12-10-2014 12:00 AM

Effect of Photoperiod on Redox Regulation of Phenotypic Plasticity and Cellular Growth in Chlorella vulgaris

Lauren E. Hollis, *The University of Western Ontario*

Supervisor: Dr Norman PA Huner, *The University of Western Ontario*

A thesis submitted in partial fulfillment of the requirements for the Doctor of Philosophy degree in Biology

EFFECT OF PHOTOPERIOD ON REDOX REGULATION OF PHENOTYPIC PLASTICITY AND CELLULAR GROWTH IN *CHLORELLA VULGARIS*

(Thesis format: Integrated Article)

by

Lauren Elisabeth Hollis

Graduate Program in Biology

A thesis submitted in partial fulfillment
of the requirements for the degree of
Doctorate of Philosophy

The School of Graduate and Postdoctoral Studies
The University of Western Ontario
London, Ontario, Canada

Abstract

Photoautotrophs are predisposed to maintain a balance between light energy absorption with the capacity to consume this energy through metabolism. An imbalance in energy flow may be a consequence of increased light intensity and is sensed as modulation of excitation pressure (EP), a measure of the redox state of quinone A. The green alga *Chlorella vulgaris* acclimated to continuous high EP exhibits a yellow-green phenotype characterized by reduced chlorophyll content and high chlorophyll a/b ratio with concomitantly reduced light-harvesting complex abundance relative to the dark green phenotype of low EP-acclimated cultures. Previous studies on acclimation to EP in green algae have been conducted under constant growth light. However, understanding how energy balance is linked to photoautotrophic form and function requires variable experimental conditions that more accurately approximate nature. To determine the role of EP in the regulation of photoacclimation in response to growth under a variable photoperiod cells were exposed to both sudden and sustained changes in the light environment. Using variable light exposure it becomes evident that EP is not the sole regulator of photoacclimation in *C. vulgaris*. Rather, photoacclimation is additionally dependent on light availability at the level of chlorophyll biosynthesis and is photoperiod-dependent. While photoperiod influences the cell cycle in *C. vulgaris*, *C. vulgaris* exhibits minimal plasticity in the capacity to upregulate metabolic sinks in response to growth light and photoperiod. I propose that perception of light in response to growth under a variable photoperiod may be involved in limiting the extent of the acclimatory response, rather than regulating photoacclimation *per se*, indirectly either through the capacity for chlorophyll biosynthesis or through the photoperiod-dependent response to high EP. Phenotypic plasticity and photoacclimation appear to be dependent on a network of intracellular sensors and signal transduction pathways integrating direct perception of light as well as perception of light as an energy source through modulation of the redox state of the photosynthetic apparatus balanced against the capacity to consume the products of photosynthesis through metabolism and ultimately growth.

Keywords

Excitation pressure
Greening
Light
Phenotype
Photoacclimation
Photoperiod
Photosynthesis
Retrograde signalling
Redox regulation

Co-Authorship Statement

A version of Chapter 1 was submitted as:

Hollis, L. & Hüner, N.P.A. (accepted). Retrograde operational sensing and signalling pathways maintain photostasis in green algae, cyanobacteria and terrestrial plants. *Trends Photochem. Photobiol.*

Contribution of co-authors:

Hollis, L., Prepared manuscript

Hüner, N.P.A., Critical comments on manuscript; principle investigator

A version of Chapter 2 was submitted as:

Hollis, L. & Hüner, N.P.A. (submitted). Relaxation of excitation pressure in *Chlorella vulgaris* (trebouxiophyceae) is light-dependent: uncoupling of redox regulation and phenotypic plasticity. *J Phycol.*

Contribution of co-authors:

Hollis, L., Conducted experiments; data analysis; preparation of manuscript

Hüner, N.P.A., Critical comments on manuscript; principle investigator

A version of Chapter 3 was submitted as:

Hollis, L. & Hüner, N.P.A. (submitted). Photoacclimation in *Chlorella vulgaris* UTEX 265 is both redox- and photoperiod-dependent. *Planta.*

Contribution of co-authors:

Hollis, L., Conducted experiments; data analysis; preparation of manuscript

Hüner, N.P.A., Critical comments on manuscript; principle investigator

A version of Chapter 4 was submitted as:

Hollis, L. & Hüner, N.P.A. (submitted). Photoperiod-dependent growth oscillations in *Chlorella vulgaris*. *J Phycol.*

Contribution of co-authors:

Hollis, L., Conducted experiments; data analysis; preparation of manuscript

Hüner, N.P.A., Critical comments on manuscript; principle investigator

Acknowledgments

Foremost, I would like to sincerely thank my supervisor, Dr. Norm Hüner. I am grateful for his time, patience and guidance and I wish I could more adequately express how thankful I am for the support and opportunities I have been given.

I am also grateful to my advisory committee members, Dr. Charles Trick and Dr. Denis Maxwell, for their thoughtful comments and advice. Additionally, I would like to thank the members of the Environmental Stress Biology Research Group for providing such an open and supportive atmosphere. In particular, Beth Szyszka for her help with techniques and friendship as well as Joseph Stinziano for his patience with statistical questions. I would also like to thank Dr. Brent Sinclair, Dr. Sheila Macfie and Dr. Ben Rubin for their advice with statistics. Additionally, Dr. Alex Ivanov and Dr. Marianna Krol for their technical expertise, on-going advice and tremendous support.

I also owe an enormous debt of gratitude to my parents for the countless opportunities they have given me as well as for never (openly) wondering why I spent so long studying algae.

And of course I need to thank my husband for his endless patience for my stressed induced antics and constant support. And to my son William; this is dedicated to you.

Table of Contents

List of Tables

List of Figures

List of Supplemental Tables

List of Supplemental Figures

List of Abbreviations

α	maximum initial slope of oxygen evolution light response curve under light limiting conditions
β-CC	β-cycloitral
ΔOD735	change in absorption at 735 nm
σ_{PSII}	effective absorption cross section of photosystem II
τ^{-1}	turnover of metabolic sinks
$\Phi_{f,D}$	sum proportions of light energy absorbed by photosystem II dissipated as fluorescence and constitutive thermal dissipation
Φ_{NPQ}	proportion of light energy absorbed by photosystem II thermally dissipated as heat through ΔpH and/or the xanthophyll cycle
Φ_{PSII}	proportion of light energy absorbed by photosystem II used to drive photochemistry
A_0	chlorophyll *a* electron acceptor in photosystem II
A_1	phylloquinone
ADP	adenosine diphosphate
AL	actinic light
ALA	aminolevulinic acid
ANOVA	analysis of variance
ATP	adenosine triphosphate
CAO	chlorophyllide *a* oxygenase
cFBPase	cytosolic fructose-1,6-bisphosphatase
CBF	c-repeat/dehydration responsive binding factor
Chl	chlorophyll
Chl*	excited chlorophyll
^{1}Chl	singlet chlorophyll
^{3}Chl*	triplet chlorophyll
Chl *a*	chlorophyll *a*
Chl *b*	chlorophyll *b*
CHLH	Mg-chlatase
Chlide *a*	chlorophyllide *a*
CL	continuous light
CO_2	carbon dioxide
COP1	constitutive photomorphogenic 1
CP	chloroplast protein
Cyt	cytochrome
D1	32 kDa reaction centre polypeptide of photosystem II
D2	34 kDa reaction centre polypeptide of photosystem II
DBMIB	2,5-dibromo-3-methyl-6-isopropy-1,4-benzoquinone
DCMU	3-(3,4-dichlorophenyl)-1,1-dimethylurea
DPOR	dark operative (or light independent) NADPH (reduced nicotinamide adenosine dinucleotide phosphate):protochlorophyllide oxidoreductase
E_K	saturating irradiance; irradiance at which photosynthetic quantum yield matches sink turnover

EP	excitation pressure
EX	executer
$F_A/F_B/F_X$	iron-sulfur cluster; electron acceptors in photosystem II
Fd	ferrodoxin
F_M'	maximum fluorescence in the light adapted state
F_M	maximum fluorescence in the dark adapted state
F_O'	minimum fluorescence in the light adapted state
F_O	minimum fluorescence in the dark adapted state
F_S	steady-state fluorescence
F_V	variable fluorescence
F_V/F_M	maximum photochemical efficiency of photosystem II
FeS	Rieske iron-sulfur protein
flu	fluorescent mutant
FNR	ferrodoxin-nictotinamide adenine phosphate oxidoreductase
FSC	forward scatter
GLK	golden 2-like
gun	genomes uncoupled mutant
GUN	genomes uncoupled
H^+	proton
H_2O_2	hydrogen peroxide
HEP	high excitation pressure
HFR1	long hypocotyl infrared
HL	high growth light
HSD	honest significant difference
HY	long hypocotyl
I	irradiance
LAF1	long after far red light
LEP	low excitation pressure
LHC	light-harvesting complex
LHCI	light-harvesting complex associated with photosystem I
LHCII	light-harvesting complex associated with photosystem II
Lhca	light-harvesting complex polypeptide of photosystem I
Lhcb	light-harvesting complex polypeptide of photosystem II
LPOR	NADPH (reduced nicotinamide adenine dinucleotide phosphate):light-dependent protochlorophyllide oxidoreductase
LL	low light
LT	low temperature
MB	measuring beam
MEcPP	methylerythritol cyclophosphate
$NADP^+$	nicotinamide adenine dinucleotide phosphate
NADPH	reduced nicotinamide adenine dinucleotide phosphate
NPQ	nonphotochemical quenching
$^1O_2$	singlet oxygen
O_2	molecular oxygen
O_2^-	superoxide
OH^-	hydroxide radical

OD735	absorbance at 735 nm
OD750	absorbance at 750 nm
OEC	oxygen evolving complex
P680	specialized reaction centre chlorophyll *a* of photosystem II
P680*	excited specialized reaction centre chlorophyll *a* of photosystem II
$P680^+$	oxidized specialized reaction centre chlorophyll *a* of photosystem II
$P680^-$	reduced specialized reaction centre chlorophyll *a* of photosystem II
P700	specialized reaction centre chlorophyll *a* of photosystem I
P700*	excited specialized reaction centre chlorophyll *a* of photosystem I
$P700^+$	oxidized specialized reaction centre chlorophyll *a* of photosystem I
P_i	inorganic phosphate
P_{MAX}	maximum carbon dioxide-saturated, light-saturated rate of oxygen evolution
Pchlide *a*	protochlorophyllide *a*
PAGE	polyacrylamide gel electrophoresis
PAM	pulse amplitude fluorometry
PC	plastocyanin
PCR	photosynthetic carbon reduction cycle
PET	photosynthetic electron transport
PGA	phosphoglyceric acid
PGE	plastid gene expression
Pheo	pheophytin
PHY	phytochrome
PIF	phytochrome interacting factor
POR	NADPH (reduced nicotinamide adenine dinucleotide phosphate): protochlorophyllide oxidoreductase
PQ^-	semiquinone
PQ	plastoquinone
PQH_2	plastoquinol (reduced plastoquinone)
PsaB	representative reaction centre polypeptide of photosystem I
PsbA	representative reaction centre polypeptide of photosystem II
PTOX	plastid terminal oxidase
Q_A	quinone A
Q_A^-	reduced quinone A
Q_A^+	oxidized quinone A
Q_B	quinone B
qL	photochemical quenching using the lake model
qN	nonphotochemical quenching
qP	photochemical quenching using the puddle model
RbcL	large-subunit rubisco
RC	reaction centre
Redox	reduction-oxidation
Resp	dark respiration
ROS	reactive oxygen species
Rubisco	ribulouse-1,5-biphosphate oxygenase/carboxylase
RuBP	ribulose bisphosphate

SDS	sodium dodecyl sulfate
SP	saturating pulse
SPS	sucrose-phosphate synthase
Y_Z	tyrosine - position161

Chapter 1

1 GENERAL INTRODUCTION

1.1 The photosynthetic apparatus

Photosynthesis is the process by which photoautotrophic organisms convert the energy available in light into biologically useful reducing power in the form of NADPH (reduced nicotinamide adenine dinucleotide phosphate) and chemical energy in the form of ATP (adenosine triphosphate). Photosynthetically derived reductants are consumed through carbon, nitrogen and sulphur metabolism, cellular respiration and ultimately growth (Figure 1.1). Virtually all life on Earth, with the exception of ancient chemolithotrophs, is dependent on the radiant energy from the sun trapped by photosynthesis. This process is responsible for virtually all molecular oxygen in the atmosphere and the fixation of 10^{11} tons of carbon annually (Falkowski 1994).

In eukaryotic algae and terrestrial plants photosynthesis occurs in specialized organelles known as chloroplasts that entered the eukaryotic lineage through an endosymbiotic event over one billion years ago (Keeling 2010). The chloroplast is composed of a system of internal thylakoid membranes organized into two distinct domains. The grana, which are composed of stacked layers of thylakoid membrane, are connected by the unstacked stroma lamallae to form a continuous membranous network enclosing a single lumenal space. The primary reactions of oxygenic photosynthesis are mediated by pigment-protein complexes embedded within the thylakoid membrane.

1.1.1 The photosystems

The initial event of photosynthesis is the absorption of light energy. Transformation of light energy into chemical energy occurs with photosystem II (PSII) and photosytem I (PSI) (Figure 1.1). Each photosystem is composed of two functional components. The

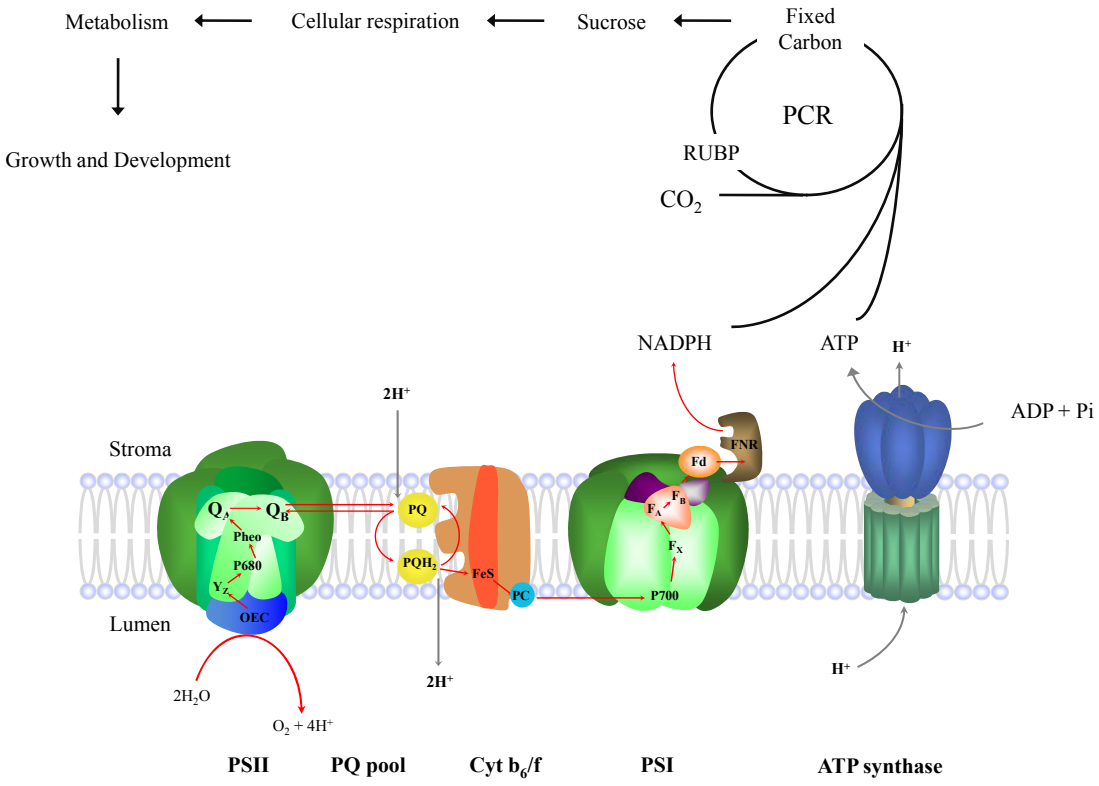
Metabolism
Cellular respiration
Sucrose
Fixed Carbon
PCR
RUBP
CO_2
Growth and Development
NADPH
ATP
H^+
ADP + Pi
$2H^+$
Stroma
Q_A
Q_B
Pheo
P680
Y_Z
OEC
PQ
PQH_2
FeS
PC
Fd
FNR
F_A
F_B
F_X
P700
Lumen
$2H_2O$
$O_2 + 4H^+$
$2H^+$
H^+
PSII
PQ pool
Cyt b_6/f
PSI
ATP synthase

Figure 1.1 Simplified model illustrating linear electron transport and carbon assimilation. Linear electron flow from water to nicotinamide adenine dinucleotide ($NADP^+$) is shown in red (discussed in text). Intersystem electron transport concentrates protons (H^+) on the lumenal side of the thylakoid membrane providing the proton motive force used to produce ATP (adenosine triphosphate) from ADP (adenosine diphosphate) and inorganic phosphate (Pi) via ATP synthase. ATP and NADPH are consumed during carbon assimilation in the photosynthetic carbon reduction (PCR) cycle; carbon dioxide (CO_2) is combined with the acceptor molecule ribulose-1,5-bisphosphate (RuBP) to generate fixed carbon in the form of triose phosphates which are transported to the cytosol for sucrose biosynthesis (discussed in text).

primary centralized component, where light energy is converted into redox potential, is termed the reaction centre. The second component is a peripheral antenna of light-harvesting pigment molecules which serve to absorb light and funnel the excitation energy to the central photosystem reaction centre. Light energy absorption is facilitated by chlorophyll (Chl) *a* and Chl *b* as well as the carotenoids, carotenes and xanthophylls, bound by light-harvesting complex polypeptides. The absorbed light energy is transferred between pigment molecules in the form of excitation energy until it reaches the reaction centre. Once excitation energy has reached the reaction centres of PSII and PSI, the specialized reaction centre Chl *a* molecules of PSII and PSI serve as electron donors that are able to trap excitation energy by transferring an electron to the primary electron acceptor, initiating charge separation. Light absorption by antenna-bound pigment molecules occurs on a timescale of subfemtoseconds ($<10^{-15}$ sec) (Shevela et al. 2013).

1.1.1.1 Photosystem II

Photosystem II is a multimeric pigment-protein complex found in terrestrial plants, algae and cyanobacteria (Burnap 2014). The crystal structure of PSII was resolved from a freshwater cyanobacterium, *Synechococcus elongatus*, at 3.8 Å resolution (Zouni et al. 2001) and more recently PSII was crystallized from a thermophilic cyanobacterium, *Thermosynechococcus vulcans* at 1.9 Å (Umena et al. 2011). PSII is the only known biological system able to generate oxidizing species capable of extracting electrons from molecular water. PSII is a large complex *in vivo* composed of over 20 proteins and approximately 60 cofactors, including 35 Chl molecules, two pheophytins, two plastoquinone (PQ) molecules and the Mn_4Ca cluster for a combined mass of approximately 700 kDa. Charge separation is conducted in the photosystem reaction centre which is composed of two proteins known as D1 and D2 (Shi et al. 2012, Burnap 2014). The D1/D2 heterodimer binds P680, a specialized Chl *a* molecule that acts as the primary electron donor within PSII as well as four additional Chl *a* molecules, two pheophytin molecules, two β-carotenes, quinone A (Q_A) and the quinone B (Q_B) binding site. Surrounding this core reaction centre complex are two proteins, CP47 and CP43, which both bind approximately 14 Chl *a* molecules and two β-carotene molecules. Oxygen evolution is catalyzed by the oxygen evolving complex (OEC), composed of four

extrinsic subunits, PsbO, PsbP, PsbR and PsbQ, as well as the four Mn^{2+} cofactors essential for oxidation of water, located on the lumenal side of PSII (Allahverdiyeva et al. 2011).

1.1.1.2 Photosystem I

The X-ray crystal structure of PSI isolated from *Pisum sativum* was determined at 3.4 Å resolution (Amunts et al. 2007, Amunts et al. 2010). The PSI reaction centre responsible for charge separation consists of a heterodimeric protein complex of PsaA and PsaB. The PsaA/PsaB heterodimer binds the electron donor and Chl *a* dimer, P700, as well as A_o, a specialized Chl *a* molecule that serves as the primary electron acceptor in PSI, A_1 (a phylloquinone) and three immobile Fe-S clusters (F_X, F_A and F_B). In addition to PsaA and PsaB, PSI is composed of approximately 10 additional proteins binding approximately 100 Chl *a* molecules and 12 to 16 β-carotene molecules (Busch et al. 2013). The PsaD and PsaE polypeptides located on the stromal side of the thylakoid membrane are involved in the docking of ferredoxin (Fd). The PsaF polypeptide, along with the PsaA/PsaB heterodimer, is involved in the binding of plastocyanin (PC), a freely diffusible copper protein located on the lumenal side of the thylakoid membrane. Photosystem I functions to catalyze the light-driven transfer of electrons from PC in the lumen to nicotinamide adenine dinucleotide phosphate ($NADP^+$) in the stroma and generates the most negative redox potential in nature (Amunts et al. 2007).

1.1.1.3 Light-harvesting complexes

The function of all light-harvesting complexes is the capture of light energy and subsequent transfer of excitation energy to the reaction centre complexes. Terrestrial plants and green algae have light-harvesting complexes associated with both PSII and PSI (LHCII and LHCI, respectively). Light-harvesting complex polypeptides are encoded by a family of nuclear genes; nine major and three minor LHCII-encoding genes and nine LHCI-encoding genes have been identified in the green algae *Chlamydomonas reinhardtii* (Minagawa and Takahashi 2004) while 15 LHCII-encoding genes and six LHCI-encoding genes have been identified in the land plant *Arabidopsis thaliana*

(Jansson 1999). Each light-harvesting complex polypeptide consists of three transmembrane domains and binds up to eight Chl *a* molecules, six Chl *b* molecules and four xanthophyll molecules.

In PSII, the major antenna complex is composed of Lhcb1, Lhcb2 and Lhcb3 along with CP29 (Lhcb4), CP26 (Lhcb5) and CP24 (Lhcb6) as well as the Chl *a*-binding core antenna proteins CP43 and CP47 (where CP refers to Chl-protein complex followed by the kDa mass of the polypeptide). The major LHCII polypeptides are arranged as trimers organized around the PSII core reaction centre; these trimers are connected to the core via the two inner, less abundant monomers, CP26 and CP29 (Rochaix 2014).

The PSI complex is asymmetrically bound to LHCI polypeptides as a crescent-shape belt around the core complex (Kargul et al. 2003, Amunts et al. 2010). The LHCI antenna is composed of six Lhca proteins (Lhac1 through Lhca6) associated with the PSI core as Lhca2 and Lhca3 homodimers as well as Lhca1/Lhca4 heterodimers; unlike LHCII which is associated with the PSII core via CP43 and CP47, LHCI is associated directly with the PSI core (Green et al. 2003).

The LHCII and LHCI systems have distinctive pigment compositions. The major LHCII and LHCI polypeptides bind both Chl *a* and Chl *b* whereas the reaction centres and core antennas of both PSII and PSI only bind Chl *a* (Green et al. 2003, Rochaix 2014). However, LHCII is preferentially enriched in Chl *b* while LHCI is enriched in Chl *a* (Lam et al. 1984, Bassi et al. 1985, Croce et al. 2002).

1.1.2 Cytochrome b_6/f

The cytochrome (Cyt) b_6/f complex is composed of seven polypeptides including the four main subunits: Cyt *f*, Cyt b_6, the Rieske Fe-S protein and subunit IV. The plastoquinol-plastocyanin/Cyt b_6 oxidoreductase activity of this complex connects PSII and PSI together in series during which movement of electrons from PSII to PSI is coupled to proton transfer across the thylakoid membrane (Hasan et al. 2013). The structure of the Cyt b_6/f complex was crystallized at 3.0 Å from the thermophilic cyanobacterium,

*Mastigloclad*us *laminosus* (Kurisu et al. 2003) and 3.1 Å from the green algae *C. reinhardtii* (Stroebel et al. 2003).

1.1.3 ATP synthase

The synthesis of ATP by photosynthesis is termed photophosphorylation (Arnon et al. 1954). ATP synthase is a multi-subunit complex composed of two subsections termed CF_o and CF_1 (chloroplastic coupling factor) and utilizes the proton motive force generated by the trans-thylakoid electrochemical proton gradient in the synthesis of ATP. The CF_0 subsection is hydrophobic and bound within the stromal lamellae in the thylakoid membrane while the CF_1 subsection protrudes into the stroma. The CF_0 complex forms a channel through the thylakoid membrane allowing protons (H^+) to move from the lumen to the stroma. The CF_1 subsection is composed of three copies of five different polypeptides; the alternating α and β subunits, as well as ɣ, ɗ and ε subunits. Rotation of ɣ induces sequential conformational changes in the structure of the αβ heterodimers (Allen 2002). The energy of the conformational movements of the CF_1 complex is converted into phospho-anhydride bond energy (Junge et al. 1997).

1.1.4 Linear electron transport

The Z, or zig-zag, scheme of photosynthesis proposed by Hill and Bendall (1960) has become the basis for our understanding of oxygenic photosynthesis where each sequential electron transfer is plotted against a vertical axis of redox potential. According to this scheme, PSII and PSI are connected in series and act in tandem to facilitate the transfer of electrons from water to $NADP^+$ (Figure 1.1). Following the absorption of a photon of light by a pigment molecule bound to LHCII, the energy contained in the photon is transferred in the form of an exciton that moves to the reaction centre Chl *a* molecule P680. The absorption of a photon and transfer of excitation energy from LHCII to P680 occurs on an extremely rapid a timescale of femtoseconds to picoseconds (10^{-15} to 10^{-12} sec); this extremely rapid transfer has been proposed to be one of the fastest biological processes (Hüner et al. 2002).

Excited P680 (P680*), the primary electron donor in PSII, is photo-oxidized to $P680^+$ with the transfer of an electron to pheophytin (Pheo), the primary electron acceptor of PSII; this results in charge separation, generating the radical pair $P680^+Pheo^-$. The electron is then passed to Q_A, resulting in the generation of the radical pair $P680^+Q_A^-$ and stable charge separation. Stable charge separation occurs on the time scale of nanoseconds to microseconds (10^{-9} to 10^{-6} sec) and results in the closure of the PSII reaction centre as $P680^+$ is not able to be further oxidized by another quantum of excitation energy. From Q_A^- the electron is transferred to a PQ at the Q_B binding site on the D1 protein. Plastoquinones are hydrophobic molecules that function as mobile electron carriers between PSII and Cyt b_6/f. Full reduction of PQ takes two electrons which requires a subsequent electron from P680. Fully reduced PQ accepts two H^+ from the stromal side of the thylakoid membrane to become plastoquinol (PQH_2). It takes 400 μs to form Q_B^{2-} and less than 1 ms to form PQH_2 which is then released from the Q_B binding site into the lipid centre of the thylakoid membrane. Therefore, full reduction of PQ to PQH_2 requires two turnovers of the PSII reaction centre. $P680^+$ is reduced by a electron donated from a tyrosine (Tyr161) located on the D1 polypeptide; reduction of $P680^+$ results in the opening of the PSII reaction centre. Tyr161 accepts an electron from water through the action of the four Mn^{2+} cluster in the OEC. Oxidation of water requires an extremely powerful reducing agent with a redox potential of + 1.25 V (Diner and Babcock 1996); this is accomplished by $P680^+$, one of the strongest biological oxidants.

Plastoquinol diffuses through the thylakoid membrane to the lumenal quinone-oxidizing (Q_o) site on the Cyt b_6 subunit of the Cyt b_6/f complex. Since oxidation of PQ pool is diffusion limited and occurs on a timescale of ms (10^{-3} sec) this reaction is believed to be the rate limiting step of photosynthetic electron transport (Haehnel 1984). When PQH_2 is oxidized by the Fe-S protein, its protons are released into the lumen. One of the two electrons carried by PQH_2 passes along a linear route to the Cyt *f* complex and subsequently through PC which shuttles the electron to PSI. The second electron carried by PQH_2 is cycled back to PQ. The second electron is transferred through two hemes (heme b_{6L} and heme b_{6H}) on Cyt b_6 before reducing PQ to semiquinone (PQ^-). A second PQH_2 and turnover of electrons is required to fully reduced PQ^- to PQ^{2-} before two H^+ are

added from the stroma and dissociation of PQH_2 occurs; this cycling of electrons around Cyt b_6/f is termed the Q-cycle. The sequential binding of PQH_2, and the cyclic nature of the Q-cycle, increases the number of protons pumped across the thylakoid membrane. For each pair of electrons to reach PSI, four protons are translocated from the stroma into the lumen. Therefore, for each pair of electrons passing through linear photosynthetic electron transport a total of six protons are contributed to the electrochemical potential across the membrane (two protons from water oxidation and four from the Q-cycle). The accumulation of these protons in the lumen generates the proton motive force required for ATP synthesis.

Following reduction by Cyt *f*, reduced PC diffuses along the lumenal side of the thylakoid membrane before it is oxidized by $P700^+$. Upon excitation by a photon of light, excited P700 (P700*), the specialized Chl *a* PSI reaction centre dimer, is photo-oxidized to $P700^+$. Following closure of the PSI reaction centre by a photon of light, the reaction centre is opened following reduction of $P700^+$ by PC. The electron donated by P700 is passed to A_o, a specialized Chl molecule that serves as the primary electron acceptor of PSI, then through A_1 and three separate Fe-S protein centres (F_X, F_A and F_B) to Fd, a soluble Fe-S protein, on the stromal side of the thylakoid membrane. Fd reduces $NADP^+$ via the enzyme ferredoxin-$NADP^+$ oxidoreductase; two electron are required to fully reduced $NADP^+$ to NADPH.

1.1.5 Carbon fixation

Photosynthetic eukaryotes assimilate carbon dioxide (CO_2) into carbohydrates through the photosynthetic carbon reduction (PCR) cycle, otherwise termed the Calvin-Benson-Bassham cycle, which is a series of biochemical redox reactions that take place in the chloroplast stroma. The enzyme ribulose bisphosphate carboxylase/oxygenase (Rubisco) catalyzes the carboxylation of the acceptor molecule ribulose bisphosphate (RuBP) by CO_2 to form two three-carbon compounds termed phosphoglyceric acid (PGA). PGA is reduced to a triose phosphate, glyceraldehyde-3-phosphate, in a two step reaction that consumes both ATP and NADPH. Continuous CO_2 assimilation requires the regeneration of RuBP. RuBP is regenerated from triose sugar-phosphates through a series of reactions

that require additional ATP. The net effect is to recycle carbon from five out of every six triose phosphates to regenerate three RuBP molecules. The sixth triose phosphate is available for sucrose and starch biosynthesis in the cytosol and chloroplast stroma, respectively. The appropiation of triose phosphates to either sucrose or starch is termed carbon allocation. Starch will be later mobilized to support respiration and metabolism during the night.

1.2 The chloroplast

Chloroplasts are descended from a free-living photoautotrophic ancestor similar to extant cyanobacteria which entered the eukaryotic lineage through an endosymbiotic event over a billion years ago (Reyes-Prieto et al. 2007, Stiller 2007, Waters and Langdale 2009). Following this event, the genome of the endosymbiont underwent significant reduction with the majority of the genes having been lost or transferred to the host nucleus (Barbrook et al. 2006, Barkan 2011). As a consequence, the chloroplast genome encodes less than 10% of the proteins required for plastid function and development (Surpin and Chory 1996, Barbrook et al. 2006, Barkan 2011). The remainder of the chloroplast-localized proteins are encoded by the nuclear genome and synthesized in the cytoplasm before import into the plastid. Such genetic heterogeneity means that many plastid localized protein complexes are molecular mosaics of plastid and nuclear-encoded gene products (Allen et al. 2011).

Establishment of photoautotrophic metabolism therefore requires considerable coordination between these two spatially separated genomes to ensure proper chloroplast biogenesis and development, while maintenance of photoautotrophic metabolism requires coordinated adjustments in nuclear- and plastid-encoded gene expression necessary to optimize photosynthesis and avoid the oxidative damage associated with excessive light energy absorption during abiotic stress. Developmental cues and environmental stimuli including light, temperature and nutrient availability are integrated to ensure proper chloroplast development and to modulate photosynthetic efficiency and capacity in mature chloroplasts.

Coordinated regulation between the nuclear and plastid genomes is achieved through the bidirectional exchange of information between the nucleus and plastids. Anterograde signals arise in the nucleus and regulate the expression of plastid localized genes (Woodson and Chory 2008). The reverse mechanism, retrograde signalling, transmits information communicating the developmental and functional state of the plastid to the nucleus to induce appropriate changes in the expression of nuclear-encoded genes involved in chloroplast function and development (Woodson and Chory 2008). *Light quality* signals are required for the proper regulation of chloroplast biogenesis and photoautotrophic architecture where as *light intensity* signals are required to regulate the structure and functionality of the photosynthetic apparatus. The former are associated with “biogenic signals” whereas the latter are referred to as “operational signals" (Pogson et al. 2008, Pogson and Albrecht 2011).

1.3 Biogenic signals

1.3.1 Photoreceptor-mediated light quality signalling during chloroplast biogenesis

In the context of biogenic control, perception of light is mediated by blue light sensitive photoreceptors (cryptochromes, phototropins and zeitlupe) and red light sensitive photoreceptors (phytochromes; Casal 2013, Kianianmomeni and Hallmann 2014). Photoreceptors are activated by absorption of specific wavelengths enabling detection of specific changes in *light quality* and are responsible for activating signalling cascades regulating light-dependent events including photomorphogensis and photoperiodic responses (Moglich et al. 2010, Pogson and Albrecht 2011, Berry et al. 2013, Jarvis and López-Juez 2013, Kianianmomeni and Hallmann 2014).

Chloroplast biogenesis is the developmental differentiation of a proplastid, the plastid progenitor, to a mature chloroplast either directly or through the dark-grown etioplast as an intermediate and ultimately leads to the establishment of photoautotrophic metabolism. Proplastids lack Chl as well as internal membranous structures. Etioplasts arise from proplastids following prolonged growth in the dark, are approximately 5 to 10

times larger than proplastids and contain the prolamellar body as well as thylakoid-like structures termed prothylakoids. The prolamellar bodies contain lipids, the Chl precursor protochlorophyllide, and the Chl biosynthesis enzyme NADPH:protochlorophyllide oxidoreductase (POR). In darkness photomorphogensis is repressed by two nuclear repressors, phytochrome interacting factors (PIFs) and constitutive photomorphogenic 1 (COP1), which prevent the accumulation of positive regulators of light-activated gene expression (Pogson et al. 2008, Casal 2013, Kianianmomeni and Hallmann 2014). Following illumination, phytochromes and cryptochromes facilitate the removal of PIFs and COP1 from the nucleus thereby allowing for the accumulation of positive transcription factors including golden2-like (GLK), long hypocotyl in far red 1 (HFR1), long hypcotyl 5 (HY5) and long after red right light 1 (LAF1; Pogson et al. 2008, Casal 2013, Kianianmomeni and Hallmann 2014). These positive transcription factors promote the expression of nuclear-encoded genes involved in photomorphogenesis and photosynthesis through *cis*-acting promoter elements (Jiao et al. 2007, Bae and Choi 2008, Casal 2013). These light signalling components are closely related to chloroplast biogenesis: PIF3 is negative regulator of chloroplast development (Stephenson et al. 2009), whereas HY5 and GLK are positive regulators of chloroplast development (Fitter et al. 2002, Kobayashi et al. 2012).

Light induces the conversion of the dark grown etioplasts to chloroplasts in a process that takes between 12 and 24 hours. Following illumination the promallelar body dissociates and the thylakoid membrane develops in a process term de-etiolation, or sometimes more informally as greening, reflecting the accumulation of Chl as the protochlorophyllide is photoreduced to Chl. The assembly of the thylakoid membrane during chloroplast biogenesis requires considerable coordination between plastid and nuclear gene expression as well as Chl biosynthesis to allow for stable accumulation of the pigment-protein structures associated with photosynthetic electron transport (PET) and establishment of a photoautotrophic lifestyle.

1.3.2 Developmental retrograde plastid signals

In addition to perception of light signals by phytochromes, the chloroplast itself mediates signals during biogenesis. When chloroplast biogenesis is blocked either by use of specific genetic backgrounds (Bradbeer et al. 1979), site specific inhibition of plastid transcription or translation by chemical inhibitors (Rapp and Mullet 1991, Barkan and Goldschmidt-Clermont 2000, Sullivan and Gray 2002), or by oxidative damage caused by carotenoid deficiency following norflurazon treatment (Foudree et al. 2010) the expression of nuclear-encoded genes involved in photosynthesis and chloroplast biogenesis are reduced. It has been postulated that signals derived from the plastid, which are dependent on plastid gene expression (PGE), control the expression of nuclear-encoded genes. These signals are believed to function to coordinate the expression of nuclear-encoded genes required for the proper biogenesis and assembly of the photosynthetic apparatus (Ruckle et al. 2007, Woodson and Chory 2008).

Significant insight into the mechanism of these PGE-dependent signalling pathways has been gained from a series of *A. thaliana* mutants that accumulate nuclear-encoded photosynthetic genes despite photobleaching caused by norflurazon treatment (Susek et al. 1993); since these mutants fail to repress nuclear gene expression they were designated *genomes uncoupled (gun)* mutants due to the apparent lesions in the plastid-to-nucleus signalling pathways. One of the mutants, *gun1*, showed de-repression of nuclear gene expression in plants treated with an inhibitor of PGE indicating a role for GUN1 in PGE-dependent retrograde signalling pathways (Koussevitzky et al. 2007). GUN1 was identified as a pentatricopeptide-repeat protein suggesting a potential role for it as a regulator of plastid-localized gene expression in a manner that influences retrograde signalling (Terry and Smith 2013).

Of the *gun* mutants isolated, four of the mutants (*gun2, gun3, gun4* and *gun5*) were demonstrated to have mutations in genes encoding enzymes in the tetrapyrrole pathway that culminates in Chl, heme and chromophore synthesis (Terry and Smith, 2013; Figure 1.2). Although the Chl biosynthesis intermediate Mg-protoporphyrin IX was

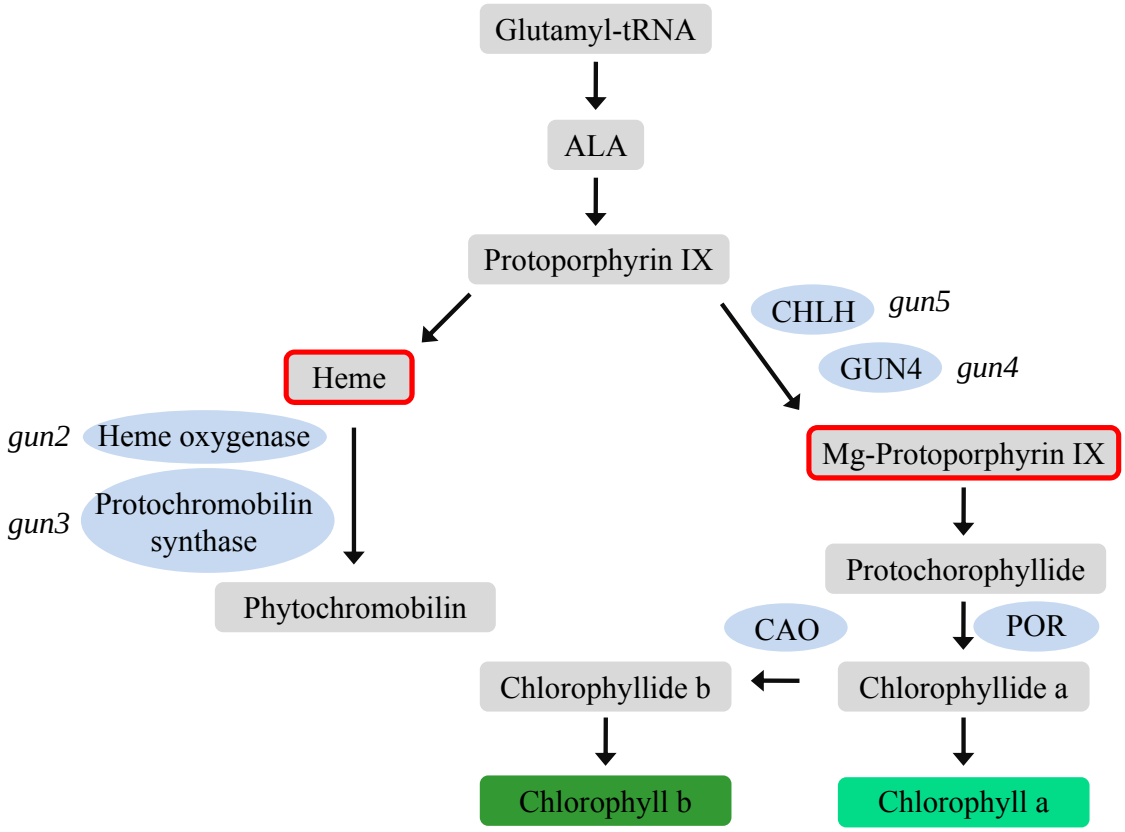

Figure 1.2 Tetrapyrrole biosynthesis pathway in plastids. Key intermediates in the pathway culminating in chlorophyll and phytochromoblin are shown in grey with key enzymes shown in blue. Molecules highlighted in red are suspected "biogenic" plastid retrograde signals (discussed in text). Location of *gun* mutations are noted. ALA, aminolevulinic acid; CAO, chlorophyllide *a* oxygenase; CHLH, Mg-chelatase; POR, protochlorophyllide oxidoreductase. Tetrapyrrole pathway adapted from Larkin 2003.

subsequently identified as a potential retrograde signal (Strand et al. 2003; Figure 1.2), the role of this intermediate remains equivocal (Mochizuki et al. 2008, Moulin et al. 2008). Recently, it has been reported that a specific heme pool may be a primary retrograde signal for chloroplast biogenesis (Woodson et al. 2011, Terry and Smith 2013; Figure 1.2).

Research suggests GUN1 may function downstream of tetrapyrrole-dependent signals and act as a convergent point for tetrapyrrole- and PGE-dependent signals (Koussevitzky et al. 2007, Woodson and Chory 2008). Convergence between multiple retrograde pathways would allow the chloroplast to integrate disparate signalling conduits that regulate similar nuclear-encoded genes (Woodson and Chory 2008). GUN1 has also been identified as a component of additional signalling pathways including those derived from the circadian clock (Hassidim et al. 2007) and de-etiolation (Mochizuki et al. 1996), as well as sugar and redox signals (Koussevitzky et al. 2007) suggesting GUN1 acts as a hub within the chloroplast coordinating multiple signalling pathways. However, GUN1-dependent plastid retrograde signalling may only function during the early stages of chloroplast development (McCormac et al. 2001, Gadjieva and Axelsson 2005).

Plastid biogenesis requires a balance between positive signals derived from phytochrome-mediated light quality sensing and negative signals derived from the functional state of the plastid itself (Waters and Langdale 2009). A genetic screen identified four mutants with a *gun* phenotype but with mutations in *cry1* alleles (Ruckle et al. 2007). Since cry1 is a strong inducer of light-harvesting gene expression, it appears that cry1 can be converted from a positive to a negative regulator of nuclear-encoded light-harvesting gene expression when chloroplast biogenesis is blocked. It was postulated that the functional state of the plastid can "remodel" biogenic light signals crucial for chloroplast biogenesis (Ruckle et al. 2007, Larkin and Ruckle 2008, Ruckle et al. 2012).

1.4 Operational signals

1.4.1 Photostasis and excitation pressure

Using phytochrome mutants, Walters et al. (1999) demonstrated that light-dependent adjustments to the structure and function of the fully developed photosynthetic apparatus of *A. thaliana* in response to changing irradiance occur independently of photoreceptors. However, the defective photoacclimation responses in the *det1* signal transduction mutant in *A. thaliana* does support some degree of cross-talk between photoreceptor-regulated responses and other regulators of photosynthetic acclimation (Walters et al. 1999). Furthermore, Fey et al. (2005) demonstrated redox signals from the photosynthetic apparatus are capable of inducing changes in nuclear-encoded gene expression independently of photoreceptor-mediated signaling.

Photoautotrophs must balance the energy trapped through the extremely fast (femtosecond to picosecond timescale), temperature-independent photophysical light absorption, energy transfer and photochemistry within the photosystems with energy utilization through much slower, temperature-sensitive metabolic sinks consisting of biochemical reactions (second to minute timescale) and subsequently growth (hours to days to weeks timescale). This energetically balanced cellular state between energy source and sink is referred to as photostasis (Hüner et al. 2003). Photostasis can be represented as:

$$\sigma_{PSII} \cdot E_K = \tau^{-1}$$

where σ_{PSII} is the effective absorption cross section of PSII and E_K is the irradiance (I) at which photosynthetic quantum yield matches sink turnover (τ^{-1}; Falkowski and Chen 2003). While light-absorption and photochemistry are also associated with PSI, PSI is not considered to be limiting during steady-state photosynthesis as its photochemical turnover rate exceeds that of PSII (Ke 2001) and is therefore excluded from the equation for photostasis.

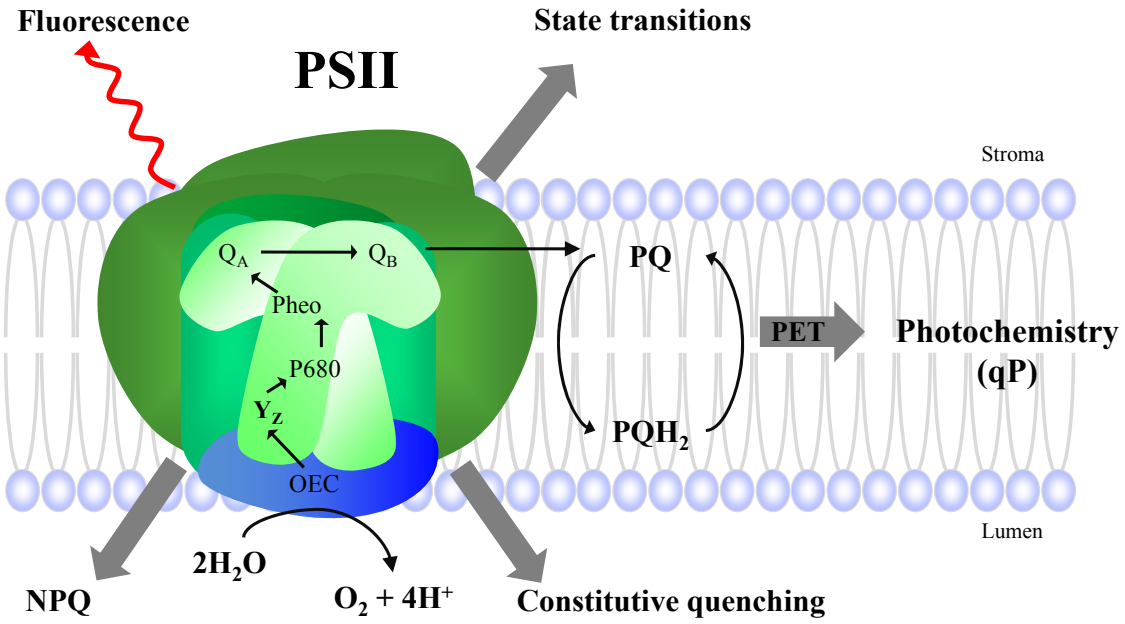

Figure 1.3 Fates of light energy absorbed by photosystem II (PSII). Light energy absorbed by the PSII antenna can be either be released as fluorescence, dissipated as heat through nonphotochemical quenching (NPQ), dissipated as heat through constitutive quenching, or used to drive photochemistry (qP) and intersystem photosynthetic electron transport (PET).

Since the maintenance of photostasis integrates temperature-insensitive photophysical and photochemical processes with temperature-dependent processes, PSII can be exposed to excessive excitation energy whenever the light energy absorbed exceeds either the turnover rate of the metabolic sinks that consume this energy through biochemistry and metabolism and/or the capacity to dissipate excess energy as heat through nonphotochemical quenching (NPQ; Demmig-Adams and Adams III 1992, Demmig-Adams and Adams III 2000; Figure 1.3). Such an imbalance in cellular energy is termed high excitation pressure (HEP) and can be represented by the inequality:

$$\sigma_{PSII} \cdot E_K > \tau^{-1}$$

(Hüner et al. 2003, Ensminger et al. 2006, Hüner et al. 2011).

An imbalanced cellular energy flow may be a consequence of the cumulative impact of changes in either, or both, light and temperature (Hüner et al. 1998). High light (HL) would satisfy this condition directly by increasing the product $\sigma_{PSII} \bullet E_K$ with minimal effects on τ^{-1} whereas low temperature (LT) satisfies the same condition by exerting minimal effects on $\sigma_{PSII} \bullet E_K$ but decreasing τ^{-1}. Since diffusion of plastoquinol (PQH_2) within the plane of the thylakoid membrane and its subsequent oxidation by the Cyt b_6/f complex is the rate limiting step of PET (Ke 2001), HEP results in the reduction of the components of PET which culminates in the accumulation of closed PSII reaction centres (Figure 1.4). This can be measured non-invasively *in vivo* by either the Chl *a* fluorescence parameter 1 - qP (Dietz et al. 1985, Hüner et al. 1998) or 1 - qL (Hendrickson et al. 2004, Kramer et al. 2004, Baker 2008) which are measures of the relative redox state of Q_A of PSII reaction centres which ultimately reflect the reduction state of the intersystem electron transport chain.

Changes in either growth irradiance or temperature will modulate excitation pressure generated within the chloroplast. The resulting reduction of the component of the PET chain represents an “operational redox signal” that can be used to re-establish photostasis and a new homeostatic cellular energy state associated with acclimation to the new

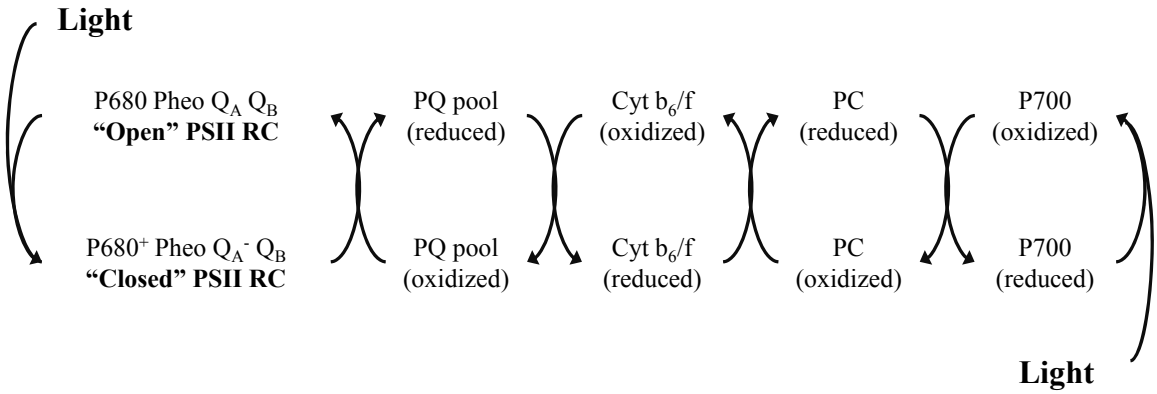

Figure 1.4 Light-dependent closure of photosystem II reaction centre (PSII RC). The PSII reaction centre consists of P680, the specialized reaction centre chlorophyll *a*, pheophytin (Pheo) and quinone A (Q_A). Excitation energy is used to excite P680 which is photo-oxidized to $P680^+$ following electron transfer to Pheo. From Pheo, the electron is passed to Q_A reducing Q_A to Q_A^-; this results in stable charge separation and closure of the PSII reaction centre ($P680^+$ Pheo Q_A^-) as $P680^+$ cannot undergo further photo-oxidation. Conversion of the "closed" PSII reaction centre to an "open" PSII reaction centre requires reduction of $P680^+$ via oxidation of water and concomitant transfer of the electron from Q_A^- to the plastoquinone (PQ) pool via Q_B. Following complete reduction, PQ is protonated to form plastoquinol (PQH_2) which leads to the step-wise reduction of the cytochrome b_6/f complex (Cyt b_6/f), plastocynanin (PC) and ultimately $P700^+$, the photo-oxidized photosystem I (PSI) reaction centre chlorophyll *a*. The proportion of closed PSII RC is measured *in vivo* as 1-qP which estimates the relative redox state of Q_A as $(Q_A^-) / ((Q_A^-) + (Q_A^+))$ which reflects the reduction state of the intersystem electron transport chain. Since reduced Q_B is in rapid equilibrium with the PQ pool, 1 - qP also reflects the redox state of the photosynthetic electron transport chain.

environment. Thus, acclimation to HL mimics acclimation to LT (Maxwell et al. 1994). Furthermore, since nutrient limitations and water availability will also induce HEP by lowering τ^{-1}, because of the nature of photoautotrophic growth, all photosynthetic organisms acclimate to changes in their environment by sensing and responding to excitation pressure, an important “operational" signal.

1.4.1.1 Green algae

Growth and development of the green algae *Chlorella vulgaris* and *Dunaliella* sp. under HL results in a typical yellow to yellow-green pigmentation relative to the dark green pigmentation typical of growth and development at low light (LL). This yellow to yellow-green phenotype is characterized, in part, by a relatively lower Chl content per cell and higher Chl a/b ratios with concomitant decreases in the level of the major LHCII pigment-binding polypeptides relative to the dark green, LL phenotype (Maxwell et al. 1994, Maxwell et al. 1995a, Maxwell et al. 1995b, Savitch et al. 1996, Król et al. 1997, Wilson and Hüner 2000, Wilson et al. 2003, Hüner et al. 2012). The xanthophyll cycle is also activated during growth under HL. Functionally, this results in a significant decrease in the apparent quantum yield for oxygen (O_2) evolution when measured on a per cell basis (Maxwell et al. 1994, Maxwell et al. 1995a, Maxwell et al. 1995b, Savitch et al. 1996, Król et al. 1997, Wilson and Hüner 2000, Wilson et al. 2003). These results are consistent with the notion that green algae respond to HL by decreasing σ_{PSII} through reductions in the physical size of LHCII as well as an increased capacity to dissipate excess energy as heat through NPQ (Escoubas et al. 1995, Maxwell et al. 1995a, Maxwell et al. 1995b, Król et al. 1997, Miskiewicz et al. 2000, Wilson and Hüner 2000, Miskiewicz et al. 2002).

As predicted, phenotype as well as photosynthetic performance during growth at HL is mimicked by growth at LT in *C. vulgaris*. This change in σ_{PSII} induced by growth at HEP imparts enhanced photoprotection and increased resistance to photoinhibition compared to LEP control cells (Maxwell et al. 1994, Maxwell et al. 1995b, Miskiewicz et al. 2000, Wilson and Hüner 2000, Miskiewicz et al. 2002). The phenotypic and photosynthetic

similarity between cells grown under HEP at either HL or LT is attributed to the observation that *C. vulgaris* is limited in its capacity to adjust either carbon metabolism (Savitch et al. 1996) or growth rates (Wilson and Hüner 2000) in response to continuous HEP. *C. vulgaris* is therefore limited in its capacity to up-regulate τ^{-1} during growth and development under continuous light. Consequently, *C. vulgaris* survives under HEP by altering the structure and function of the photosynthetic apparatus and up-regulates NPQ to reduce the capacity to absorb and trap available light energy through a decrease in σ_{PSII}. Thus, *C. vulgaris* survives and re-establishes photostasis under continuous HEP by decreasing its photosynthetic efficiency ($\sigma_{PSII} \bullet E_K$) to match its sink capacity (τ^{-1}). This increases the quantum requirement for the closure of PSII reaction centres, measured as the number of photons required to close PSII reaction centres, which accounts for the increased resistance to photoinhibition.

The yellow-green HEP phenotype in *C. vulgaris* can revert to the normal, dark green LEP phenotype following a shift from LT to moderate temperature at a constant irradiance (Wilson et al. 2003). This temperature-induced greening is associated with an increase in Chl per cell and accumulation of Lhcb2 polypeptides (Wilson et al. 2003) which is very similar to the greening observed when the green algae *C. pyrenoidosa* (Fujita et al. 1989) and *D. tertiolecta* (Sukenik and Bennett 1990) were transferred from high to low light. Temperature-induced greening in *C. vulgaris* without a change in light intensity precludes the contribution of sensors involved in light sensing *per se.*

Acclimation to HEP in *C. vulgaris* and *D. tertiolecta* is additionally mimicked by use of chemical inhibitors of PET that regulate the redox state of the PQ pool. This is accomplished through application of either 3-(3,4-dichlorophenyl)-1,1-dimethylurea (DCMU) or 2,5-dibromo-3-methyl-6-isopropy-1,4-benzoquinone (DBMIB; Escoubas et al. 1995; Wilson and Hüner 2000, Wilson et al. 2003). Since DCMU blocks the transfer of electrons from PSII to the PQ pool, the PQ pool remains oxidized in the light. DCMU mimics the effects of either LL or moderate temperature on the redox state of the PQ pool and generates the dark-green LEP phenotype characterized by relatively high Chl per cell, low Chl a/b ratio (approximately 3.0 to 4.0) and high levels of *Lhcb2* transcript and

Lhcb2 polypeptide abundance (Escoubas et al. 1995, Wilson and Hüner 2000, Wilson et al. 2003).

In contrast, DBMIB prevents the oxidation of PQH_2 by PSI in the light. Treatment with DBMIB therefore mimics the effects of HEP on the redox state of the PQ pool and generates the yellow-green HEP phenotype characterized by relatively lower Chl per cell, high Chl a/b ratio and reduced *Lhcb2* expression and Lhcb2 polypeptide abundance (Escoubas et al. 1995, Wilson and Hüner 2000, Wilson et al. 2003). Since the phenotypic and photosynthetic adjustments in *C. vulgaris* can be modulated either chemically with DMBIB and DCMU or with temperature with no change in irradiance, the attainment of photostasis is a response to "operational signals" from the chloroplast to the nucleus and does not require "biogenic signals" typically involved in photomorphogenesis. Furthermore, since PSII reaction centres are completely closed in the presence of either DCMU or DBMIB, the redox state of Q_A cannot be the sensor. Thus, it appears that the redox state of the PQ pool is an important sensor within PET and source of redox signals regulating photostasis (Hüner et al. 1996, Hüner et al. 2003, Ensminger et al. 2006).

1.4.1.2 Diverse responses to energy imbalance: species specific responses

1.4.1.2.1 Cyanobacteria

Although cyanobacteria are oxygenic, they do not exhibit a xanthophyll cycle characteristic of terrestrial plants and green algae (Hirschberg and Chamovitz 1994). Furthermore, cyanobacteria are characterized by the presence of pigment-protein complexes extrinsic to their thylakoid membranes called phycobilisomes. These phycobilisomes function to harvest light energy and transfer the energy to PSII and PSI reaction centres analogous to the major LHCII and LHCI associated with eukaryotic photoautotrophs. Do prokaryotic photosynthetic microbes respond in a similar manner to HEP as observed for green algae?

This question was addressed by examining the response of the filamentous cyanobacterium, *Plectonema boryanum*, to HEP generated by growth at either HL or LT (Miskiewicz et al. 2000, Miskiewicz et al. 2002). Similar to *C. vulgaris*, *P. boryanum* also exhibited minimal plasticity in the ability to adjust growth rates (τ^{-1}) in response to either continuous HL or LT. Consequently, this cyanobacterium alters the structure and composition of its phycobilisomes to minimize the absorption of light energy which results in a decrease in the efficiency of photosynthetic O_2 evolution (Miskiewicz et al. 2000, Miskiewicz et al. 2002). This results in a change in phenotype from the typical blue-green for control cells grown under LEP to a red-brown phenotype for cells grown at HEP. Similar to *C. vulgaris*, the HEP phenotype in *P. boryanum* is completely reversible upon a shift from low growth temperature (15 °C) to warm temperatures (29 °C) with no change in irradiance (Miskiewicz et al. 2000, Miskiewicz et al. 2002). However, unlike *C. vulgaris*, the operational signal appears to emanate downstream of the PQ pool in this cyanobacterium based on its phenotypic responses to DCMU and DBMIB (Miskiewicz et al. 2002). The precise source of the redox signal remains unclear.

1.4.1.2.2 Terrestrial plants

In contrast to green algae and cyanobacteria which respond to growth and development under HEP through reductions in σ_{PSII} due to limited capacity to adjust τ^{-1}, overwintering cultivars of wheat and rye respond to HEP through a stimulation of τ^{-1} through up-regulation of photosynthetic capacity and biomass accumulation with minimal dependence on NPQ and minimal changes in the structure and function of PSII and PSI (Gray et al. 1997, Hüner et al. 1998, Hüner et al. 2012). Consequently, in contrast to *C. vulgaris* and *P. boryanum*, the dwarf growth habit associated with cold acclimation in winter wheat and rye occurs with minimal changes in pigmentation and structure and function of PET (Dahal et al. 2012a, Dahal et al. 2012b). Rather, cold acclimated plants display a dwarf phenotype and exhibit increased cytoplasmic volume with concomitant increases in sucrose and structural carbohydrate content as well as an increase in leaf thickness such that the total biomass of the dwarf plants matches or exceeds that of those displaying the typical elongated growth habit (Boese and Hüner 1990, Strand et al. 1999, Gorsuch et al. 2010a, Gorsuch et al. 2010b, Dahal et al. 2012b).

The cold-acclimated dwarf phenotype reflects underlying changes at the molecular and biochemical level consistent with a stimulation in carbon metabolism through increased expression and activities of the carbon-fixing enzyme Rubisco (Hurry and Malmberg 1994, Strand et al. 1999, Dahal et al. 2012b) and the sucrose biosynthesis enzymes cFBPase (cytosolic fructose-1,6-bisphosphatase) and SPS (sucrose-phosphate synthase) (Hurry and Malmberg 1994, Hurry et al. 1995, Strand et al. 1999, Dahal et al. 2012a, Dahal et al. 2012b). Cold-acclimation is further associated with increased sucrose export to sink tissues and the capacity for increased carbohydrate storage in crown tissue (Pollock and Cairns 1991, Savitch et al. 2002, Stitt and Hurry 2002, Leonardos et al. 2003).

A comparable dwarf phenotype and enhanced photosynthetic capacity is generated by growth and develop of winter cereals under HL and moderate temperature. Consequently, the dwarf phenotype and enhanced photosynthetic performance is governed by excitation pressure rather than by LT *per se* (Gray et al. 1997, Hüner et al. 1998). Comparable responses to HEP with respect to dwarf phenotype and enhanced photosynthetic performance have been reported for *A. thaliana* (Savitch et al. 2001) and *Brassica napus* (Dahal et al. 2012a, Dahal et al. 2012b). Thus, although winter cereals, like green algae and cyanobacteria, maintain photostasis in response to excitation pressure, the mechanism by which they do so is quite distinct; winter hardy terrestrial plants adjust sink capacity (τ^{-1}) whereas *C. vulgaris* and *P. boryanum* adjust σ_{PSII}.

1.4.2 Photoacclimation: time-nested responses

Regulation of the structure and/or functionality of PET in response to either HL or LT maintains photostasis, a balanced cellular energy state. Depending on the severity and duration of the stress, different mechanisms are induced to restore energy balance. Falkowski and Chen (2003) suggest that transduction of the excitation pressure signal is mediated by set of responses nested, or integrated, over various timescales. According to the time-nested signal hypothesis, short term, abiotic stresses on the timescale of seconds to minutes will cause the reduction state of the PQ pool to increase leading to the

induction of highly reversible photoprotective mechanisms including a rapid increase in NPQ through the xanthophyll cycle and state transitions. These short term mechanisms function to protect the photosynthetic apparatus from photodamage by decreasing the efficiency of light energy absorption and energy transfer. However, if the energy imbalance persists over longer timescales on the order of hours to days, these short term, highly reversible mechanisms will be superseded by longer term adjustments in the structure and function of PET through changes in gene expression to physically reduce the size of the light-harvesting antenna and/or alter photosystem stoichiometry.

1.4.2.1 Nonphotochemical quenching

Nonphotochemical quenching refers to the rapidly induced and reversible changes in the effective absorption cross-section of PSII. When photosynthetic organisms are exposed to light energy in excess of what can be used to drive photochemistry, photo-excited Chl (Chl*) can convert to a triplet excited state (^{3}Chl*). Chlorophyll molecules in a triplet excited state can subsequently transfer their energy to molecular oxygen resulting in the formation of singlet O_2, a highly reactive and damaging excited form of oxygen.

Quenching of absorbed light energy through the xanthophyll cycle is considered to be the primary, inducible process contributing to photoprotection through nonphotochemical dissipation of excess light energy (Demmig-Adams and Adams III 1992, Demmig-Adams and Adams III 2000). Low lumenal pH results in the conversion of violaxanthin to zeaxanthin, the presence of which allows for thermal dissipation of excess excitation energy (Demmig-Adams et al. 1996, Gilmore 2001). Two pathways have been proposed for the conversion of excitation energy to heat. The first pathway involves direct energy transfer from the first stable excited state (S_1) of Chl to that of zeaxanthin followed by the loss of excitation energy from zeaxanthin as heat as the excited electron returns to ground state. The second pathway involves conversion of excited Chl from the S_1 state to ground state internally resulting in the loss of excitation energy as heat; this pathway requires the presence of zeaxanthin under low pH and has been proposed to involved Chl-Chl dimers

allowing for de-excitation through the introduction of additional energy levels (Demmig-Adams et al. 1996).

1.4.2.2 State transitions

State transitions are short-term (minutes) reversible changes in the absorptive cross-section of PSII and PSI involved in the redistribution of excitation energy between these two photosystems. Balanced energy flow between photosystems is achieved by the reversible phosphorylation and association of peripheral LHCII polypeptides with PSII and PSI. Over-reduction of the PQ pool is suggested to lead to the activation of a kinase responsible for phosphorylating peripheral LHCII polypeptides associated with PSII (Bellafiore et al. 2005). Following phosphorylation these LHCII polypeptides dissociate from PSII before becoming associated with PSI in a state 1-to-state 2 transition (Bellafiore et al. 2005). State transitions are contrasted against the long term (hours to days) genomic responses to imbalances in the turn-over rates of PSII and PSI involving changes in photosystem stoichiometry at the level of gene expression.

1.4.3 Redox sensing

Photosynthetic organisms constantly monitor changes in light energy availability through the redox state of the photosynthetic apparatus ("operational signals"). However, the nature of the redox sensor remains equivocal. In green algae, the ability to mimic photoacclimation and a yellow-green HL phenotype with HL, LT or inhibitors of PET has originally indicated the involvement of the redox state of the PQ pool as the primary sensor governing gene expression and phenotype (Maxwell et al. 1994, Escoubas et al. 1995, Wilson and Hüner 2000, Masuda et al. 2003, Chen et al. 2004). However, experiments with the cyanobacteria *P. boryanum* (Miskiewicz et al. 2000, Miskiewicz et al. 2002), *A. thaliana* (Piippo et al. 2006) and tobacco (Pfannschmidt et al. 2001) indicate that the PQ pool is not the primary source of redox signals in all species.

In addition to the redox state of the PQ pool, ferredoxin, thioredoxins and peroxioredoxins on the acceptor side of PSI (Dietz 2008) as well as the reducing side of

PSI (Piippo et al. 2006) have been postulated to function as components of the retrograde redox sensing and signalling network (Koussevitzky et al. 2007, Jung and Chory 2010, Barajas-López et al. 2013a). Reactive oxygen species (Apel and Hirt 2004) and PSII (Apel and Hirt 2004, Nott et al. 2006, Fernandez and Strand 2008) have additionally been implicated as redox sensing and signalling components.

Recently, much research has focused on the elucidation of retrograde operational signalling pathways between the chloroplast and the nucleus. Metabolically active chloroplasts, mitochondria and peroxisomes produce reactive oxygen species (ROS) including singlet oxygen ($^1O_2$), the hydroxyl radical ($OH^{\bullet}$), superoxide (O_2^-) and hydrogen peroxide (H_2O_2) under normal conditions. Photoautotrophs are able to maintain relatively low ROS levels due to the action of ROS scavengers such as ascorbate peroxidase and carotenoids. However, when energy absorption exceeds the capacity for utilization under abiotic stresses, including temperatures extremes, drought and HL, ROS production increases (Mullineaux and Karpinski 2002, Foyer and Allen 2003). The *A. thaliana fluorescent* (*flu*) mutant over-accumulates the Chl precursor protochlorophyllide leading to specific increases in $^1O_2$ production without increased accumulation of other ROS types (Meskauskiene et al. 2001, op den Camp et al. 2003; Figure 1.2); illumination of the *flu* mutant causes a rise in $^1O_2$ levels and increased expression of a suite of nuclear genes. Components of ROS signalling required for $^1O_2$-dependent changes in nuclear gene expression have been identified including EXECUTER 1 (EX1) and EXECUTER 2 (EX2; Lee et al. 2007). EX1 and EX2 were identified in a suppressor screen of *flu* mutants and were identified as chloroplast-localized proteins (Lee et al. 2007).

H_2O_2 produced by the chloroplast is also postulated to induce the expression of nuclear-encoded genes. Since H_2O_2 has a longer half-life relative to $^1O_2$ and a lower toxicity it may be better suited as a long distance retrograde signal (Mullineaux and Karpinski 2002). H_2O_2 generated by HL treatment has been demonstrated to increase the expression of the nuclear-encoded *APX2* in *A. thaliana* (Karpinski et al. 1999). Although H_2O_2 can be generated in different compartments under varying stresses, a specific role for

chloroplast-generated H_2O_2 has been demonstrated in tobacco plants (Yabuta and Maruta 2004) indicating a role of H_2O_2 in retrograde redox signaling.

More recently metabolites have been identified as potential sources of retrograde plastid signals during environmental stresses. Products derived from secondary metabolism including 3'-phosphoadenosine 5'-phosphate (PAP; Estavillo et al. 2011, Barajas-Lopez et al. 2013b) and methylerythritol cyclophosphate (MEcPP; Xiao et al. 2012a), and carotenoid oxidation products such as β-cycloitral (β-CC; Ramel et al. 2012) have been identified as plastid signals generated during HL and drought stress. These products function to induce changes in gene expression involved in stress responses including ROS scavenging, photoacclimation and drought tolerance (Estavillo et al. 2013). Signalling associated with these metabolites is consistent with the thesis that the chloroplast itself acts as a universal environmental sensor and as a mediator of operational signals during acclimation to environmental change. However, these chloroplast-derived metabolites may be involved in the initiation of stress response as opposed to coordination of the plastid and nuclear genomes necessary to achieve energy homeostasis *per se*.

1.5 Chlorophyll *a* fluorescence

Chlorophyll fluorescence provides an *in vivo* method to obtain information on photosynthesis and overall photoautotroph health (van Kooten and Snell 1990, Maxwell and Johnson 2000). Light energy absorbed by Chl pigment molecules can undergo one of three fates; the light energy can be (1) used for photochemistry to drive photosynthesis, (2) dissipated as heat or (3) re-emitted as light through Chl fluorescence (Figure 1.3). Of the total amount of energy absorbed, only 1 to 2% is emitted as fluorescence (Maxwell and Johnson 2000). These three processes are in competition such that an increase in any one of these pathways will lead to decreases in the other two.

When dark-adapted photosynthetic samples are exposed to exciting light, the intensity of the Chl *a* fluorescence yield follows a reproducible kinetic pattern, known as fluorescence induction, where the quantum yield of Chl *a* fluorescence mirrors the

quantum yield of photosynthesis (Papageorgiou 2012). Minimum fluorescence yield (F_O) reflects a physical state in which Q_A is oxidized and all PSII reaction centres are "open" (P680 Pheo Q_A Q_B) (Figure 1.5). Functionally, this is achieved by dark adaption (20 to 30 minutes) which results in oxidation of Q_A as well as intersystem electron transport carriers. Following the transfer of photosynthetic material into the light, an increase in Chl *a* fluorescence yield occurs. Once PSII absorbs a photon of light and Q_A accepts an electron, it is not able to accept another electron; thus the reaction centre is said to be closed ($P680^+$ Pheo Q_A^- Q_B). A strong, extremely brief saturating pulse sufficient to close all PSII reaction centres allows for measurement of the maximum fluorescence in the dark-adapted state (F_M) (Figure 1.5).

The difference between F_M and F_O is termed the variable fluorescence (F_V). F_V/F_M provides a measure of the maximum photochemical efficiency of PSII which provides a sensitive indicator of photosynthetic performance. F_V/F_M is calculated as:

$$\frac{F_V}{F_M} = \frac{F_M - F_O}{F_M}$$

When photosynthetic material is transferred from darkness to light, PSII reaction centres are progressively closed causing an increase in fluorescence within the first second of illumination. The fluorescence yield then progressively falls on a timescale of minutes, a process termed fluorescence quenching. The quenching of Chl *a* fluorescence is due to oxidation of Q_A by intersystem electron transport and PSI as well as an increase in the efficiency in which excitation energy is converted to heat. The principle mechanism to explain fluorescence quenching is an increase in the rate at which electrons are transported away from PSII through intersystem electron transport due to the light-induced activation of enzymes involved in carbon metabolism; this is termed photochemical quenching (qP) (Maxwell and Johnson 2000, Papageorgious 2012). Concomitantly, there is an increase in the efficiency to convert excitation energy to heat; this is termed nonphotochemical quenching (qN or NPQ) (Maxwell and Johnson 2000, Papageorgious 2012).

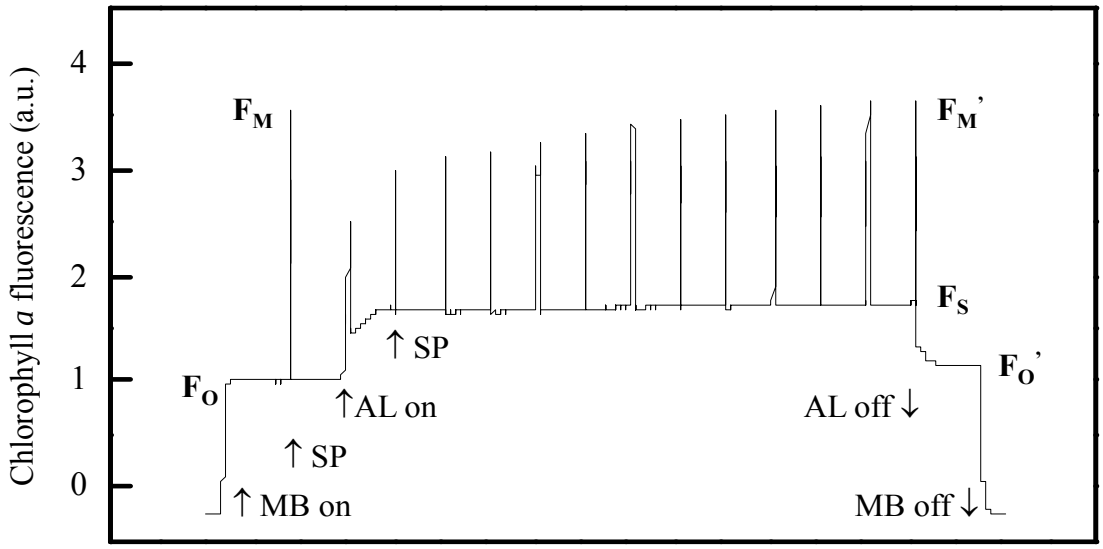

Figure 1.5 Pulse amplitude modulated (PAM) chlorophyll *a* fluorescence induction trace for *Chlorella vulgaris* grown at 28 °C and 150 µmol photons m^{-2} sec^{-1}. Cells were dark adapted for 15 minutes prior to measurement to oxidize Q_A and open all photosystem II reaction centres. Minimal fluorescence of open PSII reaction centres in the dark-adapted state (F_O) was determined using a weak measuring beam (MB) to ensure fluorescence from the antenna was not due to photochemistry. A saturating pulse (SP) of white light was applied for 800 ms to ensure complete reduction of Q_A to measure the maximum fluorescence of closed PSII reaction centres in the dark-adapted state (F_M). Continuous actinic light (AL) was subsequently applied. Steady-state fluorescence (F_S) was determined at the actinic light intensity. Maximum fluorescence in the light-adapted state (F_M') was determined by superimposing a saturating pulse every 30 seconds for five minutes. Minimum fluorescence in the light-adapted state (F_O') was measured following removal of the actinic light.

Following illumination with a constant actinic light, the fluorescent yield rapidly increases before a gradual decrease to a steady-state level (F_S) (Figure 1.5). Following illumination with the actinic light, saturating flashes of light can be used to determine the fluorescence yeild of closed PSII reaction centres in a light-adapted state (F_M') (Figure 1.5). Once the actinic light is removed, the minimum fluorescence of open PSII reaction centres in a light-adapted state (F_O') is determined (Figure 1.5). These parameters can be used to determine the proportion of photochemical (qP) and nonphotochemical (qN) quenching of the fluorescence yield as follows:

$$qP = \frac{F_M' - F_S}{F_M' - F_O'}$$

and

$$qN = 1 - \frac{F_M' - F_O'}{F_M - F_O}$$

The parameter qP is a measure of the relative oxidation state of Q_A and estimates the proportion of open PSII reaction centres. Alternatively, 1 - qP measures the relative proportion of reduced Q_A and the proportion of closed PSII reaction centres. Therefore, 1 - qP provides a measure of the reduction state of Q_A and has been used to estimate the excitation pressure on PSII which reflects the reduction state of the intersystem electron transport chain (Hüner et al. 1998).

Hendrickson et al. (2004) define the proportion of absorbed photons used to drive PSII photochemistry and intersystem photosynthetic electron transport as the quantum efficiency of photochemistry (Φ_{PSII}) and expressed in fluorescence terms as:

$$\Phi PSII = 1 - \frac{F_S}{F_M'}$$

The sum fractions of absorbed light energy lost constitutively as heat through thermal dissipation (Φ_D) and through fluorescence (Φ_f) is expressed as:

$$\Phi f, d = \frac{F_S}{F_M}$$

The proportion of light absorbed by the PSII antenna dissipated as heat through ΔpH and/or xanthophyll-dependent thermal dissipation is expressed as:

$$\Phi NPQ = \frac{F_S}{F_M'} - \frac{F_S}{F_M}$$

1.6 *Chlorella vulgaris*

Green algae represent a diverse group of oxygenic photosynthetic organisms named for their typical bright green colour. Together with terrestrial plants, green algae form a monophyletic group (Yoon et al. 2008). Green algae share chloroplasts containing Chl *a* and *b* as well as rigid cell walls with terrestrial plants. Body organization ranges from simple sphere shaped unicells, such as seen in *C. reinhardtii* or *C. vulgaris*, or complex multicellular forms with defined tissue-type, as in the *Charalas*.

The genus *Chlorella*, of the class Trebouxiophyceae, is part of the chlorophyta along with *C. reinhardtii* and *D. salina*, although these species belong to the class Chlorophycea. Characteristic of the Trebouxiophyceans, *Chlorella* occurs in freshwater and terrestrial habitats (Graham et al. 2009). *Chlorella* are small coccoid cells containing a single cup-shaped plastid and reproduce asexually by autospores (Graham et al. 2009).

Asexual reproduction by multiple fission in green algae has been suggested to be an adaptation to a naturally occurring light environment characterized by light:dark cycles such that the light period is maximally exploited to drive photoautotrophic growth (Bišová and Zachleder 2014). Division by multiple fission, such that each mother cell gives rise to 2^n daughter cells, where n is an integer between 1 and 10, is shared among the chlorophyta (Kirk 1998).

A common cell cycle consists of a growth phase (G_1 phase), followed by ena DNA replication (or synthesis) phase (S phase), a secondary growth phase (G_2 phase) and mitosis (M phase) which is closely followed by cellular division. Mitchison (1971)

proposed that this cycle proceeds as two coordinated events consisting of growth (G_1 phase) and a reproductive replication-division sequence composed of DNA replication, the G_2 growth phase and nuclear division (M phase) closely followed by cytokinesis. Alternative models suggest that progression of the cell cycle from the major growth phase to a reproductive mode characterized by the DNA replication and cellular division sequence is initiated either by signals generated by the circadian clock (Edmunds and Adams 1981, Homma and Hastings 1989, Makarov et al. 1995, Lüning et al. 1997) or following attainment of a critical point marked by the acquirement of some critical cellular volume (Vítová et al. 2011a, Vítová et al. 2011b, Bišová and Zachleder 2014).

1.7 Thesis objectives

In nature, photoautotrophic organisms are exposed to sudden shifts in the light environment due to changes in canopy cover, cloud cover and vertical mixing within a column of water as well as longer term, sustained changes in light exposure on both daily and seasonal timescales. However, previous studies on acclimation to excitation pressure in green algae have been conducted under constant growth light (Maxwell et al. 1994, Maxwell et a. 1995a, Wilson et al. 2000, Wilson and Hüner, 2003). The aim of this thesis is to address the role of excitation pressure in the regulation of photoacclimation and phenotypic plasticity in *C. vulgaris* in response to growth under a variable light environment by addressing the following questions:

1. Do the yellow-green HEP-acclimated cells of *C. vulgaris* exhibit greening in response to dark relaxation of HEP?

The yellow-green HEP phenotype in *C. vulgaris* can revert to the dark green LEP phenotype upon a shift from low growth temperature (5 °C) to warm temperatures (28 °C) with no change in irradiance (Wilson and Hüner 2000). In addition to thermodynamic relaxation of excitation pressure, PSII can be similarly be released from HEP by a decrease in irradiance at a constant temperature. I hypothesized that if excitation pressure is the sole regulator of photoacclimation in *C. vulgaris*, cells acclimated to continuous high light at 2000 μmol photons m^{-2} sec^{-1}, but subsequently released from high PSII

excitation pressure by a shift to darkness, should undergo a phenotypic reversion from the yellow-green HEP phenotype to the dark green LEP phenotype as excitation pressure is predicted to be minimal in darkness.

2. What is the effect of photoperiod on photoacclimation to excitation pressure in *C. vulgaris* with respect to σ_{PSII}?

In green algae, the ability to mimic photoacclimation and a yellow-green phenotype with HL, LT or inhibitors of PET have originally indicated PSII excitation pressure is the primary sensor governing photoacclimation and phenotype (Maxwell et al. 1994, Maxwell et al. 1995a, Maxwell et al. 1995b, Hüner et al 1998, Wilson and Hüner 2000, Wilson et al. 2003). However, these studies have been limited to growth of cell cultures under continuous light. During growth and development under alternating light:dark cycles, PSII excitation pressure should relax during the daily dark period as the absence of light will negate the photochemical closure of the PSII reaction centres. If excitation pressure is the sole regulator of photoacclimation and therefore phenotype, I hypothesized that cultures of *C. vulgaris* should photoacclimate in response to the steady-state excitation pressure during of the light period regardless of the length of the photoperiod.

3. What is the effect of growth under various photoperiods on the growth characteristics of *C. vulgaris*?

It has previously been demonstrated that *C. vulgaris* demonstrates minimal capacity to adjust either exponential growth rates or photosynthetic carbon metabolism in response to a range of continuous growth light intensities (Savitch et al. 1996, Wilson and Hüner 2000). In terrestrial plants, growth under continuous light (CL) is associated with a marked decrease in photosynthetic capacity reflecting feedback inhibition of photosynthesis which is alleviated by the introduction of a daily dark period (Stessman et al. 2002,van Gestel et al. 2005, Sysoeva et al. 2010, Velez-Ramirez et al. 2011). I

hypothesized that the insensitivity of exponential growth rates of *C. vulgaris* to growth irradiance is a consequence of growth under CL.

1.8 References

Allahverdiyeva, Y., Suorsa, M., Rossi, F., Pavesi, A., Kater, M.N., Antonacci, A., Tadini, L., Pribil, M., Schneider, A., Wanner, G., Leister, D., Aro, E.M., Barbato, R. & Pesaresi, P. 2013. Arabidopsis plants lacking PsbQ and PsbR subunits of the oxygen-evolving comolex show latered PSII super-complex organization and short-term adaptive mechanisms. *Plant J.* 75:671–684.

Allen, J.F. 2002. Photosynthesis of ATP- Electrons, proton pumps, rotors, and poise. *Cell* 110:273–276.

Allen, J.F., de Paula, W.B., Puthiyaveetil, S. & Nield, J. 2011. A structural phylogenetic map for chloroplast photosynthesis. *Trends Plant Sci.* 16:645–655.

Amunts, A., Drory, O. & Nelson, N. 2007. The structure of a plant photosystem I supercomplex at 3.4 Å resolution. *Nature* 447:58–63.

Amunts, A., Toporik, H., Borovikova, A. & Nelson, N. 2010. Structure determination and improved model of plant photosystem I. *J. Biol. Chem.* 285:3478–3486.

Apel, K. & Hirt, H. (2004). Reactive oxygen species: metabolism, oxidative stress, and signal transduction. *Annu. Rev. Plant Biol.* 55:373–399.

Arnon, D., Allen, M. & Whatley, F. 1954. Photosynthesis by isolated chloroplasts. II. Photosynthetic phosphorylation, the covnersion of light into phosphate bond energy. *J. Am. Chen. Soc.* 76:4325–6329.

Bae, G. & Choi, G. 2008. Decoding of light signals by plant phytochromes and their interacting proteins. *Annu. Rev. Plant Biol.* 59:281–311.

Baker, N.R. 2008. Chlorophyll fluorescence: a probe of photosynthesis in vivo. *Ann. Rev. Plant Biol.* 59:89–113.

Barajas-López, J. de D., Blanco, N.E. & Strand, A. 2013a. Plastid-to-nucleus communication, signals controlling the running of the plant cell. *Biochim. Biophys. Acta* 1833:425–437.

Barajas-López, J. de D., Kremnev, D., Shaikhali, J., Piñas-Fernández, A. & Strand, A. 2013b. PAPP5 is involved in the tetrapyrrole mediated plastid signalling during chloroplast development. *PLoS One* 8:e60305.

Barbrook, A.C., Howe, C.J. & Purton, S. 2006. Why are plastid genomes retained in non-photosynthetic organisms? *Trends Plant Sci.* 11:101–108.

Barkan, A. & Goldschmidt-Clermont, M. 2000. Participation of nuclear genes in chloroplast gene expression. *Biochimie* 82:559–572.

Barkan, A. 2011. Expression of plastid genes: organelle-specific elaborations on a prokaryotic scaffold. *Plant Physiol.* 155:1520–1532.

Bassi, R., Machold, O. & Simpson, D. 1985. Chlorophyll-proteins of two photosystem I preparations from maize. *Carlsberg Res. Commun.* 50:145–162.

Berry, J.O., Yerramsetty, P., Zielinski, A.M. & Mure, C.M. 2013. Photosynthetic gene expression in higher plants. *Photosynth. Res.* 117:91–120.

Bišová, K. & Zachleder, V. 2014. Cell-cycle regulation in green algae dividing by multiple fission. *J. Exp. Bot.* 25:2585–2602.

Boese, S. & Hüner, N. 1990. Effect of growth temperature and temperature shifts on spinach leaf morphology and photosynthesis. *Plant Physiol.* 94:1830–1836.

Bradbeerr, J.W., Atkinson, Y.E., Börner, T. & Hagemann, R. 1979. Cytoplasmic synthesis of plastid polypeptides may be controlled by plastid-synthesised RNA. *Nature* 279:816–817.

Burnap, R. L. 2014. Mass spectroscopy locates the extrinsic proteins of photosystem II. *Proc. Natl. Acad. Sci. U.S.A* 111:4359–4360.

Busch, A., Petersen, J., Webber-Birungi, M.T., Powikrowska, M., Lassen, L.M., Naumann-Busch, B., Nielsen, A.Z., Ye, J., Boekema, E.J., Jensen, O.N., Lunde, C. & Jensen, P.E. 2013. Composition and structure of photosystem I in the moss *Physcomitrella patens*. *J. Exp. Bot.* 64:2689–2699.

Casal, J.J. 2013. Photoreceptor signalling networks in plant responses to shade. *Ann. Rev. Plant Biol.* 64:403–427.

Chen, Y.B., Durnford, D.G., Koblizek, M. & Falkowski, P.G. 2004. Plastid regulation of *Lhcb1* transcription in the chlorophyte alga *Dunaliella tertiolecta*. *Plant Physiol.* 136:3737–3750.

Croce, R., Canino, G., Ros, F. & Bassi, R. 2002. Chromophore organization in the higher-plant photosystem II antenna protein CP26. *Biochemistry* 41:7334–7343.

Dahal, K., Kane, K., Gadapati, W., Webb, E., Savitch, L.V, Singh, J., Sharma, P., Longstaffe, F.J., Grodzinski, B. & Hüner, N.P.A. 2012a. The effects of phenotypic plasticity on photosynthetic performance in winter rye, winter wheat and *Brassica napus*. *Physiol. Plant.* 144:169–188.

Dahal, K., Gadapati, W., Savitch, L., Singh, J. & Hüner, N.P.A. 2012b. Cold acclimation and BnCBF17-over-expression enhance photosynthetic performance and energy conversion efficiency during long-term growth of *Brassica napus*. *Planta* 236:1639–1652.

Demmig-Adams, B. & Adams III, W.W. 1992. Photoprotection and other responses of plants to high light stress. *Ann. Rev. Plant Physiol.Plant Mol. Biol.* 43:599–626.

Demmig-Adams, B. & Adams III, W.W. 2000. Harvesting sunlight safely. *Nature* 403: 371,373–374.

Dietz, K.J., Schreiber, U. & Heber, U. 1985. The relationship between the redox state of Q_A and photosynthesis in leaves at various carbon-dioxide, oxygen and light regimes. *Planta* 166:219–226.

Dietz, K.J. 2008. Redox signal integration: from stimulus to networks and genes. *Physiol. Plant.* 133:459–468.

Diner, B. & Babcock, G. 1996. "Structure, dynamics, and energy conversion efficiency in photosystem II" *In* Ort, D. & Yocum, C. [Eds.] *Oxygenic Photosynthesis: the light reaction*. Kluwer Academic Publishers, Dordrecht, the Netherlands, pp. 213–247.

Edmunds, L.N. & Adams, K.J. 1981. Clocked cell cycle clocks. *Science* 211:1002–1012.

Ensminger, I., Busch, F., & Hüner, N.P.A. 2006. Photostasis and cold acclimation: sensing low temperature through photostasis. *Physiol. Plant.*126:28–44.

Escoubas, J.M., Lomas, M., LaRoche, J. & Falkowski, P.G. 1995. Light intensity regulation of cab gene transcription is signaled by the redox state of the plastoquinone pool. *Proc. Natl. Acad. Sci. U.S.A.* 92:10237–10241.

Estavillo, G.M., Crisp, P.A., Pornsiriwong, W., Wirtz, M., Collinge, D., Carrie, C., Giraud, E., Whelan, J., David, P., Javot, H., Brearley, C., Marin, E. & Pogson, B.J.

2011. Evidence for a SAL1-PAP chloroplast retrograde pathway that functions in drought and high light signalling in Arabidopsis. *Plant Cell* 23:3992–4012.

Estavillo, G.M., Chan, K.X., Phua, S.Y. & Pogson, B.J. 2013. Reconsidering the nature and mode of action of metabolite retrograde signals from the chloroplast. *Front. Plant Sci.* 3:300.

Falkowski, P.G. 1994. The role of phytoplankton photosynthesis in global biogeochemical cycles. *Photosynth. Res.* 39:235–58.

Falkowski, P.G. & Chen, Y.B. 2003. "Photoacclimation of Light Harvesting Systems in Eukaryoic Algae," *In* Green, B.R. & Green, W.W. [Eds.] *Advances in Photosynthesis and Respiration,* Vol. 13, *Light-Harvesting Antennas in Photosynthesis.* Kluwer Academic Publishers, Dordrecht, the Netherlands, pp. 423–447.

Fernandez, A.P. & Strand, A. 2008. Retrograde signalling and plant stress: plastid signals initiate cellular stress responses. *Curr. Opin. Plant Bio.* 11:509–513.

Fey, V., Wagner, R., Brautigam, K. & Pfannschmidt, T. 2005. Photosynthetic redox control of nuclear gene expression. *J. Exp. Bot.* 56:1491–1498.

Fitter, D., Martin, D. & Copley, M. 2002. GLK gene pairs regulate chloroplast development in diverse plant species. *Plant J.* 31:713–727.

Förster, T. 1965. "Delocalized excitation and excitation transfer," *In* Sinanoglu, O. [Ed.] *Modern Chemistry, Instabul Lectures: Part III: Action Quantum of Light and Organic Crystals*. Academic Press, New York, USA, pp. 93–137.

Foudree, A., Aluru, M. & Rodermel, S. 2010. PDS activity acts as a rheostat of retrograde signalling during early chloroplast biogenesis. *Plant Sign. Behav.* 5:1629–1639.

Foyer, C. & Allen, J. 2003. Lessons from redox signalling in plants. *Antioxid. Redox Signal.* 5:3–5.

Fujita, Y., Iwama, Y. & Ohki, K. 1989. Regulation of the size of light-harvesting antennae in response to light intensity in the green alga *Chlorella pyrenoidosa*. *Plant Cell Physiol.* 30:1029–1037.

Gadjieva, R., Axelsson, E., Olsson, U. & Hansson, M. 2005. Analysis of *gun* phenotype in barley magnesium chelatase and Mg-protoporphyrin IX monomethyl ester cyclase mutants. *Plant Physio. Biochem.* 43:901–908.

Gilmore, A. 2001. Xanthophyll cycle-dependent nonphotochemical quenching in photosystem II: mechanistic insights gained from *Arabidopsis thaliana* L. mutants that lack violaxanthin. *Photosynth. Res*. 67: 89–101.

Gorsuch, P.A., Pandey, S. & Atkin, O.K. 2010a. Temporal heterogeneity of cold acclimation phenotypes in *Arabidopsis* leaves. *Plant Cell Environ.* 33:244–258.

Gorsuch, P.A., Pandey, S. & Atkin, O.K. 2010b. Thermal de-acclimation: how permanent are leaf phenotypes when cold-acclimated plants experience warming? *Plant Cell Environ.*33:1124–1137.

Graham, L.E., Graham, J.M. & Wilcox, L.E. 2009. *In* Anderson, R.A. [Ed.] *Algae Second Edition*. Benjamin Cummings, New York , USA.

Gray, G.R., Chauvin, L.P., Sarhan, F. & Hüner, N. 1997. Cold acclimation and freezing tolerance l (A complex interaction of light and temperature). *Plant Physiol.* 114: 467–474.

Green, B., Anderson, J. & Parson, W. 2003. ″Photosynthetic membranes and their light-harvesting antennas,″ *In* Green, B. & Parson, W. [Eds.] *Light -harvesting antennas in Photosynthesis*. Kluwer Academic Publishers, Dordrecht, the Netherlands, pp. 1–28.

Haehnel, W. 1984. Photosynthetic electron transport in higher plants. *Ann. Rev. Plant Physiol.* 35:656–693.

Hasan, S.S., Stofleth, J.T., Yamashita, E. & Cramer, W.A. 2013. Lipid-induced conformational changes within the cytochrome b6f complex of oxygenic photosynthesis. *Biochemistry* 52:2649–2654.

Hassidim, M., Yakir, E., Fradkin, D., Hilman, D., Kron, I., Keren, N., Harir, Y., Yerushalmi, S. & Green, R. M. 2007. Mutations in CHLOROPLAST RNA BINDING provide evidence for the involvement of the chloroplast in the regulation of the circadian clock in *Arabidopsis*. *Plant J.* 51:551–562.

Hendrickson, L., Furbank, R.T. & Chow, W.S. 2004. A simple alternative approach to assessing the fate of absorbed light energy using chlorophyll fluorescence. *Photosynthesis Res.* 82:73–81.

Hirschberg, J. & Chamovitz, D. 1994. "Carotenoids in Cyanobacteria" *In* Bryan, B.A. [Ed.] *The Molecular Biology of Cyanobacteria*, Kluwer Academic Publishers, Dordrecht, the Netherland, pp. 559–579.

Hill, R. & Bendall, F. 1960. Function of the two cytochrome components in chloroplasts: A working hypothesis. *Nature* 186:136–137.

Homma, K. & Hastings, J.W. 1989. Cell growth kinetics, division asymmetry and volume control at division in the marine dinoflagellate *Gonyaulax polyedra*: a model of circadian clock control of the cell cycle. *J. Cell Sci.* 92: 303–318.

Hüner, N.P.A., Öquist, G. & Sarhan, F. 1998. Energy balance and acclimation to light and cold. *Trends Plant Sci.* 3:224–230.

Hüner, N.P.A., Ivanov, A.G., Wilson, K.E., Miskiewicz, E., Krol, M. & Öquist, G. 2002. "Energy sensing and photostasis in photoautotrophs," *In* Storey, K. & Storey, J. [Eds.] *Sensing, Signalling and Cell Adaptations*, Elsevier Science BV, Amsterdam, the Netherlands, pp. 243–255.

Hüner, N.P.A., Öquist, G. & Melis, A. 2003. "Photostasis in plants, green algae and cyanobacteria," *In* Green, B.R. & Green, W.W. [Eds.] *Advances in Photosynthesis and Respiration*, Vol. 13, *Light Harvesting Antennas in Photosynthesis,* Kluwer Academic Publishers, Dordrecht, the Netherlands, pp. 401–421.

Hüner, N.P.A, Bode, R., Dahal, K., Hollis, L., Rosso, D., Krol, M. & Ivanov, A.G. 2012. Chloroplast redox imbalance governs phenotypic plasticity: the "grand design of photosynthesis" revisited. *Front. Plant Sci.* 3:255.

Hurry, V.M., Malmberg, G., Gardestrom, P. & Öquist, G. 1994. Effects of a short-term shift to low temperature and of long-term cold hardening on photosynthesis and ribulose-1, 5-bisphosphate carboxylase/oxygenase and sucrose phosphate synthase activity in leaves of winter rye (*Secale cereale* L). *Plant Physiol.* 106:983–990.

Hurry, V.M., Strand, A., Tobiaeson, M., Gardestrom, O. & Öquist, G. 1995. Cold hardening of spring and winter wheat and rape results in differential effects on growth, carbon metabolism, and carbohydrate content. *Plant Physiol* 109:697–706.

Jansson, S. 1999. A guide to the *Lhc* genes and their relatives in *Arabidopsis*. *Trends Plant Sci.* 4:236–240.

Jarvis, P. & Lopez-Juez, E. 2013. Biogenesis and homeostasis of chloroplasts and other plastids. *Nat. Rev. Mol. Cell Biol.* 14:787–802.

Jiao, Y., Lau, O.S. & Deng, X.W. 2007. Light-regulated transcriptional networks in higher plants. *Nat.Rev. Genet.*8:217–230.

Jung, H.S. & Chory, J. 2010. Signalling between chloroplasts and the nucleus: can a systems biology approach bring clarity to a complex and highly regulated pathway? *Plant Physiol.* 152:453–459.

Junge, W., Lill, H. & Engelbrecht, S. 1997. ATP synthase: an electrochemical ransducer with rotatory mechanics. *Trends Biochem. Sci.* 22:420–423

Kargul, J., Nield, J. & Barber, J. 2003. Three-dimensional reconstruction of a light-harvesting complex I-photosystem I (LHCI-PSI) supercomplex from the green alga *Chlamydomonas reinhardtii*. Insights into light harvesting for PSI. *J. Biol. Chem.* 278:16135–16141.

Karpinski, S., Reynolds, H., Karpinska, B., Wingsle, G., Creissen, G. & Mullineaux, P. 1999. Systemic signalling and acclimation in response to excess excitation energy in *Arabidopsis*. *Science* 284:654–657.

Ke, B. 2001. "Photosytem I - introduction," *In* Govindjee [Ed.] *Advances in Photosynthesis and Respiration,* Vol. 10*,* Kluwer Academic Publishers, Dordrecht, the Netherlands, pp. 419–430.

Keeling, P.J. 2010. The endosymbiotic origin, diversification and fate of plastids. *Philos. Trans. R. Soc. Lond. B. Biol. Sci.* 265:729–728.

Kianianmomeni, A. & Hallmann, A. 2014. Algal photoreceptors: in vivo functions and potential applications. *Planta* 239:1–26.

Kirk, D.L. 2008. Volvox. *Curr. Biol.* 14:599–600.

Kobayashi, K., Baba, S., Obayashi, T., Sato, M., Toyooka, K., Kerana, M., Aro, E.M., Fukaki, H., Ohta, H., Sugimoto, K. & Masuda, T. 2012. Regulation of root greening by light and auxin/cytokinin signalling in *Arabidopsis*. *Plant Cell* 24:1081-1095.

Koussevitzky, S., Nott, A., Mockler, T.C., Hong, F., Sachetto-Martins, G., Surpin, M., Lim, J., Mittler, R. & Chory, J. 2007. Signals from chloroplasts converge to regulate nuclear gene expression. *Science* 316:715–719.

Kramer, D.M., Johnson, G., Kiirats, O. & Edwards, G.E. 2004. New fluorescence parameters for the determination of QA redox state and excitation energy fluxes. *Photosynth. Res.* 79:209–218.

Król, M., Maxwell, D.P. & Hüner, N.P.A. 1997. Exposure of *Dunaliella salina* to low temperature mimics the high light-induced accumulation of carotenoids and the carotenoid binding protein (Cbr). *Plant Cell Physiol.* 38:213–216.

Kurisu, G., Zhang, H., Smith, J.L. & Cramer, W.A. 2003. Structure of the cytochrome b6f complex of oxygenic photosynthesis: tuning the cavity. *Science* 302:1009–1014.

Lam, E., Ortiz, W. & Malkin, R. 1984. Chlorophyll *a/b* proteins of Photosystem I. *FEBS Lett.* 168*:*10–14.

Larkin, R.M. 2003. "Intracellular signalling and chlorophyll synthesis" *In* Demmig-Adams, B., Demmig, W.W. & Mattoo, A.K. [Eds.] *Photoprotection, Photoinhibition, Gene Regulation and Environment*, Springer, the Netherlands, pp. 289-301.

Larkin, R.M. & Ruckle, M.E. 2008. Integration of light and plastid signals. *Curr.Opin. Plant Biol.* 11:593–599.

Lee, K., Kim, C., Landgarf, F. & Apel, K. 2007. EXECUTER1-and EXECUTER2-dependent transfer of stress-related signals from the plastid to the nucleus of *Arabidopsis thaliana*. *Proc. Natl. Acad. Sci. U.S.A.* 104:10270–10275.

Leonardos, E.D., Savitch, L.V., Hüner, N.P.A., Oquist, G. & Grodzinski, B. 2003. Daily photosynthetic and C-export patterns in winter wheat leaves during cold stress and acclimation. *Physiol. Plant.* 117:521–531.

Lüning, K., Titlyanov, E. & Titlyanova, T. 1997. Diurnal and circadian periodicity of mitosis and growth in marine macroalgae. III. The red alga *Porphyra umbilicalis*. *Eur. J. Phycol*. 32: 167–173.

Makarov, V.N., Schoschina, E.V. & Luning, K. 1995. Dirunal and circadian periodicity of mitosis and growth in marine macroalgae. I. Junvenile sporophytes of Larminariales (Phaeophyta). *Eur. J. Phycol*. 30:261–263.

Masuda, T., Tanaka, A. & Melis, A. 2003. Chlorophyll antenna size adjustments by irradiance in *Dunaliella salina* involve coordinate regulation of *chlorophyll a oxygenase* (*CAO*) and *Lhcb* gene expression. *Plant Mol. Biol.* 51:757–771.

Maxwell, D.P., Falk, S., Trick, C.G. & Hüner, N.P.A. 1994. Growth at low temperature mimics high-light acclimation in *Chlorella vulgaris*. *Plant Physiol.* 105:535–543.

Maxwell, D.P., Falk, S. & Hüner, N.P.A. 1995a. Photosystem II excitation pressure and development of resistance to photoinhibition (I. Light-harvesting complex II abundance and zeaxanthin content in *Chlorella vulgaris*). *Plant Physiol.*107:687–694.

Maxwell, D.P., Laudenbach, D.E. & Hüner, N.P.A. 1995b. Redox regulation of light-harvesting complex II and *cab* mRNA abundance in *Dunaliella salina*. *Plant Physio.* 109:787–795.

Maxwell, K. & Johnson, G.N. 2000. Chlorophyll fluorescence-a practical guide. *J. Exp. Bot*. 51:659–668.

McCormac, A.C., Fischer, A., Kumar, A.M., Soll, D. & Terry, M. J. 2001. Regulation of *HEMA1* expression by phytochrome and a plastid signal during de-etiolation in *Arabidopsis thaliana*. *Plant J.* 25:549–561.

Meskauskiene, R., Nater, M., Goslings, D., Kessler, F., op den Camp, R. & Apel, K. 2001. FLU: A negative regulator of chlorophyll biosynthesis in *Arabidopsis thaliana. Proc. Natl Acad. Sci. U.S.A.* 98:12826–12831.

Minagawa, J. & Takahashi, Y. 2004. Structure, function and assembly of Photosystem II and its light-harvesting proteins. *Photosyn. Res.* 82:241–263.

Miskiewicz, E., Ivanov, A.G., Williams, J.P., Khan, M.U., Falk, S. & Hüner, N.P.A. 2000. Photosynthetic acclimation of the filamentous cyanobacterium, *Plectonema boryanum* UTEX 485, to temperature and light. *Plant Cell Physiol.* 41:767–775.

Miskiewicz, E., Ivanov, A.G. & Hüner, N.PA. 2002. Stoichiometry of the photosynthetic apparatus and phycobilisome structure of the cyanobacterium *Plectonema boryanum* UTEX 485 are regulated by both light and temperature. *Plant Physiol.*130:1414–1425.

Mochizuki, N., Susek, R. & Chory, J. 1996. An intracellular signal transduction pathway between the chloroplast and nucleus is involved in de-etiolation. *Plant Physiol.* 112: 1465–1469.

Mochizuki, N., Tanaka, R., Tanaka, A., Masuda, T. & Nagatani, A. 2008. The steady-state level of Mg-protoporphyrin IX is not a determinant of plastid-to-nucleus signalling in *Arabidopsis*. *Proc. Natl Acad. Sci. U.S.A.* 105:15184–15189.

Moglich, A., Yang, X., Ayers, R.A. & Moffat, K. 2010. Structure and function of plant photoreceptors. *Annu. Rev. Plant Biol.* 61:21–47.

Moulin, M., McCormac, A.C., Terry, M.J. & Smith, A.G. 2008. Tetrapyrrole profiling in *Arabidopsis* seedlings reveals that retrograde plastid nuclear signalling is not due to Mg-protoporphyrin IX accumulation. *Proc. Natl Acad. Sci. U.S.A.* 105:15178–15183.

Mullineaux, P. & Karpinski, S. 2002. Signal transduction in response to excess light: getting out of the chloroplast. *Curr. Opin. Plant Biol.*5:43–48.

Nott, A., Jung, H.S., Koussevitzky, S. & Chory, J. 2006. Plastid-to-nucleus retrograde signaling. *Ann. Rev. Plant Biol.* 57:739–759.

op den Camp, R.G., Przybyla, D., Ochsenbein, C., Laloi, C., Kim, C., Danon, A., Wanger, D., Hideg, E., Göbel, C., Feussner, I., Nater, M. & Apel, K. 2003. Rapid induction of distinct stress responses after the release of singlet oxygen in Arabidopsis. *Plant Cell* 15:2320–2337.

Papageorgiou, G.C. 2012. "Fluorescence emission from the photosynthetic apparatus," *In* Eaton-Rye, J.J., Tripathy, B.B. & Sharkey, T.D. [Eds.] *Advanves in Photosynthesis and Respiration,* Vol. 34*, Photosynthesis: Plastid Biology, Energy Conversion and Carbon Assimilation*. Springer, pp. 415 – 443.

Pfannschmidt, T., Schutze, K., Brost, M. & Oelmuller, R. 2001. A novel mechanism of nuclear photosynthesis gene regulation by redox signals from the chloroplast during photosystem stoichiometry adjustment. *J. Biol. Chem.* 276:36125–36130.

Pogson, B.J., Woo, N.S., Forster, B. & Small, I.D. 2008. Plastid signalling to the nucleus and beyond. *Trends Plant Sci.* 13:602–609.

Pogson, B.J. & Albrecht, V. 2011. Genetic dissection of chloroplast biogenesis and development: an overview. *Plant Physiol.* 155:1545–1551.

Pollock, C. & Cairns, A. 1991. Fructan metabolism in grasses and cereals. *Ann. Rev. Plant Physiol. Plant Mol. Biol.* 42:77–101.

Ramel, F., Birtic, S., Ginies, C., Soubigou-Taconnat, K., Triantaphylides, C. & Havaux, M. 2012. Carotenoid oxidation products are stress signals that mediate gene responses to singlet oxygen in plants. *Proc. Natl Acad. Sci. U.S.A.* 109: 5535–5549.

Rapp, J.C. & Mullet, J.E. 1991. Chloroplast transcription is required to express the nuclear genes *rbcS* and *cab*. Plastid DNA copy number is regulated independently. *Plant Mol. Biol.* 17:813–823.

Reyes-Prieto, A., Weber, A.P.M. & Bhattacharya, D. 2007. The origin and establishment of the plastid in algae and plants. *Annu. Rev. Genet.*41:147–68.

Rochaix, J.D. 2014. Regulation and dynamics of the light-harvesting system. *Annu. Rev. Plant Biol.* 65:287–309.

Ruckle, M.E., DeMarco, S.M. & Larkin, R.M. 2007. Plastid signals remodel light signalling networks and are essential for efficient chloroplast biogenesis in *Arabidopsis*. *Plant Cell* 19:3944–3960.

Ruckle, M.E., Burgoon, L.D., Lawrence, L.A., Sinkler, C.A. & Larkin, R.M. 2012. Plastids are major regulators of light signalling in *Arabidopsis*. *Plant Physiol.* 159: 366–390.

Savitch, L.V., Maxwell, D.P. & Hüner, N. 1996. Photosystem II excitation pressure and photosynthetic carbon metabolism in *Chlorella vulgaris*. *Plant Physiol.* 111:127–136.

Savitch, L.V., Barker-Astrom, A., Ivanov, A.G., Hurry, V. Oquist, G., Hüner, N.P. & Gardesrom, P. 2001. Cold acclimation of Arabidopsis thaliana results in incomplete recovery of photosynthetic capacity, associated with an increased reduction of the chloroplast stroma. *Planta* 2:295–303.

Savitch, L.V, Leonardos, E.D., Krol, M., Grodzinski, B., Hüner, N.P.A. & Öquist, G. 2002. Two different strategies for light utilization in photosynthesis in relation to growth and cold acclimation. *Plant Cell Environ.* 25:761–771.

Shi, L.X., Hall, M., Funk, C. & Schröder, W.P. 2012. Photosystem II, a growing complex: updates on newly discovered components and low molecular mass proteins. *Biochim. Biophys. Acta* 1817:13–25.

Shevela, D., Bjorn, L.O. & Govindjee. 2013. Oxygenic photosynthesis. *Nature* 2:13–64.

Stephenson, P.G., Fankhauser, C. & Terry, M.J. 2009. PIF3 is a repressor of chloroplast development. *Proc. Natl Acad. Sci. U.S.A.* 106:7654–7659.

Stiller, J.W. 2007. Plastid endosymbiosis, genome evolution and the origin of green plants. *Trend Plant Sci.* 12:391–396.

Stitt, M. & Hurry, V. 2002. A plant for all seasons: alterations in photosynthetic carbon metabolism during cold acclimation in *Arabidopsis*. *Curr. Opin. Plant Biol.* 5:199–206.

Strand, Å., Hurry, V., Henkes, S., Hüner, N.P.A., Gustafsson, P., Gardestrom, P. & Stitt, M. 1999. Acclimation of Arabidopsis leaves developing at low temperatures. Increasing cytoplasmic volume accompanies increased activities of enzymes in the Calvin cycle. *Plant Physiol.* 119:1387–1398.

Strand, A., Asami, T., Alonso, J., Ecker, J.R. & Chory, J. 2003. Chloroplast to nucleus communication triggered by accumulation of Mg-protoporphyrinIX. *Nature* 421: 79–83.

Stroebel, D., Choquet, Y., Popot, J.L. & Picot, D. 2003. An atypical haem in the cytochrome b(6)f complex. *Nature* 426:413–418.

Sukenik, A. & Bennett, J. 1990. Adaptation of the photosynthetic apparatus to irradiance in *Dunaliella tertiolecta*: A kinetic study. *Plant Physiol.* 92:891–898.

Sullivan, J.A. & Gray, J.C. 2002. Multiple plastid signals regulate the expression of the pea plastocyanin gene in pea and transgenic tobacco plants. *Plant J.* 32:763–774.

Surpin, M. & Chory, J. 1996. The co-ordination of nuclear and organellar genome expression in eukaryotic cells. *Essays Biochem.* 32:113–125.

Susek, R.E., Ausubel, F.M. & Chory, J. 1993. Signal transduction mutants of *Arabidopsis* uncouple nuclear *CAB* and *RBCS* gene expression from chloroplast development. *Cell* 74:787–799.

Terry, M.J. & Smith, A.G. 2013. A model for tetrapyrrole synthesis as the primary mechanism for plastid-to-nucleus signalling during chloroplast biogenesis. *Front. Plant Sci*. 4:14.

Umena, Y., Kawakami, K., Shen, J.R. & Kamiya, N. 2011. Crystal structure of oxygen-evolving photosystem II at a resolution of 1.9 Å. *Nature* 473:55–60.

van Kooten, O. & Snell, J. 1990. Progress in fluorescence research and nomenclature for quenching analysis. *Photosynth. Res*. 25:147–150.

Vítová, M., Bišová, K., Hlavová, M. & Kawano, S. 2011a. *Chlamydomonas reinhardtii*: duration of its cell cycle and phases at growth rates affected by temperature. *Planta* 234:599-608.

Vítová, M., Bišová, K., Umysová, D. & Hlavová, M. 2011b. *Chlamydomonas reinhardtii*: duration of its cell cycle and phases at growth rates affected by light intensity. *Planta* 233:75–86.

Walters, R.G., Rogers, J.J., Shephard, F. & Horton, P. 1999. Acclimation of *Arabidopsis thaliana* to the light environment: the role of photoreceptors. *Planta* 209:517–527.

Waters, M.T. & Langdale, JA. 2009. The making of a chloroplast. *EMBO J.* 28:2861–2873.

Wilson, K.E. & Hüner, N.P.A. 2000. The role of growth rate, redox-state of the plastoquinone pool and the trans-thylakoid deltapH in photoacclimation of C*hlorella vulgaris* to growth irradiance and temperature. *Planta* 212:93–102.

Wilson, K.E., Krol, M. & Hüner, N.P.A. 2003. Temperature-induced greening of *Chlorella vulgaris*. The role of the cellular energy balance and zeaxanthin-dependent nonphotochemical quenching. *Planta* 217:616–627.

Woodson, J.D. & Chory, J. 2008. Coordination of gene expression between organellar and nuclear genomes. *Nat. Rev. Genet.* 9:383–395.

Woodson, J.D., Perez-Ruiz, J.M. & Chory, J. 2011. Heme synthesis by plastid ferrochelatase I regulates nuclear gene expression in plants. *Curr. Biol.* 21:897–903.

Xiao, Y., Savchenko, T., Baidoo, E.E., Chehab, W.E., Hayden, D.M., Tolstikov, V., Corwin, J.A., Kliebenstein, D.J., Keasling, J.D. & Dehesh, K. 2012. Retrograde signalling by the plastidial metabolite MEcPP regulates expression of nuclear stress-response genes. *Cell* 149:1525–1535.

Yabuta, Y., Maruta, T., Yoshimura, K., Ishikawa, T. & Shigeoka, S. 2004. Two distinct redox signalling pathways for cytosolic APX induction under photooxidative stress. *Plant Cell Physiol.* 45:1586–1594.

Yoon, H.S., Grant, J., Tekle, Y.I., Wu, M., Chaon, B.C., Cole, J.C., Longdon, J.M., Patterson, D.J., Bhattacharya, D. & Katz, L.A. 2008. Broadly sampled multigene trees of eukaryotes. *BMC Evol. Biol.* 8:14.

Zouni, A., Witt, H.T., Kern, J., Fromme, P., Krauss, N., Saenger, W. & Orth, P. 2001. Crystal structure of photosystem II from *Synechococcus elongatus* at 3.8 Å resolution. *Nature* 409:739–743.

Chapter 2

2 RELAXATION OF EXCITATION PRESSURE IN *CHLORELLA VULGARIS* (TREBOUXIOPHYCEAE) IS LIGHT-DEPENDENT: UNCOUPLING OF REDOX REGULATION AND PHENOTYPIC PLASTICITY

2.1 Introduction

Light is required for photoautotrophic metabolism and growth. However, this resource is inherently variable on timescales ranging from seconds to days to months. The structural and functional responses of the photosynthetic apparatus to changes in growth irradiance function to maximize the capacity for light energy harvesting while minimizing the photooxidative damage due to excess light energy absorption. The classical response to high growth light (HL) in green algae is characterized by a reduction in cellular chlorophyll (Chl) content with concomitant decreases in the abundance of the major pigment-binding light-harvesting complex polypeptides (Falkowski and Owens 1980, Fujita et al. 1989, Sukenik et al. 1990, Falkowski and LaRoche 1991, Harrison et al. 1992, Webb and Melis 1995). The xanthophyll cycle is also induced under HL which dissipates excess absorbed light energy nonphotochemically as heat (Demmig-Adams and Adams III 1992, Demmig-Adams and Adams III 2000). These photoacclimation responses function to protect the photosynthetic apparatus from photodamage by decreasing the efficiency of light energy absorption and energy transfer.

While photosynthetic organisms sense changes in the light spectral quality through photoreceptors (Casal 2013, Kianianmomeni and Hallmann 2014), research using photoreceptor mutants (Walters et al. 1999), or those with lesions in the photoreceptor-mediated signal transduction pathways (Fey et al. 2005), indicate that photoreceptors are not required to adjust the structure and function of the photosynthetic apparatus in response to photoacclimation. Rather, the chloroplast, acting as a sensor of light energy

availability, is suggested to function as the major regulator of photosynthetic acclimation (Escoubas et al. 1995, Hüner et al. 1998, Falkowski and Chen 2003, Ensminger et al. 2006, Pogson et al. 2008, Pogson and Albrecht 2011, Estavillo et al. 2013). Therefore, in addition to the traditional role as an energy transducer, the chloroplast also serves a secondary role as a sensor of environmental change (Hüner et al. 1998, Brautigam et al. 2009, Murchie et al. 2009, Hüner et al. 2012, Hüner et al. 2014). Pogson and colleagues distinguish the light quality-dependent, photoreceptor-mediated sensing and signalling pathways required for chloroplast biogenesis and photomorphogenesis as "biogenic" signals and the light energy-dependent signalling pathways mediated by the mature chloroplast required for photosynthetic adjustment during photoacclimation as "operational" signals (Pogson et al. 2008, Albrecht et al. 2011, Pogson and Albrecht 2011, Estavillo et al. 2013).

Studies using the green algae *Chlorella vulgaris* and *Dunaliella* sp. demonstrated that a HL phenotype, characterized by yellow-green pigmentation as well as reduced Chl and photosystem II (PSII) light-harvesting complex polypeptide (LHCII) abundance, can be mimicked by growth at low temperature and moderate irradiance (Maxwell et al. 1994, Escoubas et al. 1995, Maxwell et al. 1995b, Król et al. 1997). The ability to mimic the structural responses to HL with low temperature in green algae has been reconciled by the contention that photosynthetic organisms photoacclimate in response to changes in PSII excitation pressure, a measure of the relative redox state of quinone A (Q_A), as opposed to either HL or low temperature *per se* (Maxwell et al. 1994, Hüner et al. 1998).

Since light energy absorption and subsequent utilization in metabolism, respiration and growth integrates extremely fast, temperature-independent photochemistry with relatively slower, temperature-dependent oxidation of intersystem electron transport components and reduction of carbon dioxide, the reduction state of Q_A can be modulated in a similar fashion by either growth temperature or light (Hüner et al. 1998). Thus, modulation of excitation pressure represents a proxy for changes in the redox state of the PQ pool and other components of the photosynthetic intersystem electron transport chain. Excessive excitation energy can be placed on PSII whenever the rate of light energy absorption

exceeds the capacity to consume this energy through metabolism and growth and/or dissipate excess energy as heat through the xanthophyll cycle and nonphotochemical quenching (NPQ).

High light most obviously increases the degree of excitation pressure on PSII as the increased photon flux rate increases the rate of Q_A reduction relative to its rate of oxidation by the PQ pool and photosystem I (PSI). While low temperature does not affect the capacity for light energy absorption, low temperature causes a similar over-reduction of Q_A since low temperature decreases the rate at which Q_A is oxidized through the PQ pool and intersystem electron transport, carbon fixation, metabolism and growth due to restrictions in the rates of temperature-sensitive enzyme catalyzed reactions (Maxwell et al. 1994, Hüner et al. 1998). Excitation pressure is a measure of the proportion of closed PSII reaction centres and can be estimated *in vivo* by the Chl *a* fluorescence parameter, 1 - qP (Dietz et al. 1985, Hüner et al. 1998), a measure of the relative redox state of Q_A of PSII which reflects the reduction state of the intersystem electron transport chain.

In green algae, the use of chemical inhibitors of photosynthetic electron transport indicate that the primary sensor governing Chl and LHCII abundance is the redox state of the plastoquinone (PQ) pool (Escoubas et al. 1995, Wilson and Hüner 2000). Application of 3-(3,4-dichlorophenyl)-1,1-dimethylurea (DCMU) to cell cultures of either *C. vulgaris* or *D. tertiolecta* mimics the dark green low excitation pressure (LEP) phenotype characterized by relatively high Chl per cell and a typical Chl a/b ratio of about 3.0 with concomitantly high levels of *Lhcb2* expression and Lhcb2 polypeptide abundance (Escoubas et al. 1995, Wilson and Hüner, 2000, Wilson et al. 2003). DCMU blocks the transfer of electrons from PSII to the PQ pool keeping the PQ pool oxidized in the light; therefore, DCMU mimics the effects of either low light or moderate temperature on the redox state of the PQ pool.

Treatment with 2,5-dibromo-3-methyl-6-isopropy-1,4-benzoquinone (DBMIB) prevents electrons from exiting the PQ pool keeping the PQ pool in a reduced state in the light; therefore, DMBIB mimics the effects of either HL or low temperature on the redox state

of the PQ pool. Under these conditions, green algae exhibit a yellow-green high excitation pressure (HEP) phenotype characterized by relatively lower Chl per cell and a higher Chl a/b ratio with reduced *Lhcb2* expression and Lhcb2 polypeptide abundance (Escoubas et al. 1995, Wilson and Hüner, 2000, Wilson et al. 2003). However, the report by Piippo et al. (2006) has challenged the role of the PQ pool in the regulation of nuclear-encoded photosynthetic genes in *Arabidopsis thaliana*.

Photosynthetic organisms are in photostasis when light-induced photochemistry is balanced against the capacity to consume absorbed light energy through metabolism and growth and/or dissipate excess energy as heat (Hüner et al. 2003). Under these conditions, the PQ pool remains oxidized and the cells exhibit a normal, dark green LEP phenotype (Maxwell et al. 1994, Wilson and Hüner 2000). However, environmental stress including HL, low temperature or any stress which inhibits the ability to consume energy through metabolism and growth will upset photostasis due to imbalances between photochemistry and the capacity for cellular energy use. Under these conditions, excitation pressure increases, the PQ pool becomes reduced and the cells develop a yellow-green HEP phenotype (Maxwell et al. 1994, Wilson and Hüner 2000).

The plasticity of this yellow-green HEP phenotype is observed when *C. vulgaris* cells are transferred from a low temperature (5 °C) to a moderate temperature (27 °C) at constant irradiance (Wilson and Hüner 2000). Following the increase in temperature the cells undergo a phenotypic reversion from the yellow-green HEP phenotype to the dark green LEP phenotype; greening of HEP cells reflects the accumulation of Chl and LHCII polypeptides with concomitant decreases in the Chl a/b ratio as Chl *b* accumulates (Wilson and Hüner 2000, Wilson et al. 2003). The change in phenotype without a change in light intensity precludes the contribution of light specific sensors.

The phenotypic reversion from the yellow-green HEP phenotype to dark green LEP phenotype can be blocked or enhanced by treatment with either DBMIB or DCMU, respectively, suggesting that the redox state of the PQ pool is the primary sensor and source of signals regulating photosynthetic acclimation and therefore phenotype in *C.*

vulgaris (Hüner et al. 1998, Wilson et al. 2003, Ensminger et al. 2006). In addition to thermodynamic relaxation of PSII excitation pressure, PSII can similarly be released from HEP by a decrease in irradiance at a constant temperature. I hypothesized that if the relative redox state of the PQ pool is the sole regulator of LHCII antenna size and phenotype in *C. vulgaris*, cells acclimated to continuous HL, but subsequently released from high PSII excitation pressure through oxidation of the PQ pool by a shift to darkness, should undergo a phenotypic reversion from the yellow-green HEP phenotype to the dark green LEP phenotype as Chl and LHCII accumulate. Furthermore, I predicted a positive linear relationship between modulation of 1 - qP by light intensity and the Chl a/b ratio, used as a proxy for phenotypic reversion, with the lowest Chl a/b ratio observed in darkness where 1 - qP is minimal.

2.2 Methods

2.2.1 Culture conditions

Cultures of *Chlorella vulgaris* Beijerinck (UTEX 265) were grown axenically in Bold's basal media (Nichols and Bold 1965) modified according to Maxwell et al. (1994). Cultures were grown as batch cultures in 400 mL Photobioreactor cultivation vessels (Photon System Instruments, Hogrova, Czech Republic) and aerated with sterile, humidified air. The temperature and light regimes were regulated by the Photobioreactor control system (Photon System Instruments, Hogrova, Czech Republic) which maintained a temperature of 28 °C and continuous light intensities of either 150 µmol photons m^{-2} sec^{-1} or 2000 µmol photons m^{-2} sec^{-1}. Growth light was supplied by an equal combination of red and blue light emitting diodes integrated into the Photobioreactor system (Photon System Instruments, Hogrova, Czech Republic).

2.2.2 Low light shift experiments

Cultures of *C. vulgaris* were grown to mid-log phase at 28 °C / 2000 µmol photons m^{-2} sec^{-1} were then shifted to either 0 (darkness), 10, 25, 50, 75, 110, 150 or 300 µmol photons m^{-2} sec^{-1} at a constant temperature of 28 °C. During the low light shift, the temperature and light regimes were maintained by the Photobioreactor control system

(Photon System Instruments, Hogrova, Czech Republic). Following the low light shift, oxygen evolution, chlorophyll content and room temperature chlorophyll *a* fluorescence were measured as a function of time.

2.2.2.1 Low light shift experiments in the presence of DCMU and DBMIB

Cultures were shifted from 28 °C / 2000 µmol photons m^{-2} sec^{-1} to 110 µmol photons m^{-2} sec^{-1} at 28 °C in the presence of either 1.0 µM DCMU 3-(3,4-dichlorophenyl)-1,1-dimethylurea or 10 µM DBMIB (2,5-dibromo-3-methyl-6-isopropy-1,4-benzoquinone) according to Wilson et al. (2003). The inhibitors were both dissolved in 95% (v/v) ethanol (Wilson et al. 2003). Following the low light shift in the presence of electron transport inhibitors, chlorophyll content and room temperature chlorophyll *a* fluorescence were measured as a function of time.

2.2.3 Chlorophyll content

Total chlorophyll content and the chlorophyll a/b ratio were calculated as previously described (Maxwell et al. 1994). Pigments were extracted in 90% acetone (v/v) using a Mini-beadbeater (BioSpec, Bartleville, USA) and chlorophyll content was calculated according to the equations of Jeffery and Humphrey (1975). To determine the chlorophyll content on a per cell basis, cells were counted using a Neubauer hemocytometer.

2.2.4 Oxygen evolution

Measurements of oxygen evolution and consumption were preformed on 1.5 mL of stirred samples at 28 °C in the presence of 5 mM $NaHCO_3$ at a series of light intensities between 0 and 600 µmol photons m^{-2} sec^{-1}. Photosynthetic rates were normalized on a per cell basis. Measurements were performed using a DW2 oxygen electrode with a LH11/R light probe controlled by the OxyLab control unit and data were collected using the OxyLab 32 v.1.15 software (Hansatech Instruments, King's Lynn, UK).

The light saturation parameter, E_k (µmol photons m^{-2} sec^{-1}) was calculated according to Talling (1957) as $E_k = P_{max} / \alpha$ where P_{max} is the maximum light-saturated, carbon dioxide-saturated rate of oxygen (O_2) evolution (mg O_2 mL^{-1} h^{-1}) and α is the maximum slope of the oxygen-evolution under light limiting conditions (mg O_2 mL^{-1} h^{-1} (µmol photons m^{-2} sec^{-1})$^{-1}$). According to the model of phytoplankton growth the parameter E_k is directly linked to the redox state of the PQ pool (Geider et al. 1996, Geider et al. 1998).

2.2.5 Sodium dodecyl sulfate-polyacrylamide gel electrophoresis (SDS-PAGE) and immunoblotting

Samples were collected during mid-log phase, centrifuged at 5,000 x g for 5 min at 4 °C, frozen with liquid nitrogen and stored at -80 °C. The resulting pellet was thawed on ice, re-suspended in 1.5 mL cold 90% (v/v) acetone and disrupted using a Mini-beadbeater (BioSpec, Bartlesville, USA). The supernatant was collected and centrifuged at 16,100 x g for 5 min at 4 °C. The resulting pellet containing total cell protein was washed with distilled water.

The pellet containing the total polypeptide constituent was solubilized at 37 °C with 4% (v/v) solubilization buffer [60 mM Tris-HCl (pH 6.8), 1% (v/v) glycerol and 4% (w/v) sodium dodecyl sulfate] to a 1:4 ratio of protein:sodium dodecyl sulfate. Protein concentration was determined using a Pierce BCA protein assay system following the specifications provided by the manufacturer (Thermo Scientific, Rockford, USA).

Prior to electrophoresis, samples containing 20 µg of protein were mixed with an equal volume of loading dye [13% (v/v) glycerol and 0.5% (w/v) bromophenol blue, 1% DTT], heated at 80 °C for 4 min then centrifuged at 16,100 x g for 1 min. Electrophoresis was performed using the discontinuous buffer system as described by Laemmli (1970) with a 5% (w/v) stacking gel and a 15% (w/v) resolving gel containing 6 M urea using a Mini-protein II apparatus (Bio-Rad, Hercules, USA) for approximately 3 h at 75 V.

The separated polypeptides were either stained [0.2% (w/v) Coomassie Blue, 50% (v/v) methanol, 7% (v/v) acetic acid] overnight or electrophoretically transferred to a

nitrocellulose membrane for immunoblotting (Bio-Rad, Hercules, USA) at 5 °C for 1 h at 100 V. Membranes were blocked in block buffer [Tris buffered saline (20mM Tris (pH 7.5), 150mM NaCl), 5% (w/v) milk powder, 0.01% (v/v) Tween 20] overnight at 5 °C then were probed with the following polyclonal primary antibodies from Agrisera (Vännäs, Sweden): Lhca2 (1:2,000 dilution), Lhcb2 (1:5,000 dilution), Lhcbm5 (1:5,000 dilution), psaB (1:4,000 dilution), psbA (1:10,000 dilution) and POR (1:2,000 dilution); as well as Rubisco (1:5,000 dilution), which was generated by Dr. Norman P.A. Hüner and PTOX (1:2,000 dilution), which was obtained from Dr. Steve Rodermel.

Following incubation with horseradish peroxidase conjugated secondary antibodies (Sigma, St. Louis, USA; 1:2,000 dilution) the antibody-protein complexes were visualized using the Amersham Biosciences enhanced chemiluminescence detection system (GE Healthcare, Little Chalfont, UK) and X-ray film (Fugi Film, Tokyo, Japan). The films were imaged and the intensity of the immunoblots were estimated using ImageJ software v1.45 (http://rsbweb.nih.gov/ij/ download.html) following the instructions provided by the manufacturer.

2.2.6 Room temperature chlorophyll *a* fluorescence

Chlorophyll *a* fluorescence measurements were performed in a temperature controlled, stirred cuvette using a XE-PAM (pulse amplitude modulated) fluorometer (XE-PAM GDEB0146; Heinz Walz, Effeltrich, Germany) with an optical unit (ED-101US/M), a photodiode detector unit (XE-PD) and a PAM data acquisition system (PDA-100). Temperature was maintained at 28 °C through the use of a temperature control unit (US-T/R). Samples were dark acclimated for 15 min in the presence of 5 mM $NaHCO_3$ prior to all measurements. Minimum fluorescence of open PSII reaction centres (F_O) was determined using a non-actinic modulated measuring beam (0.12 µmol photons m^{-2} sec^{-1}) supplied by a xenon flash lamp (XE-MF) with a BG-39 blue glass filter (Schott, Mainz, Germany). Maximum fluorescence of open PSII reaction centres (F_M) was determined using a saturating white light pulse (2600 µmol photons m^{-2} sec^{-1}, 800 ms) provided by an actinic/saturation light unit (XE-AL). Steady-state fluorescence (F_S) parameters were determined by irradiating the sample with actinic light either adjusted to the growth

irradiance or the low light shift irradiance with a saturating pulse (2600 µmol photons m^{-2} sec^{-1}, 800 ms) applied every 30 seconds for 5 min to determine the maximum fluorescence in the light (F_M'). Minimum fluorescence in the light (F_O') was determined following removal of the actinic light.

Excitation pressure was calculated as 1 - qP where qP equals (F_M'-F_S)/(F_M'-F_O') and was used as an estimation of the redox state of the PQ pool (Dietz et al. 1985, Hüner et al. 1998, van Kooten and Snell, 1990, Hendrickson et al. 2008). Alternatively, the proportion of reduced Q_A was estimated as 1 - qL where qL equals qP · (F_O/F_S) (Kramer et al. 2004, Baker 2008).

Partitioning of absorbed light energy was calculated according to Hendrickson et al. (2004). Photons absorbed by the PSII antenna allocated to PSII photochemistry and photosynthetic electron transport was calculated as $\Phi PSII = 1 - F_S/F_m'$, regulated ΔpH- and/or xanthophyll-dependent nonphotochemical quenching (NPQ) within the PSII antenna was calculated as $\Phi NPQ = F_S/F_M' - F_S/F_M$ and constitutive nonphotochemical energy dissipation was calculated as $\Phi f,d = F_S/F_M$.

2.2.7 Statistical analysis

The values given throughout are mean ± standard error of the mean (SEM). Paired Student's t-tests were conducted for statistical evaluation of change in chlorophyll content, the redox state of the PQ pool, energy partitioning and oxygen evolution at time 0 h and 24 h during greening at 110 µmol photons m^{-2} sec^{-1}. Student's t-tests were conducted using SPSS version 21. A one-way analysis of variance (ANOVA), followed by a Tukey's Honest Significant Different (HSD) post hoc test, was used to compare the chlorophyll a/b ratio and quantified plastid polypeptide abundance at 24 h following a shift to 100 µmol photons m^{-2} sec^{-1} in the absence or presence of inhibitors of photosynthetic electron transport. The chlorophyll a/b ratio was log transformed as log(chlorophyll a) - log(chlorophyll b) prior to statistical analysis. For statistical evaluation of energy partitioning, ΦNPQ was omitted as all values for one group were close to zero and the data for energy partitioning were sum constrained. Prior to statistical

analysis ΦPSII and Φf,d were log transformed. All ANOVAs were conducted using the statistical software package R version 3.0.2. Data were visually inspected for normality and homogeneity of variance. A value of $p < 0.05$ was considered significant throughout.

2.3 Results

2.3.1 Irradiance-dependent greening of high excitation pressure cells

As shown in Figure 2.1, there was an irradiance-dependence to phenotypic reversion in *C. vulgaris* in contrast to the original prediction that yellow-green HEP cells, acclimated to HL but subsequently released from high PSII excitation pressure by a shift to darkness, should revert to the dark green LEP phenotype. When grown at continuous HL at 28/2000 (°C) / µmol photons m^{-2} sec^{-1}), *C. vulgaris* cells exhibited a typical yellow-green HEP phenotype relative to the dark green LEP phenotype of cells grown under continuous low light at 28/150 (Figure 2.1A). This yellow-green phenotype at 28/2000 was characterized by a relatively high Chl a/b ratio of 6.07 and low cellular Chl content of 180 fg Chl per cell (Figure 2.1A). In contrast, when grown at 28/150, *C. vulgaris* was characterized by an approximately 2-fold lower Chl a/b ratio of 3.32 and 2-fold higher Chl per cell of 375 (Figure 2.1A).

Greening of HEP cells appeared to be inhibited in darkness as well as in dim light; within 24 h of a shift from 28/2000 to either 28/10 or complete darkness the cells remained phenotypically indistinguishable from those acclimated to continuous HEP (Figure 2.1). Consistent with this phenotype, the Chl a/b ratio remained relatively high (Chl a/b = 5.35 at 28/10 and Chl a/b = 5.55 in darkness) while cellular Chl content remained relatively low (fg Chl $cell^{-1}$ = 185 at 28/10 and fg Chl $cell^{-1}$ = 160 in darkness) such that despite 24 h at either 28/10 or in complete darkness the Chl a/b ratio and cellular Chl content remained similar to with values obtained from cells acclimated to continuous HL at 28/2000 (Figure 2.1).

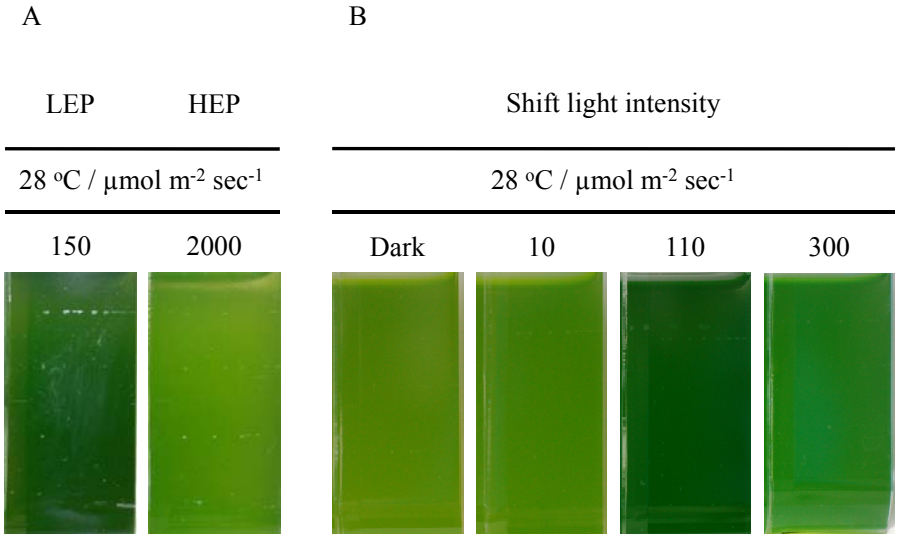

	A		B			
	LEP	HEP	Shift light intensity			
	28 °C / µmol m^{-2} sec^{-1}		28 °C / µmol m^{-2} sec^{-1}			
	150	2000	Dark	10	110	300
Chl a/b	3.32 ± 0.36	6.07 ± 0.48	5.55 ± 0.48	5.35 ± 0.31	3.56 ± 0.36	4.26 ± 0.34
fg Chl $cell^{-1}$	375 ± 77	180 ± 53	160 ± 13	185 ± 17	287 ± 33	204 ± 42

Figure 2.1 (A) Representative pigmentation for *C. vulgaris* grown under continuous low excitation pressure (LEP), at a light intensity of 150 µmol photons m^{-2} sec^{-1}, and continuous high excitation pressure (HEP), at a light intensity of 2000 µmol photons m^{-2} sec^{-1}, at 28 °C. (B) Representative change in pigmentation for cultures of *C. vulgaris* grown to mid-log phase at 2000 µmol photons m^{-2} sec^{-1} then shifted at a constant temperature of 28 °C to either 0 (darkness), 10, 110 or 300 µmol photons m^{-2} sec^{-1}. Phenotype was assayed 24 h following the low light shift. (A,B) Numbers above cultures represent temperature (°C) / growth irradiance (µmol photons m^{-2} sec^{-1}). Numbers under each culture represent either the chlorophyll (Chl) a/b ratio or total cellular Chl content (fg Chl $cell^{-1}$) measured either (A) during mid-log phase grown or (B) 24 h following the shift to low light. Values represent mean ± SEM; n = 3.

A light intensity of 110 μmol photons m^{-2} sec^{-1} was determined to be close to the optimal light intensity for phenotypic reversion from the yellow-green HEP phenotype to the dark green LEP phenotype in *C. vulgaris* based on the magnitude of change in Chl content (Figure 2.1) (Table S2.1 in Supplemental Material). Within 24 h of a shift from 28/2000 to 28/110 the cells were phenotypically indistinguishable from cells acclimated to continuous LEP at 28/150 (Figure 2.1).

The greening response at 28/110 was confirmed by measuring the accumulation of total Chl per cell over time (Figure 2.2A). The change in light regime from 28/2000 to 28/110 was accompanied by an approximate 2-fold increase in Chl per cell ($t_2 = 4.3$, $p = 0.049$) and 2-fold decrease in the Chl a/b ratio ($t_2 = 5.4$, $p = 0.033$) in the first 24 h (Table 2.1). Accumulation of Chl and the decline in the Chl a/b ratio were detected within 2 h of the shift from 28/2000 to 28/110 and by 24 h reached levels consistent with those obtained from cells acclimated to continuous LEP (Figure 2.2A).

When cells were shifted from 28/2000 to 28/110 excitation pressure declined 4.5-fold from 0.761 to 0.164 ($t_2 = 16.2$, $p = 0.004$) (Table 2.1) indicating that PSII was in a more oxidized state following the shift to 28/110. Excitation pressure can be calculated as either 1 - qP (Dietz et al. 1985, Hüner et al. 1998) or 1 - qL (Kramer et al. 2004, Baker 2008); while the absolute values of excitation pressure are dependent on whether the relative redox state of Q_A is estimated as either qP or qL, the trends were independent of the method of calculation (Table S2.2). Therefore, phenotypic reversion from the yellow-green HEP phenotype to the dark green LEP phenotype (Figure 2.1) with a corresponding decrease in the Chl a/b ratio and increase in cellular Chl content at 28/110 was correlated with a relaxation of high PSII excitation pressure as measured as a decrease in 1 - qP (Table 2.1).

Room temperature Chl *a* fluorescence induction was used to determine the functional changes associated with phenotypic reversion at 28/110. Cells either measured immediately prior to the shift to 28/110 (time 0 h) or measured 24 h following the shift to

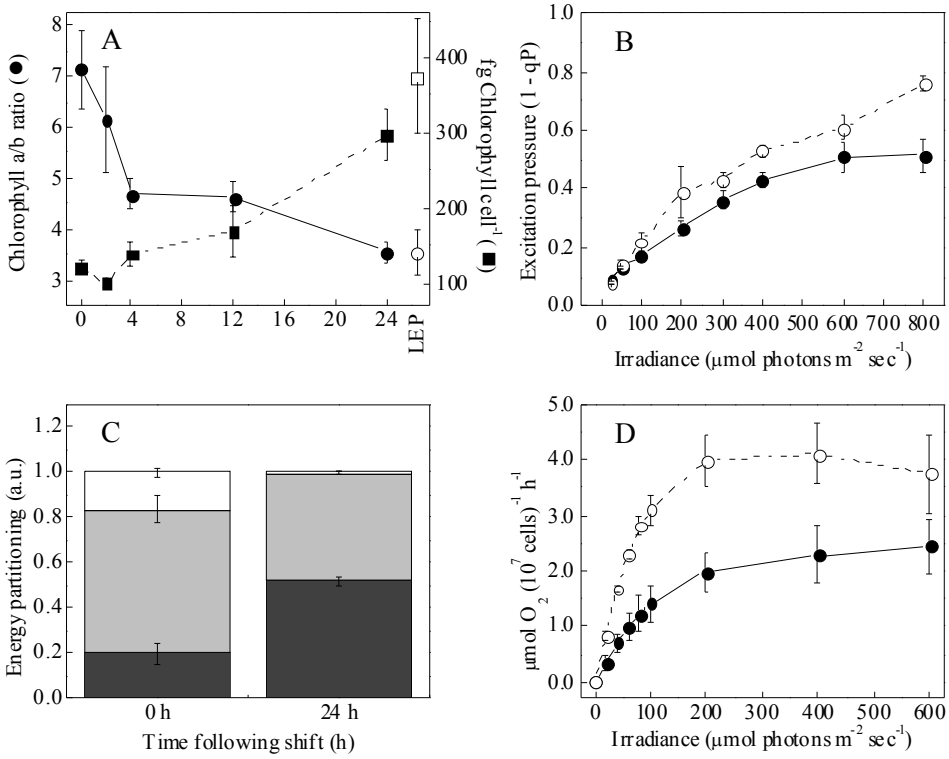
A
Chlorophyll a/b ratio (●)
fg Chlorophyll cell-1 (■)
LEP
B
Excitation pressure (1 - qP)
Irradiance (μmol photons m-2 sec-1)
C
Energy partitioning (a.u.)
0 h
24 h
Time following shift (h)
D
μmol O2 (10^7 cells)-1 h-1
Irradiance (μmol photons m-2 sec-1)

Figure 2.2 Normal greening of high excitation pressure (HEP) cells of *C. vulgaris* at 110 µmol photons m^{-2} sec^{-1}. (A) Change in chlorophyll a/b (●) and total fg chlorophyll per cell (■) during greening of HEP cells compared to the chlorophyll a/b ratio (○) and fg chlorophyll per cell (□) of *C. vulgaris* acclimated to continuous low excitation pressure (LEP). (B) Excitation pressure light response curves for *C. vulgaris* cells following phenotypic reversion. Measurements were taken at 0 h (●) and after 24 h (○) following the transfer to low light as a function of measuring light intensity. (C) Proportion of absorbed light energy consumed through photosystem II photochemistry (ΦPSII; dark gray), fluorescence and constitutive thermal dissipation (Φf,d; light gray) and xanthophyll-dependent thermal dissipation (ΦNPQ; white) during steady-state photosynthesis. (D) Oxygen evolution light response curves for *C. vulgaris*. Measurements were taken at time 0 h (●) and 24 h (○) following the shift to 110 µmol photons m^{-2} sec^{-1}. (A,B,C,D) Values represent mean ± SEM; n = 3.

Table 2.1 Chlorophyll content, steady-state chlorophyll *a* fluorescence and oxygen evolution for *C. vulgaris* grown at 2000 µmol photons m^{-2} sec^{-1} to mid-log phase then shifted at a constant temperature of 28 °C to 110 µmol photons m^{-2} sec^{-1} at time 0 h. Measurements were taken at time 0 h and 24 h following the transfer to low light. Gross oxygen evolution parameters are given on a cell count basis. Excitation pressure measurements were conducted at the growth light intensity at time 0 h and at the shift light intensity at time 24 h. Significant differences between time 0 h and 24 h are indicated by * ($p < 0.05$) and ** ($p < 0.01$). Values represent mean ± SEM; n = 3.

	Time following shift to 110µmol photons m^{-2} sec^{-1}	
	0 h	24 h
F_V/ F_M	0.654 ± 0.0251	0.645 ± 0.0202
Chlorophyll a/b	6.80 ± 0.54	3.56 ± 0.26*
fg chlorophyll $cell^{-1}$	121.0 ± 35.23	287.7 ± 33.45*
Excitation pressure (1 - qP)	0.761 ± 0.0251	0.164 ± 0.0201**
Saturating irradiance (E_K)[a]	159.0 ± 4.04	92.7 ± 4.06**
Photosynthetic capacity[b]	2.13 ± 0.44	4.43 ± 0.27**
Photosynthetic efficiency[c]	0.02 ± 0.003	0.05 ± 0.006*
Respiration[d]	0.83 ± 0.20	0.73 ± 0.15

[a]µmol photons m^{-2} sec^{-1} [b]µmol O_2 evolved $(10^7 \text{ cells})^{-1}$ h^{-1} [c]µmol O_2 evolved $(10^7 \text{ cells})^{-1}$ $(\mu\text{mol photons})^{-1}$ m^2 [d]µmol O_2 consumed $(10^7 \text{ cells})^{-1}$ h^{-1}

28/110 had comparably high PSII photochemical efficiencies (F_V/F_M) indicating neither population of cells were photoinhibited ($t_2 = 0.1$, $p = 0.906$) (Table 2.1). As shown in Figure 2.2B, 1 - qP increased with increasing measuring irradiance in *C. vulgaris* cells measured either at time 0 h (●) or 24 h (○) following a shift from 28/2000 to 28/110 reflecting the accumulation of closed PSII reaction centres. The maximum initial slope of the light response curves in Figure 2.2B provides an estimate of the quantum requirement for PSII closure, that is, the conversion of open PSII reaction centres (P680 Pheo Q_A) to closed reaction centres ($P680^+$ Pheo QA^-). The quantum requirement to close 50% of PSII reaction centres in cells measured immediately prior to the shift to 28/110 at time 0 h (Figure 2.2B, ●) was about 551 μmol photons m^{-2} sec^{-1} which decreased to approximately 275 μmol photons m^{-2} sec^{-1} in *C. vulgaris* cells shifted to 28/110 for 24 h reflecting a higher light sensitivity for PSII reaction centre closure in cells acclimated to 28/110 relative to those acclimated to 28/2000; this is consistent with the contention that the physiological responses to HEP, including reductions in Chl and LHCII abundance, function to decrease the probability of charge separation and subsequent closure of PSII reaction centres. The decreased quantum requirement for PSII reaction centre closure as well as the value of 1 - qP measured at the actinic light intensity (Table 2.1) are consistent with the observation that cells were acclimated to low PSII excitation pressure following the shift from HL to 28/110.

2.3.2 Photosynthesis and energy partitioning

There was a 60% increase in ΦPSII (dark gray) ($t_2 = 17.6$, $p = 0.003$) as well as a 25% decrease in Φf,d (light gray) ($t_2 = 1.2$, $p = 0.048$) and an almost 100% decrease in ΦNPQ (white) (Figure 2.2C) in *C. vulgaris* cells measured 24 h following a shift to 28/110 suggesting a decreased reliance on the capacity to dissipate excess excitation energy as heat through the xanthophyll cycle.

The increase in Chl per cell (Table 2.1) and decreased capacity to dissipate excess light energy as heat through the xanthophyll cycle (ΦNPQ) (Figure 2.2C) in cells shifted from HL to 28/110 for 24 h was reflected in an approximately 2-fold increase in the maximum

rate of CO_2-saturated, light-saturated O_2 evolution when measured on a per cell basis relative to HEP cells at time 0 h ($t_2 = 11.1$, $p = 0.008$) (Table 2.1 and Figure 2.2D,○). Furthermore, cells shifted from 28/2000 to 28/110 for 24 h exhibited a 2.5-fold higher photosynthetic efficiency, calculated as the initial slope of the light-response curve in Figure 2.2D ($t_2 = 5.6$, $p = 0.031$) (Table 2.1). However, no change in the rate of dark respiration was detected ($t_2 = 0.3$, $p = 0.784$) (Table 2.1).

The light-saturation parameter (E_K) is directly proportional to the redox state of the PQ pool (Geider et al. 1996). The almost 2-fold decrease in E_K in cells shifted from 28/2000 to 28/110 for 24 h ($t_2 = 10.5$, $p = 0.009$) is consistent with the detected decrease in 1 - qP and supports the fluorescence data for the relaxation of high PSII excitation pressure at 28/110 (Table 2.1).

2.3.3 Chloroplast polypeptide accumulation

Figure 2.3 shows the change in chloroplast-localized polypeptide composition during low light-induced greening of HEP cells of *C. vulgaris*. Typically, the Chl a/b ratio is inversely related to the abundance of the major Chl-binding LHCII polypeptide abundance (Porra 2005). The accumulation of Chl and decrease in the Chl a/b ratio (Figure 2.2A) during phenotypic reversion at 28/110 was accompanied by an increase in the abundance of the pigment-binding polypeptides Lhcb2 and Lhcbm5 of PSII as well as Lhca2 of PSI (Figure 2.3). While the D1 reaction centre protein of PSII (PsbA) also increased in abundance following the shift from 28/2000 to 28/110, the abundance of the PsaB reaction centre polypeptide of PSI remained relatively unchanged (Figure 2.3). The preferential accumulation of PsbA without an increase in PsaB abundance indicated an increase in the PsbA:PsaB ratio during greening of HEP cells as estimated by total protein complement of the cell. Additionally, there was a rapid increase in the abundance of PTOX, the plastid terminal oxidase (Figure 2.3). However, no noticeable changes in RbcL were detected indicating that not all chloroplast localized polypeptides change in abundance during phenotypic reversion at 28/110 (Figure 2.3).

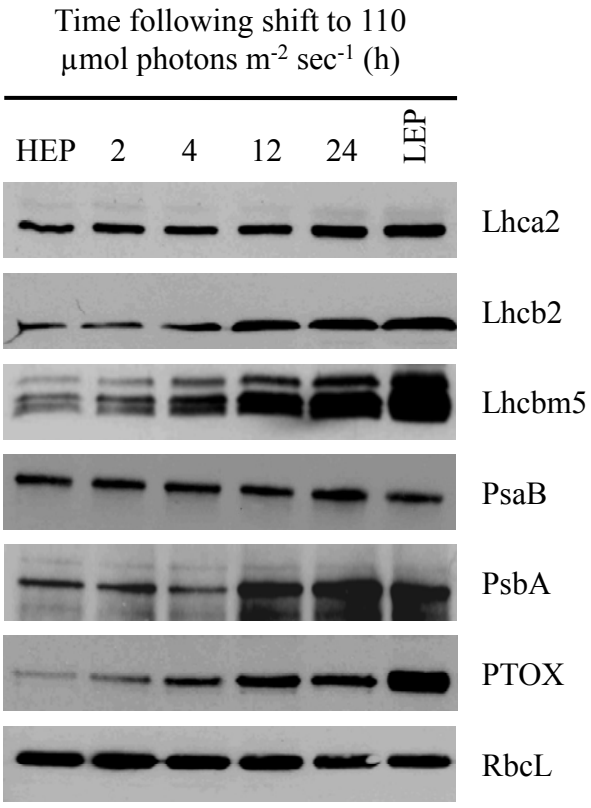

Figure 2.3 Change in chloroplast localized polypeptide during greening of high excitation pressure (HEP) cells of *C. vulgaris*. Representative immunoblots illustrating the change in abundance of light-harvesting complex polypeptides of PSI (Lhca2) and PSII (Lhcb2 and Lhcbm5), reaction centre polypeptide of PSI (PsaB), D1 reaction centre polypeptide of PSII (PsbA), plastid terminal oxidase (PTOX) and the large subunit of Rubisco (RbcL) during phenotypic reversion. Proteins collected as a function of time from cells transferred from HEP (time 0 h) to low light are followed by the whole cell polypeptide complement of cells acclimated to continuous low excitation pressure (LEP) at 28 °C and 150 µmol photons m^{-2} sec^{-1}. Each lane was loaded with 20 µg of protein. Equal loading was confirmed by staining with Coomassie Brilliant Blue (Figure S2.1).

2.3.4 Redox state of the plastoquinone pool regulates greening of high excitation pressure cells

To confirm the contribution of the redox state of the PQ pool in the regulation of PSII antenna size during low light-induced greening of HEP cells, *C. vulgaris* cells were shifted from 28/2000 to the optimal light intensity for phenotypic reversion in the presence of chemical inhibitors of photosynthetic electron transport that alternatively block either the reduction (DCMU) or the oxidation of the PQ pool (DBMIB).

When *C. vulgaris* cells grown at 28/2000 were treated with DCMU prior to the shift to 28/110, the cells greened in a manner phenotypically indistinguishable from untreated cultures (Figure 2.4A). The magnitude of decrease in the Chl a/b ratio at 24 h was similar in DCMU-treated cultures and untreated cells ($F_{2,8} = 9.9$, $p = 0.01$, Tukey's HSD $p = 0.709$) (Figure 2.4B). In contrast, when *C. vulgaris* cells grown at 28/2000 were treated with DBMIB prior to the shift to 28/110, the phenotypic reversion from the yellow-green phenotype to dark green phenotype was inhibited and cells maintained a yellow-green pigmentation visibly indistinguishable from *C. vulgaris* acclimated to continuous HEP (Figure 2.4A). At the end of the 24 h period, there was a minimal decrease in Chl a/b ratio in DBMIB treated cells such that the Chl a/b was significantly higher in DBMIB treated cells (Tukey's HSD $p < 0.05$) (Figure 2.4B).

The approximate 2-fold decrease in the Chl a/b ratio in DCMU treated cells was reflected in the accumulation of Lhcbm5 polypeptides (Figures 2.4B and 2.4C). This accumulation of LHCII polypeptides was similar in magnitude to untreated cells following a shift from continuous HL to 28/110 ($F_{2,8} = 7.9$, $p = 0.021$, Tukey's HSD $p = 0.966$) (Figure 2.4C). Similarly, the increase in PsbA abundance was similar in DCMU-treated and untreated cells ($F_{2,8} = 10.26$, $p = 0.0116$, Tukey's HSD $p = 0.453$) (Figure 2.4C). Changes in Lhcbm5 and PsbA polypeptide abundance were detected within 2 h of the shift to 28/110 in the presence of DCMU (Figure 2.4C). Similar to untreated cells, the abundance of PsaB ($F_{2,8} = 0.2$, $p = 0.823$) and RbcL ($F_{2,8} = 0.9$, $p = 0.456$) at 24 h were not affected by

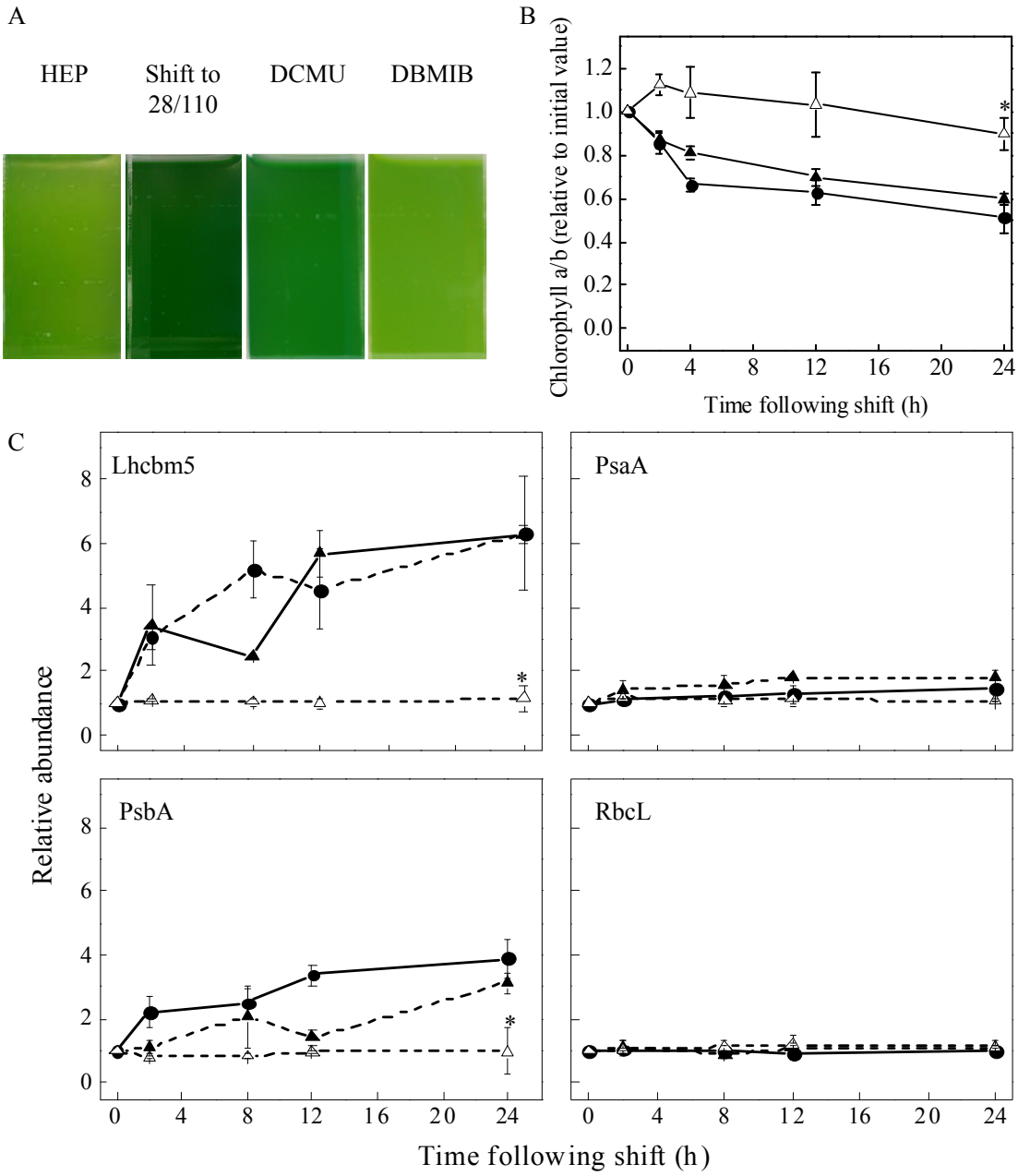
A
HEP
Shift to 28/110
DCMU
DBMIB
B
Chlorophyll a/b (relative to initial value)
Time following shift (h)
C
Lhcbm5
PsaA
PsbA
RbcL
Relative abundance
Time following shift (h)

Figure 2.4 The effect of chemical inhibitors of photosynthetic electron transport on phenotype, chlorophyll a/b ratio and chloroplast-localized polypeptides following a shift from high light to low light. (A) Phenotype was assessed 24 h following the shift to low light in presence of the chemical inhibitors DCMU and DBMIB. (B) Chlorophyll a/b ratios were taken as a function of time following the low light shift at time 0 h in the absence of chemical inhibitors (●) and in the presence of either DCMU (▲) or DBMIB (△). Chlorophyll a/b ratios are presented relative to the initial value measured at time 0 h. (C) Densitometric estimation of the relative abundance of Lhcbm5, PsaB, PsbA and RbcL. Cells were shifted either in the absence of inhibitors (●) and in the presence of either DCMU (▲) or DBMIB (△). Immunoblot films were imaged and the relative density of each band was used to estimate polypeptide abundance; change in polypeptide abundance was taken relative to the abundance of that polypeptide at time 0 h. Each lane was loaded with 20 μg of protein; equal loading was confirmed with Coomassie Brilliant Blue (Figure S2.2). (B,C) Values present mean ± SEM; n = 3. Means at 24 h were compared using an ANOVA followed by a Tukey's HSD post hoc test; means significantly different at $p < 0.05$ are indicated by *.

the change in light regime in DCMU-treated cells (Figure 2.4C). In contrast, the addition of DBMIB inhibited Lhcbm5 and PsbA accumulation in cells shifted from 28/2000 to 28/110 for 24 h such that the abundance of Lhcbm5 (Tukey's HSD $p < 0.05$) and PsbA (Tukey's HSD $p < 0.05$) was significantly lower in DBMIB treated cells (Figure 2.4C). Neither RbcL nor PsaB abundance appeared to be sensitive to DBMIB (Figure 2.4C).

2.3.5 Uncoupling of phenotypic plasticity and redox regulation

A positive linear correlation was detected between the shift light intensity and PSII excitation pressure (1 - qP) measured at the shift light intensity (Figure 2.5A, closed symbols). If PSII excitation pressure was the sole regulator of photoacclimation in *C. vulgaris*, oxidation of the PQ pool at low light (<110 µmol photons m^{-2} sec^{-1}) should be correlated with visible greening of the HEP cells and a decrease in the Chl a/b ratio. Prior to the shift in light intensity, *C. vulgaris* at 28/2000 exhibited a relatively high 1 - qP of 0.650 (Figures 2.5A, □ and S2.4). However, while a shift from 28/2000 to light intensities less than 110 µmol photons m^{-2} sec^{-1} did relax PSII excitation pressure, as measured by a decrease in 1 - qP (Figure 2.5A), there was not a corresponding decrease in the Chl a/b ratio (Figure 2.5B).

Prior to the decrease in light intensity, HEP cells at 28/2000 exhibited a relatively high Chl a/b ratio of 6.07 (Figure 2.5B, □). The lowest Chl a/b ratios of 3.56 and 3.55 were detected when *C. vulgaris* cells acclimated to 28/2000 were transferred to light intensities of either 28/110 or 28/150, respectively (Figure 2.5B, ◀ and ▶). By 24 h at either 28/150 or 28/110 the Chl a/b ratio had decreased to values which were consistent with those measured in cells acclimated to continuous LEP at 28/150 (Chl a/b = 3.32 at 28/150) (Figure 2.5B, compare ○ to ◀ and ▶). Correspondingly, when cells acclimated to 28/2000 were transferred to, and measured at, 28/110 there was a 4-fold decrease in PSII excitation pressure from 0.650 to 0.165 while 1 - qP decreased to 0.255 when cells were shifted to 28/150 (Figures 2.5A and 2.5C, ◀ and ▶).

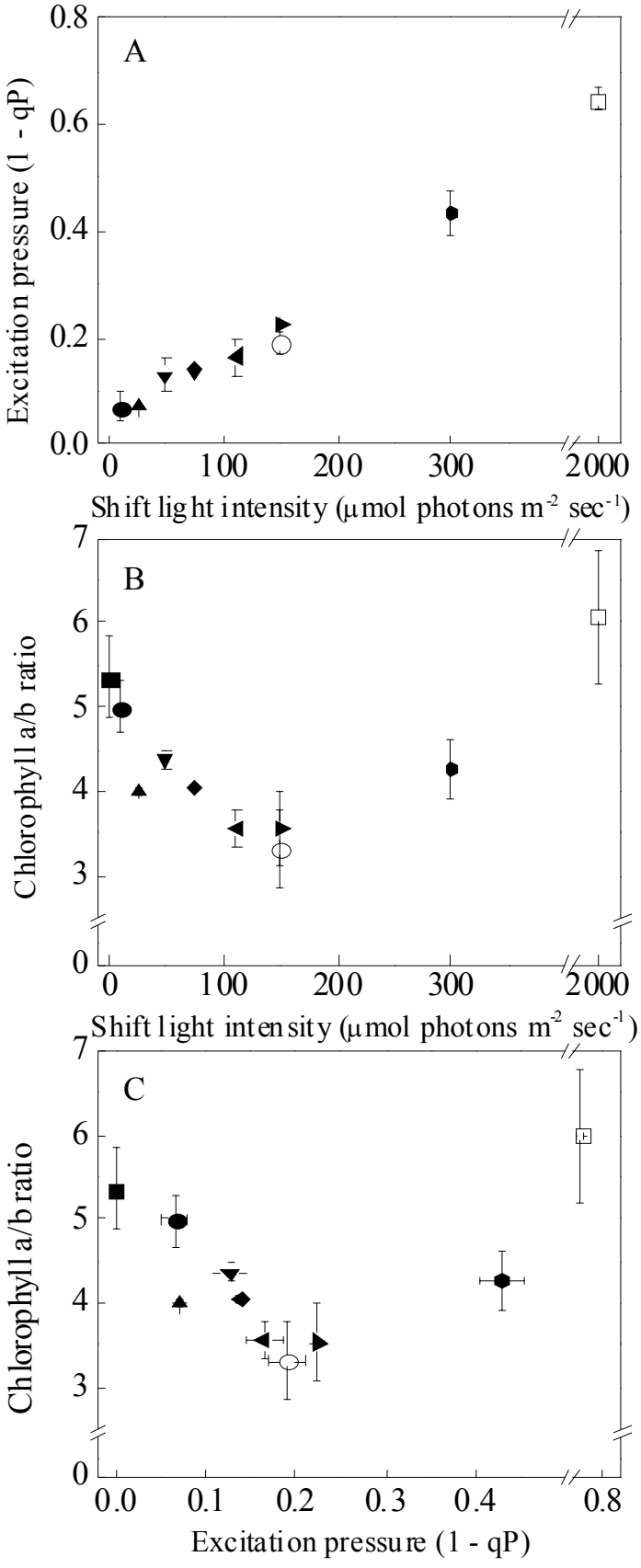
A
Excitation pressure (1 - qP)
0.0
0.2
0.4
0.6
0.8
0
100
200
300
2000
Shift light intensity (µmol photons m-2 sec-1)
B
Chlorophyll a/b ratio
0
3
4
5
6
7
0
100
200
300
2000
Shift light intensity (µmol photons m-2 sec-1)
C
Chlorophyll a/b ratio
0
3
4
5
6
7
0.0
0.1
0.2
0.3
0.4
0.8
Excitation pressure (1 - qP)

Figure 2.5 Change in chlorophyll a/b ratio following a shift from continuous high light to a series of lower light intensities. *Chlorella vulgaris* was grown to mid-log phase under either a low excitation pressure (LEP) growth regime at 28 °C / 150 µmol photons m^{-2} sec^{-1} (25/150; ○) or a high excitation pressure (HEP) growth regime at 28 °C / 2000 µmol photons m^{-2} sec^{-1} (28/2000; □). At time 0 h HEP cells of *C. vulgaris* were shifted to either darkness (0 µmol photons m^{-2} sec^{-1}; ■), 10 (●), 25 (▲), 50 (▼), 75 (◆), 110 (◀), 150 (▶) or 300 µmol photons m^{-2} sec^{-1} (⬢) at 28 °C. (A) Excitation pressure (1 - qP) measurements were conducted at either the shift light intensity 24 h following the transfer from high light to low light or at the growth light intensities for cells grown at 28/150 and 28/2000. (B) Chlorophyll a/b ratios were either measured 24 h following the transfer to a lower light intensity or during mid-log phase growth for cells grown at continuous light at 28/150 and 28/2000. (C) Chlorophyll a/b ratio was measured 24 h following the shift from continuous high light to a series of lower intensities and plotted against the excitation pressure (1 - qP) detected at the shift light intensity. (A,B,C) Values represent mean ± SEM; n = 3.

When *C. vulgaris* was transferred from 28/2000 to light intensities of either 28/150 or 28/110 the HEP cells rapidly greened such that by 24 h at either 28/150 or 28/110 the cells were phenotypically indistinguishable from those acclimated to continuous LEP (Figure 2.1). However, greening of HEP cells appeared to be inhibited at light intensities less than 25 μmol photons m^{-2} sec^{-1} as well as in darkness; within 24 h of a shift from 28/2000 to either 28/10 or 28/0 the cells remained phenotypically indistinguishable from those acclimated to continuous HEP (Figure 2.1). Consistent with this phenotype, the Chl a/b ratio remained relatively high (Chl a/b = 5.35 at 28/10 and Chl a/b = 5.55 in total darkness) such that despite 24 h at either 28/10 or in complete darkness the Chl a/b ratios remained congruent with values obtained from cells acclimated to continuous HEP at 28/2000 (Figure 2.5B, compare □ to ● and ■). However, 1 - qP had decreased from 0.650 to 0.068 when cells were shifted to, and measured at, 28/10 for 24 h indicative of oxidation of the PQ pool and extremely low PSII excitation pressure (Figure 2.5A, ●).

By 24 h following a shift from 28/2000 to either 28/10 or darkness, the yellow-green phenotype and relatively high Chl a/b ratio remained comparable to cells acclimated to continuous HEP despite a measurably low 1 - qP (Figures 2.1 and 2.5C, compare □ to ●). Since we had previously predicted that the cultures would visibly green and exhibit low Chl a/b ratios at either dim light intensities or in darkness due to relaxation of PSII excitation pressure, the failure to green at very low light intensities represented an "uncoupling" between phenotype and the redox state of the PQ pool. The "uncoupling" of 1 - qP and the expected phenotype indicated that the relative redox state of the PQ pool cannot be the sole regulator of phenotype in *C. vulgaris.* There must also exist an irradiance-dependent component to photoacclimation at the level of LHCII and Chl abundance in *C. vulgaris*.

2.3.6 Light-dependent accumulation of protochlorophyllide oxidoreductase

The use of inhibitors of photosynthetic electron transport confirmed that the relative redox state of the PQ pool did regulate LHCII antenna size during low light-induced greening at the optimal light intensity for phenotypic reversion (Figure 2.4). However, at

light intensities less than 110 μmol photons m^{-2} sec^{-1}, the decrease in 1 - qP did not result in the expected change in pigmentation (Figures 2.1 and 2.5C). This suggested that at very low light intensities the phenotype of the cells was not dependent on the redox state of the PQ pool.

Consistent with the yellow-green phenotype in cells shifted from 28/2000 to either 28/10 or total darkness, the cells exhibited a relatively low cellular Chl content and high Chl a/b ratios with concomitantly reduced LHCII polypeptide accumulation relative to HEP cells that greened at 28/110 (Figure 2.6). To determine whether failure to undergo phenotypic reversion at either very low light intensities or in total darkness represented limitations at the level of Chl biosynthesis, the accumulation of the chlorophyll biosynthesis enzyme protochlorophyllide oxidoreductase (POR) was measured following a shift from 28/2000 to darkness as well as 28/10 and 28/110. POR was detected in cells shifted from 28/2000 to 28/110, however, POR was undetectable in cells shifted to either darkness or 28/10 (Figure 2.6). Rubisco content was not affected by a similar shift in light intensity (Figure 2.6).

2.4 Discussion

Light-harvesting capacity at the level of LHCII and Chl abundance in the green algae *C. vulgaris* and *Dunaliella* sp. had previously been demonstrated to be modulated in a similar capacity by either light, temperature or the site-specific inhibitors of photosynthetic electron transport, DCMU and DBMIB (Maxwell et al. 1994, Maxwell et al. 1995a, Maxwell et al. 1995b, Król et al. 1997, Masuda et al. 2003b, Chen et al. 2004). It was therefore concluded that LHCII abundance and cellular pigmentation were controlled by the redox state of the PQ pool as reflected in changes in PSII excitation pressure as opposed to light or temperature *per se* (Maxwell et al. 1994, Hüner et al. 1998, Ensminger et al. 2006).

If the redox state of the PQ pool, estimated *in vivo* as 1 - qP, was the sole regulator of

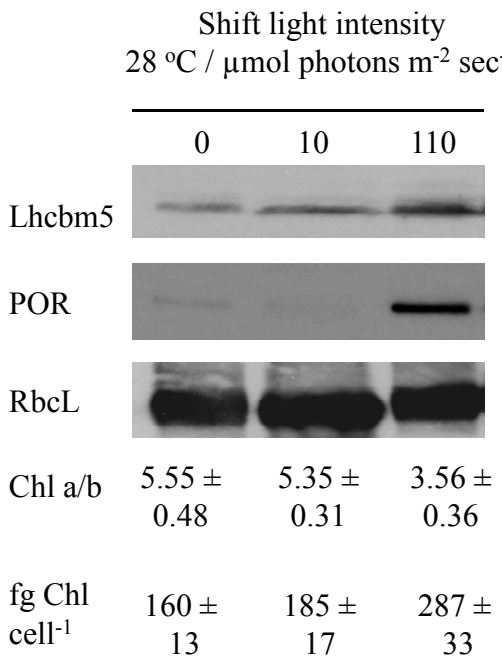

Figure 2.6 Change in LHCII (Lhcbm5), protochlorophyllide oxidoreductase (POR) and Rubisco (RbcL) polypeptide abundance for cultures of *C. vulgaris* grown to mid-log phase at 2000 µmol photons m^{-2} sec^{-1} then shifted at 28 °C to either 0 (darkness), 10 or 110 µmol photons m^{-2} sec^{-1} . Numbers above the immunoblots indicate the temperature (°C) and shift light intensity (µmol photons m^{-2} sec^{-1}). Polypeptide accumulation was assayed 24 h following the low light shift. Each lane was loaded with 20 µg of protein; equal loading was confirmed with Coomassie Brilliant Blue (Figure S2.3).

light-harvesting capacity during photoacclimation, we predicted that *C. vulgaris* cells acclimated to continuous HEP at 28/2000 and subsequently released from high PSII excitation pressure by a decrease in light intensity at a constant temperature should visibly green as the culture undergoes a phenotypic reversion from the yellow-green HEP phenotype to the dark green LEP phenotype as the PQ pool became more oxidized during the photoacclimation process. However, this is clearly not the case.

We conclude that phenotypic reversion of HEP cells is light-dependent in *C. vulgaris*. While a shift from HEP at 28/2000 to very dim light (10 μmol photons m^{-2} sec^{-1}) relaxed PSII excitation pressure, as measured by a decrease in 1 - qP, there was not a corresponding decrease in the Chl a/b ratio and concomitant reversion of the HEP phenotype (Figures 2.1 and 2.5). Based on the original predictions, this appears to indicate an "uncoupling" of excitation pressure and phenotype. This suggests that the redox state of the PQ pool cannot be the sole regulator of photoacclimation in *C. vulgaris*.

We determined that an irradiance of 110 μmol photons m^{-2} sec^{-1} was close to the optimal light intensity for low light-induced greening of HEP cells in *C. vulgaris*. Within 24 h of a shift from 28/2000 to 28/110 the rapid decrease in both 1 - qP and E_K (Table 2.1), independent measures of the relative redox state of the PQ pool, support the regulatory role of the redox state of the PQ pool in greening at the lower light intensity. As expected, within 24 h of a shift to 28/110 the HEP culture rapidly greened; this phenotypic reversion from the yellow-green HEP phenotype to dark green LEP phenotype was associated with a 2-fold increase in cellular Chl content and a 2-fold decrease in the Chl a/b ratio (Figure 2.2A) as well as an increase in the abundance of the major LHCII polypeptides with corresponding increases in other chloroplast-localized polypeptides including components of the PSII reaction centre (PsbA) as well as PTOX (Figure 2.3).

The rapid increase in PsbA abundance with relatively minor changes PsaB abundance when measured as a function of total protein complement indicate an increase in the PSII:PSI ratio. Therefore, in addition to increasing light-harvesting efficiency, there appears to be an adjustment of photosystem stoichiometry in favour of PSII during photoacclimation from HEP to LEP in *C. vulgaris*. In addition to increases in structural components of linear photosynthetic electron transport during phenotypic reversion, there was also a rapid increase in PTOX during photoacclimation. The increase in PTOX during greening is consistent with the suggestion that PTOX functions to mitigate the degree of photooxidative damage during biogenesis and assembly of the photosynthetic apparatus (Rosso et al. 2009). As no appreciable changes in PsaB and Rubisco large-subunit (RbcL) abundance were detected this indicates that not all plastid localized polypeptides change in abundance during low-light induced greening of HEP cells.

When cells were treated with DCMU, the kinetics of LHCII and PSII accumulation mimicked those of control cells (Figure 2.4). Since the accumulation of these polypeptides was blocked by DBMIB but not by DCMU this indicates that the redox sensor responsible for LHCII polypeptide and Chl accumulation during low light-induced greening of HEP cells at 28/110 is located between the bindings sites for DCMU and DBMIB on PSII and the cytochrome b_6/f complex, respectively. This is in agreement with previous reports in green algae where modulation of the redox state of intersystem electron transport through the use of chemical inhibitors have been interpreted to suggest that the redox state of the PQ pool is the primary sensor regulating photoacclimation in green algae (Escoubas et al. 1995, Wilson and Hüner 2000, Masuda et al. 2003b, Wilson et al. 2003, Chen et al. 2004). Using a similar approach Petrillo et al. (2014) recently reported that alternative splicing in the nucleus in *Arabidopsis thaliana* is also regulated by the redox state of the PQ pool. However, the lack of change in Rubisco and PsaB content indicates that not all photosynthetic components are sensitive to this redox sensing and signalling pathway.

The increased abundance of photosynthetic polypeptides encoded by the both the nuclear and plastid genomes during phenotypic reversion from the HEP to LEP phenotype

indicates coordinated changes in protein biosynthesis is required for the stable accumulation of these photosynthetic complexes (Nelson and Yocum 2006). This is consistent with the suggestion that plastid-derived signals function to coordinate the plastid and nuclear genomes during photoacclimation to changes in the environment (Woodson and Chory 2008). Since Q_A remains fully reduced in the presence of either DCMU or DBMIB, the redox state of Q_A cannot be the signal that upregulates the expression of *Lhcb* genes. Thus, in agreement with previous studies (Wilson et al. 2003), we suggest that the redox state of the PQ pool acts as a sensor of energy imbalance to regulate the accumulation of LHCII and PSII polypeptide abundance during photoacclimation at the optimal light intensity for phenotypic reversion in *C. vulgaris*. While this conclusion has been challenged by Piippo et al. (2006) using *A. thaliana*, this likely indicates that multiple components contribute to regulation of gene expression and phenotype by excitation pressure while the extent of this contribution to phenotypic plasticity may be species-dependent.

At light intensities less than 110 μmol photons m^{-2} sec^{-1}, 1 - qP was "uncoupled" from phenotype (Figures 2.1 and 2.5). Previously, modulation of 1 - qP by either light or temperature in *D. salina* have been correlated with increased *Lhcb* transcript abundance and LHCII polypeptide accumulation (Maxwell et al. 1995b). We had therefore predicted that modulation of 1 - qP in darkness would be correlated with visible greening of the HEP-acclimated culture as LHCII polypeptides and Chl accumulated. However, contrary to these predictions, HEP cells of *C. vulgaris* were unable to green in either complete darkness or at very dim light intensities (< 25 μmol photons m^{-2} sec^{-1}) (Figure 2.1). Rather, the cultures remained phenotypically indistinguishable from cells acclimated to continuous HEP. Consistent with the phenotype, cells grown at 28/2000 and shifted to either 28/0 or 28/10 exhibited relatively low cellular Chl content and high Chl a/b ratios with concomitantly low LHCII abundance characteristic of acclimation to HEP (Figure 2.6). However, cells transferred to, and measured at, 28/10 exhibited an extremely low PSII excitation pressure (Figure 2.5, ●) suggesting that redox state of the PQ cannot be the sole regulator of LHCII antenna size and, by extension, phenotype in *C. vulgaris*. This is in direct contrast to *D. salina* which exhibited rapid greening of HEP cells in

complete darkness (Maxwell et al. 1995b). As 1 - qP is predicted to be minimal in darkness, dark greening of HEP-acclimated cultures of *D. salina* was attributed to relaxation of high PSII excitation pressure (Maxwell et al. 1995b).

Normally changes in Chl abundance occur concomitantly with changes in pigment-binding LHC abundance such that Chl does not occur unbound. Furthermore, Chl *b* is required for the stability of light-harvesting complex polypeptides. Falbel et al. (1996) proposed that photosynthetic organisms may regulate light-harvesting complex polypeptide abundance by altering the rate of Chl *b* biosynthesis. Consistently, over-expressing *CAO*, which encodes the enzyme responsible for the conversion of Chl *a* to Chl *b*, in *A. thaliana* caused an increase in PSII antenna size (Tanaka et al. 2001). Based on this we propose that the yellow-green pigmentation in darkness and light levels less than 110 μmol photons m^{-2} sec^{-1} may reflect limitations at the level of Chl biosynthesis as opposed to LHCII accumulation *per se* in *C. vulgaris*.

The chlorophyll biosynthesis enzyme POR is required for the reduction of protochlorophyllide to chlorophyllide. In angiosperms, the conversion of protochlorophyllide to chlorophyllide is strictly light-dependent and is catalyzed by a light-dependent POR enzyme (LPOR) (Reinbothe et al. 2010). Greening of HEP cells at 28/110 was optimal for POR accumulation (Figure 2.6) and was associated with a 2-fold increase in cellular Chl content. A similar correlation between increased LPOR protein and Chl abundance during greening has also been observed in *Cucumis sativus* (Kuroda et al. 1995). However, cells shifted from 28/2000 to either darkness or 10 μmol photons m^{-2} sec^{-1} failed to accumulate POR (Figure 2.6). Such positive regulation of POR accumulation by light in *C. vulgaris* is similar to the positive photoregulation of the single *POR* gene in *C. sativus* (Fusada et al. 2000) and the LPOR isoform *PORC* in *A. thaliana* (Oosawa et al. 2000, Masuda et al. 2003a).

Genomic analysis suggests that *C. vulgaris* possesses the genes encoding an unrelated light-independent or dark-operative POR (DPOR) enzyme capable of facilitating the reduction of protochlorophyllide to chlorophyllide in the dark (Gabruk et al. 2012). The

presence of DPOR has been linked to dark Chl biosynthesis in photosynthetic bacteria, green algae and gymnosperms (Reinbothe et al. 2010). However, although *C. vulgaris* may possess the genes encoding DPOR the apparent inability for the dark biosynthesis of Chl necessary to relax the yellow-green HEP phenotype in either very dim light or total darkness suggests that *C. vulgaris* may not express DPOR.

In the liverwort *Marchantia paleacea,* a cell line that greened in both the light and darkness accumulated the *chlB, chlL* and *chlN* transcripts encoding DPOR equally well under both conditions (Suzuki et al. 1998). By contrast, a cell line that only greened in the light, failed to accumulate *chlB, chlL* and *chlN* transcripts in the dark (Suzuki et al. 1998) suggesting a direct link between gene expression and the ability for dark biosynthesis of Chl. Therefore, the differential ability for dark greening in *C. vulgaris* (Figure 2.1) and *D. salina* (Maxwell et al. 1995b) may be due to differential capacities for the dark biosynthesis of Chl reflecting limitations at the level of DPOR accumulation. The inability to green in darkness suggests that Chl biosynthesis may be strictly light-dependent in *C. vulgaris*. Thus, in addition to the redox state of the PQ pool, post-translational control of LHCII stability by light-dependent Chl *b* biosynthesis is likely a second important regulator of phenotypic plasticity associated with photoacclimation in *C. vulgaris*.

Therefore, we propose that photoacclimation in *C. vulgaris* requires the coordination of two distinct regulatory pathways. First, a change in light energy availability is sensed as change in the relative redox state of the PQ pool as estimated *in vivo* by PSII excitation pressure. The chemical inhibitors DCMU and DBMIB indicate the redox state of the PQ pool acts as the primary sensor for cellular energy availability and source of signals regulating LHCII abundance in *C. vulgaris*. The increase in the abundance of LHCII polypeptides following oxidation of the PQ pool is consistent with the results of this study and with those presented in previous studies which suggest that the redox state of the PQ pool as an important component of a redox retrograde sensing and signalling pathways within the photosynthetic electron transport chain regulating photoacclimation and phenotype in green algae (Escoubas et al. 1995, Wilson and Hüner 2000, Masuda et

al. 2003b, Wilson et al. 2003, Chen et al. 2004). Biochemical evidence suggests that a protein phosphorylation cascade is involved in the retrograde signal transduction of this plastid redox signal (Escoubas et al. 1995, Masuda et al. 2003b) while *cis*-acting promoter elements in algal nuclear-encoded *Lhcb* genes have been identified which are likely required for the plastidic redox regulation of nuclear genes for photoacclimation (Escoubas et al. 1995, Chen et al. 2004).

Second, based on the results of this study we suggest that the yellow-green phenotype in *C. vulgaris* may represent limitations at the level of Chl availability as opposed to the LHCII polypeptide abundance *per se* where HEP inhibits POR accumulation. Since a low light of 110 μmol photons m^{-2} sec^{-1} was optimal for the accumulation of POR, relaxation of HEP by low light is required to overcome this apparent inhibition. Moreover, the apparent positive photoregulation of POR availability in *C. vulgaris* accounts for the failure to accumulate Chl and LHCII polypeptides despite oxidation of the PQ pool at low light. We conclude that the requirement for post-translational stabilization of light-harvesting polypeptide by Chl binding therefore likely represents a second important light-dependent regulator of photoacclimation and phenotypic plasticity in *C. vulgaris.*

2.5 References

Albrecht, V., Estavillo, G.M., Cuttriss, A.J. & Pogson, B.J. 2011. Identifying chloroplast biogenesis and signalling mutants in *Arabidopsis thaliana*. *Methods Mol. Biol.* 684:257–272.

Baker, N.R. 2008. Chlorophyll fluorescence: a probe of photosynthesis *in vivo*. *Annu. Rev. Plant Biol.* 59:89–113.

Brautigam, K., Dietzel, L., Kleine, T., Ströher, E., Wormuth, D., Dietz, K.J., Radke, D., Wirtz, M., Hell, R., Dörmann, P., Nunes-Nesi, A., Schauer, N., Fernie, A.R., Oliver, S.N., Geigenberger, P., Leister, D. & Pfannschmidt, T. 2009. Dynamic plastid redox signals integrate gene expression and metabolism to induce distinct metabolic states in photosynthetic acclimation in *Arabidopsis*. *Plant Cell* 21:2715–2732.

Casal, J.J. 2013. Photoreceptor signaling networks in plant responses to shade. *Annu. Rev. Plant Biol.* 64:403–427.

Chen, Y.B., Durnford, D.G., Koblizek, M. & Falkowski, P.G. 2004. Plastid regulation of *Lhcb1* transcription in the chlorophyte alga *Dunaliella tertiolecta*. *Plant Physiol*. 136:3737–3750.

Demmig-Adams, B. & Adams III, W. W. 1992. Photoprotection and other responses of plants to high light stress. *Annu. Rev. Plant Physiol. Plant Mol. Biol.* 43:599–626.

Demmig-Adams, B. & Adams III, W.W. 2000. Harvesting sunlight safely. *Nature* 403:371–374.

Dietz, K.J., Schreiber, U. & Heber, U. 1985. The relationship between the redox state of Q_A and photosynthesis in leaves at various carbon-dioxide, oxygen and light regimes. *Planta* 166:219–226.

Ensminger, I., Busch, F. & Hüner, N.P.A. 2006. Photostasis and cold acclimation: sensing low temperature through photostasis. *Physiol. Plant.* 126:28–44.

Escoubas, J.M., Lomas, M., LaRoche, J. & Falkowski, P.G. 1995. Light intensity regulation of *cab* gene transcription is signaled by the redox state of the plastoquinone pool. *Proc. Natl. Acad. Sci. U.S A.* 92:10237–10241.

Estavillo, G.M., Chan, K.X., Phua, S.Y. & Pogson, B.J. 2013. Reconsidering the nature and mode of action of metabolite retrograde signals from the chloroplast. *Front. Plant Sci.* 3:300.

Falbel, T.G., Meehl, J.B. & Staehelin, L.A. 1996. Severity of mutant phenotype in a series of chlorophyll-deficient wheat mutants depends on light intensity and the severity of the block in chlorophyll synthesis. *Plant Physiol*. 112:821–32.

Falkowski, P.G. & Owens, T.G. 1980. Light-shade adaptation: two strategies in marine phytoplankton. *Plant Physiol.* 66:592–595.

Falkowski, P.G. & LaRoche, J. 1991. Acclimation to spectral irradiance in algae. *J. Phycol*. 27:8–14.

Falkowksi, P.G. & Chen, Y-B. 2003. "Photoacclimation of light harvesting systems in eukaryotic algae," *In* Green, B.R. & Green W.W. [Eds.] *Advance in Photosyntheis and Respiration*, Vol. 13, *Light Harveting Antennas in Photosynthesis*. Kluwer Academic Publishers, Dordrecht, the Netherlands, pp. 423–447.

Fey,V., Wagner, R., Braütigam, K., Wirtz, M., Hell, R., Dietzmann, A., Leister, D., Oelmüller, R. & Pfannschmidt, T. 2005. Retrograde plastid redox signals in the expression of nuclear genes for chloroplast proteins of *Arabidopsis thaliana*. *J. Biol. Chem*. 280:5318–5328.

Fujita, Y., Iwama, Y., Ohki, K., Murakami, A. & Hagiwara, N. 1989. Regulation of the size of light harvesting antennae in response to light intensity in the green alga *Chlorella pyrenoidosa*. *Plant Cell Physiol.* 30:1029–1037.

Fusada, N., Masuda, T., Kuroda, H., Shiraishi, T., Shimada, H., Ohta, H. & Takamiya, K. 2000. NADPH-protochlorophyllide oxidoreductase in cucumber is encoded by a single gene and its expression is transcriptionally enhanced by illumination. *Photosyn. Res.* 64:147–154.

Gabruk, M., Grzyb, J., Kruk, J. & Mysliwa-Kurdziel, B. 2012. Light-dependent and light-independent protochlorophyllide oxidoreductases share similar sequence motifs - *in silico* studies. *Photosynthetica* 50:529–540.

Geider, R.J., MacIntrye, H.L. & Kana, T.M. 1996. A dynamic model of photoadaptation in phytoplankton. *Limnol. Oceanogr.* 4:1–15.

Geider, R.J., MacIntrye, H.L. & Kana, T.M. 1998. A dynamic regulatory model of phytoplanktonic acclimation to light, nutrients, and temperature. *Limnol. Oceanogr.* 43:679–694.

Harrison, M.A., Melis, A. & Allen, J.F. 1992. Restoration of irradiance-stressed *Dunaliella salina* (green alga) to physiological growth conditions: changes in antenna size and composition of photosystem II. *Biochim. Biophys. Acta* 1100:83–91.

Hendrickson, L., Furbank, R.T. & Chow, W.S. 2004. A simple alternative approach to assessing the fate of absorbed light energy using chlorophyll fluorescence. *Photosynth. Re*s. 82:73–81.

Hüner, N.P.A., Öquist, G. & Sarhan, F. 1998. Energy balance and acclimation to light and cold. *Trends Plant Sci.* 3:224–230.

Hüner, N.P.A., Oquist, G. & Melis, A. 2003. "Photostasis in plants, green algae and cyanobacteria: the role of light harvesting antenna complexes", *In* Green, B.R. & Green, W.W. [Eds.] *Advances in Photosynthesis and Respiration,* Vol. 13*, Light*

Harvesting Antennas in Photosynthesis. Kluwer Academic Publishers, Dordrecht, the Netherlands, pp. 401–421.

Hüner, N.P., Bode, R., Dahal, K., Hollis, L., Rosso, D., Król, M. & Ivanov, A.G. 2012. Chloroplast redox imbalance governs phenotypic plasticity: the "grand design of photosynthesis" revisited. *Front. Plant Sci.* 3:255.

Hüner, N.P., Dahal, K., Kurepin, L.V., Savitch, L., Singh, J., Ivanov, A.G., Kane, K. & Sarhan, F. 2014. Potential for increased photosynthetic performance and crop productivity in response to climate change: role of CBFs and gibberellic acid. *Front. Chem.* 2:18.

Jeffrey, S.W. & Humphrey, G.F. 1975. New spectrophotometric equations for determining chlorophylls a1, b1, c1 and c2 in higher plants, algae and natural phytoplankton. *Biochem. Physiol. Pflanz*. 167: 191–194.

Kianianmomeni, A. & Hallmann, A. 2014. Algal photoreceptors: in vivo functions and potential applications. *Planta* 239:1–26.

Kramer, D.M., Johnson, G., Kiirats, O. & Edwards, G.E. 2004. New fluorescence parameters for the determination of Q_A redox state and excitation energy fluxes. *Photosynth. Res.* 79:209–218.

Król, M,. Maxwell, D.P. & Hüner, N.P.A. 1997. Exposure of *Dunaliella salina* to low temperature mimics the high light-induced accumulation of carotenoids and the carotenoid binding protein (Cbr). *Plant Cell Physiol.* 38:213–216.

Kuroda, H., Masuda, T., Ohta, H., Shioi, Y. & Takamiya, K. 1995. Light-enhanced gene expression of NADPH-protochlorophyllide oxidoreductase in cucumber. *Biochem. Biophys. Res. Commun.* 210:310–316.

Laemmli, U. 1970. Clevage of structural proteins during the assembly of the head of bacteriophage T4. *Nature* 227: 680–685.

Masuda, T., Fusada, N., Oosawa, N., Takamatsu, K., Yamamoto, Y.Y., Ohto, M., Nakamaura, K., Goto, K., Shibata, D., Shirano, Y., Hayashi, H., Kato, T., Tabata, S., Shimada, H., Ohta, H. & Takamiya, K. 2003a. Functional analysis of isoforms of NADPH: protochlorophyllide oxidoreductase (POR), PORB and PORC, in *Arabidopsis thaliana*. *Plant Cell Physiol.* 44:963–974.

Masuda, T., Tanaka, A. & Melis, A. 2003b. Chlorophyll antenna size adjustments by irradiance in *Dunaliella salina* involve coordinate regulation of chlorophyll a oxygenase (CAO) and *Lhcb* gene expression. *Plant Mol. Biol.* 51:757–771.

Maxwell, D.P., Falk, S., Trick, C.G. & Hüner, N.P.A. 1994. Growth at low temperature mimics high-light acclimation in *Chlorella vulgaris*. *Plant Physiol.* 105:535–543.

Maxwell, D.P., Falk, S. & Hüner, N.P.A. 1995a. Photosystem II excitation pressure and development of resistance to photoinhibition (I. Light harvesting complex II abundance and zeaxanthin content in *Chlorella vulgaris*). *Plant Physiol.* 107:687–694.

Maxwell, D.P., Laudenbach, D.E. & Hüner, N.P.A. 1995b. Redox regulation of light harvesting complex II and *cab* mRNA abundance in *Dunaliella salina*. *Plant Physiol*. 109:787–795.

Murchie, E.H., Pinto, M. & Horton, P. 2009. Agriculture and the new challenges for photosynthesis research. *New Phytol*. 181:532–552.

Nelson, N. & Yocum, C.F. 2006. Structure and function of photosystems I and II. *Annu. Rev. Plant Biol.* 57:521–565.

Nichols, S.H.W & Bold, H.C. 1965. *Trichosarcina polymorpha* gen. et sp. nov. *J. Phycol*. 1:34–38.

Oosawa, N., Masuda, T., Awai, K., Fusada, N., Shimada, H., Ohta, H. & Takamya, K. 2000. Identification and light-induced expression of a novel gene of NADPH-protochlorophyllide oxidoreductase isoform in *Arabidopsis thaliana*. *FEBS Lett*. 474:133–136.

Petrillo, E., Godoy Herz, M.A., Fuchs, A., Reifer, D., Fuller, J., Yanovsky, M.J., Simpson, C., Brown, J.W.S., Barta, A., Kalyna, M. & Kornblihtt, A.R. 2014. A chloroplast retrograde signal regulates nuclear alternative splicing. *Science* 344:427–430.

Piippo, M., Allahverdiyeva, Y., Paakkarinen, V., Suoranta, U.M., Battchickova, N. & Aro, E.M. 2006. Chloroplat-mediated regulation of nuclear genes in *Arabidopsis thaliana* in the absence of light stress. *Physiol. Genomics* 25:142–152.

Pogson, B.J., Woo, N.S., Förster, B. & Small, I.D. 2008. Plastid signalling to the nucleus and beyond. *Trends Plant Sci*. 13:602–609.

Pogson, B.J. & Albrecht, V. 2011. Genetic dissection of chloroplast biogenesis and development: an overview. *Plant Physiol.* 155:1545–1551.

Porra, R.J. 2005. "The chequered history of the development and use of simultaneous equations for the accurate determination of chlorophylla *a* and *b*," *In* Govindgee, Beatty, J.T., Gest, H. & Allen, J.F. [Eds]. *Advances in Photosynthesis and Respiration*, Vol. 20, *Discoveries in Photosynthesis*. Springer, Dordrecht, the Netherlands, pp. 633–670

Reinbothe, C., El Bakkouri, M., Buhr, F., Muraki, N., Nomata, J., Kurisu, G., Fujita, Y. & Reinbothe, S. 2010. Chlorophyll biosynthesis: spotlight on protochlorophyllide reduction. *Trends Plant Sci*. 15:614–624.

Rosso, D., Bode, R., Li, W., Król, M., Saccon, D., Wang, S., Schillaci, L.A., Rodermel, S.R. Maxwell, D.P. & Hüner, N.P.A. Photosynthetic redox imbalance governs leaf sectoring in the *Arabidopsis thaliana* variegation mutants *immutans*, *spotty*, *var1*, and *var2*. *Plant Cell* 21:3473–3492.

Sukenik, A., Bennett, J., Mortain-Bertrand, A. & Falkowski, P.G. 1990. Adaptation of the photosynthetic apparatus to irradiance in *Dunaliella tertiolecta:* A kinetic study. *Plant Physiol.* 92:891–898.

Suzuki, T., Takio, S. & Satoh, T. 1998. Light-dependent expression in liverwort cells of *chlL/N* and *chlB* identified as chloroplast genes involved in chlorophyll synthesis in the dark. *J. Plant Physiol.* 152:31–37.

Talling, J.F. 1957. The phytoplankton population as a compound photosynthetic system. *New Phytol.* 56:133–149.

Tanaka, R., Koshino, Y., Sawa, S., Ishiguro, S., Okada, K. & Tanaka, A. 2001. Overexpression of chlorophyllide a oxygenase (CAO) enlarges the antenna size of photosystem II in *Arabidopsis thaliana*. *Plant J.* 26:365–373.

van Kooten, O. & Snel, J.F. 1990. The use of chlorophyll nomenclature in plant stress physiology. *Photosyn. Res.* 25:147–150.

Walters, R.G., Rogers, J.J., Shephard, F. & Horton, P. 1999. Acclimation of *Arabidopsis thaliana* to the light environment: the role of photoreceptors. *Planta* 209:517–527.

Webb, M. & Melis, A. 1995. Chloroplast response in *Dunaliella salina* to irradiance stress (effect on thylakoid membrane protein assembly and function). *Plant Physiol.* 107:885–893.

Wilson, K.E. & Hüner, N.P.A. 2000. The role of growth rate, redox-state of the plastoquinone pool and the trans-thylakoid (delta)pH in photoacclimation of *Chlorella vulgaris* to growth irradiance and temperature. *Planta* 212:93–102.

Wilson, K.E., Król, M. & Hüner, N.P.A. 2003. Temperature-induced greening of *Chlorella vulgaris*. The role of the cellular energy balance and zeaxanthin-dependent nonphotochemical quenching. *Planta* 217:616–627.

Woodson, J.D. & Chory, J. 2008. Coordination of gene expression between organellar and nuclear genomes. *Nat. Rev.* 9:383–395.

2.6 Supplemental Material

2.6.1 Supplemental Tables

Supplemental Table S2.1 Total change in chlorophyll a/b ratio (ΔChl a/b) measured as a function of time over a 24 h period following a shift from continuous high light of 2000 µmol photons m^{-2} sec^{-1} to a series of lower light intensities at 28 °C. Values represent mean ± SEM; n = 3.

	Shift light intensity (µmol photons m^{-2} sec^{-1})							
	0	10	25	50	75	110	150	300
ΔChl a/b	1.35 ± 0.59	1.29 ± 0.17	2.00 ± 0.21	2.53 ± 0.36	2.86 ± 0.34	3.25 ± 0.79	2.86 ± 0.22	1.18 ± 0.44

Supplemental Table S2.2 Estimation of the proportion of closed photosystem II reaction centres. Measurements were taken at time 0 h and 24 h following the change in light regime from 2000 µmol photons m^{-2} sec^{-1} to 110 µmol photons m^{-2} sec^{-1} at a constant temperature of 28 °C. The proportion of closed reaction centres was calculated as either 1 - qP or 1 - qL where qP and qL estimates the proportion of reduced Q_A as $(Q_A)_{reduced}$ / $[(Q_A)_{reduced} + (Q_A)_{oxidized})]$ where $qP = (F_M' - F_S)/(F_M' - F_O')$[a] and $qL = qP \cdot (F_O/F_S)$[b]. Values represent mean ± SEM; n = 3.

	Time following shift	
	0 h	24 h
1 - qP	0.761 ± 0.0251	0.164 ± 0.0201
1 - qL	0.843 ± 0.0325	0.341 ± 0.0218

[a](Dietz et al. 1985, Hendrickson et al. 2004) [b](Kramer et al. 2004)

2.6.2 Supplemental Figures

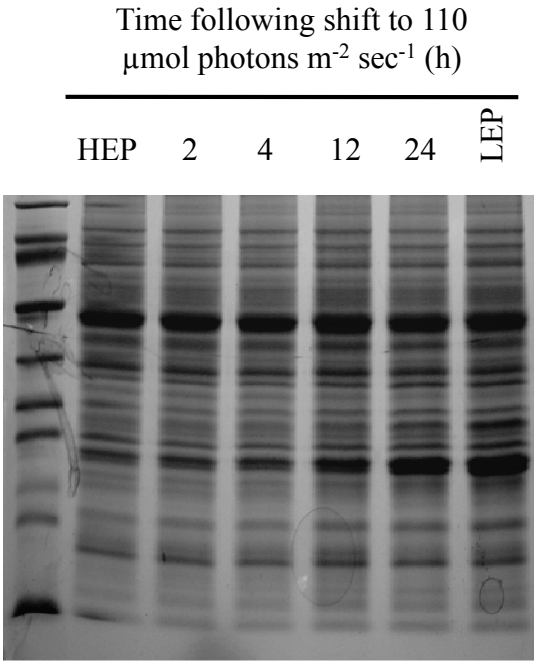

Supplemental Figure S2.1 Separated whole cells polypeptides for cultures of *C. vulgaris* grown to mid-log phase at a high excitation pressure (HEP; time 0 h) growth regime of 2000 µmol photons m^{-2} sec^{-1} before being transferred at a constant temperature of 28 °C to 110 µmol photons m^{-2} sec^{-1} at time 0 h. Proteins collected as a function of time following the transfer to low light are followed by the whole cell polypeptide complement of cells acclimated to continuous low excitation pressure (LEP) at 28 °C and 150 µmol photons m^{-2} sec^{-1}. Each lane was loaded with 20 µg of protein.

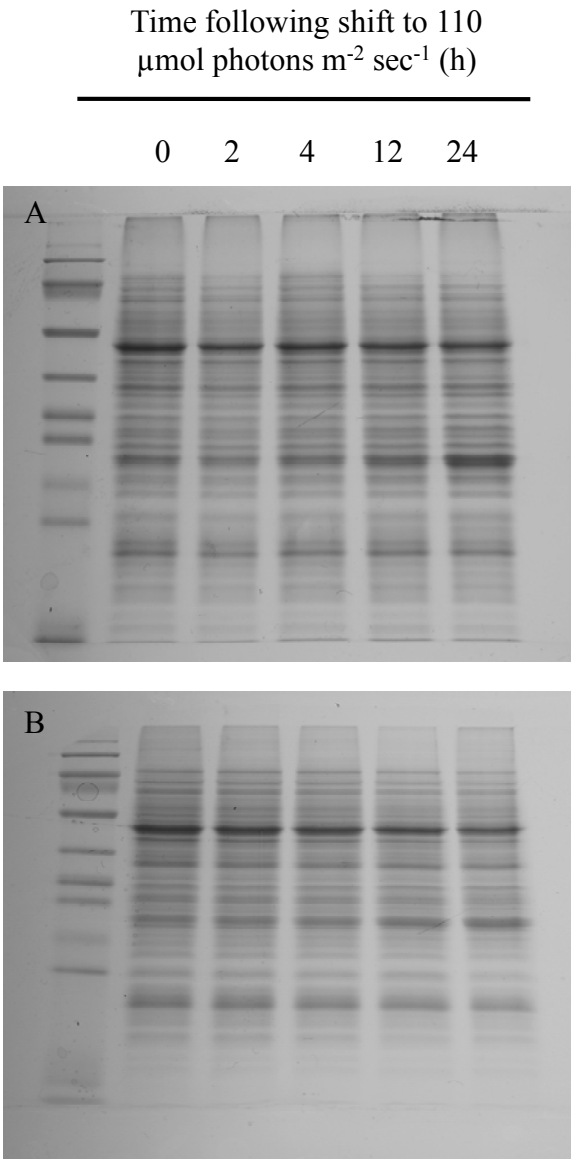

Supplemental Figure S2.2 Separated whole cells polypeptides for *C. vulgaris* grown to mid-log phase at a high excitation pressure growth regime of 2000 µmol photons m^{-2} sec^{-1} then transferred to 110 µmol photons m^{-2} sec^{-1} at 28 °C at time 0 h in the presence of either (A) DCMU or (B) DBMIB. Proteins were collected as a function of time following the transfer to low light. Each lane was loaded with 20 µg of protein.

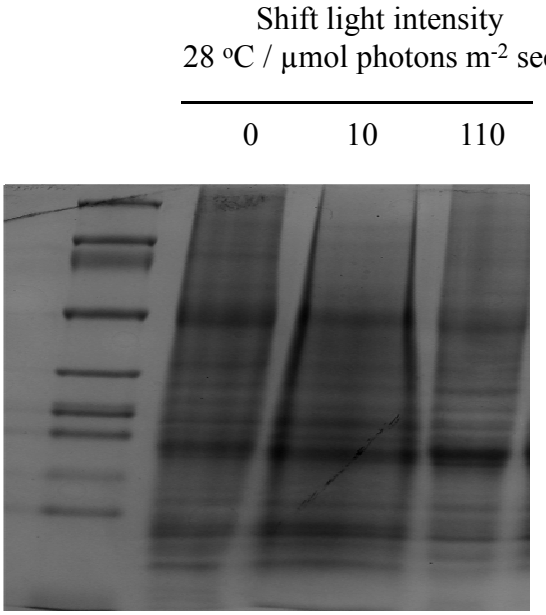

Supplemental Figure S2.3 Separated whole cells polypeptides for *C. vulgaris* grown to mid-log phase at a high excitation pressure growth regime of 2000 µmol photons m^{-2} sec^{-1} before transfer to either 0, 10 or 110 µmol photons m^{-2} sec^{-1} at a constant temperature of 28 °C. Proteins were collected 24 h following the transfer to low light. Each lane was loaded with 20 µg of protein.

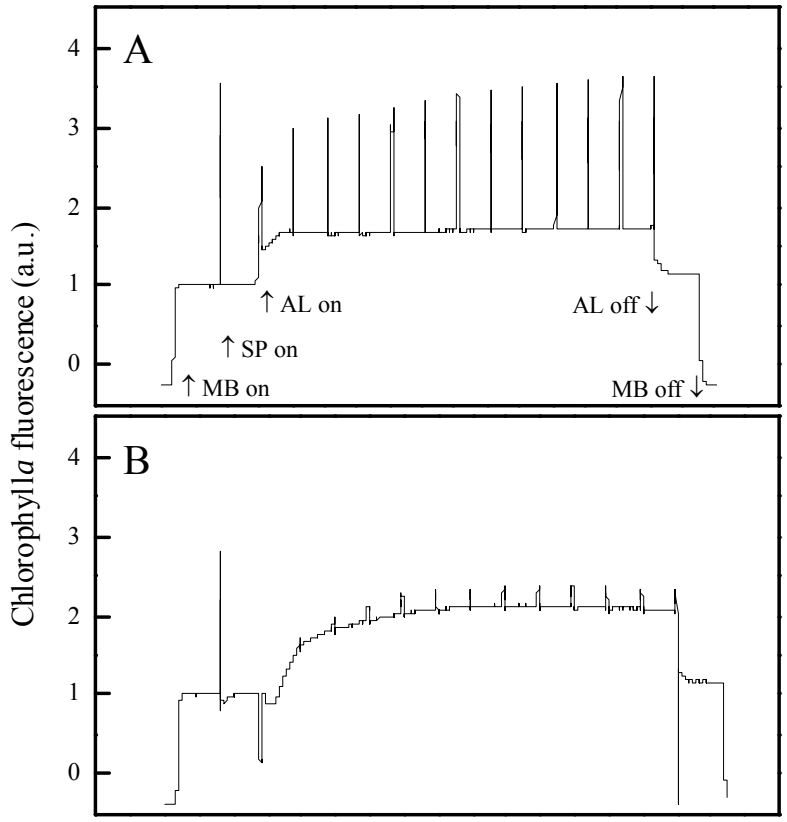

Supplemental Figure S2.4 Representative room temperature chlorophyll *a* fluorescence inductions curves for cultures of *Chlorella vulgaris* grown at either (A) a low excitation growth regime (28 °C and 150 µmol photons m^{-2} sec^{-1}) or (B) a high excitation pressure growth regime (28 °C and 2000 µmol photons m^{-2} sec^{-1}). Measurements were taken during mid-log phase growth at the growth light intensity. AL, actinic light; MB, measuring beam; SP, saturating pulse.

Chapter 3

3 PHOTOACCLIMATION IN *CHLORELLA VULGARIS* UTEX 265 IS BOTH REDOX- AND PHOTOPERIOD-DEPENDENT

3.1 Introduction

Differences in the wavelengths of light (light quality) are sensed by photosynthetic organisms through specialized blue light sensitive cryptochromes, phototropins and zeitlupe, and red light sensitive phytochromes (Möglich et al. 2010, Casal 2013, Kianianmomeni and Hallmann 2014). These photoreceptors serve a vital role in photoautotrophic growth and development by regulating the biosynthesis and assembly of thylakoid membranes and associated protein complexes during chloroplast biogenesis as well as photomorphogenesis; the photoreceptor-mediated sensing and signalling pathways that enable responses to light quality are defined as "biogenic" controls (Pogson et al. 2008, Pogson and Albrecht 2011, Estavillo et al. 2013). In addition to photoreceptor-mediated light quality sensing, photoautotrophs sense changes in the light environment through changes in light energy availability (Anderson et al. 1995; Hüner et al. 1998, Pfannschmidt 1999, Hüner et al. 2012). Changes in light energy availability are sensed by mature chloroplasts through modulation of the reduction-oxidation (redox) state of intersystem photosynthetic electron transport (Anderson et al. 1995; Hüner et al. 1998, Pfannschmidt 2003; Hüner et al. 2003, Ensminger et al. 2006, Hüner et al. 2012).

Despite a role in light quality sensing, it has been demonstrated that photoreceptors do not play a major role in photoacclimation of the photosynthetic apparatus in mature chloroplasts. Walters et al. (1999) used *Arabidopsis thaliana* phytochrome mutants to demonstrate that adjustments to the structure and functionality of the photosynthetic apparatus in response to changing irradiance occur independently of light quality sensing through photoreceptors. Fey et al. (2005) further demonstrated redox signals from the photosynthetic apparatus are capable of inducing changes in nuclear-encoded gene

expression independently of signalling mediated by photoreceptors. Rather, signals derived from the mature chloroplast are believed to act as the major regulators of photoacclimation (Hüner et al. 1998).

Optimal photoautotrophic performance requires a balance between the energy obtained through photochemistry with the energy required for metabolism, growth and development. Imbalances in cellular energy flow occur whenever the rate of light energy absorption and transformation by temperature-insensitive photochemistry exceeds the capacity to dissipate excess light energy as heat through the xanthophyll cycle and/or utilize absorbed light energy through carbon, nitrogen and sulphur metabolism, respiration and ultimately growth (Hüner et al. 1998, Ensminger et al. 2006, Hüner et al. 2012). Changes in cellular energy balance are sensed as changes in the redox state of photosynthetic electron transport through modulation of photosystem II (PSII) excitation pressure (Hüner et al. 1998).

Excitation pressure is a measure of the relative redox state of quinone A (Q_A), the first stable electron acceptor of PSII, and is estimated *in vivo* by the room temperature chlorophyll (Chl) *a* fluorescence induction parameter as 1 - qP where qP estimates the proportion of reduced Q_A as $Q_{A(reduced)} / (Q_{A(reduced)} + Q_{A(oxidized)})$ (Dietz et al. 1985, Hüner et al. 1998). Sensing and signalling of light energy availability by mature chloroplasts is defined as "operational" control (Pogson et al. 2008, Pogson and Albrecht 2011, Estavillo et al. 2013). These signals coordinate regulation of the structure and efficiency of the photosynthetic apparatus in mature, fully developed cells to ensure optimal photosynthetic performance while mitigating the harmful effects of excess light energy in the face of an ever changing environment. In this manner, the mature chloroplast serves dual roles; both as an energy transducer and as a sensor for changes in the environment (Hüner et al. 1998, Murchie et al. 2009, Hüner et al. 2012).

Research in the green alga *Dunaliella* sp. (Escoubas et al. 1995, Maxwell et al. 1995b, Król et al. 1997) and *Chlorella vulgaris* (Maxwell et al. 1994, Maxwell et al. 1995a, Wilson and Hüner 2000) indicate that the central sensor for changes in cellular energy

poise of photosynthetic electron transport in green algae is the redox state of the plastoquinone (PQ) pool. This was based on the observation that a typical high light phenotype, characterized by yellow-green pigmentation, relatively low Chl content per cell and relatively high Chl a/b ratio with concomitantly reduced abundance of the major pigment-binding light-harvesting complex polypeptides associated with PSII (LHCII) could be mimicked by application of the herbicide 2,5-dibromo-3-methyl-6-isopropy-1,4-benzoquinone (DBMIB) in the green algae *D. tertiolecta* (Escoubas et al. 1995) and *C. vulgaris* (Wilson et al. 2003). DBMIB mimics the effects of high light on the redox state of the PQ pool by preventing oxidation of the PQ pool by the Cyt b_6/f complex thereby keeping the PQ pool reduced in the light. In contrast, cultures developed a dark green pigmentation characterized by a relatively low Chl a/b ratio and high cellular Chl content when treated with 3-(3,4-dichlorophenyl)-1,1-dimethylurea (DCMU) which keeps the PQ pool oxidized in the light by blocking the transfer of electrons from Q_A to quinone B (Q_B) and subsequently to the intersystem PQ pool (Escoubas et al. 1995, Wilson et al. 2003)

The yellow-green, high light phenotype in green algae can additionally be mimicked by growth at low temperature (Maxwell et al. 1994, Maxwell et al. 1995a, Maxwell et al. 1995b, Król et al. 1997, Wilson and Hüner 2000, Wilson et al. 2003). Since light energy absorption and subsequent utilization in metabolism, respiration and growth integrates extremely fast, temperature-independent photochemistry with much slower, temperature-dependent biochemistry, the reduction state of Q_A can be modulated in a similar fashion by either low temperature or high light. High light will increase the rate of Q_A reduction through the increased photon flux rate. Although low temperature does not affect photochemistry, low temperature limits the reaction rates of the temperature-sensitive, enzyme-mediated reactions that consume photosynthetically generated electrons. Therefore, low temperature will cause an over-reduction of photosynthetic electron transport chain and an increase in PSII excitation pressure by limiting metabolism and growth.

Since the yellow-green phenotype can be mimicked by either high light or low temperature, these green algae photoacclimate in response to changes in PSII excitation

pressure as opposed to light or temperature *per se* (Maxwell et al. 1994, Hüner et al. 1998). Changes in cellular energy balance by either growth irradiance or temperature will modulate excitation pressure within the mature chloroplast. Furthermore, since nutrient limitations and water availability will also limit the capacity to consume photosynthetically generated electrons and increase excitation pressure, because of the nature of photoautotrophic growth, all photosynthetic organisms acclimate to changes in their environment by sensing and responding to excitation pressure, an important "operational" signal.

When photoautotrophs are in photostasis the rate of light-induced photochemistry is balanced by the capacity to consume photosynthetically generated electrons through metabolism and growth and/or dissipate excess absorbed light energy nonphotochemically as heat through the xanthophyll cycle and nonphotochemical quenching (NPQ) (Hüner et al. 1998, Falkowski and Chen 2003, Hüner et al. 2003). Under these conditions, PSII excitation pressure is low, the PQ pools remains oxidized as estimated by a relatively low 1 - qP, and cultures of green algae display a typical dark green, low excitation pressure (LEP) phenotype. Environmental stresses including high light and low temperature cause an increase in excitation pressure by causing an imbalance between light energy absorption through photochemistry and the capacity for cellular energy use (Maxwell et al. 1994, Escoubas et al. 1995, Maxwell et al. 1995a, Wilson and Hüner 2000). Under these conditions, the PQ pool becomes reduced and excitation pressure is high reflecting the accumulation of closed PSII reaction centres ($P680^+$ Pheo QA^-). Cultures acclimated to high excitation pressure (HEP) display a yellow-green pigmentation characterized by retrograde redox suppression of the nuclear-encoded *Lhcb* expression leading to decreased pigment-binding LHCII polypeptide abundance with concomitantly reduced cellular Chl content and increased Chl a/b ratio (Maxwell et al. 1994, Escoubas et al. 1995, Savitch et al. 1996, Chen et al. 2004). The reduction in the accumulation of LHCII polypeptides protects the photosynthetic apparatus by decreasing the efficiency of light energy absorption. Green algae photoacclimate to HEP by adjusting the structure and function of the photosynthetic apparatus as they are believed to be limited in the capacity to stimulate either growth rate

(Wilson and Hüner 2000) or carbon fixation (Savitch et al. 1996) in response to imbalances in cellular energy flow.

Photosynthetic organisms are subjected to short term variations in the light environment due to changes in cloud and canopy cover as well as longer term diurnal and seasonal changes in photoperiod. However, previous studies on acclimation to excitation pressure in green algae have been conducted under constant illumination (Maxwell et al. 1994, Maxwell et al. 1995a, Wilson and Hüner 2000, Wilson et al. 2003). In addition to redox retrograde regulation (Escoubas et al. 1995, Maxwell et al. 1995b, Chen et al. 2004), the major nuclear-encoded light harvesting complex genes have additionally been demonstrated to be regulated by other factors including the circadian clock (Millar et al. 1985, Rochaix 2014). To determine the effects of changes in photoperiod on acclimation to excitation pressure cultures of *C. vulgaris* were grown under what has been demonstrated to be a LEP growth regime at 28 °C and 150 µmol photons m^{-2} sec^{-1} and a HEP growth regime at 28 °C and 2000 µmol photons m^{-2} sec^{-1} (Maxwell et al. 1994; Maxwell et al. 1995a) with decreasing photoperiods.

During growth and development under alternating light:dark cycles, PSII excitation pressure should relax during the daily dark period as the absence of light will negate the photochemical closure of the PSII reaction centres. We hypothesized that if excitation pressure is the sole regulator of photoacclimation and therefore phenotype, cultures of *C. vulgaris* should photoacclimate in response to the steady-state excitation pressure during of the light period regardless of the length of the photoperiod. In this report, we test this hypothesis and show that photoacclimation in *C. vulgaris* is dependent upon both photoperiod and photosynthetic redox imbalance.

3.2 Methods

3.2.1 Culture conditions

Cultures of *Chlorella vulgaris* Beijerinck (UTEX 265) were grown axenically in Bold's basal media (Nichols and Bold, 1965) modified according to Maxwell et al. 1994.

Cultures were grown 400 mL capacity Photobioreactor cultivation vessels (FMT 150) which maintained at a constant temperature of 28 °C and light intensities of either 150 or 2000 μmol photons m^{-2} sec^{-1} supplied by an equal combination of red and blue light emitting diodes. Cultures were grown under continuous light (24 h photoperiod), an 18 h photoperiod or 12 h photoperiod in a 24 h cycle at both light intensities. The temperature and photoperiod regimes were maintained by the Photobioreactor control system (Photon System Instruments, Hogrova, Czech Republic).

3.2.2 Chlorophyll content

Total chlorophyll content and the chlorophyll a/b ratio were calculated as previously described (Maxwell et al. 1994). Pigments were extracted in 90% acetone (v/v) using a Mini-beadbeater (BioSpec, Bartleville, USA) and chlorophyll content was calculated according to the equations of Jeffery and Humphrey (1975). To determine the chlorophyll content on a per cell basis, cells were counted using a PhytoCyt flow cytometer (C6) with C-Plus data acquisition software (Turner Designs, Sunnyvale, USA). For cultures grown under continuous light, measurements were taken during mid-log phase. For cultures grown under a photoperiod, measurements were taken immediately following the start of the light period during mid-log phase growth.

3.2.3 Measurements of oxygen evolution

Measurements of oxygen evolution and consumption were performed on 1.5 mL of stirred samples at 28 °C in the presence of 5 mM $NaHCO_3$. Measurements were performed using a DW2 oxygen electrode with a LH11/R light probe controlled by the OxyLab control unit and data were collected using the OxyLab 32 v.1.15 software (Hansatech Instruments, King's Lynn, UK) at a series of light intensities between 0 and 600 μmol photons m^{-2} sec^{-1}. Photosynthetic rates were normalized on a per cell basis. For all photoperiods, measurements were taken within two hours of the start of the light period in mid-log phase cells.

The light saturation parameter, E_k (μmol photons m^{-2} sec^{-1}) was used to estimate the redox state of the PQ pool (Geider et al. 1996, Geider et al. 1998). E_K was calculated as $E_k = P_{max} / \alpha$ where P_{max} is the maximum light-saturated, carbon dioxide-saturated rate of oxygen (O_2) evolution (mg O_2 mL^{-1} h^{-1}) and α is the maximum slope of the oxygen-evolution under light limiting conditions (mg O_2 mL^{-1} h^{-1} (μmol photons m^{-2} sec^{-1})$^{-1}$) (Talling 1957).

3.2.4 SDS-PAGE and immunoblotting

Samples were collected during mid-log phase immediately following the start of a light period, centrifuged at 5,000 x g for 5 min at 4 °C, frozen with liquid nitrogen and stored at -80 °C. For cultures grown under continuous light, samples were collected during mid-log phase. For cultures grown under a photoperiod, samples were collected immediately following the end of a dark period during mid-log phase. Total protein was extracted with 90% (v/v/) acetone using a using a Mini-beadbeater (BioSpec, Bartlesville, USA) and pelleted by centrifugation at 16, 100 x g for 5 min at 5 °C. The pellet containing the total polypeptide was solubilized with 4% (v/v) solubilization buffer [60 mM Tris-HCl (pH 6.8), 1% (v/v) glycerol and 4% (w/v) sodium dodecyl sulfate] at 37 °C to a 1:4 ratio of protein:sodium dodecyl sulfate. Protein concentration was determined using a Pierce BCA protein assay system (Thermo Scientific, Rockford, USA).

Prior to electrophoresis, samples containing 20 μg of protein were mixed with an equal volume of loading dye [2% (v/v) β-mercaptoethanol, 13% (v/v) glycerol and 0.5% (w/v) bromophenol blue, 1% DTT]**,** heated at 80 °C for 4 min before centrifugation at 16,100 x g for 1 min to remove any unsolubilized debris. Electrophoresis was performed using the discontinuous buffer system of Laemmli (1970) with a 5% (w/v) stacking gel and a 15% (w/v) resolving gel containing 6 M urea for 3 h at 75 V. The separated polypeptides were either stained with Coomassie blue [0.2% (w/v) Coomassie blue, 50% (v/v) methanol, 7% (v/v) acetic acid] at room temperature overnight or electrophoretically transferred to a nitrocellulose membrane (Bio-Rad, Hercules, USA) at 5 °C for 1 hour at 100 V. The nitrocellulose membranes were then blocked in Block buffer [Tris buffered saline (20mM Tris (pH 7.5), 150mM NaCl), 5% (w/v) milk powder, 0.01% (v/v) Tween 20] overnight

at 5 °C before being probed with one of the following polyclonal primary antibodies from Agrisera (Vännäs, Sweden): Lhca2 (1:2,000 dilution), Lhcb2 (1:5,000 dilution), PHYA (1:10,000), PIF3, (1:10,000 dilution), psaB (1:4,000 dilution) and psbA (1:10,000 dilution); as well as Rubisco (1:5,000 dilution), which was generated by NPAH. Following incubation with horseradish peroxidase-conjugated secondary antibodies (Sigma, St. Louis, USA; 1:2,000 dilution) the antibody-protein complexes were visualized with the Amersham Biosciences enhanced chemiluminescence detection system (GE Healthcare, Little Chalfont, UK) and X-ray film (Fugi Film, Tokyo, Japan).The density of each band was quantified using Image J using ImageJ software v1.45 (http://rsbweb.nih.gov/ij/download.html) following the instructions provided by the manufacturer to determine relative changes in polypeptides abundance.

3.2.5 Room temperature chlorophyll *a* fluorescence induction

Chlorophyll *a* fluorescence induction measurements were performed on cells placed in a temperature controlled stirred cuvette using XE-PAM fluorometer (XE-PAM GDEB0146; Heinz Walz, Effeltrich, Germany) with an optical unit (ED-101US/M), a photodiode detector unit (XE-PD) and a PAM data acquisition system (PDA-100). Temperature was maintained at 28 °C through the use of a temperature control unit (US-T/R). Steady-state fluorescence parameters were determined by irradiating the sample with actinic light adjusted to the growth irradiance with a saturating pulse (2600 µmol photons m^{-2} sec^{-1}, 800 ms) applied every 30 seconds for 5 mins. For cultures grown under continuous light (CL) measurements were taken during mid-log phase. For cultures grown under a specific photoperiod, measurements were taken on mid-log phase cells immediately following the end of a dark period.

Excitation pressure was calculated as $1 - qP = (F_S - F_O')/(F_M' - F_O')$ and was used as an estimation of the redox state of the PQ pool (van Kooten and Snell, 1990) where 1 - qP estimates the proportion of closed PSII reaction centres. Partitioning of absorbed light energy was calculated where photons absorbed by the PSII antenna allocated to PSII photochemistry and photosynthetic electron transport was calculated as $\phi PSII = 1 - F_S/F_{M'}$, regulated ΔpH- and/or xanthophyll-dependent nonphotochemical quenching

(NPQ) within the PSII antenna was calculated as $\Phi NPQ = F_S/F_{M'} - F_S/F_M$ and the non-regulated, constitutive nonphotochemical energy dissipation (f,d) was calculated as $\phi f,d = F_S/F_M$ (Hendrickson et al. 2004).

3.2.6 Statistical analysis

A two-way analysis of variance (ANOVA) was conducted with irradiance and photoperiod as explanatory variables followed by a Tukey's Honest Significant Difference (HSD) multiple compression post hoc test to determine overlapping means. If an insignificant interaction term between irradiance and photoperiod was determined, the main effects of each of the factors were examined. Data were visually inspected for normality and homogeneity of variance. If equality of variance was not determined, the data were log transformed to achieve equal variance; the log transformed data were inspected for normality and equal variance. Chlorophyll a/b ratios were log transformed as log(chlorophyll a) - log(chlorophyll b) prior to statistical analysis. For statistical evaluation of energy partitioning, ΦNPQ was omitted as all values for one group were close to zero and the values for energy partitioning were sum constrained. Prior to statistical analysis ΦPSII and Φf,d were log transformed. A value of 0.05 was considered significant throughout. All statistical analysis was conducted using the statistical software package R version 3.0.2.

3.3 Results

3.3.1 Effect of photoperiod on phenotype

During growth at 28/150 (°C / µmol photons m^{-2} sec^{-1}), *C. vulgaris* developed a typical dark green LEP phenotype regardless of photoperiod (Figure 3.1A, B and C). Cells of *C. vulgaris* exhibited a typical yellow-green HEP phenotype when grown at 28/2000 under

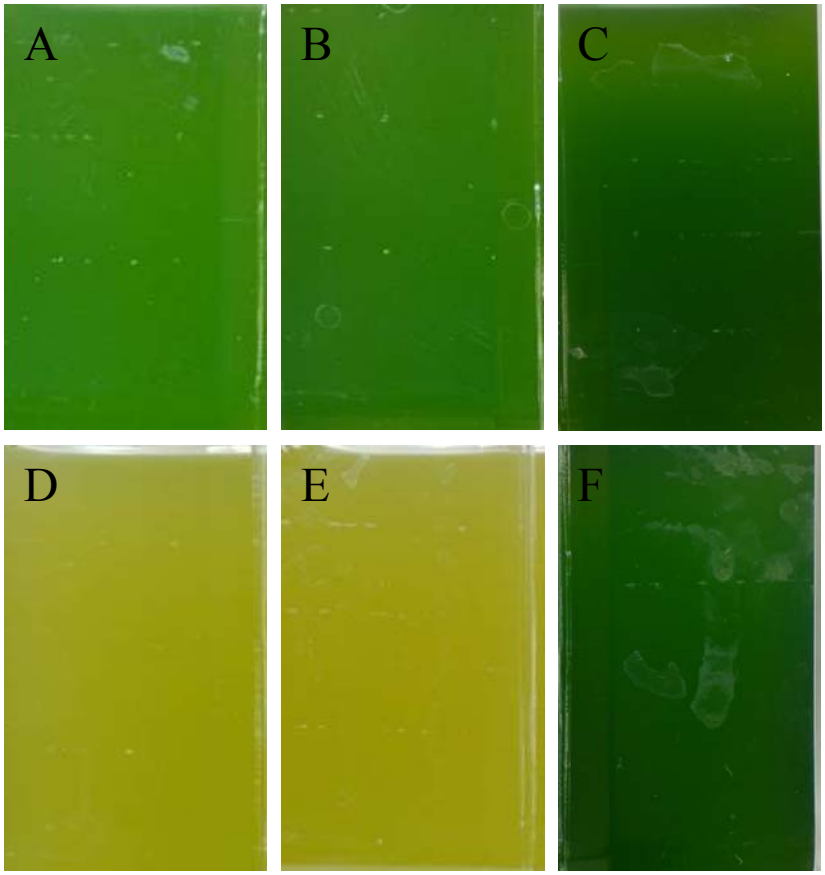

Figure 3.1 Representative phenotype for cultures of *C. vulgaris* grown at 28 °C / 150 µmol photons m^{-2} sec^{-1} and 28 °C / 2000 µmol photons m^{-2} sec^{-1} under either 24 h, 18 h and 12 h photoperiods. Phenotype was assayed immediately following the end of a dark period during mid-log phase growth. (A) 28/150 24L:0D, (B) 28/150 18L:6D, (C) 28/150 12L:12D, (D) 28/2000 24L:0D, (E) 28/2000 18L:6D, (F) 28/2000 12L:12D where values represent temperature (°C) / irradiance (µmol photons m^{-2} sec^{-1}) with length of light (L) and dark period (D) in a 24 h cycle.

continuous light (CL) (Figure 3.1D). Despite the introduction of a 6 h dark period, *C. vulgaris* grown at 28/2000 under an 18 h photoperiod still exhibited a comparable yellow-green phenotype visually indistinguishable from cells grown at 28/2000 under CL (Figure 3.1, compare D and E). However, the introduction of a 12 h dark period caused *C. vulgaris* cells grown at 28/2000 but a 12 h photoperiod to exhibit a dark green phenotype indistinguishable from low light-grown cells at 28/150 (Figure 3.1; compare A, B and C to F).

3.3.2 Effect of photoperiod on PSII excitation pressure

Figure 3.2 shows representative room temperature Chl *a* fluorescence induction traces for cells of *C. vulgaris* grown at 28/150 and 28/2000 under either CL, an 18 h photoperiod or 12 h photoperiod. Excitation pressure was measured *in vivo* using the Chl *a* fluorescence parameter 1 - qP where 1 - qP estimates the proportion of closed PSII reaction centres ($P680^+$ Pheo QA^-) (Dietz et al. 1985, Hüner et al. 1998). Cells of *C. vulgaris* grown at 28/150 exhibited comparable steady-state 1 - qP values of 0.22 to 0.27 during the light period which were approximately 3-fold lower than the steady-state of 1 - qP values of 0.69 to 0.82 exhibited by *C. vulgaris* grown at 28/2000 (irradiance, $p < 0.0001$, Table 3.2) (Table 3.1); however, within a light intensity, there were no differences in 1 - qP across the various photoperiods (photoperiod, $p = 0.0563$, Tables 3.2) (Table 3.1). Therefore, when compared at the same photoperiod, *C. vulgaris* grown at 28/150 were exposed to a relatively low PSII excitation pressure during the light period relative to cells grown at 28/2000 which were exposed to a relatively high PSII excitation pressure during the daily light period.

At 28/150, typical fluorescence induction for *C. vulgaris* grown under 18 h and 12 h photoperiods closely resembled the fluorescence induction pattern characteristic of cells grown at 28/150 under CL (Figure 3.2A, B and C). Typical Chl *a* fluorescence induction traces for cells grown under CL at 28/2000 were characterized by an initial, but transient, quenching of the fluorescence signal below F_O upon illumination by the actinic light (indicated by *), followed by a slow rise of F_S during illumination with the actinic light to a steady-state level (F_S) accompanied by an almost complete quenching of F_M' relative to

Table 3.1 Chlorophyll characteristics and steady-state chlorophyll *a* fluorescence for cultures of *C. vulgaris* grown at 28 °C / 150 µmol photons m^{-2} sec^{-1} and 28 °C / 2000 µmol photons m^{-2} sec^{-1} with 24 h, 18 h and 12 h photoperiods. Numbers under growth regime indicate growth temperature (°C) / irradiance (µmol photons m^{-2} sec^{-1}) and the length of the light (L) and dark (D) periods in a 24 h cycle. Values represent mean ± SEM; n = 3 expect Chl a/b where n = 5. Means were compared using a two-way ANOVA followed by a Tukey's HSD post hoc test; means not connected by the same letter are statistically different ($p < 0.05$). 1 - qP, photosystem II excitation pressure; Chl, chlorophyll; F_V/F_M, photosystem II photochemical efficiency.

	Growth regime					
	28/150			28/2000		
	24L:0D	18L:6D	12L:12D	24L:0D	18L:6D	12L:12D
F_V/F_M	0.67 ± 0.05[a]	0.63 ± 0.03[a]	0.64 ± 0.04[a]	0.68 ± 0.06[a]	0.59 ± 0.05[a]	0.59 ± 0.07[a]
Chl a/b	2.97 ± 0.18[b]	3.11 ± 0.44[b]	3.35 ± 0.16[b]	6.36 ± 0.54[a]	5.82 ± 0.53[a]	3.17 ± 0.28[b]
fg Chl/cell	375 ± 77[a]	328 ± 67[a]	338 ± 64[a]	180 ± 53[b]	126 ± 27[b]	300 ± 15[a]
1 - qP	0.22 ± 0.02[b]	0.25 ± 0.03[b]	0.27 ± 0.03[b]	0.69 ± 0.01[a]	0.82 ± 0.02[a]	0.80 ± 0.04[a]

Table 3.2 Results for statistical analysis (two-way ANOVA) for *C. vulgaris* grown at 150 and 2000 µmol photons m^{-2} sec^{-1} under either a 24 h, 18 h or 12 h photoperiod at 28 °C. I, irradiance; PP, photoperiod. n = 3; expect Chl a/b where n = 5.

Response variable	Source of variation	Result	Conclusion (Tukey's HSD post hoc test)
1 - qP	I	$F_{1,12} = 99.9$, $p < 0.0001$	LL < HL
	PP	$F_{2,12} = 3.7$, $p = 0.0563$	
	I * PP	$F_{2,12} = 1.4$, $p = 0.283$	
Chl a/b	I	$F_{1,24} = 39.6$, $p < 0.0001$	
	PP	$F_{2,24} = 6.9$, $p = 0.00413$	
	I * PP	$F_{2,24} = 13.3$, $p = 0.0001$	LL24h = LL18h = LL12h = HL12h < HL24h = HL18h
Chl $cell^{-1}$	I	$F_{1,12} = 36.1$, $p < 0.0001$	
	PP	$F_{2,12} = 5.0$, $p = 0.0263$	
	I * PP	$F_{2,12} = 4.6$, $p = 0.0324$	HL24h = HL18h < LL24h = LL18h = LL12h = HL12h
F_V/F_M	I	$F_{1,12} = 4.5$, $p = 0.0556$	
	PP	$F_{1,12} = 1.3$, $p = 0.325$	
	I * PP	$F_{2,12} = 0.2$, $p = 0.797$	
Φ_{PSII}	I	$F_{2,12} = 155.2$, $p < 0.0001$	HL< LL
	PP	$F_{2,12} = 2.2$, $p = 0.160$	
	I * PP	$F_{2,12} = 0.717$, $p = 0.508$	
$\Phi_{f,d}$	I	$F_{2,12} = 7.4$, $p = 0.0188$	LL< HL
	PP	$F_{2,12} = 4.5$, $p = 0.0350$	24h=12h<18h

	I * PP	$F_{2,12} = 1.7$, $p = 0.220$	
P_{MAX}	I	$F_{1,12} = 21.1$, $p = 0.0006$	
	PP	$F_{2,12} = 24.3$, $p < 0.0001$	
	I * PP	$F_{2,12} = 7.4$, $p = 0.008$	HL24h = HL18h < LL24h = LL18h = LL12h = HL12h
Slope	I	$F_{2,12} = 25.6$, $p = 0.0003$	
	PP	$F_{2,12} = 16.3$, $p = 0.0004$	
	I * PP	$F_{2,12} = 4.3$, $p = 0.0391$	HL24h = HL18h < LL24h = LL18h = LL12h = HL12h
Respiration	I	$F_{1,12} = 0.2$, $p = 0.694$	
	PP	$F_{2,12} = 2.0$, $p = 0.173$	
	I * PP	$F_{2,12} = 0.9$, $p = 0.439$	
E_K	I	$F_{2,12} = 17.3$, $p = 0.001$	LL < HL
	PP	$F_{2,12} = 2.3$, $p = 0.140$	
	I * PP	$F_{2,12} = 15.5$, $p = 0.261$	

HL, high light; HL24h, HL18h and HL12h, high light with 24 h, 18 h and 12 h photoperiod, respectively; LL, low light; LL24h, LL18h and LL12h, low light with 24 h, 18 h and 12 h photoperiod, respectively.

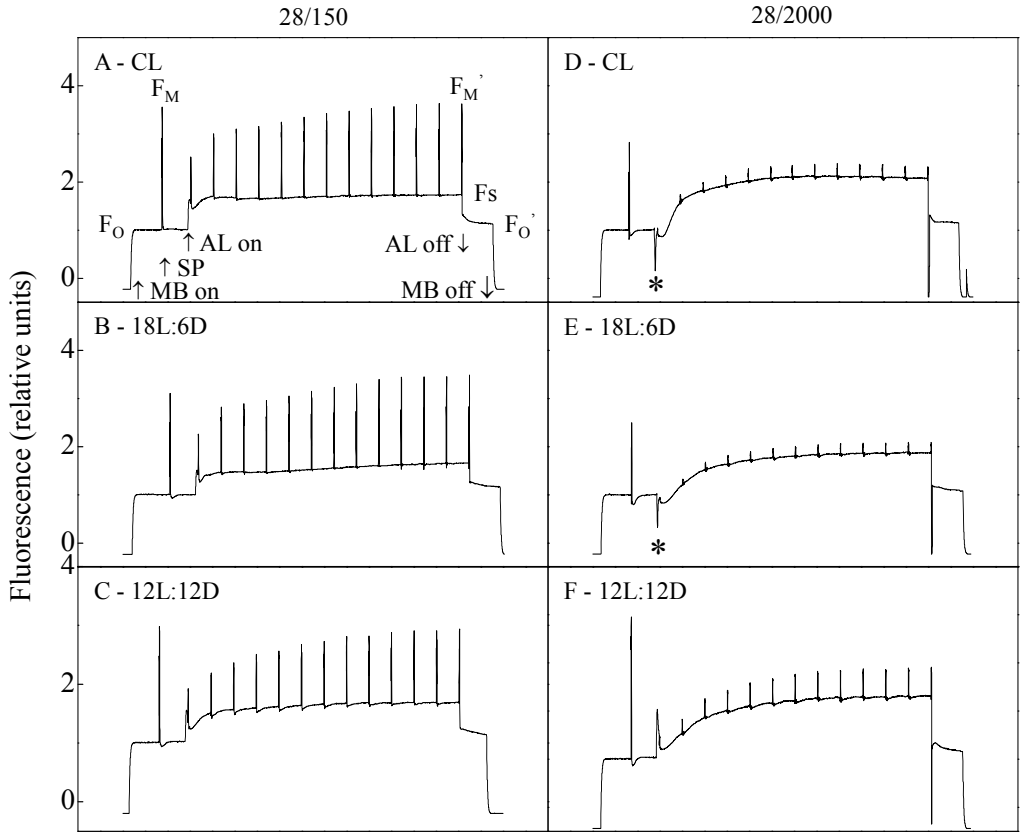

Figure 3.2 Representative room temperature chlorophyll *a* fluorescence induction curves for *C. vulgaris* grown at 28 °C / 150 µmol photons m^{-2} sec^{-1} and 28 °C / 2000 µmol photons m^{-2} sec^{-1} with 24 h, 18 h and 12 h light periods in a 24 h cycle. (A) 28/ 150 24L:0D, (B) 28/150 18L:6D, (C) 28/150 12L:12D, (D) 28/2000 24L:0D, (E) 28/2000 18L:6D and (F) 28/2000 12L:12D where values indicate growth temperature (°C) / irradiance (µmol photons m^{-2} sec^{-1}) and the length of light (L) and dark (D) periods in a 24 h cycle. AL, actinic light; MB, measuring mean; SP, saturating pulse.

cells grown under CL but 28/150 (Figure 3.2, compare A to D). At 28/2000, fluorescence induction of cells grown under an 18 h photoperiod resembled the induction pattern characteristic of C. *vulgaris* grown at 28/2000 under CL (Figure 3.2D and E). However, the introduction of a 12 h dark period at 28/2000 caused the initial, transient quenching of the fluorescence signal to disappear and the kinetics for the rise in F_S to more closely resemble the induction pattern characteristic of cells grown at 28/150 (Figure 3.2, compare A,B and C to F); however, the extent of quenching of F_M' appeared to be more characteristic of *C. vulgaris* at 28/2000 under either CL or an 18 h photoperiod (Figure 3.2E).

3.3.3 Effect of photoperiod of Chl content

Consistent with the dark green phenotype, cells of *C. vulgaris* grown at LEP at 28/150 exhibited comparably low Chl a/b ratios of 2.97 to 3.35 across all photoperiods (irradiance*photoperiod, $p = 0.0001$, Tukey's HSD $p > 0.05$, Table 3.2) (Table 3.1). Similarly, consistent with the yellow-green HEP phenotype, cells grown at HEP at 28/2000 under either CL or an 18 h photoperiod exhibited 2-fold higher Chl a/b ratios of 6.36 and 5.82, respectively, relative to LEP cells (Tukey's HSD $p < 0.05$, Table 3.2) (Table 3.1). However, compared to HEP cells grown at 28/2000 under either CL or an 18 h photoperiod, *C. vulgaris* grown at HEP but a 12 h photoperiod exhibited a 2-fold lower Chl a/b ratio of 3.17 (Tukey's HSD $p < 0.05$, Table 3.2) despite growth and development at a high light intensity (Table 3.1); furthermore, the Chl a/b ratio exhibited by HEP cells grown at 28/2000 under a 12 h photoperiod was similar to that of cells grown at LEP (Tukey's HSD $p > 0.05$, Table 3.2).

A similar pattern for the effect of photoperiod was obtained for total cellular Chl content (irradiance*photoperiod, $p = 0.0234$, Table 3.2) (Table 3.1). Cells of *C. vulgaris* grown either at LEP or at HEP with a 12 h photoperiod exhibited Chl contents that were approximately 2-fold higher (Tukey's HSD $p < 0.05$, Table 3.2) relative to HEP cells grown at 28/2000 under either CL or an 18 h photoperiod (Table 3.1). Thus, the presence of the dark-green, LEP phenotype, with concomitantly low Chl a/b ratio and high cellular

Chl content, in *C. vulgaris* grown at HEP at 28/2000 under a 12 h indicated an "uncoupling" of daytime PSII excitation pressure and the predicted phenotype.

3.3.4 Effect of photoperiod on polypeptide accumulation

The relative abundance of the representative light-harvesting complex polypeptide of PSII, Lhcb2, remained comparable across all photoperiods in *C. vulgaris* grown at 28/150 (Figure 3.3). The marked increase in the Chl a/b ratio in HEP cells grown at 28/2000 under either CL or an 18 h photoperiod was reflected in an approximately 40% lower Lhcb2 polypeptide abundance relative to LEP cells grown at 28/150 at all photoperiods (Figure 3.3 and Table 3.1). In contrast, the low Chl a/b ratio in *C. vulgaris* grown at HEP but a 12 h photoperiod was reflected in an approximately 30% increase in Lhcb2 abundance relative to HEP cells grown at 28/2000 under either CL or an 18 h photoperiod (Figure 3.3 and Table 3.1). Furthermore, HEP cells of *C. vulgaris* grown at 28/2000 under a 12 h photoperiod exhibited Lhcb2 levels comparable to growth at LEP (Figure 3.3).

The abundance of the representative light harvesting polypeptide of PSI, Lhca2, followed a similar trend to that of Lhcb2 (Figure 3.3). The abundance of Lhca2 was comparable across all photoperiods for LEP cells grown at 28/150 whereas HEP cells grown at 28/2000 under either CL or an 18 h photoperiod exhibited approximately 43% and 61% decreases in Lhca2 abundance, respectively (Figure 3.3). In contrast, Lhca2 abundance increased 2.5-fold during growth at 28/2000 but a 12 h photoperiod relative to cells grown at HEP under either CL or an 18 h photoperiod (Figure 3.3). Thus, *C. vulgaris* displayed a dark green phenotype at 28/150 which was mimicked by growth at HEP but a 12 h photoperiod (Figure 3.1). Concomitantly, these cells grown at 28/2000 under a 12 h photoperiod exhibited increases in LHCII and LHCI polypeptide abundance relative to the yellow-green cells grown at HEP under either CL or an 18 h photoperiod (Figure 3.3).

While photoperiod did not affect the relative abundance of the representative PSII reaction centre polypeptide PsbA in cells grown at 28/150, PsbA levels were sensitive to photoperiod as a consequence of growth at HEP and decreased by up to 45% with

A

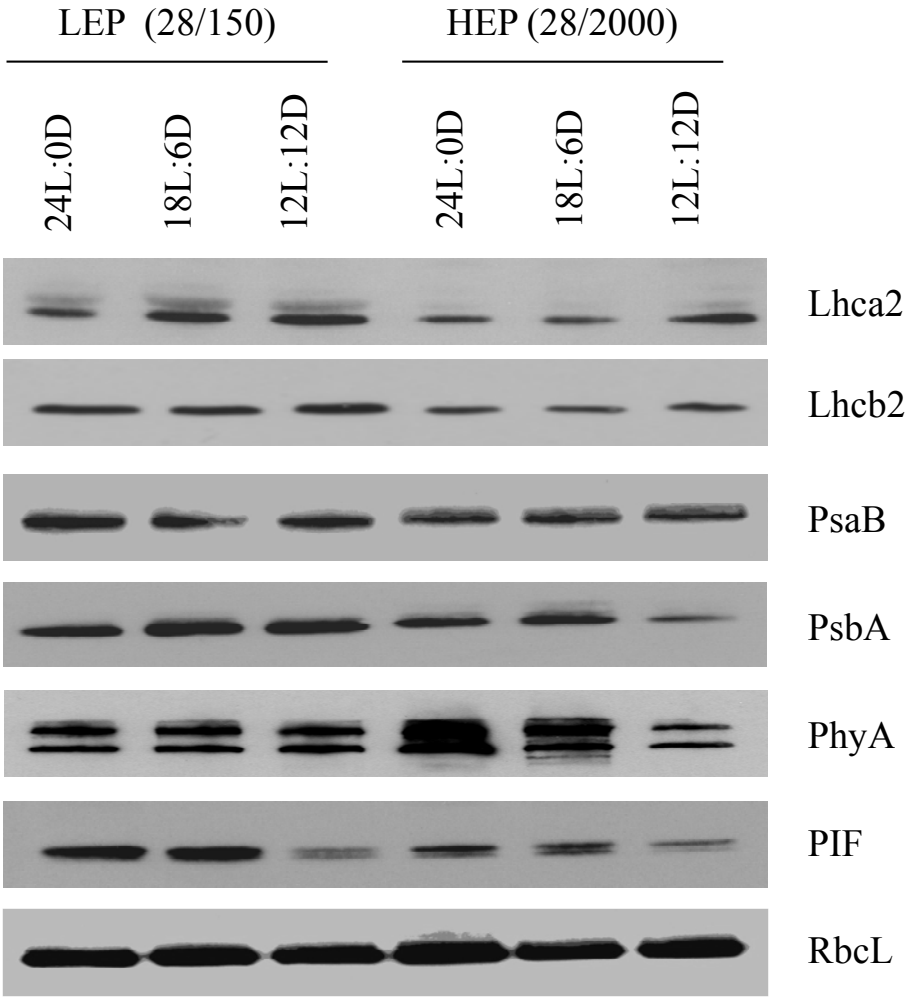
LEP (28/150)
HEP (28/2000)
24L:0D
18L:6D
12L:12D
24L:0D
18L:6D
12L:12D
Lhca2
Lhcb2
PsaB
PsbA
PhyA
PIF
RbcL

B

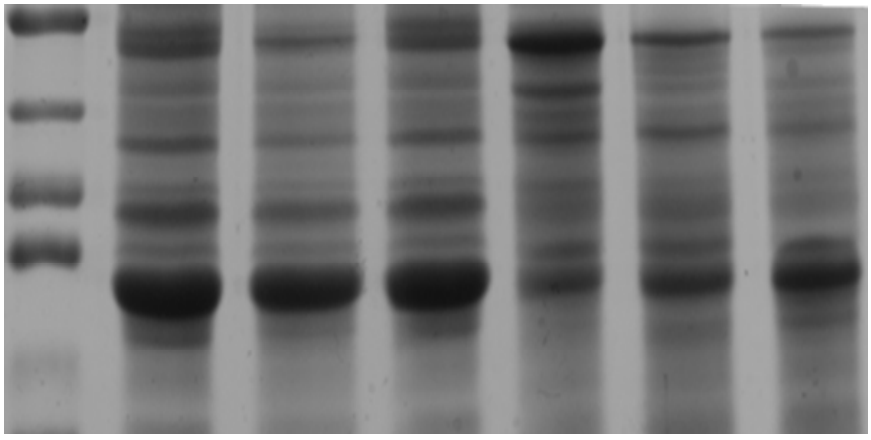

Figure 3.3 Change in polypeptide abundance for cultures of *C. vulgaris* grown at low excitation pressure (LEP) at 28 °C / 150 µmol photons m^{-2} sec^{-1} and high excitation pressure (HEP) at 28 °C / 2000 µmol photons m^{-2} sec^{-1} with 24 h, 18 h and 12 h light periods in a 24 h cycle. Numbers above the immunoblots indicate growth temperature (°C) / irradiance (µmol photons m^{-2} sec^{-1}) followed by the length of light (L) and dark (D) periods in a 24 h cycle. (A) Representative immunoblots against LHCI (Lhca2), LHCII (Lhcb2), PSI reaction centre polypeptide (PsaB), D1 polypeptide of PSII (PsbA), phytochrome A (PhyA), phytochrome interacting factor 3 (PIF3), and the large subunit of Rubisco (RbcL). (B) Representative Coomassie Brilliant Blue stained gel showing separated polypeptides; each lane was loaded with 20 µg of protein.

decreasing photoperiod at 28/2000; moreover, when compared at the same photoperiod, LEP cells had a relatively greater abundance of PsbA polypeptides relative to HEP cells (Figure 3.3). However, no changes in the abundance of either PsaB, a representative PSI reaction centre polypeptide, or RbcL, the large-subunit of Rubisco, were detected regardless of growth light intensity and photoperiod (Figure 3.3). This indicated that not all plastid-localized polypeptides changed in abundance during growth and development under varying photoperiods in *C. vulgaris*.

Light quality perception mediated by light sensitive photoreceptors such as phytochromes is critical for the generation of "biogenic" signals involved in photomorphogenesis (Pogson et al. 2008, Pogson and Albrecht, 2011, Casal 2013, Kianianmomeni and Hallmann 2014). To assess the impact of PSII excitation pressure and photoperiod on components of phytochrome signalling the levels of phytochrome A (PHYA) and the phytochrome-interacting factor 3 (PIF3) were assessed (Figure 3.3). There was a 2-fold decrease in the abundance of PIF3 at the 12 h photoperiod in both LEP and HEP cells as well as a 3-fold decrease in PHYA at the 12 h photoperiod in HEP grown cells (Figure 3.3).

3.3.5 Effect of photoperiod on PSII functionality

All cultures exhibited comparably high PSII photochemical efficiencies, as measured by F_V/F_M (irradiance, $p = 0.0556$; photoperiod $p = 0.325$, Table 3.2), indicating that none of the cultures were photoinhibited (Table 3.1). Figure 4 demonstrates the response of excitation pressure, estimated as 1 - qP, to increased measuring light intensity. In all cultures, 1 - qP increased with increasing irradiance reflecting the closure of PSII reaction centres (Figure 3.4). The maximum initial slope of the light response curves in Figure 3.4 estimates of the number of photons required to convert an open PSII reaction centre (P680 Pheo Q_A) to a closed reaction centre ($P680^+$ Pheo QA^-), providing an estimate of the quantum requirement for PSII closure. The quantum requirement to close 50% of PSII reaction centres in LEP cells grown at 28/150 was about 574, 432 and 491 for the 24 h, 18 h and 12 h photoperiods, respectively. The quantum requirement increased to

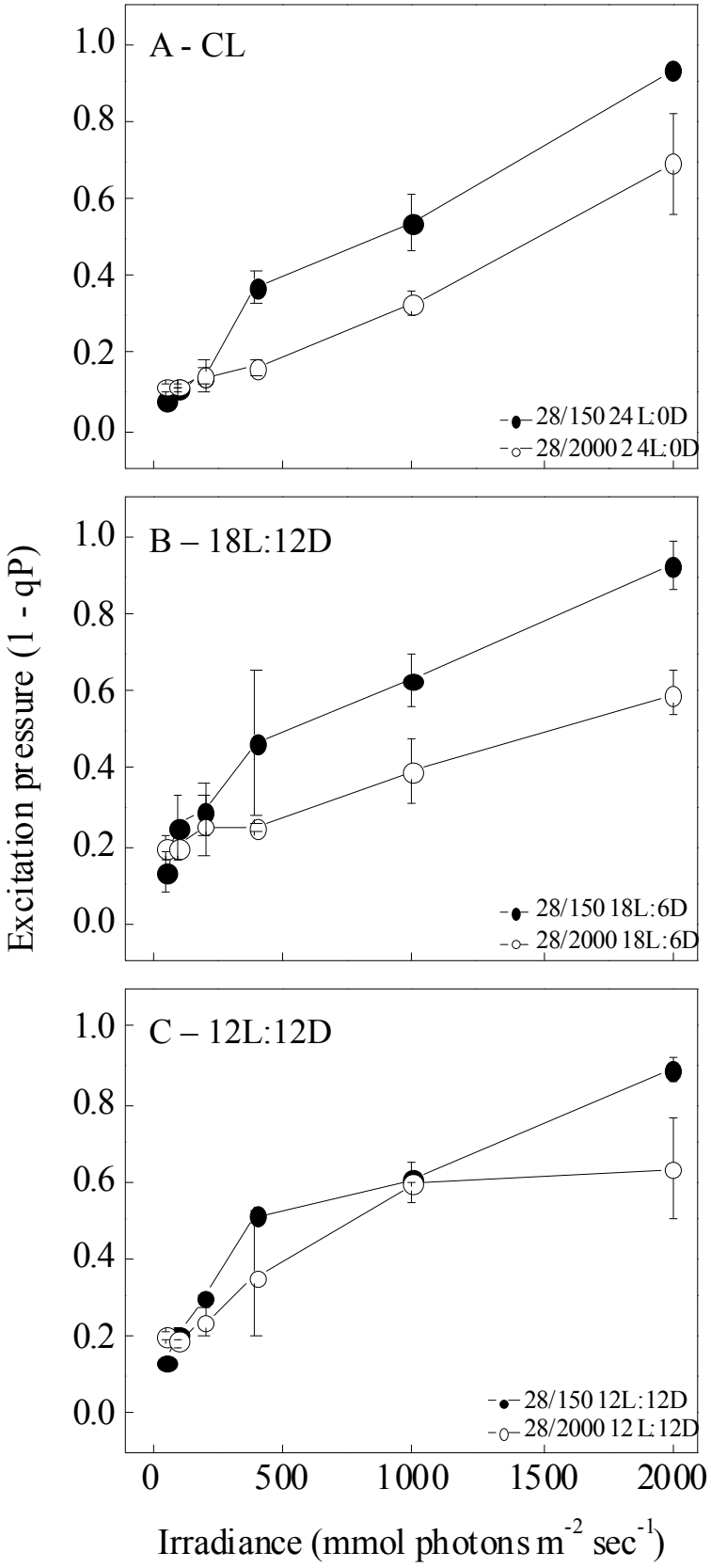
A - CL
B – 18L:12D
C – 12L:12D
28/150 24 L:0D
28/2000 2 4L:0D
28/150 18L:6D
28/2000 18L:6D
28/150 12L:12D
28/2000 12 L:12D
Excitation pressure (1 - qP)
Irradiance (mmol photons m-2 sec-1)
0.0
0.2
0.4
0.6
0.8
1.0
0
500
1000
1500
2000

Figure 3.4 Excitation pressure light responses curves for *C. vulgaris* grown at low excitation pressure (LEP; 28 °C / 150 µmol photons m^{-2} sec^{-1}) and high excitation pressure (HEP; 28 °C / 2000 µmol photons m^{-2} sec^{-1}) under either continuous light (24L:0D), an 18 h photoperiod (18L:6D) or a 12 h (12L:12D) photoperiod. Closed symbols represent LEP cells. Open symbols represent HEP cells. Numbers in the legends indicate temperature (°C) / irradiance (µmol photons m^{-2} sec^{-1}) and the length of the light (L) and dark (D) periods in a 24 h cycle. Values represent mean ± SEM; n = 3.

approximately 700, 612 and 725 for *C. vulgaris* grown at HEP at either CL, an 18 h photoperiod or a 12 h photoperiod, respectively. The 22 to 48% increase in the quantum requirement for PSII closure for HEP cells grown at 28/2000 relative to cells grown at LEP but the same photoperiod reflects a decreased probability of reaction centre closure in cells grown at HEP regardless of photoperiod.

HEP cells of *C. vulgaris* grown at 28/2000 exhibited an approximately 4-fold reduction in the capacity to use absorbed light energy to drive PSII photochemistry (ϕPSII) (irradiance, $p < 0.0001$, Table 3.2) as well as induction of the capacity to dissipate excess energy through regulated thermal dissipation through nonphotochemical quenching (ϕNPQ) (Figure 3.5). Cells grown under HL at 28/2000 demonstrated a significantly higher capacity for energy dissipation through constitutive quenching (irradiance, $p = 0.0188$, Table 3.2) (ϕf,d) (Figure 3.5). Furthermore, there was a significant increase ϕf,d in cells grown under an 18 h photoperiod (photoperiod, $p = 0.0350$, Tukey's HSD $p < 0.05$, Table 3.2) (Figure 3.5). When compared at the same photoperiod, *C. vulgaris* grown at HEP under a 12 h photoperiod exhibited a 25% increase in the capacity for energy dissipation through constitutive quenching relative to cells grown at LEP and the same photoperiod (ϕf,d) (Figure 3.5). There was a 10% increase in ϕf,d in HEP cells grown at 28/2000 under an 18 h photoperiod and only a 2% increase in ϕf,d in HEP cells under CL relative to the LEP cells grown at 28/150 under an 18 h photoperiod and CL, respectively (Figure 3.5). Therefore, while cells grown at HEP under a 12 h photoperiod were similar to cells grown at LEP in terms of pigmentation (Figure 3.2), cellular Chl content (Table 3.1) and Lhcb2 levels (Figure 3.3), they differed in the capacity for energy partitioning and more closely resembled cells grown at HEP under either CL or an 18 h photoperiod (Figure 3.5).

3.3.6 Effect of photoperiod on oxygen evolution

When grown under CL, the dark green LEP cells of *C. vulgaris* grown at 28/150 exhibited an approximately 2.5-fold higher maximum, light-saturated rate of oxygen evolution relative to the yellow-green HEP cells grown at CL but 28/2000 (irradiance*photoperiod, $p = 0.008$, Tukey's HSD $p = 0.010$, Table 3.2) (Figure 3.6A,○).

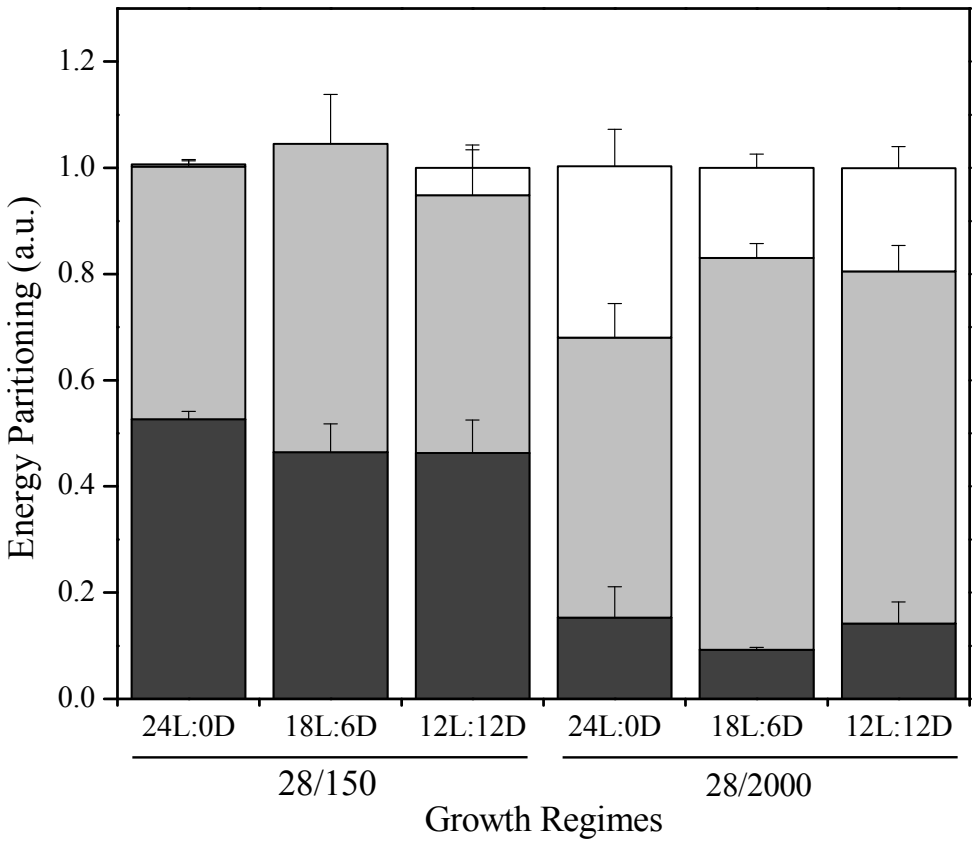

Figure 3.5 Proportion of absorbed light energy consumed through photosystem II photochemistry (ΦPSII) (dark gray), fluorescence and constitutive thermal dissipation (Φf,d) (gray) and xanthophyll-dependent thermal dissipation (ΦNPQ) (white) during steady-state photosynthesis for *C. vulgaris* grown at 28 °C / 150 µmol photons m^{-2} sec^{-1} and 28 °C / 2000 µmol photons m^{-2} sec^{-1} with 24 h, 18 h and 12 h light periods in a 24 h cycle. Numbers under bars indicate temperature (°C) / irradiance (µmol photons m^{-2} sec^{-1}) and the length of the light (L) and dark (D) periods in a 24 h cycle. Values represent mean ± SEM; n = 3.

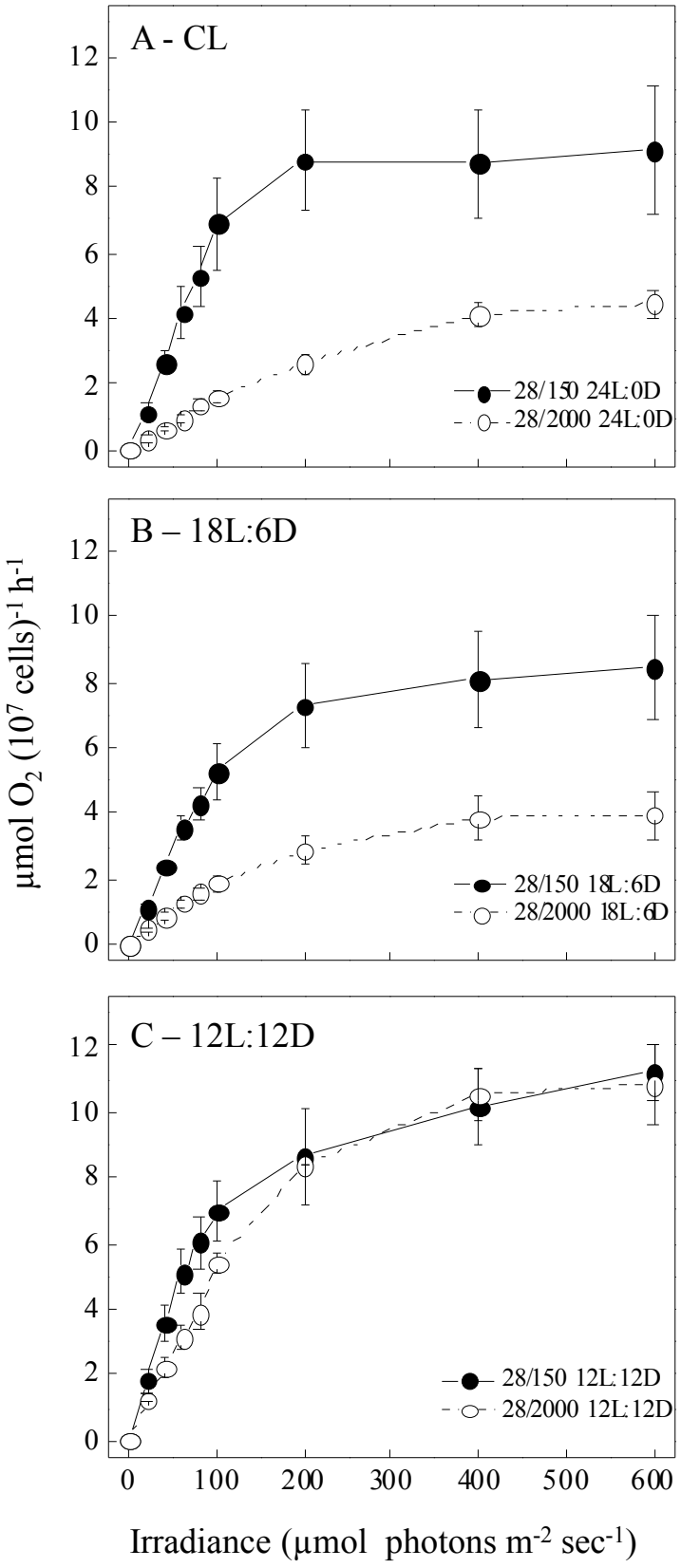
A - CL
B – 18L:6D
C – 12L:12D
28/150 24L:0D
28/2000 24L:0D
28/150 18L:6D
28/2000 18L:6D
28/150 12L:12D
28/2000 12L:12D
µmol O2 (10^7 cells)^-1 h^-1
Irradiance (µmol photons m^-2 sec^-1)
0
2
4
6
8
10
12
0
100
200
300
400
500
600

Figure 3.6 Oxygen evolution light response curves for *C. vulgaris* grown at low excitation pressure (LEP) at 28 °C / 150 µmol photons m^{-2} sec^{-1} and high excitation pressure (HEP) at 28 °C / 2000 µmol photons m^{-2} sec^{-1} under either continuous light (CL; 24L:0D), an 18 h photoperiod (18L:6D) or a 12 h photoperiod (12L:12D). Measurements presented are for gross oxygen evolution. Numbers in the legends indicate temperature (°C) / irradiance (µmol photons m^{-2} sec^{-1}) and the length of the light (L) and dark (D) periods in a 24 hour cycle. Values represent mean ± SEM; n= 3 (where not visible, error bars are smaller than the symbol).

Similar results were observed for cells grown at either LEP or HEP but an 18 h photoperiod (Tukey's HSD = 0.012, Table 3.2) (Figure 3.6B). However, under a 12 h photoperiod, *C. vulgaris* grown at 28/2000 exhibited comparable light-saturated rates of oxygen evolution relative to LEP cells grown at 28/150 (Tukey's HSD p = 0.99, Table 3.2) (Figure 3.6C). Therefore, when compared on a per cell basis, cultures of *C. vulgaris* with a dark green LEP phenotype exhibited 2-fold higher photosynthetic capacities relative to cells displaying a yellow-green HEP pigmentation (Figure 3.2, and Tables 3.2 and 3.3).

A similar trend for the effect of photoperiod on photosynthetic efficiency, calculated as the maximum initial slopes of the light response curves for oxygen evolution in Figures 3.6A, B and C, was measured (irradiance*photoperiod, p = 0.039, Table 3.2). Photosynthetic efficiency was 2-fold higher in LEP cells of *C. vulgaris* grown at 28/150 under either CL or an 18 h photoperiod relative to HEP cells grown at 28/2000 under either CL (Tukey's HSD p = 0.034, Table 3.2) or an 18 h photoperiod, respectively (Tukey's HSD p = 0.0026), Table 3.2) (Figures 3.6A and B). However, photosynthetic efficiency was comparable in LEP grown cells and HEP cells grown under a 12 h photoperiod (Tukey's HSD p = 0.425, Table 3.2) (Figure 3.6C). Thus, LEP cells of *C. vulgaris* grown at 28/150 were photosynthetically comparable regardless of the day length (Figure 3.6 and Table 3.3). Consistent with the recovery of the dark-green pigmentation in HEP cells grown at 28/2000 under a 12 h photoperiod (Figure 3.1), these cells were photosynthetically comparable to *C. vulgaris* grown at LEP (Figure 3.6C and Table 3.3). However, neither irradiance nor photoperiod significantly affected the rate of dark respiration (irradiance, p = 0.694; photoperiod, p = 0.173, Tables 3.2) (Table 3.3).

The light-saturation parameter (E_K) represents the light intensity at which the electrons generated through PSII photochemistry match the capacity to consume these electrons through metabolic sinks (Falkowski and Chen 2003). E_K is calculated directly from the oxygen evolution light response curves and is independent of the variable used to normalize measurements. E_K has further been suggested to provide an estimation of the relative redox state of the PQ pool (Geider et al. 1996). LEP cells of *C. vulgaris* grown at

Table 3.3 Oxygen evolution for *C. vulgaris* grown at 28 °C / 150 µmol photons m^{-2} sec^{-1} and 28 °C / 2000 µmol photons m^{-2} sec^{-1} with 24 h, 18 h and 12 h photoperiods. Numbers under growth regime indicate growth temperature (°C) / irradiance (µmol photons m^{-2} sec^{-1}) and the length of the light (L) and dark (D) periods in a 24 h cycle. Values represent mean ± SEM; n = 3. Means were compared using a two-way ANOVA followed by Tukey's HSD test; means not connected by the same letter are statistically different ($p < 0.05$). E_K, saturating irradiance (µmol photons m^{-2} sec^{-1}); P_{MAX}, photosynthetic capacity (µmol O_2 evolved $(10^7$ cells$)^{-1}$ h^{-1}); Resp., dark respiration (µmol O_2 consumed $(10^7$ cells$)^{-1}$ h^{-1}); Slope, initial slope or photosynthetic efficiency (µmol O_2 $(10^7$ cells$)^{-1}$ (µmol photons m^{-2} $sec^{-1})^{-1}$).

	Growth regime					
	28/150			28/2000		
	24L:0D	18L:6D	12L:12D	24L:0D	18L:6D	12L:12D
P_{MAX}	9.80 ± 0.93[a]	8.95 ± 1.28[a]	9.19 ± 1.32[a]	4.06 ± 0.36[b]	3.17 ± 0.45[b]	9.80 ± 0.95[a]
Slope	0.04 ± 0.002[a]	0.05 ± 0.006[a]	0.05 ± 0.003[a]	0.02 ± 0.007[b]	0.02 ± 0.002[b]	0.05 ± 0.006[a]
E_K	180 ± 17[a]	137 ± 37[a]	160 ± 10[a]	210 ± 31[b]	201± 9[b]	255 ± 56[b]
Resp.	1.69 ± 0.42[a]	1.54 ± 0.39[a]	1.66 ± 0.50[a]	0.96 ± 0.24[a]	1.11 ± 0.32[a]	1.88 ± 0.19[a]

28/150 exhibited E_K values of 137 to 180 µmol photons m^{-2} sec^{-1} which were between 15% and 37% lower than the E_K values of 201 to 255 µmol photons m^{-2} sec^{-1} exhibited by HEP cells grown at 28/2000 (irradiance, p = 0.001, Table 3.2) (Table 3.3); however, there was no difference in E_K across photoperiod (photoperiod, p = 0.140, Tables 3.2) (Table 3.3). The relatively higher values for E_K obtained from the light response curves for oxygen evolution supported the data for excitation pressure which was based on Chl *a* fluorescence induction (Tables 3.1 and 3.3).

3.4 Discussion

LHCII polypeptide abundance has been demonstrated to be reduced in a similar capacity by either continuous high light, low temperature or DBMIB in green algae (Maxwell et al. 1994, Escoubas et al. 1995, Maxwell et al. 1995, Maxwell et al. 1995b, Król et al. 1997). Based on these findings, it was concluded that LHCII accumulation is regulated by PSII excitation pressure as opposed to light or temperature *per se* under steady illumination in green algae (Maxwell et al. 1994; Hüner et al. 1998; Ensminger et al. 2006). These findings in green algae are supported by the work of Walters and colleagues who demonstrated that photoacclimation of the photosynthetic apparatus to changes in irradiance occur independently of sensing and signalling pathways mediated by photoreceptors in *A. thaliana* (Walters et al. 1999). The results of this study show that although PSII excitation pressure is a factor regulating photoacclimation, it is not the sole regulator of photoacclimation in *C. vulgaris*.

When grown at a LEP growth regime at 28/150, the duration of the daily photoperiod did not appear to influence the photoacclimation response in *C. vulgaris*. LEP cells grown at 28/150 under either an 18 h photoperiod or 12 h photoperiod exhibited the dark green pigmentation (Figure 3.1), high Chl per cell as well as low Chl a/b (Table 3.1) with concomitantly high LHCII abundance (Figure 3.3) typical of cells acclimated under CL at LEP. These trends remained consistent irrespective of whether samples were taken at the start or end of the light period (Supplemental Figure S3.1). As both 1 - qP and E_K, independent measures of the relative redox state the PQ pool, indicate cells were exposed to comparably low PSII excitation pressure during the light period, we suggest that

despite the introduction of a dark period during growth and development at LEP, PSII antenna size as well as the associated phenotype appear to be insensitive to photoperiod.

At HEP (28/2000), however, the length of the photoperiod had a distinct effect on PSII antenna size as measured by Chl and LHCII abundance. Cells of *C. vulgaris* grown at HEP under a 12 h photoperiod exhibited the dark-green phenotypic response (Figure 3.1F) typical of growth and development under LEP and displayed a characteristically high cellular Chl content per cell and low Chl a/b ratio (Table 3.1). At 28/2000, when the photoperiod was increased above 12 h to either a 14 h or 16 h photoperiod the values obtained for the Chl a/b ratio, a proxy for phenotype, never yielded a clear pattern (Supplemental Table S3.1). Only when the photoperiod was increased to a 18 h light period did the phenotypic response become reproducible.

Despite the introduction of a 6 h dark period, HEP cells of *C. vulgaris* grown at 28/2000 under an 18 h photoperiod exhibited the yellow-green pigmentation (Figure 3.1E), low Chl per cell and high Chl a/b (Table 3.1) with concomitantly reduced LHCII abundance (Figure 3.3) as well as reduced photosynthetic capacity and efficiency (Figure 3.6B) typical of cells acclimated to continuous high PSII excitation pressure at 28/2000 under CL. This indicates that cells of *C. vulgaris* grown at 28/2000 under an 18 h photoperiod both structurally and functionally mimic *C. vulgaris* photoacclimated to continuous high PSII excitation pressure. Although the introduction of a dark period should relax excitation pressure due to the absence of light energy required to close PSII reaction centres, these cells appear to remain locked in a HEP-acclimated state despite the six hours of darkness. Similarly, Post et al. (1984) demonstrated that photoacclimation in the cells of the diatom *Thalassiosira weisflogii* did not respond to the daily 12 h photoperiod as the cells did not photoacclimate in response to darkness; rather photoacclimation was correlated with the average irradiance during the light period.

At 28/2000 under a 12 h photoperiod, based on phenotype (Figure 3.1), Chl content (Table 3.1), LHCII abundance (Figure 3.3), as well as photosynthetic capacity and efficiency (Figure 3.6) we conclude that *C. vulgaris* are both structurally and

photosynthetically comparable to cells grown at LEP at 28/150. Surprisingly, these cells appear to mimic the responses characteristic of photoacclimation to LEP despite exposure to HEP. Thus, regulation of phenotype in *C. vulgaris* UTEX 265 can be "uncoupled" from the relative redox state of the PQ pool by the duration of the photoperiod. Consequently, the redox state of the PQ pool cannot be the sole determinate of phenotype and photoacclimation in *C. vulgaris* during growth and development under variable photoperiods. In contrast to previous reports that assume that excitation pressure alone regulates photoacclimation in *C. vulgaris* is incorrect (Maxwell et al. 1994, Maxwell et al. 1995a, Maxwell et al. 1995b, Hüner et al. 1998, Wilson and Hüner 2000, Wilson et al. 2003, Hüner et al. 2012), we conclude that photoacclimation in *C. vulgaris* is both redox- and photoperiod-dependent.

The comparable levels of both Chl and LHCII in *C. vulgaris* grown at HEP but a 12 h photoperiod relative to cells grown at LEP were surprising as cells grown at 28/2000 are exposed to approximately 13-times more photons during the 12 h light period relative to cells grown at 28/150. Therefore, a mechanism must be in place to provide protection from the potential photodamage associated with prolonged exposure to high light. Normally, exposure to high light elicits short-term photoprotective mechanisms including the induction of the xanthophyll cycle that protect against photodamage of the photosynthetic apparatus by decreasing the efficiency of light energy transfer (Demmig-Adams and Adams III 2000). Consistently, despite the phenotypic similarities, *C. vulgaris* at 28/2000 under a 12 h photoperiod exhibit an 80% increase in the capacity to dissipate excess light energy as heat through the xanthophyll cycle (ΦNPQ) and a 4-fold reduction in the capacity to use light energy to drive PSII photochemistry (ΦPSII) relative to cells at grown under 28/150 (Figure 3.5). Quenching of absorbed light energy through the xanthophyll cycle is considered to be the primary, inducible process contributing to photoprotection through nonphotochemical dissipation of excess light energy (Demmig-Adams and Adams III 1992, Demmig-Adams and Adams III 2000). Low lumenal pH results in the conversion of violaxanthin to zeaxanthin, the presence of which allows for thermal dissipate of excess excitation energy (Demmig-Adams et al. 1996, Gilmore 2001). *C. vulgaris* grown at 28/2000 under a 12 h photoperiod also exhibit

the greatest increase in the capacity for constitutive thermal dissipation (Φf,d) (Figure 3.5). The mechanism for non-regulated constitutive quenching of excitation energy remains equivocal but it has been suggested to reflect PSII reaction centre quenching (Hüner et al. 2003). Therefore, while structurally *C. vulgaris* at grown 28/2000 under a 12 h photoperiod mimics LEP cells grown at 28/150, in terms of the cellular capacity for energy dissipation these cells are functionally comparable to high-light grown cultures.

We conclude that the structural responses at the level of PSII antenna size appear to be dependent on both the extent of excitation pressure during the light period as well as the duration of the daily light period. This raises several questions. Firstly, how do cells measure day length? During photoperiodic development photoreceptors provide light input signals to the circadian clock while phytochromes specifically enable responses the far-red/red range of light (Casal 2013; Kianianmomeni and Hallmann 2014). Light-quality specific signal transduction is facilitated by phytochrome-specific target proteins including phytochrome-interacting factors (Shin et al. 2013). Interestingly, distinct responses for PHYA and the PIF3 in response to photoperiod were measured as both PIF3 and PHYA abundance decreased during growth under a 12 h photoperiod (Figure 3.6). The reduced accumulation of both PhyA and PIF3 under a 12 h photoperiod may indicate a differential impact on the core oscillator and clock function in a manner that potentially influences clock output signals under this photoperiod.

Length of the daily light period has a distinct response on photosynthetic acclimation in *C. vulgaris*. This is analogous to research in *A. thaliana* where acclimation to a short-day photoperiod mimicked the structural responses, including increased Chl content, increased leaf biomass and decreased Chl a/b ratio, characteristic of shade acclimated leaves (Lepisto et al. 2009). Photoperiod has additionally been demonstrated to differentially influence the stress response to hydrogen peroxide and ozone in *A. thaliana* (Queval et al. 2007, Queval et al. 2012) and *Trifolium subterraneum* (Vollsnes et al. 2009), respectively. In *A. thaliana,* day length specific responses appear to be under the control of a genetic program as opposed to representing a response to differential exposure time to stressful conditions *per se* (Chaouch and Queval 2010; Chaouch and

Noctor 2010). Based on the distinct and discrete responses elicited by 18 h and 12 h photoperiods at 28/2000, and the differential accumulation of PHYA and PIF3, we suggest that the phenotypic response to high PSII excitation pressure under 18 h and 12 h photoperiods in *C. vulgaris* likely represents a response to intrinsic measures of day length. It appears that photoperiod may play a crucial role in conditioning the acclimation response to a variety of environmental stresses.

Secondly, how do signals pertaining to the length of the light period interact with plastid-derived redox signals? A clear consensus has emerged that that "operational" signals derived from mature chloroplasts act the major regulators of chloroplast ultra structure and the structure of the photosynthetic apparatus (Hüner et al. 1998, Pfannschmidt et al. 1999, Ensminger et al. 2006, Piippo et al. 2006, Hüner et al. 2012). In this study however, the apparent "uncoupling" of high PSII excitation pressure and the expected photoacclimation response indicates that excitation pressure cannot be the sole regulator of photoacclimation under a variable light regime.

We conclude that photoacclimation in *C. vulgaris* likely represents a complex interplay between "biogenic" phytochrome-mediated sensing and "operational" redox sensing and signalling pathways (Pogson et al. 2008, Pogson and Albrecht 2011). Signals pertaining to day length must be able to interact with, or override the interpretation of, photosynthetic redox signals to modify the photoacclimation response. Interaction between light specific receptors and chloroplast redox signals during leaf acclimation in terrestrial plant has been proposed (Ruckle et al. 2007; Ruckle and Larkin 2009). Similarly, the defective photoacclimation responses in the *det1* signal transduction mutant in *A. thaliana* does support some degree of cross-talk between photoreceptor-regulated responses and other regulators of photosynthetic acclimation (Walters et al. 1999). Currently only fragments of these signalling pathways are known. The elucidation of cross-talk between photoreceptor-mediated "biogenic" pathways and plastid-mediated redox "operational" pathways and the extent to which cross-talk alters acclimation of the photosynthetic apparatus to different light intensities and photoperiods remains an

interesting question of general relevance to understanding how stress signals impact photoautotrophic function.

3.5 References

Anderson, J.M., Chow, W.S. & Park, Y.I. 1996. The grand design of photosynthesis: acclimation of the photosynthetic apparatus to environmental cues. *Photosyn. Res.* 46:129–139.

Casal, J.J. 2013. Photoreceptor signaling networks in plant responses to shade. *Annu. Rev. Plant Biol*. 64:403–427.

Chaouch, S. & Noctor, G. 2010. Myo-inositol abolishes salicylic acid-dependent cell death and pathogen defence responses triggered by peroxisomal hydrogen peroxide. *New Phytol*. 188:711–718.

Chaouch, S., Queval, G., Vanderauwera, S., Mhamdi, A., Vandorpe, M., Langlois-Meurinne, M., Van Breusegem, F., Saindrenan, P. & Noctor, H. 2010. Peroxisomal hydrogen peroxide is coupled to biotic defense responses by ISOCHORISMATE SYNTHASE1 in a daylength-related manner. *Plant Physiol*. 153:1692–1705.

Chen, Y.B., Durnford, D.G., Koblizek, M. & Falkowski, P.G. 2004. Plastid regulation of *Lhcb1* transcription in the chlorophyte alga *Dunaliella tertiolecta*. *Plant Physiol.* 136:3737–3750.

Demmig-Adams, B. & Adams III, W.W. 1992. Photoprotection and other responses of plants to high light stress. *Annu. Rev. Plant Physiol. Plant Mol. Biol.* 43:599–626.

Demmig-Adams, B., Gilmore, A. & Adams III, W.W. 1996. Carotenoids 3: in vivo function of carotenoids in higher plants. *FASEB J.* 10: 403–412.

Demmig-Adams, B. & Adams III, W.W. 2000. Harvesting sunlight safely. *Nature* 403:371,373–374.

Dietz, K., Schreiber, U. & Heber, U. 1985. The relationship between the redox state of Q_A and photosynthesis in leaves at various carbon-dioxide, oxygen and light regimes. *Planta* 166:219–226.

Ensminger, I., Busch, F. & Hüner, N.P.A. 2006. Photostasis and cold acclimation: sensing low temperature through photostasis. *Physiol. Plant* 126:28–44.

Escoubas, J.M., Lomas, M., LaRoche, J. & Falkowski, P.G. 1995. Light intensity regulation of *cab* gene transcription is signaled by the redox state of the plastoquinone pool. *Proc. Natl. Acad. Sci. U.S.A.* 92:10237–10241.

Estavillo, G.M., Chan, K.X., Phua, S.Y. & Pogson, B.J. 2013. Reconsidering the nature and mode of action of metabolite retrograde signals from the chloroplast. *Front. Plant Sci*. 3:300.

Falkowksi, P.G. & Chen, Y-B. 2003. "Photoacclimation of light harvesting systems in eukaryotic algae," *In* Green, B.R. & Green W.W. [Eds.] *Advance in Photosyntheis and Respiration*, Vol. 13, *Light Harveting Antennas in Photosynthesis*. Kluwer Academic Publishers, Dordrecht, the Netherlands, pp. 423–447.

Fey, V., Wagner, R., Brautigam, K. & Pfannschmidt, T. 2005. Photosynthetic redox control of nuclear gene expression. *J. Exp. Bot.* 56:1491–1498.

Geider, R.J., MacIntrye, H.L. & Kana, T.M. 1996. A dynamic model of photoadaptation in phytoplankton. *Limnol. Oceanogr.* 4:1–15.

Geider, R.J., MacIntrye, H.L. & Kana, T.M. 1998. A dynamic regulatory model of phytoplanktonic acclimation to light, nutrients, and temperature. *Limnol. Oceanogr.* 43:679–694.

Gilmore, A.M. & Yamamoto, H.Y. 1993. Linear models relating xanthophylls and lumen acidity to non-photochemical fluorescence quenching. Evidence that antheraxanthin explains zeaxanthin-independent. *Photosynth. Res*. 35:67–78.

Hendrickson, L., Furbank, R. & Chow, W. 2004. A simple alternative approach to assessing the fate of absorbed light energy using chlorophyll fluorescence. *Photosynth. Res.* 82:73–81.

Hüner, N.P.A., Öquist, G. & Sarhan, F. 1998. Energy balance and acclimation to light and cold. *Trends Plant Sci*. 3:224–230.

Hüner, N.P.A., Öquist, G. & Melis, A. 2003. "Photostasis in plants, green algae and cyanobacteria: the role of light harvesting antenna complexes," *In* Green, B.R. & Green, W.W. [Eds.] *Advances in Photosynthesis and Respiration,* Vol. 13*, Light Harvesting Antennas in Photosynthesis*. Kluwer Academic Publishers, Dordrecht, the Netherlands, pp. 401–421.

Hüner, N.P.A, Bode, R., Dahal, K., Hollis, L., Rosso, D., Król, M. & Ivanov, A.G. 2012. Chloroplast redox imbalance governs phenotypic plasticity: the "grand design of photosynthesis" revisited. *Front. Plant Sci.* 3:255.

Kianianmomeni, A. & Hallmann, A. 2014. Algal photoreceptors: in vivo functions and potential applications. *Planta* 239:1–26.

Król, M., Maxwell, D.P. & Hüner, N.P.A. 1997. Exposure of *Dunaliella salina* to low temperature mimics the high light-induced accumulation of carotenoids and the carotenoid binding protein (Cbr). *Plant Cell Physiol.* 38:213–216.

Lepisto, A., Kangasjarvi, S., Luomala, E.M., Brader, G., Sipari, N., Keränen, M. & Rintamäki, E. 2009. Chloroplast NADPH-thioredoxin reductase interacts with photoperiodic development in *Arabidopsis*. *Plant Physiol.* 149:1261–1276.

Masuda, T., Tanaka, A. & Melis, A. 2003. Chlorophyll antenna size adjustments by irradiance in Dunaliella salina involve coordinate regulation of chlorophyll *a* oxygenase (*CAO*) and *Lhcb* gene expression. *Plant Mol. Biol.* 51:757–771.

Maxwell, D.P., Falk, S., Trick, C.G. & Hüner, N.P.A. 1994. Growth at low temperature mimics high-light acclimation in *Chlorella vulgaris*. *Plant Physiol.*105:535–543.

Maxwell, D.P., Falk, S. & Hüner, N.P.A. 1995a. Photosystem II excitation pressure and development of resistance to photoinhibition (I. Light-harvesting complex II abundance and zeaxanthin content in *Chlorella vulgaris*). *Plant Physiol.* 107:687–694.

Maxwell, D.P., Laudenbach, D.E. & Hüner, N.P.A. 1995b. Redox regulation of light-harvesting complex II and *cab* mRNA abundance in *Dunaliella salina*. *Plant Physiol*. 109:787–795.

Millar, A.J., Straume, M., Chory, J., Chua, N.H. & Kay, S.A. 1995. The regulation of circadian period by phototransduction pathways in *Arabidopsis*. *Science* 267:1163–1166.

Möglich, A., Yang, X., Ayers, R.A. & Moffat, K. 2010. Structure and function of plant photoreceptors. *Annu. Rev. Plant Biol*. 61:21–47.

Murchie, E.H., Pinto, M. & Horton, P. 2009. Agriculture and the new challenges for photosynthesis research. *New Phytol.* 181:532–552.

Nichols, S.H.W & Bold, H.C. 1965. *Trichosarcina polymorpha* gen. et sp. nov. *J. Phycol*. 1:34–38.

Pfannschmidt, T., Nilsson, A., Tullberg, A., Link, G. & Allen, J.F. 1999. Direct transcriptional control of the chloroplast genes *psbA* and *psaAB* adjusts photosynthesis to light energy distribution in plants. *IUBMB Life* 48:271–276.

Piippo, M., Allahverdiyeva, Y., Paakkarinen, V., Suoranta, U.M., Battchikova, N. & Aro, E.M. 2006. Chloroplast-mediated regulation of nuclear genes in *Arabidopsis thaliana* in the absence of light stress. *Physiol. Genomics* 25:142–152.

Pogson , B.J., Woo, N.S., Forster, B. & Small, I.D. 2008. Plastid signalling to the nucleus and beyond. *Trends Plant Sci.* 13:602–609.

Pogson, B.J. & Albrecht, V. 2011. Genetic dissection of chloroplast biogenesis and development: an overview. *Plant Physiol.* 155:1545–1551.

Post, A.F., Dubinsky, Z., Wyman, K. & Falkowski, P.G. 1984. Kinetics of light-intensity adaptation in a marine planktonic diatom. *Mar. Biol*. 83:231–238.

Queval, G., Issakidis-Bourguet, E., Hoeberichts, F.A., Vandorpe, M., Gakière, B., Vanacker, H., Miginiac-Maslow, M., Van Breusegem, F. & Noctor, G. 2007. Conditional oxidative stress responses in the *Arabidopsis* photorespiratory mutant *cat2* demonstrate that redox state is a key modulator of daylength-dependent gene expression, and define photoperiod as a crucial factor in the regulation of H_2O_2-induced cell death. *Plant J.* 52:640–657.

Queval, G., Neukermans, J., Vanderauwera, S., Van Breusegem, G. & Noctor, G. 2012. Day length is a key regulator of transcriptomic responses to both CO_2 and H_2O2 in *Arabidopsis*. *Plant Cell Environ.* 35:374–387.

Rochaix, J.D. 2014. Regulation and dynamics of the light-harvesting system. *Annu. Rev. Plant Biol.* 65:287–309.

Ruckle, M.E., DeMarco, S.M. & Larkin, R.M. 2007. Plastid signals remodel light signaling networks and are essential for efficient chloroplast biogenesis in *Arabidopsis*. *Plant Cell* 19:3944–3960.

Ruckle, M.E. & Larkin, R.M. 2009. Plastid signals that affect photomorphogenesis in *Arabidopsis thaliana* are dependent on GENOMES UNCOUPLED 1 and cryptochrome 1. *New Phytol*. 367–379.

Savitch, L.V., Maxwell, D.P. & Hüner, N.P.A. 1996. Photosystem II excitation pressure and photosynthetic carbon metabolism in *Chlorella vulgaris*. *Plant Physiol*. 111:127–136.

Shin, J., Anwer, M.U. & Davis, S.J. 2013. Phytochrome-interacting factors (PIFs) as bridges between environmental signals and the circadian clock: diurnal regulation of growth and development. *Mol. Plant* 6:592–595.

Vollsnes, A.V., Eriksen, A.B., Otterholt, E., Kvaal, K., Oxaal, U. & Futsaether, C.M. €€€ 2009. Visible foliar injury and infrared imaging show that daylength affects short-term recovery after ozone stress in *Trifolium subterraneum. J. Exp. Bot.* 60:3677–3686.

Yanovsky, M. J. and Kay, S. A. 2002. Molecular basis of seasonal time measurement in *Arabidopsis*.Nature 419:308–312.

Walters, R.G., Rogers, J.J., Shephard, F. & Horton, P. 1999. Acclimation of *Arabidopsis thaliana* to the light environment: the role of photoreceptors. *Planta* 209:517–527.

Wilson, K.E. & Hüner, N.P.A. 2000. The role of growth rate, redox-state of the plastoquinone pool and the trans-thylakoid deltapH in photoacclimation of *Chlorella vulgaris* to growth irradiance and temperature. *Planta* 212:93–102.

Wilson, K.E., Król, M. & Hüner, N.P.A. 2003. Temperature-induced greening of *Chlorella vulgaris*. The role of the cellular energy balance and zeaxanthin-dependent nonphotochemical quenching. *Planta* 217:616–627.

3.6 Supplementary Material

3.7 Supplemental Tables

Supplemental Table S3.1 Mean chlorophyll a/b ratio, standard error of the mean and variance for cultures of *C. vulgaris* grown at 28 °C / 2000 µmol photons m^{-2} sec^{-1} under either a 16 h or 14 h photoperiod. Chlorophyll a/b ratio was assayed immediately following the start of a daily light period (n = 3).

	28/2000	
	16 h	14 h
Chlorophyll a/b	4.80	4.32
Standard Error of the Mean	1.22	1.25
Variance	1.51	1.57

3.8 Supplemental Figures

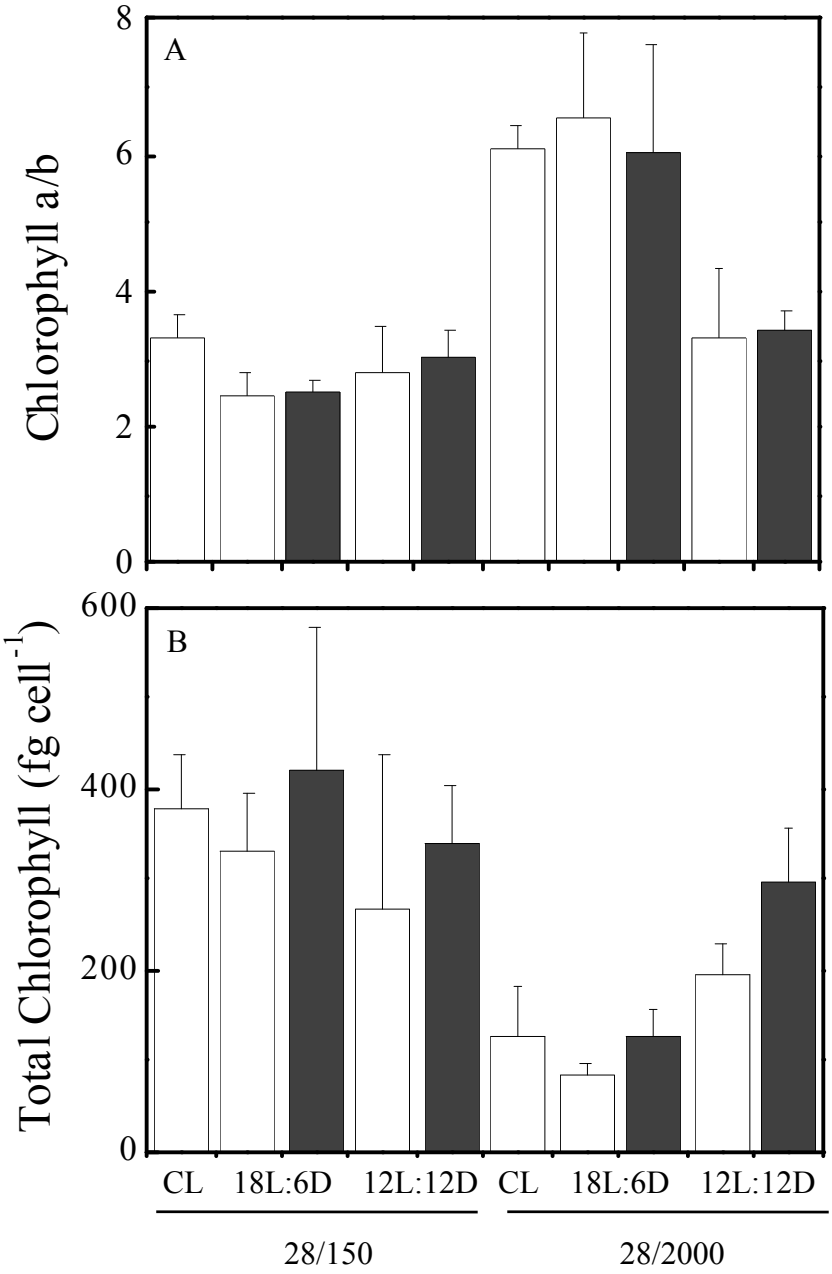

Supplemental Figure S3.1 Change in (A) chlorophyll a/b ratio and (B) total cellular chlorophyll content during the light period. Cultures of *C. vulgaris* were grown at 28 °C / 150 µmol photons m^{-2} sec^{-1} or 28 °C / 2000 µmol photons m^{-2} sec^{-1} with 24 h, 18 h and 12 h light periods in a 24 h cycle. Chlorophyll content was measured at the start of the light period (open bars) and end of the light period (closed bars) during mid-log phase growth. Numbers under growth regime represent temperature (°C) / irradiance (µmol photons m^{-2} sec^{-1}) with length of light (L) and dark period (D) in a 24 h cycle for cultures grown under a photoperiod. For cultures grown under continuous light (CL). Chlorophyll content was measured during mid-log phase growth. Values represent mean ± SEM; n = 3.

Chapter 4

4 PHOTOPERIOD-DEPENDENT GROWTH OSCLLATIONS IN *CHLORELLA VULGARIS*

4.1 Introduction

Photoautotrophic metabolism, development and growth are tightly regulated by the prevailing environmental conditions. Light quality and quantity, as well as photoperiod, together with temperature and nutrient availability influence photoautotrophic morphology and the timing of developmental phases. Among these environmental cues, day length provides the most reliable indicator of diurnal and seasonal progression due to its high degree of predictability on a daily and yearly level. The ability to anticipate changes in the light environment accurately, and coordinate metabolism and growth to external light:dark cycles, has been demonstrated to confer a selective advantage by enhancing fitness in *Arabidopsis thaliana* (Kulheim et al. 2002, Dodd et al. 2005).

The circadian clock is a series of interconnected transcriptional feedback loops that provides internal measures of time that serve to synchronize photoautotrophic physiology with the external light:dark cycle by regulating downstream targets. Clock-controlled biological oscillations demonstrating circadian rhythms exhibit periods of approximately 24 h that persist under continuous light (CL) (McClung 2006, Harmer 2009). Light and temperature signals serve as the major regulators used to entrain the clock to the environment (Salome and McClung 2005, Eckardt 2005). The circadian clock has been implicated in the regulation of photosynthesis, both nuclear and plastid-localized gene transcription, starch metabolism as well as cellular division (Dodd et al. 2005, Graf and Smith 2011, Staiger et al. 2013, Dodd et al. 2014).

Asexual cellular division by multiple fission in green algae has been suggested to be an adaptation to a naturally occur light environment characterized by light:dark cycles such that the light period is maximally exploited to drive photoautotrophic growth (Bišová and

Zachleder 2014). Reproduction by multiple fission, where each mother cell gives rise to 2^n daughter cells where n is an integer between 1 and 10, is shared among the chlorophyta algae (Kirk 2004).

A cell cycle consists of a growth phase (G_1 phase), followed by a DNA replication (or synthesis) phase (S phase), a secondary growth phase (G_2 phase) and mitosis (M phase) which is closely followed by cellular division. Mitchison (1971) proposed that this cycle proceeds as two coordinated events consisting of growth (G_1 phase) and a DNA replication-division sequence composed of DNA replication (S phase), the G_2 growth phase and nuclear division (M phase) closely followed by cytokinesis. Alternative models suggest that progression of the cell cycle from the major growth phase to a reproductive mode characterized by the DNA replication and cellular division sequence is initiated either by signals generated by the circadian clock (Edmunds and Adams 1981, Homma and Hastings 1989, Makarov et al. 1995, Lüning et al. 1997) or following attainment of a critical point marked by the acquirement of a critical cellular volume (Vítová et al. 2011a, Vítová et al. 2011b, Bišová and Zachleder 2014).

It has previously been demonstrated that *C. vulgaris* demonstrates minimal capacity to adjust either exponential growth rates or carbon metabolism in response to a range of continuous growth light intensities (Savitch et al. 1996, Wilson and Hüner 2000). In terrestrial plants, growth under CL is associated with a marked decrease in photosynthetic capacity and growth reflecting feedback inhibition of photosynthesis (Stessman et al. 2002,van Gestel et al. 2005, Sysoeva et al. 2010, Velez-Ramirez et al. 2011). We hypothesized the insensitivity of exponential growth rates of *Chlorella vulgaris* to growth irradiance is an consequence of growth under continuous light (CL). To test this hypothesis, cells were grown at constant temperature of 28 °C, under CL, an 18 h photoperiod or a 12 h photoperiod at either high light (HL; 2000 μmol photons m^{-2} sec^{-1}) or low light (LL; 150 μmol photons m^{-2} sec^{-1}).

4.2 Methods

4.2.1 Cell culture conditions

4.2.1.1 Photobioreactor

Cultures of *Chlorella vulgaris* Berjiernick (UTEX 265) were grown axenically in Bold's basal media (Nichols and Bold 1965) with modifications according to Maxwell et al. 1994. Cultures were grown as batch cultures in 400 mL capacity Photobioreactor cultivation vessels (FMT 150) (Photon System Instruments, Hogrova, Czech Republic) and aerated with sterile, humidified air. The temperature and light regimes were regulated by the Photobioreactor control system (Photon System Instruments, Hogrova, Czech Republic) which maintained a temperature of 28 ^{o}C ± 1 ^{o}C and CL intensities of either 150 (28/150) or 2000 µmol photons m^{-2} sec^{-1} (28/2000) supplied by an equal combination of red and blue light emitting diodes. Cells were grown under either CL (24 h photoperiod), an 18 h photoperiod or 12 h photoperiod (Photon System Instruments, Hogrova, Czech Republic) at both low light (LL; 28/150) or high light (HL; 28/2000).

Optical density was measured at 680 and 735 nm by a densitometer integrated into the Photobioreactor system (Photon System Instruments, Hogrova, Czech Republic). Maximum fluorescence (F_M') of photosystem II reaction centres and steady-state fluorescence (Fs) at the growth irradiance were measured using a fluorometer integrated into the Photobioreactor system (Photon System Instruments, Hogrova, Czech Republic). Both optical density and Chl *a* fluorescence induction measurements were taken at 30 minute intervals and were automatically recorded by the Photobioreactor control system (Photon System Instruments, Hogrova, Czech Republic).

4.2.1.2 Growth tube

For comparison, the growth pattern of *C. vulgaris* in Photobioreactors were compared to the traditional growth of cells in 150 mL capacity pyrex growth tubes suspended in temperature controlled aquaria which maintained a temperature of 28 ^{o}C (Maxwell et al.

1994). During cultivation in growth tubes, cells were illuminated by a bank of white florescent lights (Sylvania T12 daylight) which supplied growth light of either 150 or 2000 μmol photons m^{-2} sec^{-1}. Growth tube-grown cells were aerated with sterile air. Samples were removed at 24 h intervals and growth was assayed as change in optical density at 750 nm using a spectrophotometer.

4.2.2 Growth rate

Cellular growth rates were measured as a change in light scattering at 735 nm measured at 30 minute intervals via the integrated densitometer (Photon System Instruments, Hogrova, Czech Republic). Specific growth rates were calculated for the exponential growth phase using natural log transformed absorbance readings at 735 nm as $\mu = \ln(N_1/N_O)/(t_1-t_0)$ where μ is the pseudo-first order growth constant ($days^{-1}$), and N_0 and N_1 represent optical density at 735 nm at time 0 (t_0) and time 1 (t_1), respectively (Wood et al. 2005). Doubling time was calculated as $\ln 2/\mu$ (Wood et al. 2005).

4.2.3 Cell size

Cell size was estimated using a PhytoCyt Flow Cytometer (C6) equipped with a 488 nm argon laser (Turner, California, USA). Forward scatter (FSC) was used as an indicator of relative cell diameter; FSC is light from the illumination beam that has been deflected at a small angle as it passes throughout the cells in suspension and is proportional to cell size. A Flow Cytometry Size Calibration kit with nonfluorescent size calibration standards of 1, 2, 4, 6, 10 and 15 μm were used to determine cell size following the instruction provided by the manufacturer (Molecular Probes, Eugene, Oregon, USA).

4.2.4 DNA stain and cell cycle tracking

Samples were either removed from the Photobioreactor immediately prior to the end of the light period as well as immediately prior to the end of the dark period during exponential growth for cells grown under either an 18 h or 12 h photoperiod, or were collected during exponential growth for cells grown under CL. Vybrant DyeCycle Green stain was used to estimate DNA mass (Molecular Probes, Eugene, Oregon, USA).

Background fluorescence was measured on 50 µL of unstained cells using the 488 nm excitation and 530/30 emission wavelengths (Molecular Probes, Eugene, Oregon, USA). DNA content was estimated in stained cells using the instructions provided by the manufacturer; 4 µL of dye was added to 1 mL cells for a final concentration of 10 µM and incubated at 37 ^{o}C for 30 min in the dark (Molecular Probes, Eugene, Oregon, USA). A 50 µL sample of the stained cells was then measured using the PhytoCyt Flow Cytometer (Turner, California, USA) where the Vybrant DyeCycle Green:DNA complex was analyzed using the 488 nm excitation and green emission wavelengths (Molecular Probes, Eugene, Oregon, USA). The normalized fluorescence signal was calculated as the difference between the mean fluorescence signal of stained and unstained cells.

4.2.5 Carbohydrate analysis

Carbohydrate analysis was conducted on exponentially growing cells harvested by centrifugation at 5, 000 x g for 5 min and stored at - 80 ^{o}C until analysis. Samples were collected from the Photobioreactor immediately prior to the end of the light period as well as immediately prior to the end of the dark period for cells grown under either an 18 h or 12 h photoperiod; or under CL, mid-log phase cells harvested during exponential growth. Pigments were extracted from thawed cells with hot 80% (v/v) ethanol until cells were completely pigment free. Total starch content was quantified using the Megazyme Total Starch Assay Kit (Megazyme, Wicklow, Ireland) and total sucrose content was quantified using the Sigma Sucrose Assay Kit (Sigma-Aldrich, Missouri, USA) according to the manufacturers' recommendations with modifications specific for measurements conducted from microalgal samples according to Lee et al. (2013).

4.2.6 Statistical analysis

Doubling times in Photobioreactor or growth tube-grown cells of *C. vulgaris* grown at 28/150 and 28/2000 under CL were compared using a two-way analysis of variance (ANOVA) using growth light intensity and cultivation vessel type as explanatory variables. Doubling time, rate of change in absorbance at 735 nm and rate of starch consumption for cells grown at both 28/150 and 28/2000 in Photobioreactors under either

CL, an 18 h photoperiod or 12 h photoperiod were compared using a two-way ANOVA using growth irradiance and photoperiod as explanatory factors. Two-way ANOVAs were conducted using the statistical software package R version 3.0.2 and followed by Tukey's Honest Significant Different (HSD) post hoc tests.

Three-way repeated measures ANOVAs were conducted on diel changes in cellular volume, starch content and sucrose content for cells grown at both 28/150 and 28/2000 under either an 18 h or 12 h photoperiod with two between subject factor (irradiance and photoperiod) and one within subject factor (end of light period and end of dark period). Tukey's HSD post hoc tests were performed on significant single factor and two factor interactions. The significant three-way interaction for change in cellular volume was examined by running two-way repeated measures ANOVAs for each light intensity separately with time as the within subject factor and photoperiod as the between subject factor. All repeated measures ANOVAs were conducted using the statistical software package R version 3.0.2. Prior to each test, the data were visually inspected for normality and homoscedasticity. A value of $p < 0.05$ was considered significant throughout.

4.3 Results

4.3.1 Growth of *Chlorella vulgaris* under CL

Figure 4.1A shows representative growth curves for cultures of *Chlorella vulgaris* grown in Photobioreactors under CL at either 28/150 or 28/2000. Growth was measured as a change in cell density, monitored at 735 nm (OD_{735}), over time using a densitometer integrated into the Photobioreactor system (Figure S4.1A). Change in cell density in cultures of *C. vulgari*s grown at either 28/150 or 28/2000 under CL exhibited a typical sigmodial growth pattern with distinct lag, exponential growth and stationary phases (Figure 4.1A). Typical growth curves for *C. vulgaris* grown in Photobioreactors at 28/150 and 28/2000 under CL resembled the representative growth patterns of cells grown in more traditional growth tubes under the same growth light and temperature regimes (Figures 4.1B and S4.2). The doubling times for Photobioreactor-grown cultures as well

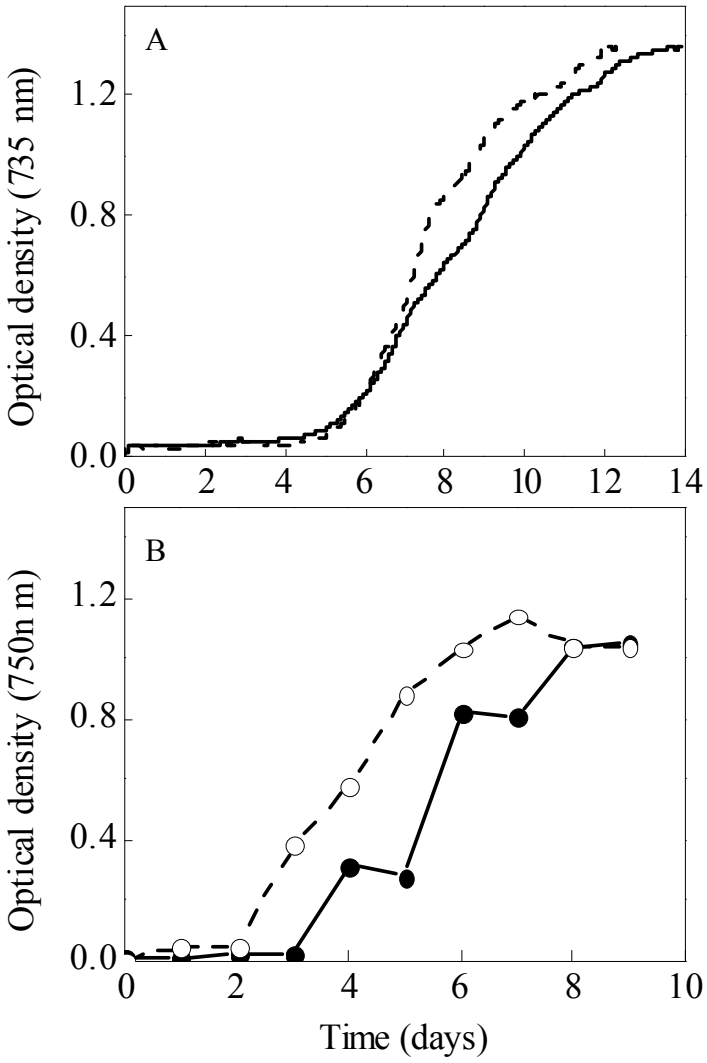
A
B
Optical density (735 nm)
Optical density (750n m)
Time (days)
0.0
0.4
0.8
1.2
0
2
4
6
8
10
12
14

Figure 4.1 (A) Representative growth curves for *C. vulgaris* grown at either 150 (solid line) or 2000 (dashed line) µmol photons m^{-2} sec^{-1} at 28 °C under CL in Photobioreactors. Light scattering at 735 nm was measured at 30 minutes via a densitometer integrated into the Photobioreactor control system. (B) Representative growth curves for *C. vulgaris* grown at either 150 (solid line; closed symbols) or 2000 (dashed line; open symbols) µmol photons m^{-2} sec^{-1} at 28 °C under CL in growth tubes. Cell density was measured as a change in optical density 750 nm in samples removed from the growth tubes at 24 h intervals.

as growth tube cultures of *C. vulgaris* grown under CL appeared to be independent of growth light intensity (Table 4.1); however, Photobioreactor grown cultures exhibited a 2-fold longer doubling time relative to cells grown in the more traditional growth tubes (Table 4.1) (irradiance, $F_{1,16} = 3.1$, $p = 0.0979$; cultivation vessel, $F_{1,16} = 40.5$, $p < 0.0001$; irradiance*cultivation vessel, $F_{1,16} = 0.5$, $p = 0.475$).

The Photobioreactor system simultaneously measured change in chlorophyll (Chl) content over time at 680 nm (OD_{680}) (Figure S4.1B). The increase in Chl abundance (Figures 4.2B and 4.3B) closely paralleled the increase in optical density (Figures 4.2A and 4.3A) for cultures of *C. vulgaris* grown at either 28/150 or 28/2000 under CL. The integrated fluorometer additionally measured change in Chl *a* fluorescence induction over time. Increases in F_M', the maximum light-adapted Chl *a* fluorescence (Figures 4.2C and 4.3C; closed symbols), and F_S, steady-state Chl *a* fluorescence (Figures 4.2C and 4.3C; open symbols), were measured in cultures grown at both 28/150 and 28/2000 under CL that paralleled the increase in optical density (Figures 4.2A and 4.3A). Since nearly identical patterns were obtained for F_M' and F_S at both the red and blue excitation irradiances, the response for the blue light only will be presented (Figure S4.3).

4.3.2 Effect of photoperiod on cell growth

Figures 4.2 and 4.3 show representative diurnal growth dynamics for cultures of *C. vulgaris* grown at either 28/150 or 28/2000, respectively, under varying photoperiods. Although, the overall sigmodial growth patterns exhibited by cells of *C. vulgaris* grown under either an 18 h photoperiod (Figures 4.2D and 4.3D) or 12 h photoperiod (Figures 4.2G and 4.3G) were similar to those observed under CL (Figures 4.2A and 4.3A), growth under either an 18 h or 12 h photoperiod was dominated by transient oscillations in OD_{735} at both growth light intensities. At both 28/150 and 28/2000 there was a rapid rise in OD_{735} during the light period followed by a marked decline in optical density that corresponded with the start of the dark period (Figure 4.4). Oscillations in OD_{735} occurred with a period of approximately 24 h and appeared to be independent of the growth light intensity. However, the amplitude of these oscillations did dampen as the cells approached the stationary growth phase (Figures 4.2 and 4.3). Similar oscillation

Table 4.1 Comparison of growth characteristic for *C. vulgaris* cultivated in either Photobioreactors or growth tubes. Cells were grown to mid-log phase at either 150 or 2000 µmol photon m^{-2} sec^{-1} under continuous growth light at 28 ^{o}C. Numbers under growth regime indicate growth temperature (^{o}C) / irradiance (µmol photons m^{-2} sec^{-1}). The doubling times of Photobioreactor-grown cells as well as growth tube-grown cells of *C. vulgaris* were compared using a two-way ANOVA followed by a Tukey's HSD post hoc test; means not connected by the same letter were statistically different at $p < 0.05$. Values represent mean ± SEM; n = 5.

Characteristic	Growth regime			
	Photobioreactor		Growth tube	
	28/150	28/2000	28/150	28/2000
Doubling time (h)	20.26 ± 0.48^{a}	25.58 ± 1.18^{a}	12.75 ± 0.75^{b}	14.12 ± 1.27^{b}

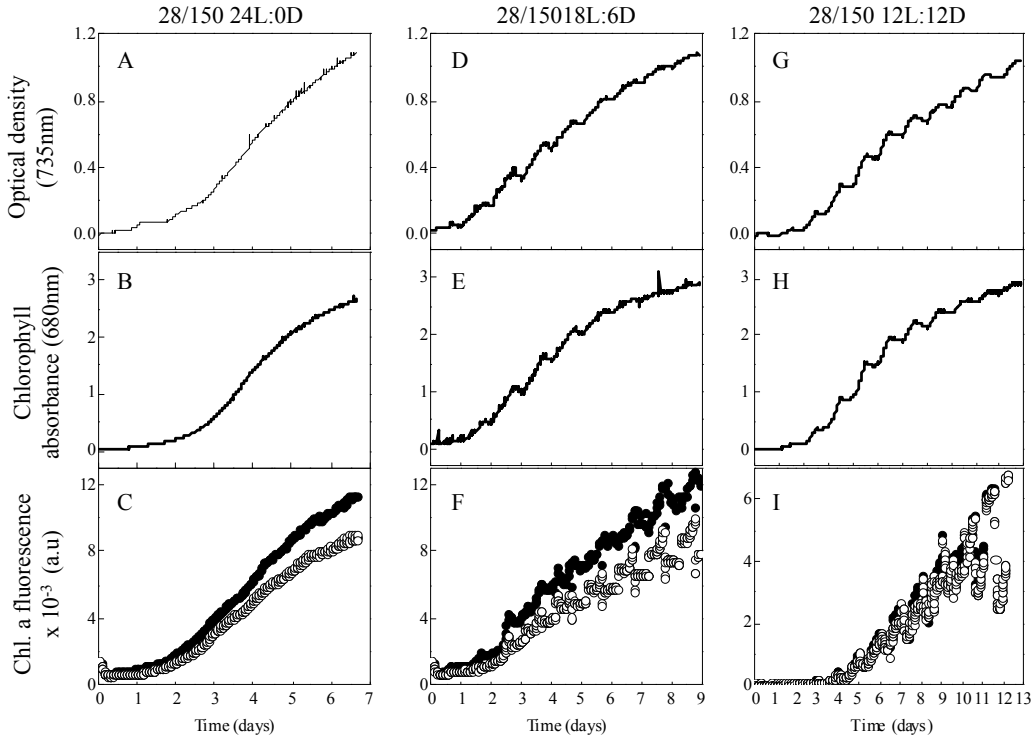

Figure 4.2 Representative growth curves for cells of *C. vulgaris* grown at 28 ^{o}C / 150 photons m^{-2} sec^{-1} under either 24 h, 18 h or 12 h photoperiods in a 24 h cycle. An integrated densitometer measured change in cell density over time which was monitored as light scattering at 735 nm as well as change in chlorophyll mL^{-1} at 680 nm at 30 minute intervals. An integrated fluorometer simultaneously measured light-adapted Chl *a* fluorescence (F_M'; closed circles) and the steady-state chlorophyll *a* fluorescence (F_S; open circles) using blue excitation light at 30 minute intervals. Values above the columns represent temperature (^{o}C) / growth irradiance (µmol photons m^{-2} sec^{-1}) followed by the length of the light (L) and dark (D) periods in a 24 h cycle.

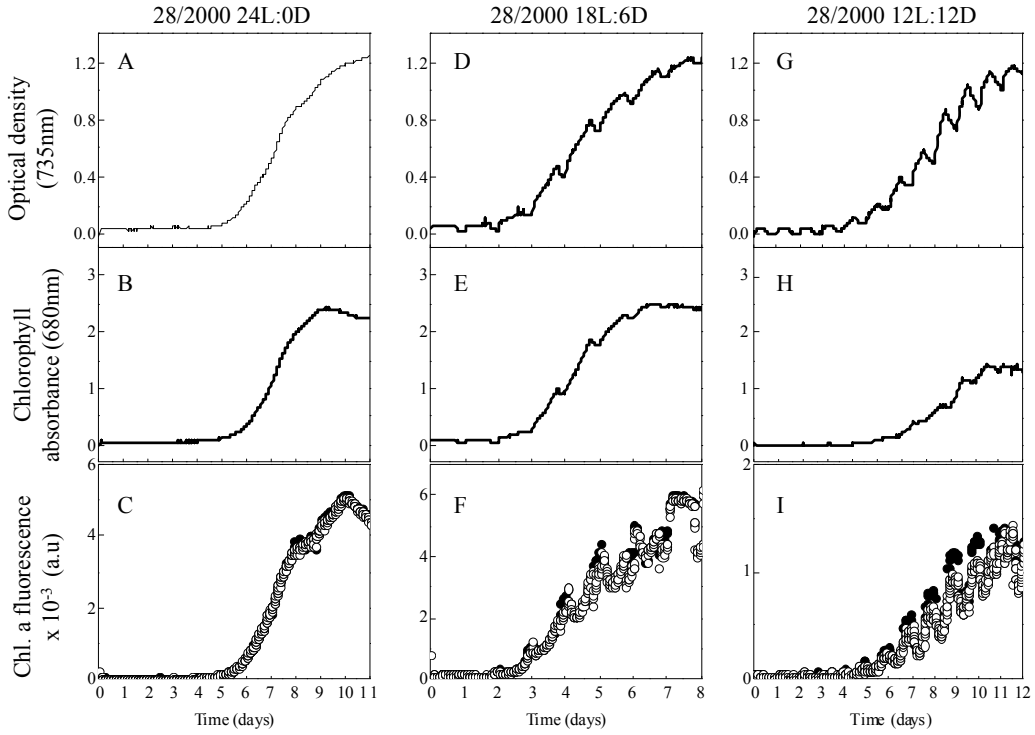

Figure 4.3 Representative growth curves for cells of *C. vulgaris* grown at 28 ^{o}C / 2000 photons m^{-2} sec^{-1} under either 24 h, 18 h or 12 h photoperiods in a 24 h cycle. An integrated densitometer measured change in cell density over time which was monitored as light scattering at 735 nm as well as change in chlorophyll mL^{-1} at 680 nm at 30 minute intervals. An integrated fluorometer simultaneously measured light-adapted Chl *a* fluorescence (F_M'; closed circles)and the steady-state chlorophyll *a* fluorescence (F_S; open circles) using blue excitation light at 30 minute intervals. Values above the columns represent temperature (^{o}C) / growth irradiance (μmol photons m^{-2} sec^{-1}) followed by the length of the light (L) and dark (D) periods in a 24 h cycle.

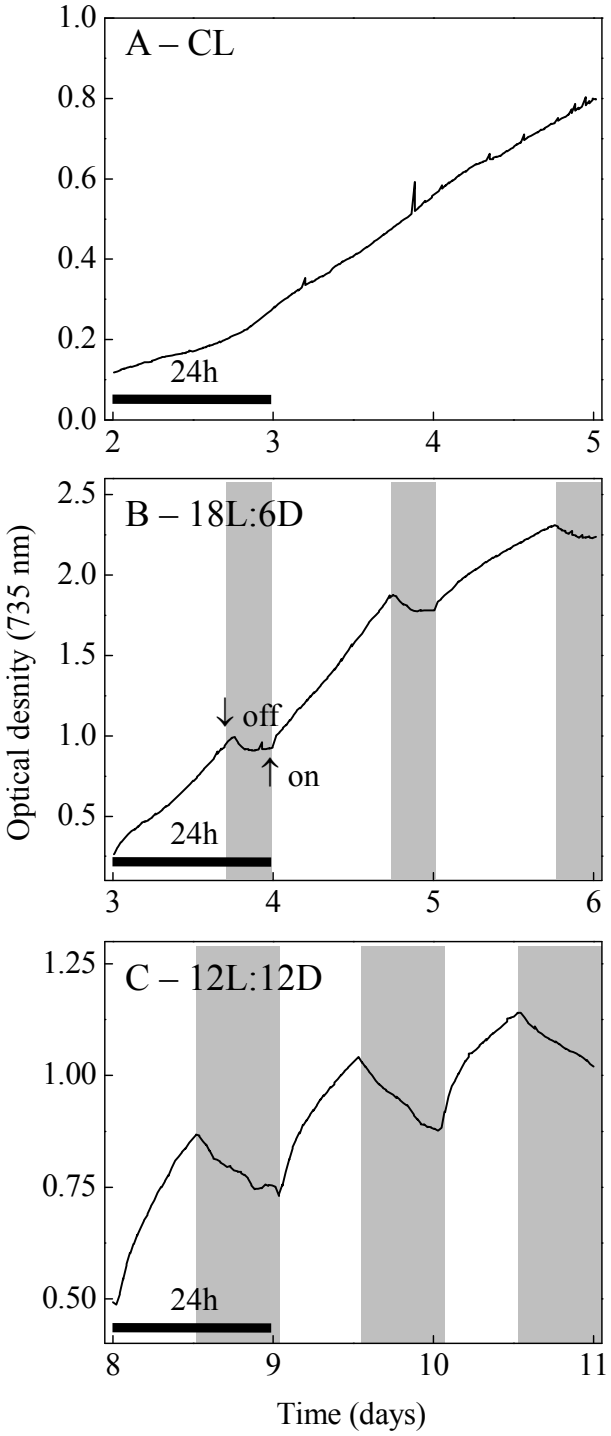
A – CL
24h
B – 18L:6D
off
on
24h
C – 12L:12D
24h
Optical desnity (735 nm)
Time (days)

Figure 4.4 Change in optical density and chlorophyll content over a three day period. Cultures of *C. vulgaris* were grown to mid-log phase at 28 ^{o}C /150 µmol photons m^{-2} sec^{-1} under either (A) continuous light (CL), (B) an 18h photoperiod (18L:6D) or (C) 12h photoperiod (12L:12D). Optical density was measured at 735 nm while chlorophyll per mL was measured as absorption at 680 nm. Open bars represent the daily light period while closed bars represents the daily dark period in a 24 h cycle. Numbers in the panels represent the length of the light period (L) and dark period (D) in a 24 h cycle.

patterns were observed for Chl accumulation (Figure 4.2E and 4.2H; Figures 4.3E and 4.3H) as well as Chl *a* fluorescence (Figures 4.2F and 4.2I; Figures 4.3F and 4.3I).

Doubling times remained relatively constant at about 24 h across the range of photoperiods and growth light intensities (irradiance, $F_{1,24} = 3.1$, $p = 0.092$; photoperiod, $F_{2,24} = 0.9$, $p = 0.404$; irradiance*photoperiod, $F_{2,24} = 0.2$, $p = 0.828$) (Table 4.2). However, the rate of change in OD_{735} over time during the light period was approximately 2-fold greater in *C. vulgaris* grown at 28/2000 compared to cells grown at 28/150 when compared at the same photoperiod (irradiance, $F_{1,8} = 13.9$, $p = 0.00575$; photoperiod, $F_{1,8} = 0.01$, $p = 0.924$; irradiance*photoperiod, $F_{1,8} = 0.447$, $p = 0.523$) (Table 4.3).

When cells of *C. vulgaris* grown under a daily light:dark cycle were shifted to CL at the same growth light intensity and temperature, the oscillations in both OD_{735} (Figure 4.5A) and OD_{680} (Figure 4.5B) were dampened immediately following the transfer. In contrast, the daily oscillations in Chl *a* fluorescence did persist in the absence of a photoperiod for several cycles (Figure 4.5C).

4.3.3 Physiological basis underlying growth oscillations

4.3.3.1 Effect of photoperiod on starch content

Since starch granules are opaque, the presence or absence of these granules may contribute to the photoperiod-dependent changes in the optical properties of the cells. To test this, total starch content was assayed biochemically. There was a significant decrease in total starch content on a per cell basis during the daily dark period (time, $p < 0.0001$, Table 4.4) (Figure 4.6A). Total starch content decreased by 88 and 86% by the end of the dark period in *C. vulgaris* grown at 28/150 under an 18 h and 12 h photoperiod, respectively, while starch content decreased by 95 and 92% in cells grown at 28/2000 under an 18 h and 12 h photoperiod, respectively (Figure 4.6A). However, there were no significant main effects of either the growth light intensity or the duration of the

Table 4.2 Growth rates of *C. vulgaris* grown at 150 and 2000 μmol photon m^{-2} sec^{-1} at 28 ^{o}C under either continuous light, an 18 h photoperiod or 12 h photoperiod. Doubling times were measured in exponentially growing cultures. Numbers under growth regime indicate growth temperature (^{o}C) / irradiance (μmol photons m^{-2} sec^{-1}) followed by the length of light (L) and dark (D) periods in a 24 h cycle. Values represent mean ± SEM; n = 5. Means for either specific growth rate or doubling time were compared using a two-way ANOVA; means not connected by the same letter were significantly different at $p < 0.05$.

Growth regime		Doubling time (h)
28/150	24L:0D	20.26 ± 0.48^{a}
	18L:6D	24.84 ± 1.41^{a}
	12L:12D	24.14 ± 0.63^{a}
28/2000	24L:0D	25.58 ± 1.18^{a}
	18L:6D	27.40 ± 1.26^{a}
	12L:12D	26.94 ± 1.31^{a}

Table 4.3 Change in light scattering at 735 nm (OD_{735}) over time during a daily light period for *C. vulgaris* grown at 150 and 2000 µmol photon m^{-2} sec^{-1} at 28 ^{o}C under either an 18 h photoperiod or 12 h photoperiod. Numbers under growth regime indicate growth temperature (^{o}C) / irradiance (µmol photons m^{-2} sec^{-1}) followed by the length of light (L) and dark (D) periods in a 24 h cycle. Values represent mean ± SEM; n = 3. Means were compared using a two-way ANOVA followed by a Tukey's HSD post hoc test; means not connected by the same letter were significantly different at $p < 0.05$.

Growth regime		ΔOD_{735} / h
28/150	18L:6D	0.19 ± 0.05^{b}
	12L:12D	0.16 ± 0.13^{b}
28/2000	24L:0D	0.30 ± 0.03^{a}
	18L:6D	0.32 ± 0.05^{a}

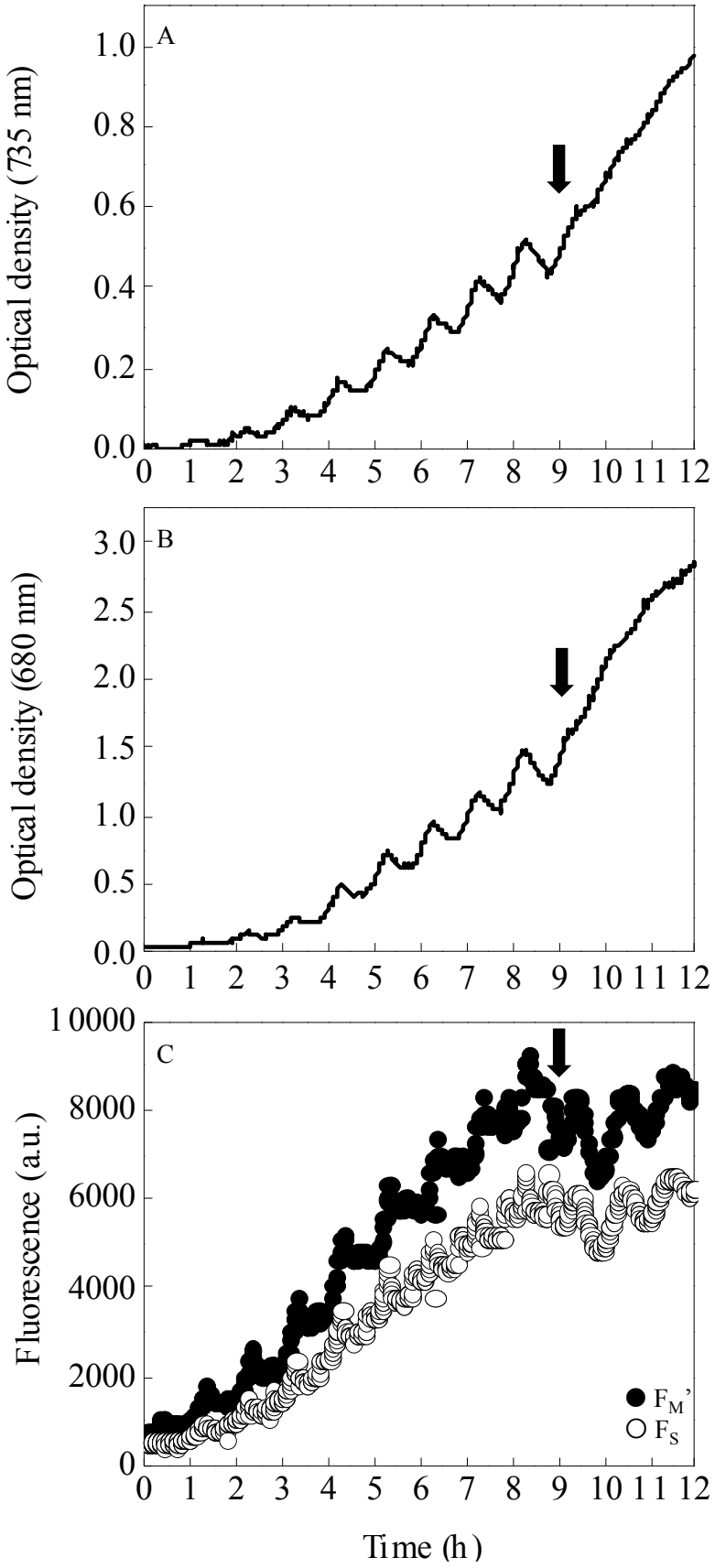
A
Optical density (735 nm)
1.0
0.8
0.6
0.4
0.2
0.0
0 1 2 3 4 5 6 7 8 9 10 11 12
B
Optical density (680 nm)
3.0
2.5
2.0
1.5
1.0
0.5
0.0
0 1 2 3 4 5 6 7 8 9 10 11 12
C
Fluorescence (a.u.)
10000
8000
6000
4000
2000
0
F_M'
F_S
0 1 2 3 4 5 6 7 8 9 10 11 12
Time (h)

Figure 4.5 Cells of *C. vulgaris* grown to mid-log phase at 28 ^{o}C /150 µmol photons m^{-2} sec^{-1} under a 12 h photoperiod were shifted to continuous light, indicated by an arrow, during the exponential growth phase. Change in (A) optical density (735 nm), (B) chlorophyll content per mL (680 nm) and (C) the chlorophyll *a* fluorescence parameters F_M' and F_S were measured at 30 minute intervals. Trends were confirmed by independent biological replicates.

Table 4.4 Results for statistical analysis (three-way repeated measures ANOVA) for *C. vulgaris* grown at 150 and 2000 µmol photons m^{-2} sec^{-1} under either an 18 h or 12 h photoperiod at 28 ^{o}C. I, irradiance; PP, photoperiod, T, time.

Response variable	Source of variation	Result	Conclusion (post hoc test)
Starch	I	$F_{1,8} = 23.2$, $p = 0.261$	
	PP	$F_{1,8} = 17.3$, $p = 0.327$	
	T	$F_{1,8} = 76.1$, $p < 0.0001$	EL > ED
	I*T	$F_{1,8} = 0.07$ $p = 0.793$	
	PP*T	$F_{1,8} = 0.3$, $p = 0.590$	
	I*PP	$F_{1,8} = 30.2$, $p = 0.205$	
	I*PP*T	$F_{1,8} = 1.3$, $p = 0.294$	
Sucrose	I	$F_{1,8} = 405.9$, $p < 0.0001$	HL > LL
	PP	$F_{1,8} = 91.3$, $p < 0.0001$	PP18h > PP12h
	T	$F_{1,8} = 161.3.2$, $p < 0.0001$	ED > EL
	I*T	$F_{1,8} = 26.9$, $p = 0.0008$	HL:ED > HL:EL > LL:ED > LL:EL
	PP*T	$F_{1,8} = 6.7$, $p = 0.0320$	18h:ED > 18h:EL = 12h:ED > 12h:EL
	I*PP	$F_{1,8} = 7.4$, $p = 0.026$	HL18h = HL12h > LL18h > LL12h
	I*PP*T	$F_{1,8} = 3.4$, $p = 0.102$	
Cell volume	I	$F_{1,8} = 63.8$, $p < 0.0001$	HL > LL
	PP	$F_{1,8} = 20.9$, $p = 0.002$	PP18h > PP12h
	T	$F_{1,8} = 22.8$, $p = 0.001$	EL > ED

	I*T	$F_{1,8} = 0.04$, $p = 0.852$	
	PP*T	$F_{1,8} = 0.2$, $p = 0.0.649$	
	I*PP	$F_{1,8} = 3.4$, $p = 0.104$	
	I*PP*T	$F_{1,8} = 5.8$, $p = 0.043$	See two-way ANOVAs for LL and HL, respectively
LL	PP	$F_{1,4} = 3.4$, $p = 0.139$	
	T	$F_{1,4} = 5.9$, $p = 0.072$	
	PP*T	$F_{1,4} = 1.0$, $p = 0.364$	
HL	PP	$F_{1,4} = 23.1$, $p = 0.009$	PP18h > PP12h
	T	$F_{1,4} = 57.8$, $p = 0.002$	EL > ED
	PP*T	$F_{1,4} = 5.8$, p 0.041	PP18h:EL > PP18h:ED = PP12h:EL = PP12:ED

ED, end dark; EL, end light; HL, high light; LL, low light; PP18h, 18h photoperiod; PP12h, 12h photoperiod.

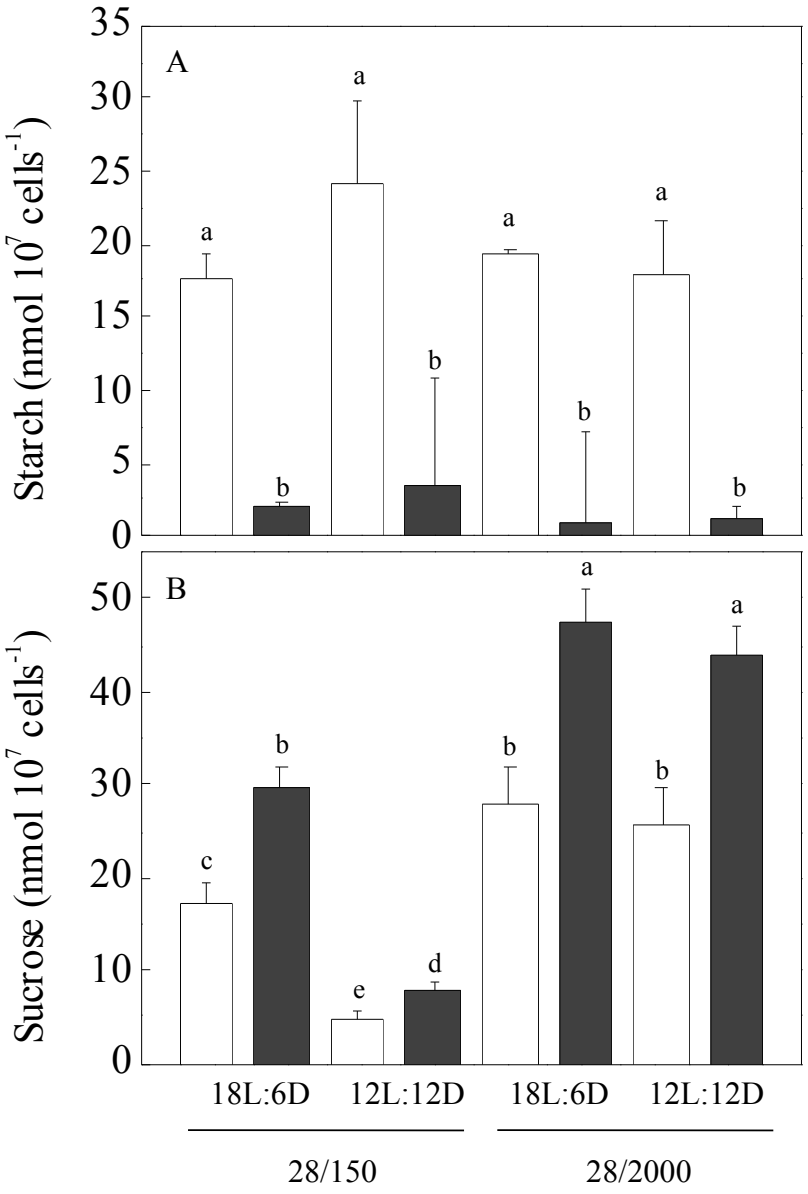
A
B
Starch (nmol 10^7 cells^-1)
Sucrose (nmol 10^7 cells^-1)
0
5
10
15
20
25
30
35
40
50
a
b
a
b
a
b
a
b
c
b
e
d
b
a
b
a
18L:6D
12L:12D
18L:6D
12L:12D
28/150
28/2000

Figure 4.6 Effect of photoperiod on starch (A) and sucrose (B) content during a daily dark period in *C. vulgaris* cells grown at either 150 or 2000 µmol photons under either an 18 h or 12 h photoperiod at 28 ^{o}C. Carbohydrate content was measured immediately following the end of a daily light period (open bars) and immediately following the end of the daily dark period (closed bars). Means not connected by the same letter are significantly different at $p < 0.05$.Values represent mean ± SEM; n = 3.

photoperiod on total starch content (irradiance, p = 0.261; photoperiod, 0 = 0.327, Table 4.4) (Figure 4.6A and Table S4.1).

As expected, the reduction in starch reserves during the dark period coincided with an increase in cellular sucrose content (time, p < 0.0001, Table 4.4) (Figure 4.6B). Sucrose content increased by approximately 60% by the end of the dark period at both the 18 h and 12 h photoperiods for cells grown at either 28/150 or 28/2000 (Figure 4.6B). Furthermore, the interaction between growth irradiance and photoperiod on cellular sucrose content was significant (irradiance*photoperiod, p = 0.026, Table 4.4) (Figure 4.6B). The length of the photoperiod only had a significant effect on cellular sucrose content at low light; there was an approximately 3.6-fold decrease in sucrose content at the 12 h photoperiod relative to the 18 h photoperiod at 28/150 (Tukey's HSD p = 0.0015) while there was no effect of photoperiod at 28/2000 (Tukey's HSD p = 0.232) (Figure 4.6B and Tables 4.4 and S4.1).

4.3.3.2 Effect of photoperiod on cellular volume

Changes in cell size may additionally account for the transient, photoperiod-dependent oscillations in OD_{735}. To test this, diel changes in cellular volume were measured in cultures of *C. vulgaris* grown at both 28/150 and 28/2000 under either an 18 h or 12 h photoperiod; cell size was measured immediately prior to the end of the light period (open bars) as well as immediately prior to the end of the dark period (closed bars) (Figure 4.7A). The response of cellular volume was dominated by a three-way interaction (irradiance*photoperiod*time, p = 0.043, Table 4.4). At low light (28/150), there was no significant change in cellular volume during the dark period (time, p = 0.072, Table 4.4) (Figure 4.7A). However, at high light, while there was a significant 30% decrease in cellular volume during the dark period in *C. vulgaris* grown under an 18 h photoperiod (Tukey's HSD p = 0.0069), there was no significant change in cell volume in cells grown at high light but a 12 h photoperiod (photoperiod*time, p = 0.041, Tukey's HSD p = 0.628, Table 4.4) (Figure 4.7A). However, there was a shift in the distribution of cell sizes such that there was a greater abundance of cells with a smaller diameter, estimated

A

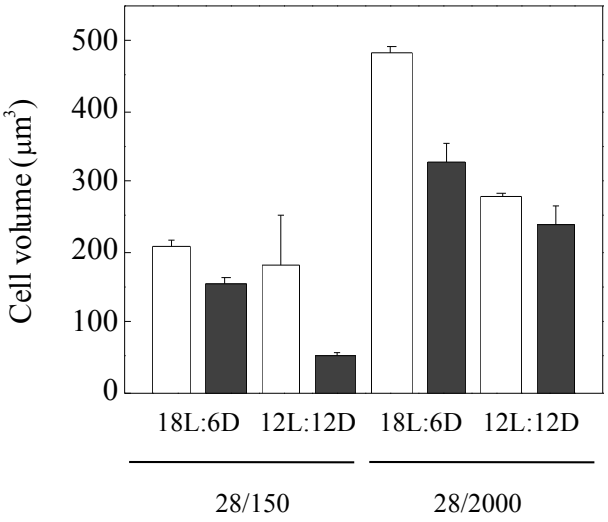
Cell volume (μm³)
500
400
300
200
100
0
18L:6D
12L:12D
18L:6D
12L:12D
28/150
28/2000

B

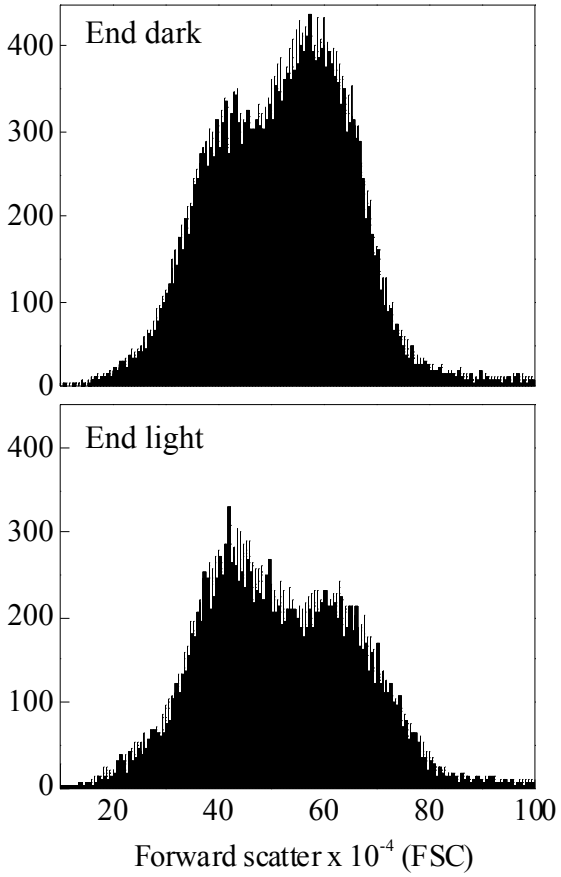
End dark
End light
400
300
200
100
0
20
40
60
80
100
Forward scatter x 10⁻⁴ (FSC)

Figure 4.7 (A) Change in cellular volume during a daily dark period. *C. vulgaris* was grown at either 150 or 2000 µmol photons m^{-2} sec^{-1} at 28 ^{o}C under either a 12 h photoperiod (12L:12D) or 18 h photoperiod (18L:6D) photoperiod. Cellular volume was measured immediately prior the end of a daily light period (open bars) as well as immediately prior to the end of the daily dark period (closed bars). See Table 4.4 for statistical differences in cellular volume. Values represent mean ± SEM; n = 3. (B) Representative histograms illustrating the distribution of cell sizes, where cellular diameters was estimated using flow cytometry as forward scatter (FSC), take immediately prior to the end of the light period (end light) as well as prior to the end of the dark period (end dark).

by flow cytometry as forward scatter (FSC), at the end of a dark period relative to the end of the light period (Figure 4.7B). Thus, while there was not significant effect of dark exposure on the mean cell volume under all conditions, there was shift in the distribution of cell sizes that may not be reflected by changes in the mean cell volume (Figure 4.7B).

4.3.3.3 Cell cycle tracking

Photoperiod-dependent cell division could also account for the observed transient oscillations in OD_{735}. To test this, the change in cellular DNA content was assayed using a cell membrane-permeable fluorescent dye. A stably low Vybrant green fluorescence signal was observed during the light period followed by a 4-fold increase in the fluorescence signal at the light-to-dark transition in *C. vulgaris* grown under a daily photoperiod (Figure 4.8A). The fluorescence signal returned to baseline levels by the end of the dark period (Figures 4.8A). Furthermore, a 4-fold increase in cellular volume appeared to precede the increase in the DNA fluorescence signal by 6 h (Figure 4.8B).

4.4 Discussion

Contrary to the original hypothesis, the specific growth rates of Photobioreactor-grown cultures of *C. vulgaris* were independent of both growth light intensity as well as the length of the photoperiod (Tables 4.1 and 4.2). Thus, consistent with previous reports for *C. vulgaris* (Wilson and Hüner 2000), this species appears unable to up-regulate growth rate in response to increased growth light intensity. While we did not detect an effect of light intensity on the absolute specific growth rate during the exponential growth phase at either 28/150 or 28/2000, the rate of change in OD_{735} over time during the daily light period was 2-fold greater in cells grown at 28/2000 relative to those grown at 28/150 when *C. vulgaris* was grown under a daily light:dark cycle (Tables 4.2 and 4.3). This is analogous to studies in *Chlamydomonas* sp. which demonstrated an increased growth rate with increased light intensity (Vítová et al. 2011a, Vitova et al. 2011b). However, in *C. vulgaris* this positive relationship between growth rate and light intensity appears to be

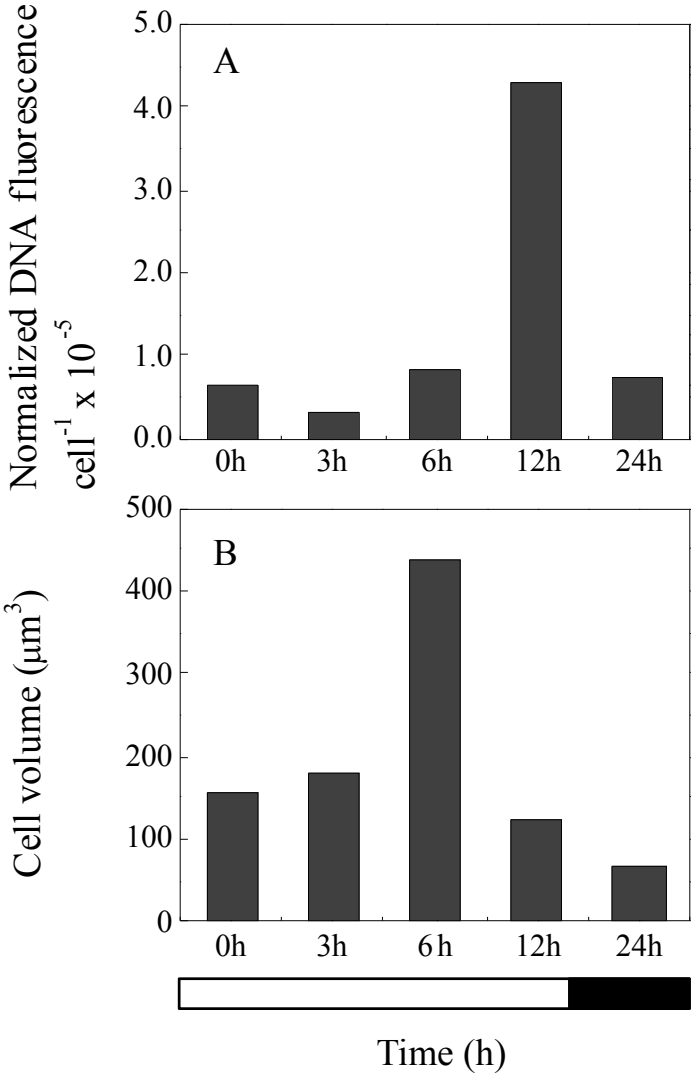
A
B
Normalized DNA fluorescence
cell^{-1} x 10^{-5}
Cell volume (µm^3)
5.0
4.0
3.0
2.0
1.0
0.0
500
400
300
200
100
0
0h
3h
6h
12h
24h
Time (h)

Figure 4.8 Representative diel changes in cell density, cellular DNA content and cellular volume for a culture of *C. vulgaris* grown to mid-log phase at 28 ^{o}C / 150 µmol photons m^{-2} sec^{-1} under a 12 h photoperiod. (A) Daily changes in DNA fluorescence were assayed using flow cytometry as a function of time where time 0 h represents the start of a 12 h light period for cells grown under a 12 h photoperiod. (B) Cellular volume was measured using flow cytometry at the same time points. Trends were confirmed with independent biological replicates. The open bar under the graph represents the daily light period while the closed bar represents the daily dark period.

limited to periods of light exposure only, as the specific growth rates during the exponential growth phase of *C. vulgaris* were ultimately independent of both growth light intensity and photoperiod.

We propose that the daily oscillations in OD_{735} observed during growth and development under various photoperiods are reflective of synchronization of the cell cycle by the light:dark cycle. During growth under an alternating light:dark cycle, the majority of cells appear to be in the G_0/G_1 phase of the cell cycle during the light period as characterized by a relatively constant but low DNA fluorescence signal where the relatively low fluorescence signal would correspond to cells in the G_0/G_1 phases. There was an approximately four-fold increase in the DNA fluorescence signal corresponding to increased DNA content in mitotic cells that occurred at the light-to-dark transition during growth under a 12 h light:dark cycle (Figure 4.8A) which has been demonstrated to immediately precede nuclear and cell division in green algae (Bišová and Zachleder 2014). This marked increase in the fluorescence signal at the end of the daily light period corresponded with a shift in the distribution of cells such that there was a greater proportion of high fluorescence cells, corresponding to cells with an increased DNA content in the G_2/M phase of the cell cycle, at the end of the light period relative to cells measured at the end of the dark period (Figures S4.4). This is in contrast to cells grown under CL where cells were equally distributed between the G_0/G_1 and G_2/M phases (Figure S4.4) characteristic of an unsynchronized population of cells. Furthermore, the 4-fold increase in cellular volume that preceded the increase in DNA cellular content (Figure 4.8B) is characteristic of the attainment of a critical size during cell cycle progression that precedes a commitment to divide in green algae (Bišová and Zachleder 2014).

The results of this study are consistent with early work by Tamiya and colleagues in synchronous cultures of green algae which demonstrated that the separation of mother cells following mitosis was confined to the dark periods during growth under daily light:dark cycles (Hase et al. 1959, Morimura 1959, Tamiya and Morimuta 1961, Morimura et al. 1964). Similarly, mitosis occurs predominately during dark period in the

macroalgal species *Ulva pseudocurvata* (Titlyanov et al. 1996) and *Porphyra umbilicus* (Lüning et al. 1997), as well as the unicellular green alga *Chlamydomonas reinhardtii* (Goto and Johnson 1995) during growth and development under various photoperiods. The temporal separation of photosynthesis and photosynthetic carbon metabolism during the day and DNA replication-division during the night has been suggested to confer an evolutionary advantage by allowing for optimization of growth during the light period when energy is readily available (Bišová and Zachleder 2014).

In addition to growth rate, starch content additionally appears insensitive to both photoperiod and growth irradiance (Figure 4.6A and Table S4.1). Therefore, consistent with the previous studies using CL (Savitch et al. 1996), we conclude *C. vulgaris* exhibits a minimal capacity to upregulate absolute metabolic sink capacity. While there was a significant decrease in starch content during the dark period at both the 18 h and 12 h photoperiods when cells were grown at either 28/150 or 28/2000, the apparent consumption rate of starch during the daily dark period was 2-fold lower when *C. vulgaris* was grown under a 12 h photoperiod relative to an 18h photoperiod at both light intensities (Table S4.2). This suggests that photoperiod may modify carbohydrate metabolism in *C. vulgaris*. Similarly, growth under a short-day photoperiod has been demonstrated to decrease the rate of starch degradation during the dark relative to growth under a long-day photoperiod in *A. thaliana* which is believed to prevent pre-mature depletion of starch reserves during the night (Lu et al. 2005, Gibon et al. 2009). Although the mechanisms regulating transient starch formation and degradation in green algae are not well understood, the corresponding increase in sucrose content during the dark period is consistent with the suggested mechanism of feedback inhibition from carbohydrate metabolism (Lepisto and Rintamaki 2012).

Studies in *C. reinhardtii* indicate starch is required both to supply energy for the metabolic demands of the cell during the dark period as well as for use as a vital energy supply for cellular division as starch reserves were consumed in this species during cellular division in the light where the energy required for division could be supplied directly by photosynthesis (Vítová et al. 2011b). This suggests a close relationship

between the cellular energy stores and growth rate. We therefore suggest that the apparent inability to up-regulate growth rate in *C. vulgaris* in response to increased growth irradiance may be ultimately reflective of limitations at the level of the capacity to increase starch reserves.

Despite reasonable correlation between OD_{735} and cell counts during growth under CL (Figure S4.1) it appears OD_{735} is influenced by other optical, or light scattering properties of the cells, including cell size as well as the presence of highly light scattering carbohydrate reserves. The results for diel changes in cell size, DNA content and carbohydrate content appear consistent with recent models of cellular division in green algae (Bišová and Zachleder 2014) and indicate that oscillation in OD_{735} are likely reflective of cell cycle progression in *C. vulgaris*. Diurnal cell division has been observed in multiple species of microalgae (Nelson and Brand 1979). Many models account for this periodicity in cell division by suggesting the cell cycle, or cell cycle machinery, is regulated by an endogenous circadian clock (Edmunds and Adams 1981, Homma and Hastings 1989). However, we suggest a model of cell division regulated by an endogenous clock is likely not applicable to *C. vulgaris* as the diel oscillations in OD_{735} disappeared immediately in CL (Figure 4.5). This is in direct contrast to the green alga *Nannochloropsis gaditana* (Braun et al. 2014) as well as the cyanobacteria *Cyanothece* sp. (Nedbal et al. 2008) where photobioreactor-grown cultures of *N. gaditana* and *Cyanothece* sp. both exhibited similar diel oscillations in OD_{735} during growth and development under a 12 h photoperiod; however, unlike *C. vulgaris*, these oscillations in OD_{735} persisted in CL (Nedbal et al. 2008, Braun et al. 2014). This likely indicates that regulation of growth by light and photoperiod in photoautotrophic microbes is species specific.

The apparent immediate synchronization of cellular division in *C. vulgaris* in response to changes in light availability following a shift to CL (Figure 4.5) supports a model for direct regulation of the cell cycle by the environmental light:dark cycle. Recently, the cell cycle in *C. reinhardtii* (Vítová et al. 2011a, Vítová et al. 2011b) and the multicellular algal *Ulva compressa* (Kuwano et al. 2008, Kuwano et al. 2014) have been demonstrated

to be regulated independently of an endogenous clock. Alternative models propose that cell cycle progression is regulated directly by the light:dark cycle (Vítová et al. 2011a, Vítová et al. 2011b, Bišová and Zachleder 2014, Kuwano et al. 2014). These models propose that cell volume increases in the light period using the energy supplied by photosynthesis until a critical size, termed the commitment point, is reached and DNA replication-division occurs (Vítová et al. 2011a, Vítová et al. 2011b, Bišová and Zachleder 2014, Kuwano et al. 2014).

Oscillations in OD_{680}, a measure of Chl concentration, were detected that paralleled the response of OD_{735} to the daily light:dark cycle where there was a steady increase in OD_{680} during the light period and decrease during the dark period (Figures 4.2 and 4.3). Consistent with the immediate dampening of oscillations on OD_{735} in CL, oscillations in OD_{680} also immediately disappeared following a transfer to CL (Figure 4.5). The strictly diurnal increase in OD_{680} suggests that Chl biosynthesis is positively regulated by light in *C. vulgaris*. The light-dependent photoreduction of protochlorophyllide to chlorophyllide is catalyzed by the enzyme protochlorophyllide oxidoreductase (POR) (Reinbothe et al. 2010). However, a second structurally unrelated dark operative POR enzyme found in photoautotrophic bacteria, algae and gymnosperms is capable of catalyzing this reaction in the dark (Reinbothe et al. 2010). Although the genes encoding the subunits of this dark operative, or light independent, POR enzyme have been detected in *C. vulgaris* (Gabruk et al. 2012), the strictly diurnal increase in OD_{680} may indicate that *C. vulgaris* does not express this enzyme under these conditions. Interestingly, circadian oscillations in δ-aminolevulinic acid (ALA), a early precursor to Chl biosynthesis, have been observed in *Hordeum vulgare* (Beator and Kloppstech 1993, Kruse et al. 1997). However, the strict diurnal increases in both OD_{735} and OD_{680} suggests that growth as well as Chl accumulation is light-dependent in *C. vulgaris* providing an environmental control to coordinate Chl biosynthesis to periods of light exposure.

While oscillations in OD_{680} and OD_{735} were immediately dampened following a transfer from growth under a light:dark cycle to CL, oscillations in both F_M' and F_S persisted in CL (Figure 4.5). This indicates PSII photochemistry may oscillate independently of

cellular division in *C. vulgaris*. Similar circadian oscillations in PSII quantum yield (Φ_{PSII}) have been detected in *Kalanchoe daigremontiana* using modulated Chl *a* fluorescence induction (Wyka et al. 2005). Circadian regulation of light harvesting capacity was first described in algae (Sweeney and Haxo 1961). Circadian oscillations in photosynthetic oxygen evolution (Sweeney and Haxo 1961) and electron transport (Mackenzie and Morse 2011) have since additionally been detected in algae. Early work by Sweeney and colleague (1961) demonstrating oscillations in photosynthesis occur in anucleated *Acetabularia* (Sweeney and Haxo 1961) was later followed by the finding that oscillations in peroxiredoxin redox state occur independently of the nuclear-encoded circadian oscillator in *Ostreococcus tauri* (O'Neill et al. 2011). The persistent oscillations in Chl *a* fluorescence in CL in the absence of apparent rhythms in cellular division may similarly indicate the presence of plastid-autonomous circadian rhythms. However, more work is required to confirm this in *C. vulgaris*.

Growth of *C. vulgaris* under an alternating light:dark cycle is dominated by oscillations in OD_{735}, OD_{680} and Chl *a* fluorescence induction that are not observed during growth at development under CL. We suggest that the nocturnal decrease in OD_{735} principally reflects changes in the light-scattering, or optical properties of the cells, including a decrease in cell size and consumption of starch reserves. Furthermore, we suggest that the nocturnal catabolism of starch reserves in conjunction with the diurnal changes in DNA content and cellular volume indicate that these oscillations reflect synchronized cellular division in *C. vulgaris*.

4.5 References

Beator, J. & Kloppstech, K. 1993. The circadian oscillator coordinates the synthesis of apoproteins and their pigments during chloroplast development. *Plant Physiol.* 103: 191–196.

Bišová, K. & Zachleder, V. 2014. Cell-cycle regulation in green algae dividing by multiple fission. *J. Exp. Bot*. 25:2585–2602.

Braun, R., Farré, E.M., Schurr, U. & Matsubara, S. 2014 . Effects of light and circadian clock on growth and chlorophyll accumulation of N annochloropsis gaditana. *J Phycol*. 50:515–525.

Dodd, A.N., Kusakina, J., Hall, A., Gould, P.D. & Hanaoka, M. 2014. The circadian regulation of photosynthesis. *Photosynth. Res.* 119:181–190.

Dodd, A.N., Salathia, N., Hall, A., Kever, E., Toth, R., Nagy, F., Hibberd, J.M., Millar, A.J. & Webb, A.A.R. 2005. Plant circadian clocks increase photosynthesis, growth, survival, and competitive advantage. *Science* 309:630–633.

Eckardt, N.A. 2005. Temperature entrainment of the *Arabidopsis* circadian clock. *Plant Cell* 17:645–647.

Edmunds, L.N. & Adams, K.J. 1981. Clocked cell cycle clocks. *Science* 211:1002–1012.

Gabruk, M., Grzyb, J., Kruk, J. & Mysliwa-Kurdziel, B. 2012. Light-dependent and light-independent protochlorophyllide oxidoreductases share similar sequence motifs — in silico studies. *Photosynthetica* 50:529–540.

Gibon, Y., Pyl, E.T., Sulpice, R., Lunn, J.E., Hogne, M., Gunther, M. & Stitt, M. 2009. Adjustment of growth, starch turnover, protein content and central metabolism to a decrease of the carbon supply when *Arabidopsis* is grown in very short photoperiods. *Plant Cell Environ.* 32:859–74.

Goto, K. & Johnson, C. 1995. Is the cell division cycle gated by a circadian clock? The case of *Chlamydomonas reinhardtii*. *J. Cell Biol.* 129:1061–1069.

Graf, A. & Smith, A.M. 2011. Starch and the clock: the dark side of plant productivity. *Trends Plant Sci*. 16:169–175.

Harmer, S.L. 2009. The circadian system in higher plants. *Annu. Rev. Plant Biol.* 60:357–377.

Hase, E., Otsuka, H., Mihara, S. & Tamiya, H. 1959. Role of sulfur in the cell division of *Chlorella*, studied by the technique of synchronous culture. *Biochim. Biophys. Acta* 35:180–189.

Homma, K. & Hastings, J.W. 1989. Cell growth kinetics, division asymmetry and volime control at division in the marine dinoflagellate *Gonyaulax polyedra*: a model of circadian clock control of the cell cycle. *J. Cell Sci.* 92: 303–318.

Kirk, D.L. 2004. Volvox. Curr. Biol. 14:599–600.

Kruse, E., Grimm, B., Beator, J. & Kloppstech, K. 1997. Developmental and circadian control of the capacity for δ-aminolevulinic acid synthesis in green barley. *Planta* 202: 235–241.

Kulheim, C., Agren, J. & Jansson, S. 2002 Rapid regulation of light harvesting and plant fitness in the field. *Science* 297:91–93.

Kuwano, K., Abe, N., Nishi, Y., Seno, H., Nishihara, G.N., Iima, M. & Zachleder, V. 2014 . Growth and cell cycle of *Ulva compressa* Ulvophyceae under LED illumination*. J. Phycol.* 50:744–752.

Kuwano, K., Sakurai, R., Motozu, Y., Kitade, Y. & Saga, N. 2008. Diurnal cell division regulated by gating the G1/S transition in *Enteromorpha compressa* chlorophyta. *J. Phycol*. 44:364–373.

Lee, Y.K., Chen, W., Shen, H., Han, D., Li, Y., Jones, H.D.T., Timlin, J.A. & Hu, Q. 2013. "Basic culturing and analytical meaurement techniques," *In* Richmond, A. & Hu, Q. [Eds.] *Handbook of Applied Microalgal Culture: Applied Phycology and Biotechnology, Second Edition,* Wiley-Blackwell, West Sussex, the United Kingdom, pp. 37–68.

Lepisto, A. and Rintamaki, E. 2012. Coordination of plastid and light signaling pathways upon development of *Arabidopsis* leaves under various photoperiods. Mol. Plant 5:799–816.

Lüning, K., Titlyanov, E. & Titlyanova, T. 1997. Diurnal and circadian periodicity of mitosis and growth in marine macroalgae. III. The red alga *Porphyra umbilicalis*. *Eur. J. Phycol*. 32: 167–173.

Maxwell, D.P., Falk, S., Trick, C.G. & Hüner, N.P.A. 1994. Growth at low temperature mimics high-light acclimation in *Chlorella vulgaris*. *Plant Physiol.* 105:535–543.

Mackenzie, T.D.B. & Morse, D. 2011. Circadian photosynthetic reductant flow in the dinoflagellate *Lingulodinium* is limited by carbon availability. *Plant Cell Environ.* 34:669–680.

McClung, C.R. 2006. Plant circadian rhythms. *Plant Cell* 18:792–803.

Makarov, V.N., Schoschina, E.V. & Luning, K. 1995. Dirunal and circadian periodicity of mitosis and growth in marine macroalgae. I. Junvenile sporophytes of Larminariales (Phaeophyta). *Eur. J. Phycol*. 30:261–263.

Mitchison, J.M. 1971. *The biology of the cell cycle*. Cambridge University Press, Cambridge, the United Kingdom.

Morimura, Y. 1959. Synchronous culture of *Chlorella* I. Kinetic analysis of the life cycle of Chlorella ellipsoidea as affected by changes of temperature and light intensity. *Plant Cell Physiol.* 1:49–62.

Morimura, Y., Yanagi, S. & Tamiya, H. 1964. Synchronous mass-culture of *Chlorella*. *Plant Cell Physiol.* 5.

Nedbal, L., Brezina, V., Cerveny, J. & Trtilek, M. 2005. Photosynthesis in dynamic light: systems biology of unconventional chlorophyll fluorescence transients in *Synechocystis* sp. PCC 6803. *Photosynth Res.* 84:99–106.

Nedbal, L., Trtilek, M., Cerveny, J., Komarek, O. & Pakrasi, H.B. 2008. A photobioreactor system for precision cultivation of photoautotrophic microorganisms and for high-content analysis of suspension dynamics. *Biotechnol. Bioeng*. 100:902–910.

Nelson, D. & Brand, L. 1979. Cell division peridicity in 13 species of marine phytoplankton on a light:dark cycle. *J. Phycol.* 15:65–75.

Nichols, S.H.W & Bold, H.C. 1965. *Trichosarcina polymorpha* gen. et sp. nov. *J. Phycol*. 1:34–38.

O'Neill, J., Van Ooijen, G., Dixon, L., Troein, C. Corellou, F. Bouget, F-Y., Reddy, A.B. & Millar, A.J. 2011. Circadian rhythms persist without transcription in a eukaryote. *Nature* 369:554–558.

Reinbothe, C., Bakkouri, M., Buhr, F., Muraki, N., Nomata, J., Kurisu, G., Fujita, Y. & Reinboth, S. 2010. Chlorophyll biosynthesis: spotlight on protochlorophyllide reduction. *Trends Plant Sci.* 15:614–624.

Salone, P.A. & McClung, C.R. 2005. What makes the *Arabidopsis* clock tick on time? A review on entrainment. *Plant Cell Environ*. 28:21–38

Savitch, L.V., Maxwell, D.P. & Hüner N.P.A. 1996. Photosystem II excitation pressure and photosynthetic carbon metabolism in *Chlorella vulgaris*. *Plant Physiol.* 111:127–136.

Staiger, D., Shin, J., Johansson, M. & Davis, S.J. 2013. The circadian clock goes genomic. *Genome Biol*. 14:208.

Stressman D., Millar, A., Spalding, M. & Rodermel, S. 2002. Regulation of photosynthesis during *Arabidopsis* lead development in continuous light. *Photosynth. Res*. 72:27–37.

Sysoeva, M., Markovskaya, E.F. & Shibaeva, T.G. 2010. Plants under continuous light: a review. Plant Stress 4:5–17.

Tamiya, H. & Morimura, Y. 1961. Mode of nuclear division in synchronous cultures of *Chlorella*: comparison of various methods of synchronization. *Plant Cell Physiol.* 2:383–403.

Titlyanov, E., Titlyanova, T.V. & Lunning, K. 1996. Diurnal and circadian periodicity of mitosis and growth in marine macroalgae. II. The green alga *Ulva pseudocurvata*. *Eur. J. Phycol*. 31: 181–188.

van Gestel, N.C., Nesbit, A.D., Gordon, E.P., Green, C., Pare, P.W., Thompson, L., Pefflet, E.B. & Tissue, D.T. 2005. Continuous light may induce photosynthetic downregulation in onion - consequences for growth and biomass partitioning. *Physiol. Plant* 125:235–246.

Velez-Ramirz, A., van Ieperen, W. Vreugdenhil, D. & Millenaar, F.F. 2011. Plants under contunuous light. Trends Plant Sci. 16:310–316.

Vítová, M., Bišová, K., Hlavová, M. & Kawano, S. 2011a. *Chlamydomonas reinhardtii*: duration of its cell cycle and phases at growth rates affected by temperature. *Planta* 234:599-608.

Vítová, M., Bišová, K., Umysová, D. & Hlavová, M. 2011b. *Chlamydomonas reinhardtii*: duration of its cell cycle and phases at growth rates affected by light intensity. *Planta* 233:75–86.

Wilson, K.E. & Hüner, N.P.A. 2000. The role of growth rate, redox-state of the plastoquinone pool and the trans-thylakoid deltapH in photoacclimation of *Chlorella vulgaris* to growth irradiance and temperature. *Planta* 212:93–102.

Wood, A.M., Everroad, R.C. & Wingard, L.M. 2005. "Measuring growth rates in microalgal cultures," *In* Anderson, R.A. [Ed.] *Algal Culturing Techniques,* Elsevier Academic Publishers, Burlington, United States of America, pp. 269–286.

Wyka, T.P., Duarte, H.M. & Lüttge, U.E. 2005. Redundancy of stomatal control for the circadian photosynthetic rhythm in *Kalanchoë daigremontiana* Hamet et Perrier. *Plant Biol.* 7:176–181.

4.6 Supplementary Material

4.6.1 Supplementary Tables

Supplemental Table S4.1 Comparison of starch and sucrose abundance during a daily light period for cells of *C. vulgaris* grown at 28 ^{o}C and either 150 or 2000 µmol photons m^{-2} sec^{-1} under 24 h, 18 h and 12 h photoperiods. Values under growth regime represent temperature (°C) / irradiance (2000 µmol photons m^{-2} sec^{-1}) with the length of light (L) and dark (D) exposure in a 24 h cycle. Values represent mean ± SEM; n = 3. A two-factorial ANOVA followed by a Tukey's HSD post hoc test was used to compare means. Data were visually inspected for normality and equality of variance. When equal variances were not observed, the data were log transformed to achieve equal variances. Means not connected by the same letter are significantly differentat $p < 0.05$.

	Growth regime					
	28/150			28/2000		
	24L:0D	18L:6D	12L:12D	24L:0D	18L:6D	12L:12D
Starch (nmol 10^7 $cells^{-1}$)	25.94 ± 2.52^{a}	17.71 ± 1.74^{a}	24.23 ± 2.22^{a}	15.78 ± 3.18^{a}	19.29 ± 3.95^{a}	17.89 ± 3.71^{a}
Sucrose (nmol 10^7 $cells^{-1}$)	18.88 ± 1.38^{ab}	17.29 ± 2.07^{b}	4.82 ± 0.99^{c}	35.20 ± 3.86^{a}	27.91 ± 4.19^{ab}	25.69 ± 3.84^{ab}

Starch: irradiance, $F_{1,12} = 2.8$, $p = 0.177$; photoperiod, $F_{1,12} = 0.3$, $p = 0.738$; irradiance * photoperiod, $F_{1,12} = 1.4$, $p = 0.289$.

Sucrose: irradiance, $F_{1,12} = 63.8$, $p < 0.0001$; photoperiod, $F_{1,12} = 20.3$, $p = 0.0001$; irradiance * photoperiod, $F_{1,12} = 10.8$, $p = 0.002$.

Supplemental Table S4.2 Change in total starch content over time during a daily light period for *Chlorella vulgaris* grown at either 150 or 2000 µmol photon m^{-2} sec^{-1} at 28 ^{o}C under either an 18 h photoperiod or 12 h photoperiod. Change in starch content over time was calculated as the difference between starch content at the start and end of a daily period dark divided by the length of the dark period (h). Numbers under growth regime indicate growth temperature (^{o}C) / irradiance (µmol photons m^{-2} sec^{-1}) followed by the length of light (L) and dark (D) periods in a 24 h cycle. Values represent mean ± SEM; n = 3. Means were compared with a two-way ANOVA followed by a Tukey's HSD post hoc test; means not connected by the same letter were considered significant at $p < 0.05$.

Growth regime		nmol starch consumed 10^7 $cells^{-1}$ / h
28/150	18L:6D	3.05 ± 0.63^{a}
	12L:12D	1.38 ± 0.31^{b}
28/2000	24L:0D	2.62 ± 0.22^{a}
	18L:6D	1.74 ± 0.22^{b}

irradiance, $F_{1,8} = 0.7$, $p = 0.407$; photoperiod, $F_{1,8} = 20.2$, $p = 0.002$; irradiance x photoperiod, $F_{1,8} = 0.09$, $p = 0.77$.

4.6.2 Supplementary Figures

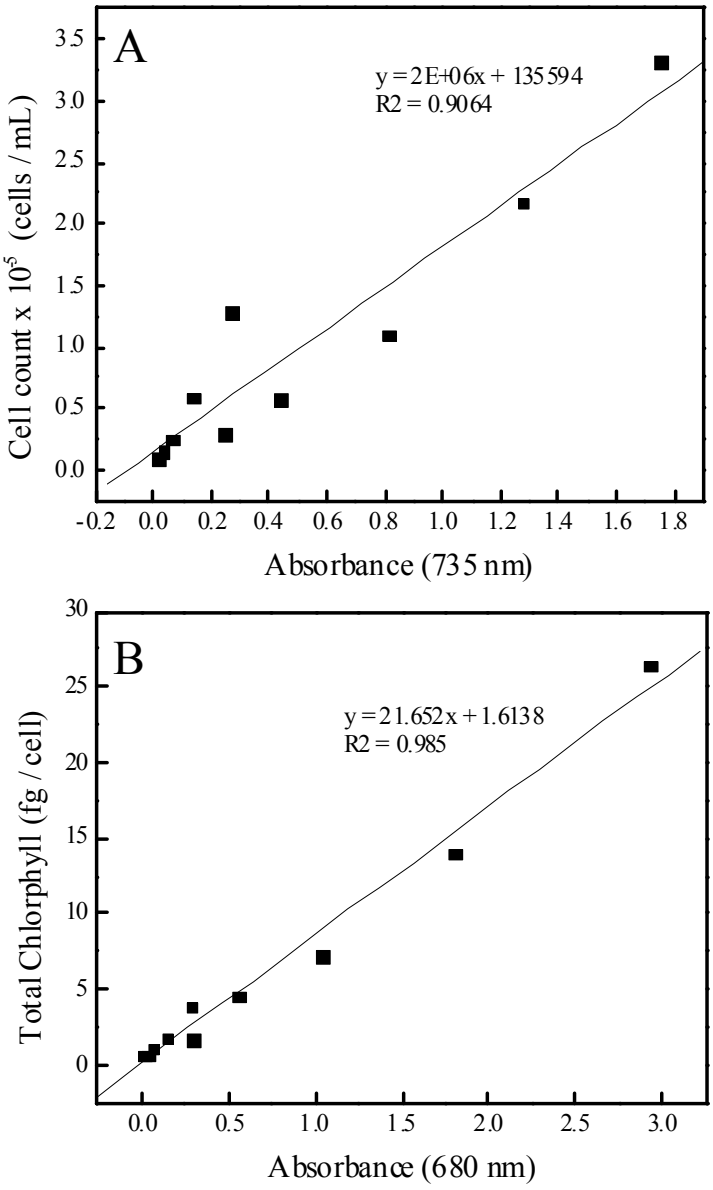

Supplemental Figure S4.1 (A) Correlation between optical density measured at 735 and independent cell counts made using flow cytometry. (B) Correlation between optical density measured at 680 and independent measures of chlorophyll content using spectrophotometry.

A

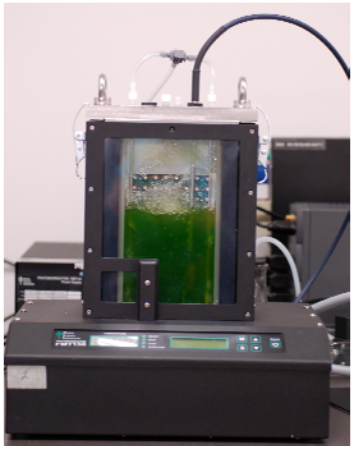

B

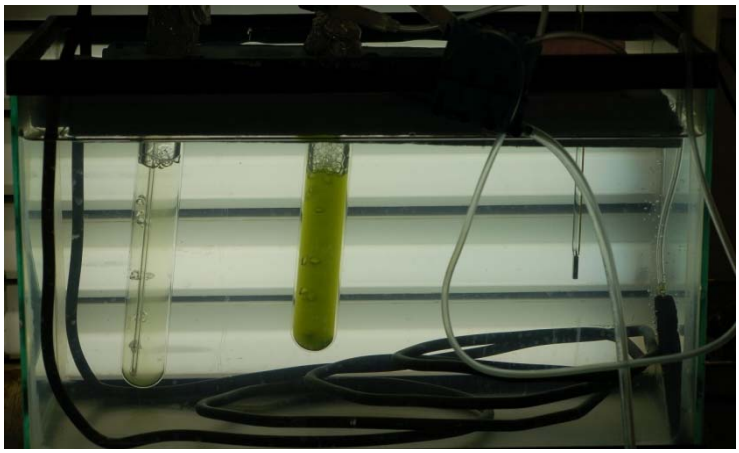

Supplemental Figure S4.2 (A) Cells of *Chlorella vulgaris* cultivated in a 400mL capacity Photobioreactor. Light was supplied by light emitting diodes integrated into the Photobioreactor system. Light and temperature regimes were maintained by the Photobioreactor control system. (B) *C. vulgaris* cells cultivated in 150 mL capacity growth tubes suspended in a temperature controlled water bath. Light was supplied by a bank of fluorescent lights behind the aquarium.

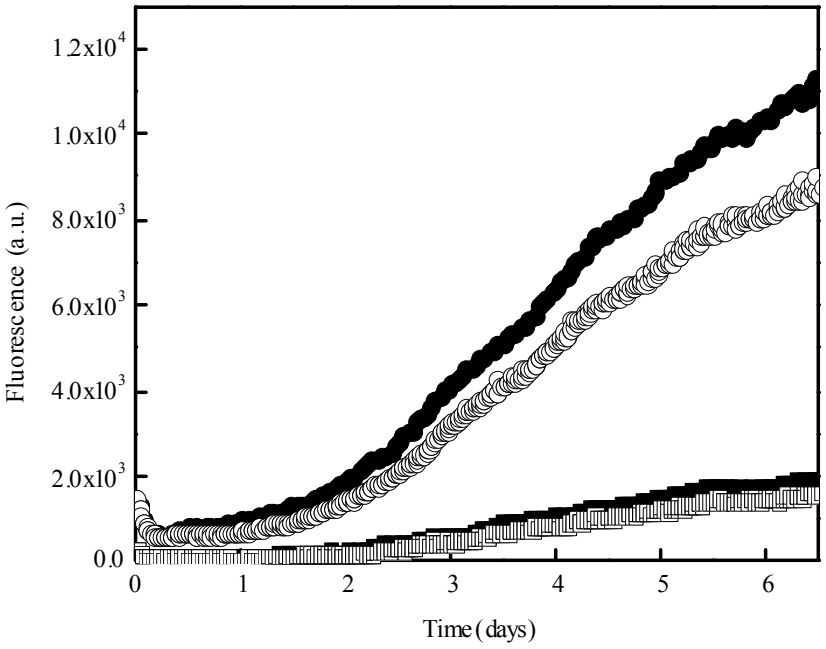

Supplemental Figure S4.3 Representative change in chlorophyll *a* fluorescence induction in cells of *Chlorella vulgaris* grown at 28 ^{o}C and 150 μmol photons m^{-2} sec^{-1}. Chlorophyll fluorescence was alternatively excited by the blue (circles; F_M', closed circles and F_S, open circles) and red light (squares; F_M', closed squares and F_S, open squares) emitting diodes at 30 minute intervals. Fluorescence was measured by a fluorometer integrated into the Photobioreactor system and recorded by the control system.

A – Continuous light

B – Alternating light:dark cycle

Start light (End dark)

End light

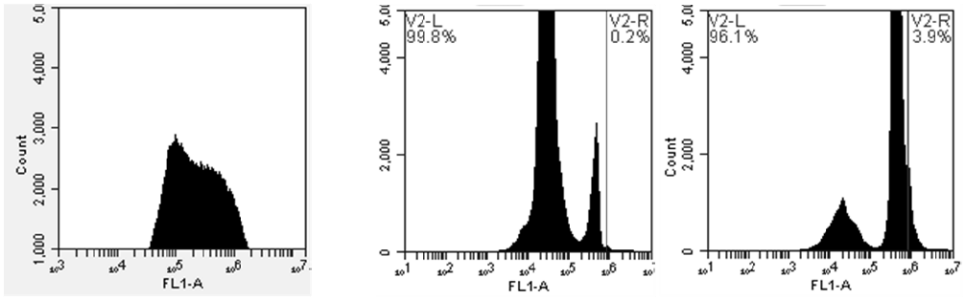

Supplemental Figure S4.4 Representative histograms showing DNA:Vybrant Green fluorescence for cells of C. vulgaris grown under (A) continuous light or (B) an alternating light:dark cycle where samples were collected either at the start of the light period (corresponding the end of the previous dark perod) or end of the dark period. Relatively low fluorescence cells in the G_0/G_1 phases are separated by cells in the S-phase from the relatively higher fluorescence cells with an increased DNA content in the G_2/M phase.

Chapter 5

5 SUMMARY AND PERSPECTIVES

A clear consensus has emerged that "operational" signals derived from mature chloroplasts serve as the major signals regulating the structure and function of the photosynthetic apparatus in response to environmental change (Hüner et al. 1998, Pfannschmidt et al. 2003, Ensminger et al. 2006, Hüner et al. 2012). Previous studies on acclimation to excitation pressure in green algae have been conducted under constant growth light (Maxwell et al. 1994, Maxwell et a. 1995a, Wilson et al. 2000, Wilson and Hüner, 2003). If PSII excitation pressure is the sole regulator of photoacclimation and phenotype in the green alga *Chlorella vulgaris,* then phenotypic, structural and functional responses should correlate with 1 - qP, an *in vivo* measure of the redox state of Q_A and intersystem photosynthetic electron transport, despite sudden or sustained changes in photoperiod. However, based on the results of this thesis I suggest that excitation pressure is not the sole regulator of photoacclimation.

Phenotypic reversion from the yellow-green HEP phenotype to the dark green LEP phenotype in response to a shift from high light to low light at a constant temperature was correlated with relaxation of high PSII excitation pressure during the photoacclimation process as measured by decreases in both E_K and 1 - qP (Chapter 2). The use of inhibitors of photosynthetic electron transport in Chapter 2 are in agreement with earlier studies implicating the PQ pool as the principle sensor for changes in cellular energy balance and regulator of phenotypic plasticity in green algae (Escoubas et al. 1995, Wilson and Hüner 2000, Masuda et al. 2003, Wilson et al. 2003, Chen et al. 2004). However, this conclusion has been challenged in cyanobacteria (Miskiewicz et al. 2000, Miskiewicz et al. 2002) and *Arabidopsis thaliana* (Piippo et al. 2006). Clearly, multiple components may contribute to regulation of gene expression and phenotype by excitation pressure while the extent of this contribution to phenotypic plasticity may be species-dependent as well as likely dependent on the developmental stage and degree of energy imbalance. The end result of retrograde redox sensors is the remodeling of the photosynthetic

apparatus to re-establish a new photostatic state in response to environmental change. However, based on the observation that PSII excitation pressure can be "uncoupled" from the expected phenotypic adjustment in *C. vulgaris* by a shift to darkness, the results from Chapter 2 indicate that the redox state of the PQ pool cannot be the sole role regulator of phenotype and photoacclimation in *C. vulgaris* following a sudden shift in the light environment.

Based on the results of Chapter 2, I propose that photoacclimation in *C. vulgaris* requires the coordination of two distinct regulatory pathways. First, during a change in growth light at a constant temperature, a change in light energy availability is sensed as change in the relative redox state of the PQ pool. The increased abundance of LHCII polypeptides following oxidation of the PQ pool is consistent with the results of this thesis and with those presented in previous studies which suggest that the redox state of the PQ pool as an important component of a retrograde redox sensing and signalling pathway within the photosynthetic electron transport chain regulating the transcription of nuclear-encoded *Lhcb* genes (Escoubas et al. 1995, Wilson and Hüner 2000, Masuda et al. 2003, Wilson et al. 2003, Chen et al. 2004). Second, I propose that concomitant changes in Chl availability are required for the post-translational stabilization of LHCII polypeptides during greening of the yellow-green HEP cells.

I suggest that the yellow-green phenotype in *C. vulgaris* may ultimately represent limitations at the level of Chl availability where pre-exposure to HEP inhibits POR accumulation. Since a low light of 110 µmol photons m^{-2} sec^{-1} was optimal for the accumulation of POR, relaxation of HEP by low light is required to overcome this apparent inhibition. Therefore, I propose that modulation of *de novo* Chl biosynthesis by the redox state of photosynthetic electron transport may represent a supplementary mechanism to regulate σ_{PSII} during imbalances in energy flow (Figure 5.1); however, more work is required to confirm regulation of Chl biosynthesis by the redox state of photosynthetic electron transport.

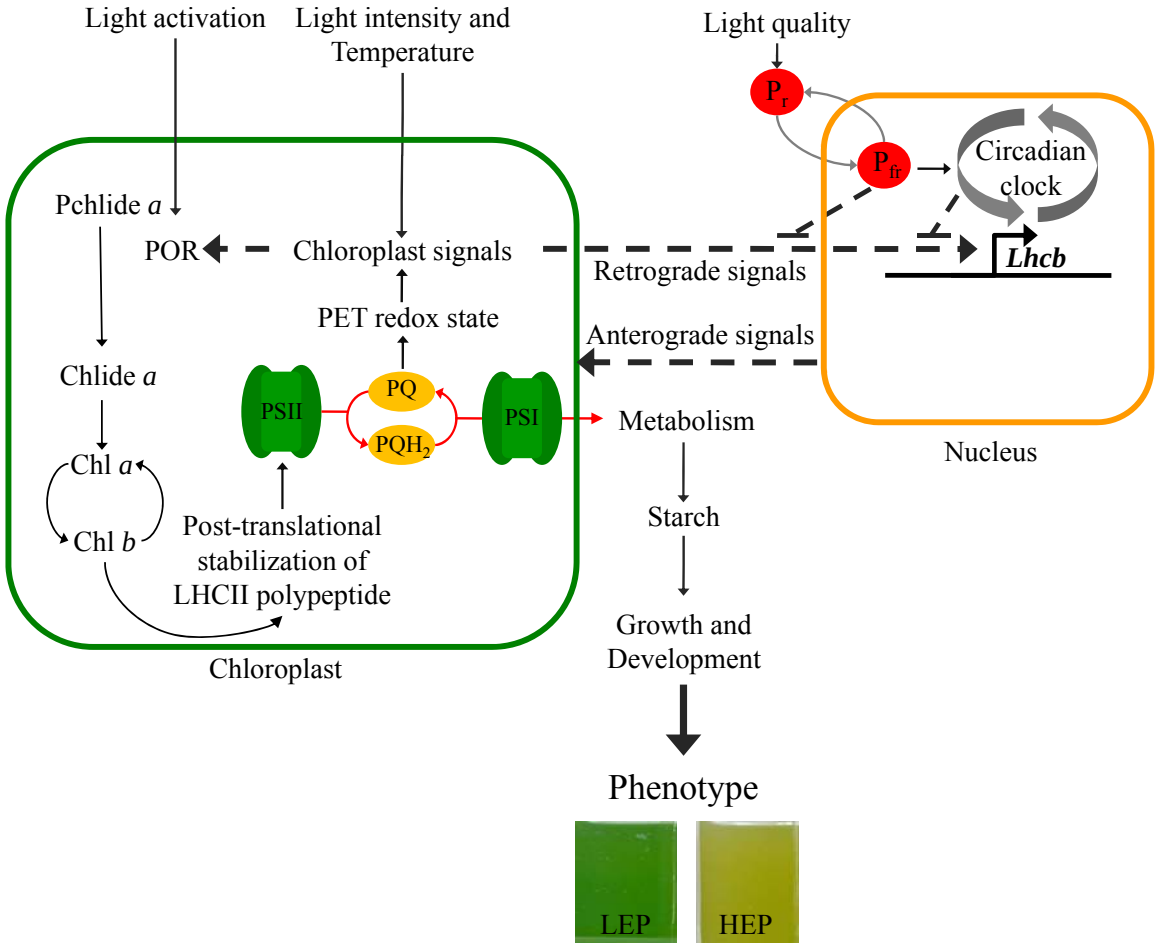
Light activation
Light intensity and Temperature
Light quality
Pr
Pfr
Circadian clock
Pchlide a
POR
Chloroplast signals
Retrograde signals
Lhcb
PET redox state
Anterograde signals
Chlide a
PSII
PQ
PQH2
PSI
Metabolism
Chl a
Chl b
Post-translational stabilization of LHCII polypeptide
Nucleus
Starch
Growth and Development
Chloroplast
Phenotype
LEP
HEP

Figure 5.1 Model illustrating environmental regulation of phenotypic plasticity through integration of chloroplast redox sensing and light-dependent pathways during growth under a variable photoperiod. Imbalance between light as an energy source and metabolic sink capacity is sensed by the mature chloroplast through modulation of the redox state of photosynthetic electron transport; an imbalance in cellular energy flow may be a consequence of the cumulative impact of changes in either, or both, light and temperature. In green algae, changes in the redox state of PET regulate the structure and efficiency of the photosynthetic apparatus to re-establish photostasis; these signals derived from the functional state of the mature chloroplast, are defined as "operational" signals. "Operational" redox signals may additionally modulate *de novo* Chl biosynthesis to match light-harvesting capacity to the energy requirements of the cell to re-establish photostasis. However, the light-dependency for Chl biosynthesis is another important regulator of photoacclimation due to the requirement for post-transcriptional stability of LHCII polypeptides.The phytochrome-mediated sensing and signalling pathways that enable responses to change in light quality are defined as "biogenic" signals. Phytochromes may modulate the extent of photoacclimation in response to a specific photoperiod by potentially modulating the capacity of the nucleus to perceive the plastid redox signal. Photoacclimation in green algae is likely reflective of cross-talk between direct perception of light mediated by phytochromes as well as chloroplast-mediated photosynthetic events. Remodeling of the photosynthetic apparatus in green algae is ultimately reflected as a change in pigmentation. Chl *a*, chlorophyll *a*; Chl *b*, chlorophyll *b*; Chlide *a*, chlorophyllide *a*; Pchlide *a*, protochlorophyllide *a*; HEP, high excitation pressure; LHCII, light-harvesting complex associate with photosystem II; LEP, low excitation pressure; Pfr, far-red absorbing phytochrome; Pr, red absorbing phytochrome; PET, photosynthetic electron transport; POR, protochlorophyllide oxidoreductase; PSI, photosystem I; PSII, photosystem II; PQ, plastoquinone; PQH_2, plastoquinol.

In addition to redox regulation, the apparent positive photoregulation of Chl biosynthesis represents an import independent, yet light-dependent, regulator of light-harvesting antenna size and phenotypic plasticity in *C. vulgaris*. The "uncoupling" of low PSII excitation pressure and the expected dark green phenotype in *C. vulgaris* shifted from a high excitation pressure growth regime to either darkness or very dim light is reconciled by the observation that *C. vulgaris* is unable to accumulate the Chl biosynthesis enzyme POR in darkness and dim light (Chapter 2). Light is therefore a major regulator of plastid function, not only because light is required to relax high PSII excitation pressure, but also because Chl biosynthesis in *C. vulgaris* is light-dependent (Figure 5.1). While changes in light energy availability are conveyed to the nucleus through retrograde redox signal transduction pathways to re-establish photostasis, the requirement for post-translational stabilization of light-harvesting polypeptides by Chl binding likely represents a second important light-dependent regulator of plastid function and phenotypic plasticity in *C. vulgaris* in response to variable light exposure (Figure 5.1). However, subsequent studies should focus on quantifying the abundance of intermediates in the Chl biosynthesis pathway to confirm the presence of a limiting step in Chl biosynthesis at low light and in darkness.

Typically, *Lhcb* mRNA levels are inversely related to irradiance while LHCII protein abundance is directly correlated with *Lhcb* mRNA suggesting *Lhcb* genes are primarily controlled at the level of transcription in green algae (LaRoche et al. 1991, Maxwell et al. 1995b, Webb and Melis 1995, Masuda et al. 2002, Chen et al. 2004). Furthermore, *cis*-acting promoter elements in nuclear-encoded *Lhcb* genes in *Dunaliella* sp. have been identified that are likely required for the plastic redox regulation of nuclear genes during photoacclimation (Escoubas et al. 1995, Chen et al. 2004). It has therefore been assumed that regulation of σ_{PSII} by excitation pressure in green algae in general is primarily controlled at the level of *Lhcb* transcription. However, down regulation of LHCII abundance in *C. reinhardtii* in response to high light appears to be governed through both transcriptional and post-transcriptional mechanisms (Durnford et al. 2003). It remains unclear whether retrograde redox signals directly coordinate Chl and LHCII accumulation in *C. vulgaris* directly through coordinated transcriptional regulation of Chl

biosynthesis enzyme and nuclear-encoded *Lhcb* gene expression in parallel or whether LHCII abundance is primarily regulated post-transcriptionally through a regulatory mechanism involving redox modulation of Chl *b* biosynthesis and post-translational stabilization on LHCII polypeptides.

Efforts to thoroughly characterize *Lhcb* as well as chlorophyll biosynthesis enzyme mRNA abundance, transcript stability and transcription rates in response to modulation of excitation pressure in future studies may be difficult in *C. vulgaris* both due to the difficultly in quickly rupturing the cell wall in this species to extract genetic material as well as the lack of a fully sequenced nuclear genome as of this time. Whether the conclusions gained from other study organisms regarding retrograde signal transduction components and the mechanisms of redox regulation of gene expression can be applied across the chlorophyte algae is unclear. However, the presence of common TCTAA sites in the promoters of *Lhcb* genes in *D. tertiolecta*, *C. reinhardtii* and *Arabidopsis* does suggest that some components of the retrograde signal transduction pathways are highly conserved (Chen et al. 2004).

In addition to sudden shifts in the light environment, photoautotrophs are exposed to sustained fluctuations in the light environment through alternating light:dark cycles at both daily and seasonal levels. Similar to the conclusions of Chapter 2, the results from Chapter 3 indicate previous models assuming excitation pressure is the sole regulator of photoacclimation and phenotypic plasticity in green algae neglect the potential contributions of additional light-sensitive pathways during growth under a variable photoperiod. The "uncoupling" of high PSII excitation pressure and the expected yellow-green phenotype during growth and development under a 12 h photoperiod at high light in Chapter 3 indicates excitation pressure cannot be the sole regulator of phenotype in *C. vulgaris* during growth and development under alternating light:dark cycles.

The results from Chapter 3 indicate that modulation of the structure and function of the photosynthetic apparatus as well as phenotype appear to be dependent on both the degree of excitation pressure during the light period as well as the duration of photoperiod where

growth under HL and an 18 h photoperiod mimicked the structural and photosynthetic traits typical of photoacclimation to HEP while growth under at HL but a 12 h photoperiod mimicked acclimation to LEP (Chapter 3). However, since growth under intermediate photoperiods failed to yield reproducible results I suggest that the length of photoperiod likely influences the interpretation of the retrograde redox signal in a manner analogous to an "on/off switch". While no evidence has been found to support a direct role for photoreceptors or photoreceptor signalling in the fine tuning of the chloroplast to the environment *per se* (Maxwell et al. 1995, Walters et al. 1999, Wilson et al. 2003, Fey et al. 2005), phytochromes may play a role in gating the circadian clock in a manner that induces photoperiod-specific modifications to σ_{PSII} in *C. vulgaris* potentially by directly blocking nuclear perception of the plastid redox signal or impairing the retrograde signal transduction pathway (Figure 5.1).

Clearly future work is required to confirm the role of circadian clock in the capacity to photoacclimate to HEP during growth under a light:dark cycle. However, as I have noted before, molecular work in *C. vulgaris* may be inherently problematic due to the difficulty in quickly rupturing the cell wall. However, I do not believe that we would have pursued the response to photoperiod in another species more amenable to molecular work, such as *Dunaliella* sp., as this species has demonstrated the capacity to green in darkness (Maxwell et al. 1994). In contrast to Post et al. (1994) who concluded that photoacclimation is not a response to light:dark cycles, but rather a response to the average irradiance during the photoperiod, the results in Chapter 3 demonstrate that the length of the photoperiod, in concert with excitation pressure, is a crucial regulator of photoacclimation. I suggest that the effect of the duration of the photoperiod on photoacclimation may be largely underappreciated.

Consistent with previous studies (Savitch et al. 1996, Wilson and Hüner 2000), *C. vulgaris* exhibits a minimal plasticity to adjust either starch stores or growth rate in response to growth light intensity (Chapter 4). In contrast to higher plants where feedback inhibition of photosynthesis is an artifact of growth under continuous light (Velez-Ramirez et al. 2011), sink capacity appears insensitive to photoperiod in *C. vulgris*. The

results in Chapter 4 indicate that *C. vulgaris* demonstrates a minimal plasticity in τ^{-1} in response to both growth light as well as photoperiod. Consequently, *C. vulgaris* photosynthetic apparatus to reduce the capacity to absorb and trap available light energy through a decrease in σ_{PSII}. However, while starch abundance and exponential growth rates exhibit limited responses to photoperiod, the length of photoperiod had a distinct response on cellular growth (Chapter 4) in *C. vulgaris*.

Growth of *C. vulgaris* under varying photoperiods was associated with oscillations in optical density that were correlated with diel changes in cell size, starch content and DNA content (Chapter 4) that suggest DNA replication occurs at the light to dark transition, following an increase in cell volume during the light period, while separation of mother cells occurs late in the dark period (Figure 5.2). The results in Chapter 4 appear consistent with early work which identified that DNA replication occurs as a single wave at the light to dark transition in green algae while separation of daughter cells was exclusively confined to the dark period during growth under an alternating light:dark cycle (Tamiya et al. 1961, Wanka and Mulders 1967, Wanka et al. 1970).

The increase in cellular volume during the light period as well as the rapid dampening of growth oscillations in continuous light in Chapter 4 align with models in *Chlamydomonas reinhardtii* suggesting that the cell cycle in green algae is regulated by cell size where progression from growth to reproductive phases is achieved following attainment of a predetermined critical cell volume that denotes a critical point in the cell cycle (Vítová et al. 2011a, Vítová et al. 2011b, Bišová and Zachleder 2014) as well as discredits the involvement of an internal clock in the regulation of the cell cycle. Figure 5.2 illustrates a model for cellular growth in *C. vulgaris* where, during growth and development under an alternating light:dark cycle, the light period is dedicated to increases in cellular volume and accumulation of starch reserves which are subsequently degraded during the dark period to provide the energy required for the DNA replication, and the nuclear and cellular division sequence.

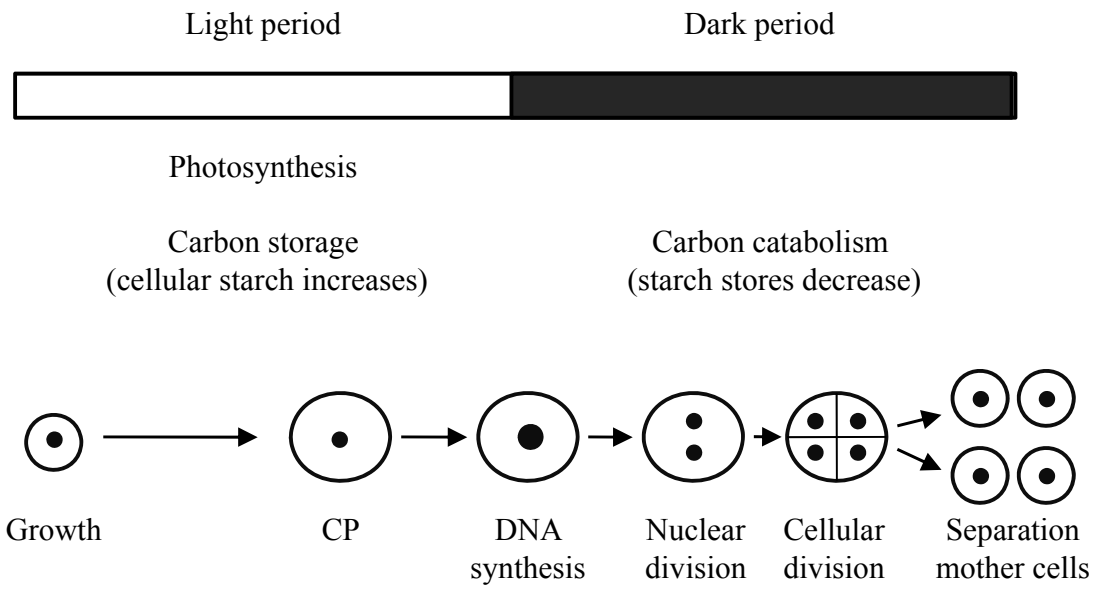

Figure 5.2 Model of cell cycle progression in *C. vulgaris* during growth under a photoperiod. During the light period starch accumulates and the cell increases in volume until a critical cellular volume is obtained; obtainment of this critical volume marks a critical point, or commitment point (CP), in the cell cycle which serves as a switch between growth and cellular reproduction. DNA is replicated at the light-to-dark transition. DNA synthesis is quickly followed by nuclear division and the cellular division sequence. Separation of mother cells likely occurs at the end of the dark period. Starch stores are consumed during the dark period to provide the energy for cellular metabolism and the DNA replication, and nuclear and cellular division sequence. Diurnal availability of light energy and the capacity to store starch in metabolic sinks is suggested to be the major regulator of growth potential. CP, commitment point.

The length of photoperiod additionally modifies carbohydrate metabolism in *C. vulgaris* such that the starch degradation rate appears reduced in response to growth under a 12 h photoperiod as opposed to an 18 h photoperiod (Chapter 4). The mechanisms regulating transient starch formation and degradation under varying photoperiods has not been rigorously addressed in green algae. However, feedback inhibition by sucrose accumulation and redox regulation of enzyme transcription via a thioredoxin system have been proposed for *A. thaliana* (Lepistö and Rintamäki 2012). The relationship between starch metabolism and cellular division appears close as starch reserves are consumed when cells divided in the light (Vítová et al. 2011a; Vítová et al. 2011b); however, this relationship needs to be comprehensively addressed in *C. vulgaris*. I suggest that the inability of *C. vulgaris* to upregulate growth rate (τ^{-1}) in response to increased growth light may ultimately reflect limitations at the capacity to store starch. Therefore, cell growth may be forced into daily periodicity by diurnal light energy availability and the capacity to store photosynthate in metabolic sinks at the level starch abundance.

Previous studies on acclimation to excitation pressure in green algae have been conducted under constant growth light (Maxwell et al. 1994, Maxwell et a. 1995a, Wilson et al. 2000, Wilson and Hüner, 2003); this approach has yield vital insights into the role of the mature chloroplast in the regulation of the structure and function of the photosynthetic apparatus. However, understanding how energy balance is linked to photoautotrophic form and function requires variable experimental conditions that more accurately approximate nature. Using both sudden and sustained variations in photoperiod, it becomes evident that excitation pressure is not the sole regulator of photoacclimation in *C. vulgaris*.

During growth under a variable photoperiod, daily light availability regulates the capacity for Chl biosynthesis (Chapter 2), contributes to the regulation of structure and function of the photosynthetic apparatus (Chapters 2 and 3) as well as regulates the cell cycle (Chapter 4) in *C. vulgaris*. Perception of light in response to growth under a variable photoperiod may be involved in limitating the extent of the acclimation response, rather than affecting photoacclimation itself, indirectly either through the capacity for Chl

biosynthesis or through phytochromes and the photoperiod-dependent capacity to potentially perceive or transmit the retrograde redox signal. It has been suggested that regulation of photosynthetic acclimation must have multiple pathways to address the full range of responses to environmental change (Anderson et al. 1995). While all photosynthetic organisms sense environmental change through modulation of excitation pressure, it is likely ultimately the source-sink relationship that governs the observed phenotype. Phenotypic plasticity and photoacclimation appears to be dependent on a network of intracellular sensors and signal transduction pathways integrating direct perception of light as well as perception of light as an energy source through modulation of the redox state of the photosynthetic apparatus balanced against the capacity to consume the products of photosynthesis through metabolism and ultimately growth (Figure 5.1).

5.1 References

Anderson, J.M., Chow, W.S. & Park, Y.I. 1996. The grand design of photosynthesis: acclimation of the photosynthetic apparatus to environmental cues. *Photosyn. Res.* 46:129–139.

Bišová, K. & Zachleder, V. 2014. Cell-cycle regulation in green algae dividing by multiple fission. *J. Exp. Bot*. 65:2585–2602.

Chen, Y.B., Durnford, D.G., Koblizek, M. & Falkowski, P.G. 2004. Plastid regulation of *Lhcb1* transcription in the chlorophyte alga *Dunaliella tertiolecta*. *Plant Physiol.* 136:3737–3750.

Durnford, D.G., Price, J.A., McKim, S.M. & Sarchfield, M.L. 2003. Light-harvesting complex gene expression is controlled by both transcriptional and post-transcriptional mechanisms during photoacclimation in *Chlamydomonas reinhardtii*. *Physiol. Plant* 118:193–205.

Ensminger, I., Busch, F., & Hüner, N.P.A. 2006. Photostasis and cold acclimation: sensing low temperature through photostasis. *Physiol. Plant.*126:28–44.

Escoubas, J.M., Lomas, M., LaRoche, J. & Falkowski, P.G. 1995. Light intensity regulation of *cab* gene transcription is signaled by the redox state of the plastoquinone pool. *Proc. Natl. Acad. Sci. U.S.A.* 92:10237–10241.

Fey, V., Wagner, R., Brautigam, K. & Pfannschmidt, T. 2005. Photosynthetic redox control of nuclear gene expression. *J. Exp. Bot.* 56:1491–1498.

Hüner, N.P.A., Öquist, G. & Sarhan, F. 1998. Energy balance and acclimation to light and cold. *Trends Plant Sci.* 3:224–230.

Hüner, N.P.A., Bode, R., Dahal, K., Hollis, L., Rosso, D., Krol, M. & Ivanov, A.G. 2012. Chloroplast redox imbalance governs phenotypic plasticity: the "grand design of photosynthesis" revisited. *Front. Plant Sci.* 3:255.

LaRoche, J., Mortain-Bertrand, A. & Falkowski, P.G. 1991. Light intensity-induced changes in *cab* mRNA and light harvesting complex II apoprotein levels in the unicellular chlorophyte *Dunaliella tertiolecta*. *Plant Physiol*. 97:147–153.

Masuda, T., Polle, J.E.W. & Melis, A. 2002. Biosynthesis and distribution of chlorophyll among the photosystems during recovery of the green alga *Dunaliella salina* from irradiance stress. *Plant Physiol.* 128:603–614.

Masuda, T., Tanaka, A. & Melis, A. 2003. Chlorophyll antenna size adjustments by irradiance in *Dunaliella salina* involve coordinate regulation of *chlorophyll a oxygenase* (*CAO*) and *Lhcb* gene expression. *Plant Mol. Biol.* 51:757–771.

Maxwell, D.P., Falk, S. & Hüner, N.P.A. 1995a. Photosystem II excitation pressure and development of resistance to photoinhibition (I. Light-harvesting complex II abundance and zeaxanthin content in *Chlorella vulgaris*). *Plant Physiol.*107:687–694.

Maxwell, D.P., Laudenbach, D.E. & Hüner, N.P.A. 1995b. Redox regulation of light-harvesting complex II and *cab* mRNA abundance in *Dunaliella salina*. *Plant Physio.* 109:787–795.

Miskiewicz, E., Ivanov, A.G., Williams, J.P., Khan, M.U., Falk, S. & Hüner, N.P.A. 2000. Photosynthetic acclimation of the filamentous cyanobacterium, *Plectonema boryanum* UTEX 485, to temperature and light. *Plant Cell Physiol.* 41:767–775.

Miskiewicz, E., Ivanov, A.G. & Hüner, N.PA. 2002. Stoichiometry of the photosynthetic apparatus and phycobilisome structure of the cyanobacterium *Plectonema boryanum* UTEX 485 are regulated by both light and temperature. *Plant Physiol.*130:1414–1425.

Pffanschmidt, T. 2003. Chloroplast redox signals: how photosynthesis controls its own genes. Trends Plant Sci. 8:33–41.

Piippo, M., Allahverdiyeva, Y., Paakkarinen, V., Suoranta, U.M., Battchikova, N. & Aro, E.M. 2006. Chloroplast mediated regulation of nuclear genes in *Arabidopsis thanliana* in the absence of light stress. *Physiol. Genomics* 25:142–152.

Savitch, L.V., Maxwell, D.P. & Hüner, N.P.A. 1996 Photosystem II excitation pressure and photosynthetic carbon metabolism in *Chlorella vulgaris*. *Plant Physiol*. 111:127–136.

Tamiya, H., Morimura, Y. , Mizue, Y. & Kunieda, R. 1961 Mode of nuclear division in synchronous cultures of *Chlorella*: comparison of various methods of synchronization. *Plant Cell* 2:383–403.

Velez-Ramirez, A.L., van Iperen, W., Vreugenhil, D. & Millenaar, F.F. 2011. Plants under continuous light. *Trends Plant Sci.* 16:310–318.

Vítová, M., Bišová, K., Hlavová, M., Kawano, S., Zachleder, V. & Cížková, M. 2011a. *Chlamydomonas reinhardtii*: duration of its cell cycle and phases at growth rates affected by temperature. *Planta* 234:588–608.

Vítová, M., Bišová, K., Umysová, D., Hlavová, M., Kawano, S., Zachleder, V. & Cížková, M. 2011b. *Chlamydomonas reinhardtii*: duration of its cell cycle and phases at growth rates affected by light intensity. *Planta* 233:75–86.

Walters, R.G., Rogers, J.J., Shephard, F. & Horton, P. 1999. Acclimation of *Arabidopsis thaliana* to the light environment: the role of photoreceptors. *Planta* 209:517–527.

Wanka, F., Joosten, H. & De Grip, W. 1970. Composition and synthesis of DNA in synchronously growing cells of *Chlorella pyrenoidosa*. *Arch. Mikrobiol*. 75:25–36.

Wanka, F. & Mulders, P. 1967. The effect of light on DNA synthesis and related processes in synchronous cultures of *Chlorella*. *Arch. Mikrobiol*. 58:257–269.

Webb, M. & Melis, A. 1995. Chloroplast response in *Dunaliella salina* to irradiance stress (effect on thylakoid membrane protein assembly and function). *Plant Physiol*. 107: 885–893.

Wilson, K.E. & Hüner, N.P. 2000. The role of growth rate, redox-state of the plastoquinone pool and the trans-thylakoid deltapH in photoacclimation of *Chlorella vulgaris* to growth irradiance and temperature. *Planta* 212:93–102.

Wilson, K.E., Krol, M. & Hüner, N.P. 2003. Temperature-induced greening of *Chlorella vulgaris*. The role of the cellular energy balance and zeaxanthin-dependent nonphotochemical quenching. *Planta* 217:616–627.

Curriculum Vitae

Name:	Lauren Elisabeth Hollis
Post-secondary Education and Degrees:	University of Western Ontario London, Ontario, Canada 2003 to 2007 H.B.Sc. Genetics The University of Western Ontario London, Ontario, Canada 2007 to 2014 Ph.D. Biology * Maternity leave from May 1, 2012 to April 30, 2013
Honours and Awards:	NSERC USRA, 2007
Related Work Experience:	Teaching Assistant University of Western Ontario 2007 to 2014

Publications and Contributions:

Hollis, L. & Hüner, N.P.A. (accepted). Retrograde operational sensing and signalling pathways maintain photostasis in green algae, cyanobacteria and terrestrial plants. *Trends Photochem. Photobiol.*

Hollis, L. & Hüner, N.P.A. (submitted). Relaxation of excitation pressure in *Chlorella vulgaris* (trebouxiophyceae) is light-dependent: uncoupling of redox regulation and phenotypic plasticity. *J Phycol.*

Hollis, L. & Hüner, N.P.A. (submitted). Photoacclimation in *Chlorella vulgaris* UTEX 265 is both redox- and photoperiod-dependent. *Planta.*

Hollis, L. & Hüner, N.P.A. (submitted). Photoperiod-dependent growth oscillations in *Chlorella vulgaris*. *J Phycol.*

Hüner, N.P.A, Bode, R., Dahal, K., **Hollis, L**., Rosso, D., Krol, M. & Ivanov, A.G. 2012. Chloroplast redox imbalance governs phenotypic plasticity: the "grand design of photosynthesis" revisited. *Front. Plant Sci.* 3:255.

Hollis, L.E. and Hüner, N.P.A. (2014). Photoacclimation is both redox- and photoperiod-dependent. Oral presentation at the Eastern Regional Meeting of the Canadian Society of Plant Biologists. Guelph, Ontario, Canada.

Hollis, L.E. and Hüner, N.P.A. (2013). Chlorophyll biosynthesis and gene regulation are coupled to regulate greening in *Chlorella vulgaris*. Oral presentation at the Eastern Regional Meeting of the Canadian Society of Plant Biologists. Mississauga, Ontatio, Canada.

Hollis, L.E. and Hüner, N.P.A. (2013). Photoperiod influences acclimation to excitation pressure in *Chlorella vulgaris*. Poster presented at the 16th International Congress on Photosynthesis Research. St Louis, Missouri, USA.

Hollis, L.E. and Hüner, N.P.A. (2011). Kinetics of dark relaxation of excitation pressure in *Chlorella vulgaris*. Poster presented at the joint international meeting of the Canadian Society of Plant Physiologists and the American Society of Plant Biologists. Montreal, Quebec, Canada.

Hollis (nee Pellar), L.E. and Hüner, N.P.A. (2009). Dark relaxation of excitation pressure in *Chlorella vulgaris*. Poster presented at the Eastern Regional Meeting of the Canadian Society of Plant Physiologists. Burnaby, British Columbia, Canada.